

Copyright
by
Harpreet Singh
2012

**The Thesis Committee for Harpreet Singh
Certifies that this is the approved version of the following thesis:**

**Assessing Reservoir Performance and Modeling Risk Using Real
Options**

**APPROVED BY
SUPERVISING COMMITTEE:**

Sanjay Srinivasan, Supervisor

Larry W. Lake

**Assessing Reservoir Performance and Modeling Risk Using Real
Options**

by

Harpreet Singh, B.Tech

Thesis

Presented to the Faculty of the Graduate School of

The University of Texas at Austin

in Partial Fulfillment

of the Requirements

for the Degree of

Master of Science in Engineering

The University of Texas at Austin

May 2012

Dedication

This thesis is dedicated to my mother, and God.

Acknowledgements

I would like to express my sincere gratitude to my supervisor, Dr. Sanjay Srinivasan, for his guidance, support, patience, and motivation throughout my master's studies at the University of Texas at Austin. I am thankful to him for providing me the opportunity of pursuing my graduate studies under his guidance. I am grateful to him for his good suggestions and wisdom on the challenges that I faced outside my research. Without him, I would not have achieved this milestone. I would also like to thank Dr. Larry Lake for reading this thesis and providing valuable comments and suggestions.

I would like to thank my research group, especially Ankesh Anupam, Cesar Mantilla, and Sayantan Bhowmik. I learned a lot from them. I am especially grateful to Ankesh Anupam for being my unofficial research mentor. I am also thankful to the rest of my office mates and friends, specifically, Brandon Henke, Namdi Azom, Selin Erzybek, Aarti Punase, Hoonyoung Jeong, and Young Kim. Other past group members that I have had the great pleasure to work with or alongside of are John Littlepage, Hapiz Zulkipli, Nader Bukhamseen, and Nitish Koduru.

I would like to thank the friendly staff, each of whom helped in providing the resourceful environment for the research. Specifically, Jin Lee for her help with the administrative support, Dr. Roger Terzian for his help with the computer support, and all other staff members at the Department of Petroleum and Geosystems Engineering. I would also like to thank CMG Ltd. for providing me with full license of their simulator for the research.

I would like to thank my mother, to whom I owe absolutely everything in life. Finally, I wish to thank Garima Bajwa for her constant support and encouragement throughout this time.

Abstract

Assessing Reservoir Performance and Modeling Risk Using Real Options

Harpreet Singh, M.S.E

The University of Texas at Austin, 2012

Supervisor: Sanjay Srinivasan

Reservoir economic performance is based upon future cash flows which can be generated from a reservoir. Future cash flows are a function of hydrocarbon volumetric flow rates which a reservoir can produce, and the market conditions. Both of these functions of future cash flows are associated with uncertainties. There is uncertainty associated in estimates of future hydrocarbon flow rates due to uncertainty in geological model, limited availability and type of data, and the complexities involved in the reservoir modeling process. The second source of uncertainty associated with future cash flows come from changing oil prices, rate of return etc., which are all functions of market dynamics. Robust integration of these two sources of uncertainty, i.e. future hydrocarbon flow rates and market dynamics, in a model to predict cash flows from a reservoir is an essential part of risk assessment, but a difficult task. Current practices to assess a reservoir's economic performance by using Deterministic Cash Flow (DCF) methods have been unsuccessful in their predictions because of lack in parametric capability to robustly and completely incorporate these both types of uncertainties.

This thesis presents a procedure which accounts for uncertainty in hydrocarbon production forecasts due to incomplete geologic information, and a novel real options methodology to assess the project economics for upstream petroleum industry. The modeling approach entails determining future hydrocarbon production rates due to incomplete geologic information with and without secondary information. The price of hydrocarbons is modeled separately, and the costs to produce them are determined based on market dynamics. A real options methodology is used to assess the effective cash flows from the reservoir, and hence, to determine the project economics. This methodology associates realistic probabilities, which are quantified using the method's parameters, with benefits and costs. The results from this methodology are compared against the results from DCF methodology to examine if the real options methodology can identify some hidden potential of a reservoir's performance which DCF might not be able to uncover. This methodology is then applied to various case studies and strategies for planning and decision making.

Table of Contents

Table of Contents	ix
List of Tables	xii
List of Figures	xiii
Chapter 1: Introduction	1
Motivation.....	1
Uncertainties In Upstream Petroleum Industry Projects.....	2
Thesis Outline	3
Chapter 2: Real Options.....	5
Introduction.....	5
Discounted Cash Flow	5
Real Options Valuation.....	6
DCF vs. ROV	7
Black-Scholes Equation	7
Chapter 3: Model Updating and Value of Information.....	18
Introduction.....	18
Research Approach	19
Incorporating Reservoir Uncertainty In ROV.....	19
Assessing The Value Of Information	22
Static Reservoir Modeling	23
Flow Modeling.....	31
ROV Analysis	36
Results And Discussions.....	39
Chapter 4: Assessing Economic Implications of Reservoir Modeling Decisions ..	42
Introduction.....	42
Assessing The Impact Of Detailed Geological Modeling	43
Assessing The Impact Of Detailed Flow Modeling.....	69

Chapter 5: Binomial-Lattice Option Valuation.....	77
Introduction.....	77
Use Of The Model	78
Method For Constructing The Lattice.....	80
Relationship Of BLOV With Black-Scholes Model For ROV	86
Chapter 6: Analyzing the Prospects of an Undeveloped Field	88
Introduction.....	88
Description of the problem	89
Modeling Approach	89
Static Reservoir Modeling	91
NPV Distribution Forecast.....	94
Option Valuation By BLOV	97
Results And Discussions.....	101
Chapter 7: Uncertainty Analysis by Model Selection and Economic Evaluation Using a Binomial Lattice.....	106
Introduction.....	106
Model Selection Algorithm.....	106
Case Description	108
Static Reservoir Modeling	109
Well History.....	115
Final Set of Models by Model Selection Algorithm.....	117
Results.....	119
Discussions	128
Chapter 8: Summary, Conclusions, and Future Recommendations	130
summary.....	130
conclusions.....	131
recommendations for future work.....	132
Appendix A: Simulation Data Files for CMG-IMEX.....	134
A.1 Reservoir Model: 50 x 50 x 1Grid Dimension, 5 Production Wells (Chapter 3)	134

A.2 Reservoir Model: 200 x 200 x 1Grid Dimension, 5 Production Wells (Chapter 4)	142
A.3 Reservoir Model: 200 x 200 x 1Grid Dimension, 5 Production Wells, Well testing (Chapter 7)	151
Appendix B: MatLab Codes to Perform General Operations	168
B.1 Importing Data From GSLIB Format Files To MatLab	168
B.2 Making a Data File With GSLIB Format From MatLab Workspace	169
B.3 Calling CMG-IMEX From Matlab To Retrieve Bottom Hole Pressure (BHP) Data	171
B.4 Calling CMG-IMEX From Matlab To Retrieve Production Rate Data	174
B.5 Computing Production Rate Through Decline Curve Analysis	177
B.6 PV, NPV And ROV Analysis	180
B.7 NPV And Reserve Estimation By STOOIP	185
B.8 BLOV Anlysis	188
B.9 Calling GSLIB Executable 'TRANS' From MatLab And Retrieving The Resultant Data	193
B.10 Generating Sample Data And Their Co-Ordinates From A Gridded Data	195
B.11 Computing Permeability By Drawdown/Buildup Well Testing Data	198
Appendix C: MatLab Codes for Specific Cases and Chapters	209
C.1 Model Updating And Value Of Information (Chapter 3)	209
C.2 Assessing Economic Implications of Reservoir Modeling Decisions (Chapter 4)	217
C.3 Analyzing the Prospects of an Undeveloped Field (Chapter 6)	224
C.4 Analyzing Reservoir Performance by Model Selection (Chapter 7)	229
Bibliography	239

List of Tables

Table 3-1: Hard (core) data of porosity and permeability obtained at the 5 producing well locations	23
Table 3-2: Hard data of porosity and permeability after drilling an additional well (in yellow) .	26
Table 4-1: Hard data of porosity and permeability from 5 reference wells.....	45
Table 4-2: Conditioning data at well locations in form of two facies	51
Table 6-1: Hard data of porosity from 5 wells and their locations	91
Table 7-1: Hard data of porosity and permeability from 5 reference wells.....	110
Table 7-2: Threshold values of permeability and porosity with their corresponding marginal probabilities.....	113
Table 7-3: Locations of 5 wells	115

List of Figures

Figure 3-1: Algorithm for incorporating reservoir uncertainty in ROV	21
Figure 3-2: Porosity (%) and permeability (md) model on left and right, respectively, for the base case.....	25
Figure 3-3: Two realizations of each porosity (left side; in %) and permeability (right side; in md), respectively, after drilling an exploratory well (green colored circle)	28
Figure 3-4: a) Secondary data mimicking seismic; b) Two realizations of each porosity (%) and permeability (md) model on left and right, respectively, after acquiring seismic	30
Figure 3-5: Two phase relative permeability curve for oil-water phase	32
Figure 3-6: Reservoir model setup in CMG for simulations	33
Figure 3-7: Uncertainty in production rate profiles for a) base case, b) after an exploratory well, c) after seismic	34
Figure 3-8: Change in uncertainty of oil production forecast after obtaining information from drilling an exploratory well.....	35
Figure 3-9: Change in uncertainty of oil production forecast after conditioning to secondary data mimicking seismic.	35
Figure 3-10: Change in uncertainty of oil production forecast.....	36
Figure 3-11: Variation of project volatility with time during the life of the reservoir	38
Figure 3-12: Comparison of uncertainty in cumulative DCF for scenarios 1 and 2 with base case	39
Figure 3-13: Uncertainty in ROV due to uncertainty in production forecasts.....	40
Figure 3-14: Uncertainty in PV due to uncertainty in production forecasts.....	40
Figure 4-1: Reference Model for porosity (left; in %) and permeability (right; in md)	46
Figure 4-2: Isotropic model fit (black) for experimental semivariograms (red) of porosity in four directions.....	47
Figure 4-3: Isotropic model fit (black) for experimental semivariograms (red) of permeability in various directions.....	48
Figure 4-4: Maps from SGSIM.....	50
Figure 4-5: Maps from SISIM	51
Figure 4-6: TI used as input in the SNESIM program.....	52
Figure 4-7: Maps from SNESIM	53
Figure 4-8: Average of SGSIM (top), SISIM (middle) and SNESIM (bottom) maps over the suite of 100 realizations.....	54
Figure 4-9: Two phase oil-water relative permeability curve assumed for the flow simulations.	56
Figure 4-10: Reservoir model setup in CMG for simulations	57
Figure 4-11: Uncertainty in oil production forecast obtained using SGSIM.....	58
Figure 4-12: Uncertainty in oil production forecast obtained using SISIM	58
Figure 4-13: Uncertainty in oil production forecast obtained using SNESIM	59
Figure 4-14: Comparison of production rate distributions (histograms) from 3 geological models with the reference truth	60
Figure 4-15: Variation of project volatility with time for different models and reference truth ..	62
Figure 4-16: Comparison of uncertainty in cumulative DCF from SGSIM, SISIM, and SNESIM with that	63

Figure 4-17: Uncertainty in PV forecast obtained using SGSIM	64
Figure 4-18: Uncertainty in PV forecast obtained using SISIM	65
Figure 4-19: Uncertainty in PV forecast obtained using SNESIM	65
Figure 4-20: Uncertainty in ROV forecast obtained using SGSIM	66
Figure 4-21: Uncertainty in ROV forecast obtained using SISIM	66
Figure 4-22: Uncertainty in ROV forecast obtained using SNESIM	67
Figure 4-23: Comparison of mean production profiles from different models	68
Figure 4-24: Comparison of ROV corresponding to mean production profiles from different models	68
Figure 4-25: Uncertainty in oil production forecast determined using CMG	73
Figure 4-26: Uncertainty in oil production forecast determined using decline curve analysis	73
Figure 4-27: Uncertainty in PV obtained using CMG	74
Figure 4-28: Uncertainty in PV obtained using Decline Curve	74
Figure 4-29: ROV obtained using CMG	75
Figure 4-30: ROV obtained using Decline Curve	75
Figure 5-1: Example of a lattice showing underlying asset values	79
Figure 5-2: Example of a lattice showing option values	79
Figure 5-3: Construction of lattice for an underlying asset illustrating the process of construction of lattice for an underlying asset. The value of the asset is first constructed by going from left to right. Subsequently, the option value is computed by traversing the lattice from right to left.	81
Figure 5-4: Probability distribution of future payoffs obtained from the values in the terminal nodes of the underlying lattice	82
Figure 5-5: Construction of Option Valuation Lattice	85
Figure 5-6: Evolution of Option Valuation Lattice	86
Figure 6-1: Porosity with reference data only	92
Figure 6-2: Seismic map on a 50 x 50 x 1 grid scale	93
Figure 6-3: Porosity with reference data and seismic	94
Figure 6-4: Distribution of NPV values for a) Scenario 1. The reservoir models have been generated conditioned to only 5 well data; b) Scenario 2. The reservoir models have been generated conditioned to 5 well data and the pseudo-seismic data	95
Figure 6-5: P10, P25, P50, P75, and P90 values retrieved from the NPV distribution for Scenario 1 and Scenario 2	96
Figure 6-6: a) Illustration for constructing lattice of the underlying asset; b) Calculation of underlying asset value using 5 well data for 1 time step.	98
Figure 6-7: a) Illustration for constructing option valuation lattice; b) Calculation of option valuation lattice using 5 well data for 1 time step.	99
Figure 6-8: Lattice of the underlying asset with reference data only	101
Figure 6-9: Option valuation lattice with reference data only	102
Figure 6-10: Lattice of the underlying asset with reference data and seismic	102
Figure 6-11: Option valuation lattice with reference data and seismic	103
Figure 6-12: Uncertainty in option values generated using P-values of the NPV	104
Figure 7-1: Algorithm for model selection by distance-metric approach	108
Figure 7-2: Isotropic model fit (black) for experimental variograms (red) of porosity in various directions	111

Figure 7-3: Isotropic model fit (black) for experimental variograms (red) of permeability in various directions	112
Figure 7-4: Single realization for each porosity (%) and permeability (md).....	114
Figure 7-5: Multiple realizations of permeability field.....	114
Figure 7-6: Reservoir model setup in CMG for flow simulation.....	115
Figure 7-7: Well bottom hole pressure during drawdown and buildup well test for well-1	116
Figure 7-8: Well bottom hole pressure during drawdown and buildup well test for well-2.....	117
Figure 7-9: Uncertainty in oil flow rates from the reservoir before and after model selection ..	118
Figure 7-10: NPV distribution before model selection.....	120
Figure 7-11: Key percentile values of the NPV distribution before model selection.....	121
Figure 7-12: NPV distribution after the model selection.....	122
Figure 7-13: Key percentiles of the NPV distribution after the model selection.....	122
Figure 7-14: Variation of project volatility with time for models before and after selection, and reference truth	124
Figure 7-15: Underlying lattice of the reference truth model	125
Figure 7-16: Option lattice of the reference truth model	126
Figure 7-17: Underlying lattice before the model selection	126
Figure 7-18: Option lattice before the model selection	127
Figure 7-19: Underlying lattice after the model selection	127
Figure 7-20: Option lattice after the model selection	128
Figure 7-21: Uncertainty in option values generated using P-values of the NPV	129

Chapter 1: Introduction

MOTIVATION

Project evaluation under uncertainty is a key aspect of reservoir engineering and management that has assumed a critical role in recent times because of the depletion of easy to produce hydrocarbon resources and the increasing hostile operating environments faced by oil and gas operators. However, there is a significant gap between theory as developed in academic literature and the practical manner in which project evaluation is carried out in the industry. There is also a gap in the way uncertainty is assessed using modern reservoir modeling tools and the assumptions employed in economic tools for project evaluation. In light of the geological, technical, economical and political uncertainties that confront major projects – flexibility in making development decisions is essential. Thus we need options to change the capacity of facilities, the scale of a project, the timing of investment etc. and these options must be evaluated under technical and market uncertainties.

These motivate the use of real options valuation (ROV) for strategic planning and decision-making. ROV is a technique that provides flexibility for including any changes that may be associated with a project. Standard implementations of ROV for petroleum projects reveal a distinct gap between the technologies for uncertainty assessment available within reservoir modeling workflows and the representation of uncertainty in typical options evaluation. The objective of this thesis is to expose some of these gaps and subsequently suggest a new workflow for incorporating reservoir uncertainties in ROV analysis. The research also sheds some light on

issues such as optimum resolution of reservoir models, the level of detail in flow modeling etc. as viewed from the standpoint of ROV analysis.

UNCERTAINTIES IN UPSTREAM PETROLEUM INDUSTRY PROJECTS

Decisions to invest in projects related to upstream petroleum engineering are made in the presence of multiple sources of uncertainty. These decisions are based on future economic value as determined by forecasting future hydrocarbon production from the reservoir, the cost associated with production of those hydrocarbons, and the forecast of oil price prevailing during the time period of hydrocarbon production.

Some of the uncertainties associated with valuing an upstream project are (Lin 2008):

1. Subsurface Uncertainty:
 - a. Geologic uncertainty - Uncertainty in predicting porosity, permeability, shape of reservoir, fault structures etc.
 - b. Flow related uncertainty - Can include uncertainty in fluid properties, uncertainty in reservoir drive mechanisms, uncertainty in sweep efficiency etc.
2. Surface Uncertainty: This type of uncertainty may include shut in of the well due to changes in operating conditions such as weather (in case of offshore fields), failure in operation of surface facilities etc.
3. Cost Uncertainty: This includes uncertainty in capital costs, operational costs etc.
4. Market Uncertainty: Such as changes in oil and gas prices, interest rates etc.

Although in reality, these uncertainties may exhibit coupled behavior rendering the analysis very difficult, in this thesis, the focus is on geologic uncertainty and its manifestation in the ROV analysis.

THESIS OUTLINE

The general research questions addressed in this thesis are:

1. How do we integrate geological uncertainty obtained by reservoir modeling within the ROV framework?
2. How can we use ROV analysis to address important modeling issues such as optimal representation of geology in reservoir models and the role of complex flow models for uncertainty assessment?
3. What is the economic worth of incremental data for reservoir modeling?

Chapter 2 presents a review of real option valuation using the Black-Scholes model, and the concepts associated with its application to projects in the upstream petroleum industry. This concept will be used subsequently to value projects under geologic uncertainty. Chapter 3 presents a strategy for updating reservoir models as new information becomes available. The economic forecasts of the project after integrating two sources of information are compared using both deterministic cash flow technique and real options Black-Scholes model. Comparison of results from both these techniques suggest that project valuation by the Black-Scholes model results in a more robust assessment of the worth of additional data. Chapter 4 explores and compares reservoir performance obtained by complex reservoir modeling (geological model and reservoir simulation) and simple reservoir modeling for valuing long term E&P projects. Chapter 5 extends the real option valuation technique using Binomial Lattice, and the concepts associated with its application to projects in upstream petroleum industry. Chapter 6 applies the framework

of Binomial Lattice Option Valuation (BLOV) to analyze the economic prospects of an undeveloped, but discovered field. Chapter 7 proposes a strategy to save computational time for doing uncertainty analysis, in context of reservoir performance and risk assessment, by employing the use of model selection algorithm. The final chapter outlines conclusions and presents recommendations for future work.

Chapter 2: Real Options

INTRODUCTION

An option is a form of contract between two members for future commercial transaction. An important aspect of an option is that it is essentially a member's right, but not an obligation, to form a contract with another member. A real option is an analogy of the financial options applicable to projects and activities outside the stock market. A real option allows forming a contract for future transactions in physical/real assets. Typically, this could be the option to develop, abandon, expand etc. a capital intensive project. Another difference between financial and real options is the time to expiration, which is the date on which the contract expires, and after which the option becomes worthless. In financial options the date of expiration typically ranges from one to two quarters, whereas in real options the date of expiration ranges in several years.

Before embarking on a review of real option valuation, a brief look at a more traditional approach to economic analysis is warranted.

DISCOUNTED CASH FLOW

Discounted Cash Flow (DCF) is a technique to value a project using the concept of time value of money. In this technique, future cash flows are determined and discounted to obtain Present Values (PV), and the sum of all PVs is the Net Present Value (NPV). NPV assumes all the risks in a project are completely accounted for by the rate of return (r), and it does not allow for uncertainty, changing circumstances etc.

$$NPV = Benefits - Costs = \frac{F(t)}{(1+r)^t}$$

Where,

$F(t)$ = future cash flow at time t

r = rate of return

REAL OPTIONS VALUATION

Real Options Valuation (ROV) is also a form of project valuation technique, but more advanced than DCF. ROV is a process of valuing a physical/real asset with real uncertainties. As opposed to NPV, ROV incorporates multi-domain uncertainties. Simply put, ROV is an extension to Net Present Value (NPV)/Present Value (PV) analysis:

$$NPV / PV = Benefits - Cost$$

$$ROV = Benefits \times P(x) - Cost \times P(y)$$

Where, $P(y)$ represents the probability that the option will be positive (i.e. the benefit is greater than the cost). If the option has been exercised (i.e. the costs have been incurred and cannot be recovered), $P(x)$ represents the probability that subsequent benefits are also positive. Here x and y are the variables through which these probabilities are quantified. It is evident from the above equation that a major difference between the the NPV/PV evaluation and the ROV evaluation is the introduction of uncertainty in current and future benefits through the probabilities $P(\bullet)$. The ROV can be estimated through a closed-form equation known as Black-Scholes equation. The variables x and y will be defined in the upcoming section on Black-Scholes equation.

DCF vs. ROV

The focus of this chapter is on the concept of ROV, and the focus in the next two chapters is on the application of ROV to evaluate models for geologic uncertainty, data integration etc. In order to assess why ROV may be more realistic and flexible in valuing assets compared to NPV, here are two reasons (Johnson 2010) that may specifically apply to petroleum E&P industry:

1. When an investment is valued using NPV, it is assumed that production rates are fixed and there is no allowance for changes in future production rates that might occur due to changing circumstances. However, as opposed to NPV, the ROV concept allows for changing circumstances and in considering changes in future production rates.
2. The ability of ROV make use of more available information such as project volatility due to oil price fluctuations as well as geologic uncertainty, schedule uncertainty etc.

DCF is still the basis to appraise potential investments for most oil companies. It is easy and requires less information to appraise the valuation. It is believed (Coy 1999) that ROV yields more realistic asset evaluation than DCF because the ROV model incorporates the variability and uncertainty in the model parameters. ROV may highlight extra value for projects, where DCF fails to see the hidden value, or may highlight low value of falsely bloated value projects by DCF (Bailey et al. 2003). The strength of ROV is based on the accuracy of the parameters used in its models and parameter selection is a vital part of ROV (Bailey et al. 2003).

BLACK-SCHOLES EQUATION

There are various derivations of the Black-Scholes equation. However, we present here the derivation that invokes the usage of a formula in stochastic calculus known as Ito's lemma.

We assume that our reservoir's asset price (present value) evolves according to the stochastic process, called Brownian motion, given by the following stochastic differential equation (SDE):

$$\frac{dS}{S} = \mu dt + \sigma dW$$

where,

$$dW = \varepsilon \sqrt{dt}, \text{ and } \varepsilon \sim N(0,1)$$

W = Brownian motion

S = Asset price at instantaneous time ' t ' (Present Value)

$V(S, T)$ = Asset price accumulated till the time of maturity ' T ' (Net Present Value)

μ = Constant drift

σ = Volatility

A simple interpretation of the above equation is that the fluctuations in an asset's prices can be decomposed into a trend component and an additional stochastic residual. Given the asset value S at a particular time t , to determine how $V(S, T)$ evolves as a function of T , we use Ito's lemma. Ito's lemma is a rule for calculating differentials of quantities dependent on stochastic processes. It is an extension of the chain rule in ordinary calculus.

The lemma states that for an Ito drift diffusion process:

$$dX_t = \mu_t dt + \sigma_t dW_t$$

If $f(t, X_t)$ be a twice differentiable function of stochastic variable X_t and t , then:

$$df(t, X_t) = \left(\frac{\partial f}{\partial t} + \mu \frac{\partial f}{\partial x} + \frac{\sigma_t^2}{2} \frac{\partial^2 f}{\partial x^2} \right) dt + \sigma_t \frac{\partial f}{\partial x} dW_t \quad \text{--- (2.1)}$$

Equation (2.1) is referred to as Ito's lemma (or Ito's formula). Ito's lemma is derived by first using the Taylor expansion to expand df in the second order and replace dX_t ,

with $dX_t = \mu_t dt + \sigma_t dW_t$. The second degree terms are ignored and $(dW)^2$ term is substituted with dt .

In case of reservoir as an asset the Ito's lemma can be used by replacing f with V and x with S . Therefore, after invoking the usage of Ito's lemma for a reservoir as an asset we get the following partial differential equation (PDE) which is known as the Black-Scholes equation:

$$\frac{\partial V}{\partial t} + \frac{1}{2} \sigma^2 S^2 \frac{\partial^2 V}{\partial S^2} + rS \frac{\partial V}{\partial S} - rV = 0 \quad \text{--- (2.2)}$$

Equation (2.2) is a parabolic PDE, that relates the asset's price at time of maturity, $V(S, T)$, to parameters for a fixed risk-free interest rate (r), fixed volatility of the cash flow from the reservoir (σ), the asset price at any time (S).

Remarks

- The Black Scholes PDE has a well known mathematical form which is similar to the ubiquitous Advection-Diffusion-Reaction (ADR) PDE, a specific form of Material Balance PDE, in reservoir engineering. Both the Black Scholes PDE and Material Balance PDE have similar mathematical form which will be evident in the next section from the fact that on change of variables from Black-Scholes PDE we derive the heat equation (a specific form of Material Balance PDE) in order to find analytical solution to the Black-Scholes PDE.
- In Black-Scholes PDE the term $\frac{\partial V}{\partial t}$ is analogous to the accumulation term, $rS \frac{\partial V}{\partial S}$ is analogous to the advection term, $\frac{1}{2} \sigma^2 S^2 \frac{\partial^2 V}{\partial S^2}$ is analogous to the diffusion term, and rV is analogous to the source/reaction term in ADR equation, respectively.

Derivation for Closed Form Solution of the Black-Scholes Equation

In order to derive the closed form of the Black-Scholes equation for real options valuation, we use change of variables technique to transform the Black-Scholes PDE (Equation 2.1) to the well known heat equation. The solution to that heat equation, and its transformation to the original variables of the Black-Scholes partial differential equation, gives the closed form solution of the Black-Scholes equation for real options valuation. Depending on the boundary conditions and final condition employed, different solutions can be obtained.

Using the following variable transformation:

$$\tau = T - t$$

$$u = Ce^{r\tau}$$

$$x = \ln(S / X) + (r - \frac{\sigma^2}{2})\tau$$

Where,

T = Time, (where t=1,2,...,T)

(T-t) = Time to maturity

$C(S, t)$ = Real option value (ROV)

$S = F(t)$ = Future Cash flow, undiscounted, at time t

X = Capital expenditure (Capex), undiscounted

r = rate of return

σ = project volatility (volatility of the underlying asset i.e. reservoir model)

Based on the above change of variables, the Black-Scholes PDE assumes a form similar to the heat conduction equation:

$$\frac{\partial u}{\partial \tau} = \frac{\sigma^2}{2} \frac{\partial^2 u}{\partial x^2} \quad \text{--- (2.3)}$$

In order to solve this PDE (Equation 2.3), we need to specify the final condition and boundary conditions. Because at the time of maturity T, the value of a call option is exactly known, we get the following final condition and boundary conditions, respectively:

F.C: $C(S, T) = \max(S - X, 0)$

1st B.C: $C(S, t) \rightarrow S$ as $S \rightarrow \infty$

2nd B.C: $C(0, t) = 0$ for all t

The first boundary condition states that if the future cash flow goes to infinity, the value of the option will equal the value of the future cash flow. The second boundary condition states that the option to delay is worthless if the future cash flows are zero.

Using the above final condition and boundary conditions, we get one of the closed form solution of the Black-Scholes equation which is also known as the real options equation (Ugur 2008):

$$C(S, t) = SN(d_1) - Xe^{-r(T-t)}N(d_2) \quad \text{--- (2.4)}$$

Where,

$N(d_1)$ and $N(d_2)$ = cumulative normal probability values of d_1 and d_2

$$d_1 = \frac{\ln\left(\frac{S}{X}\right) + \left(r + \frac{\sigma^2}{2}\right)(T-t)}{\sigma\sqrt{T-t}}, \text{ and } d_2 = d_1 - \sigma\sqrt{T-t}$$

$S = F(t)$ = Future Cash flow, undiscounted, at time t

X = Capital expenditure (Capex), undiscounted

r = rate of return

σ = the project volatility (volatility of the underlying asset i.e. reservoir model)

T = Time, (where $t=1, 2, \dots, T$)

$(T-t)$ = Time to maturity

$C(S, t)$ = Real option value (ROV)

Conceptually, the term $N(d_1)$ is the probability that the value of the option will pay off, and $N(d_2)$ is the probability that the option will be exercised (DePamphilis 2009). Mathematically, these two terms are the Z scores from the normal probability function. These terms take risk into account.

Remarks on ROV

- In traditional ROV implementations, the price of oil is a major factor driving S and σ . In subsequent chapters we incorporate geologic uncertainty into the computation of S and σ .
- Option value = $\max(\text{value}, 0)$. Option value is not negative because philosophically it is defined as our right but not the obligation to make the investment, never wanting to run into loss.

Traditional Project Volatility Model

The volatility of a particular property is a statistical measure of the dispersion of that property under given condition. Volatility of the ROV model, or project volatility, refers to the frequency and severity with which the economic returns for a particular project fluctuate.

Volatility significantly impacts option valuation, and it is perhaps the most difficult and critical factor to quantify. Higher volatility increases the possible option values and lower volatility decreases the possible option values. Volatility is the only variable quantity which affects option values and which is not directly evident either in the option type or in the market. It must be estimated and estimating the underlying asset (reservoir) volatility is one of the most important problems faced by practitioners wanting to use real options models. It is difficult to estimate

volatility in practice, because before project execution, it is impossible to assess the fluctuations of the underlying real asset and the very process of exercising an option will introduce fluctuations that are impossible to assess *a priori*. It may be useful to estimate the volatility for the project without options by considering the project without options as the underlying asset. There are several approaches, some of which are briefly reviewed next:

Logarithmic Ratio Method:

In this approach, the ratio of the present value at two successive time instants are calculated and used to define the volatility as the sample standard deviation:

$$\sigma = \sqrt{\frac{1}{n-1} \sum_{i=1}^n (x_i - \bar{x})^2} \quad \text{--- (2.5)}$$

where, $x = \ln \left[\frac{PV_i}{PV_{i-1}} \right]$ and \bar{x} is the mean ratio over all time instants. The project volatility is thus the sample standard deviation of the ratio of present value at successive time instants.

This method is simple and easy to use; however it does not work well if the cash flows are negative over certain period of time as the logarithm of a negative number does not exist.

An alternative is to consolidate all future cash flow values into two sets of present values in the following way (Mun 2002):

$$G = \ln \left[\frac{\sum_{i=1}^n PV_i}{\sum_{i=0}^n PV_i} \right] \quad \text{--- (2.6)}$$

The volatility σ is calculated as the standard deviation of G.

However both approaches (EquationS 2.5 and 2.6) are unreliable if some of the cash flows are negative.

Copeland and Antikarov Method:

Copeland and Antikarov (Copeland & Antikarov 2001) presented a method to estimate the volatility parameter in ROV based on hypothetical simulated distribution of returns to account for the lack of historical distribution of returns from a project. For each simulation trial, the value of the returns is estimated at two different points in time. These two estimates are generated independently because it is assumed that the value of a project through time will follow a random walk, regardless of the pattern of cash flows (Samuelson 1965). The ratio of these two estimated underlying asset values gives an estimate of the rate of return. A rate of return distribution is generated by compiling the rate of return estimates from all simulations.

The detailed steps for calculating the project volatility by the Copeland and Antikarov method are outlined below:

$F(0)$ = Known cash flow in year 0

$F(t)$ = [Future incoming cash flow (revenue) – Opex] = Uncertain cash flow in the t^{th} year,

where $t=1, 2, \dots, T$

r = continuously compounded discount rate (the rate used to discount future cash flows to their present values)

$MV(n)$ = Market value of the project at time n (expectation over the future cash flows)

$PW(n)$ = Present worth of the project at time n (expectation over the future cash flows)

$k(n)$ = a random variable that represents the continuously compounded rate of return on the project between time $n-1$ and time n .

The present value at any time t is calculated by multiplying the future cash flow, $F(t)$, with the discount factor, $DV(t)$ i.e.

$$PV(t) = F(t) \times DV(t)$$

For a fixed discount rate, r , discretely compounded over time, t :

$$DV(t) = \frac{1}{(1+r)^t}$$

For a fixed continuously compounded discount rate:

$$DV(t) = e^{-rt}$$

Denoting the present value at time n of future cash flows as $MV(n)$:

$$MV(n) = \sum_{t=n+1}^T F(t).e^{-r(t-n)}$$

Adding the cash flow at time n , we get the present worth $PW(n)$.

$$PW(n) = MV(n) + F(n) = \sum_{t=n}^T F(t).e^{-r(t-n)}$$

In other words:

$$PW(n) = MV(n-1).e^{k(n)}$$

$$\text{and so } k(n) = \ln \left[\frac{PW(n)}{MV(n-1)} \right] \quad \text{--- (2.7)}$$

Since the cash flows are uncertain, the corresponding $PW(n)$ are actually random variables (outcomes from simulation). We therefore get a distribution for $k(n)$ using equation (2.7) and the standard deviation of this distribution is the project volatility i.e.

$$\sigma(n) = std(k(n))$$

If the volatility of the project changes with time, this method can still be used to compute time varying volatility by computing distributions of k for different times and standard deviation of each k will generate volatility for each year.

The Oil Price Model

The three types of processes used in modeling financial commodities are geometric Brownian motion (GMB) process, Mean Reverting (MR) process, and mean reversion with jumps (MRJ) process. However, mean reverting (MR) processes are the most widely used to model financial commodities. Ornstein and Uhlenbeck (Ornstein & Uhlenbeck 1930) is the most popular MR model.

Mean reverting processes incorporate the concept of demand and supply i.e. when prices are ‘too high’, demand will reduce and supply will increase, producing a counter-balancing effect. When prices are ‘too low’ the opposite will occur, again pushing prices back towards the long term mean. Some of the properties of this model are:

- The price is said to follow MR process if price follows a log-normal diffusion.
- Price changes in MR models are not independent.
- MR models have a long term equilibrium price and mean reversion rate.

The Ornstein-Uhlenbeck method is widely used for modelling a mean reverting process. We start by defining the terms and some concepts to be used:

W_t = a Brownian- Motion, also called Weiner process. $\rightarrow dW_t \sim N(0, \sqrt{dt})$

λ = the speed of mean reversion

μ = the ‘long run mean’, to which the process tends to revert.

σ = a measure of the process volatility

t = time

Δt = small time

P_t = Price of oil at time ‘ t ’

Now we present the formulae to be used based on Ornstein-Uhlenbeck model (Dias 2004).

The process of fluctuation in oil price ‘ P ’ is modeled as:

$$dP = \lambda(\mu - P)dt + \sigma dW_t \quad \text{--- (2.8)}$$

The exact formula of the Ornstein-Uhlenbeck mean reverting process which is obtained as a solution to the differential equation (2.8) that holds for any size of Δt is:

$$P_t = e^{-\lambda\Delta t} P_{t-1} + (1 - e^{-\lambda\Delta t})\mu + \sigma \sqrt{\frac{(1 - e^{-2\lambda\Delta t})}{2\lambda}} dW_t$$

To estimate the three parameters of MR model, we must have historical data of oil price. Then parameter estimation can be done using well known techniques for parameter estimation such as Least Square regressions, and Maximum Likelihood.

Once we have historical data of oil prices, we can examine the distribution of annual changes in the natural logarithm of price, as oil prices are usually said to follow a log-normal distribution.

Instead of using deterministic values for long-term mean, reversion speed and volatility of oil prices, we can replace them with their distribution values (min., most likely and max.).

Chapter 3: Model Updating and Value of Information

INTRODUCTION

This chapter presents:

- An economic analysis procedure that accounts for uncertainty in production forecasts arising due to incomplete geologic information.
- A procedure to assess the worth of progressive updating of reservoir models using additional data.

For the first objective, a workflow to model reservoir uncertainty and its economic analysis is presented and a procedure for economic analysis is developed. The workflow also demonstrates how to incorporate flow rate uncertainty in the ROV calculations.

For the second objective of our research, we compared the value of information obtained by either drilling an additional exploratory well or acquiring seismic for developing a reservoir model. The base case reservoir model is obtained conditioned data along 5 production wells and the value of information is assessed both in terms of uncertainty reduction and increase in economic returns. Even though in this particular case neither of the two information brought significant improvement to the economic forecast over the base case forecast, the example demonstrates the workflow for updating reservoir models and assessing the value of information.

RESEARCH APPROACH

For geostatistical modeling we used stochastic simulation algorithms like sequential Gaussian Simulation SGSIM (Deutsch & Journel 1997), and cosimulation COSGSIM (Xu et al. 1992). We used the histogram transformation program TRANS to ensure that the final stochastic reservoir models reflect the target histogram accurately. For these techniques we performed variogram. Through geostastical modeling we get multiple realizations of porosity and permeability models.

For flow modeling we used the CMG simulator (CMG-IMEX 2009) in order to obtain production rates. Geostatistical modeling followed by flow modeling is essential for uncertainty assessment of reservoir performance. Finally for economic analysis we use a deterministic discounted cash flow (DCF) technique, as well as real options valuation (ROV) that utilize the uncertainty models explicitly.

INCORPORATING RESERVOIR UNCERTAINTY IN ROV

An algorithm is presented to forecast reservoir flow uncertainty and its corresponding economic analysis. The steps for incorporating flow rate uncertainty in the ROV calculations are:

- I. We develop multiple realizations of reservoir model using appropriate geostatistical technique.
- II. These stochastic reservoir models are then input into the reservoir flow simulator to determine future hydrocarbon production rates. We obtain as many realizations of production rates as the number of stochastic reservoir models. The uncertainty in the stochastic reservoir models is carried to the hydrocarbon production rates. This uncertainty is represented by the different realizations of production rate profiles.

- III. Using these production rates, oil price, and operational expenses, we can determine future cash flows.
- IV. These future cash flows are used to determine project volatility using an appropriate model for project volatility such as the method by Copeland and Antikarov (2001).
- V. Finally, future cash flows, capital expenses, project volatility, and rate of return are used in the Black-Scholes ROV model to determine the option value for investing in the project at a certain time in future.

The above steps to incorporate flow rate uncertainty in the ROV calculations are detailed in Figure 3-1:

Algorithm

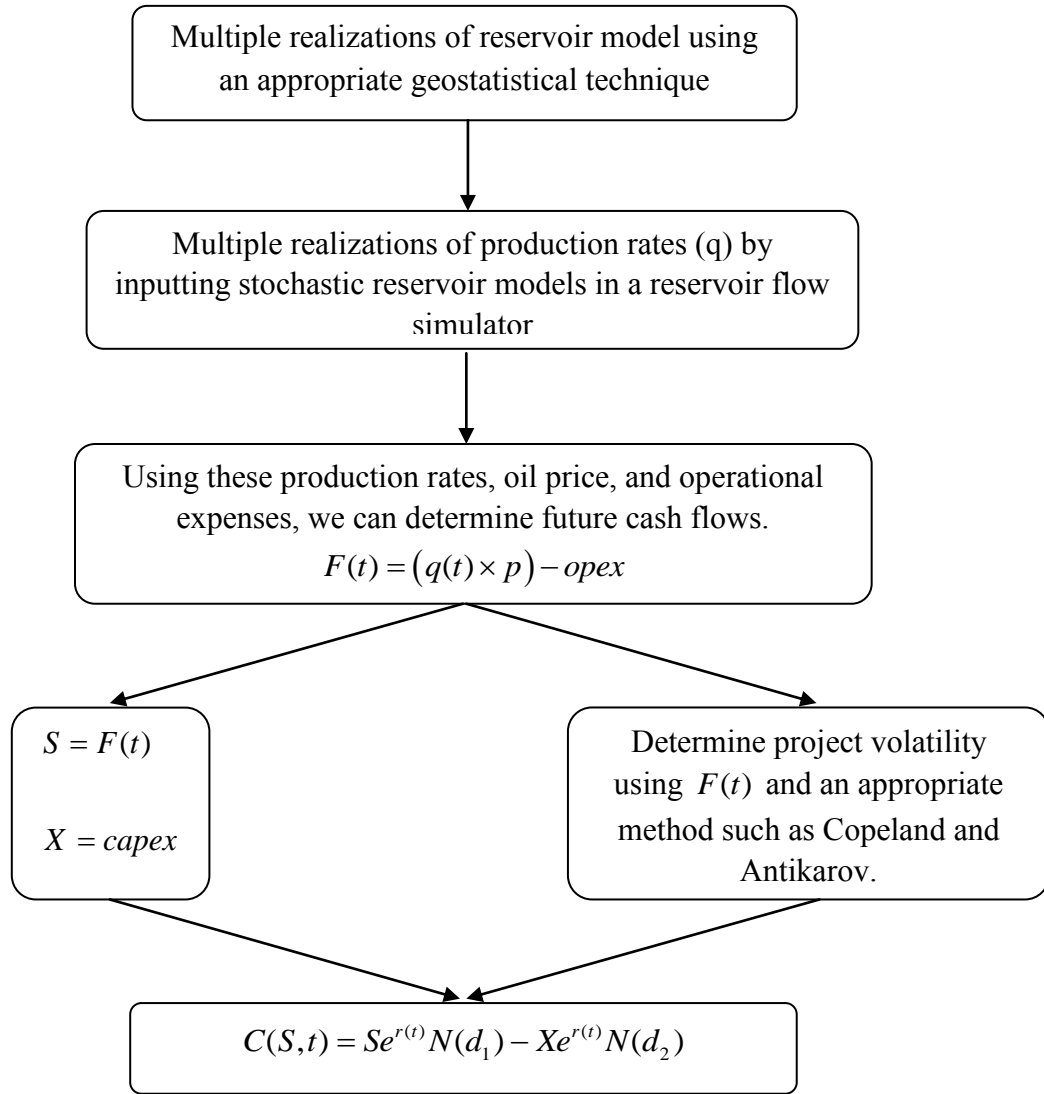


Figure 3-1: Algorithm for incorporating reservoir uncertainty in ROV

As pointed out in the previous chapter, $N(d_1)$ and $N(d_2)$ are normal probability values corresponding to d_1 and d_2 that can be calculated knowing the cash flow, rate of return r and

project volatility σ . The algorithm above describes the workflow of converting the reservoir uncertainty into economic returns from the reservoir.

ASSESSING THE VALUE OF INFORMATION

Description of the Problem

We assume a reservoir with grid dimension of 50 x 50 x 1 that initially has 5 production wells only. Basic information available about the reservoir characteristics such as porosity and permeability is from these 5 production wells. Using this base information we can develop multiple realizations of the reservoir model and future economic performance of the reservoir. Having multiple scenarios for economic performance of the reservoir enables us to perform risk analysis and take appropriate decisions regarding further development of the reservoir.

These multiple realizations of future economic performance of the reservoir represent uncertainty, and in order to reduce this uncertainty in predicting future economic performance we need to gain more information about our reservoir. We can adopt one of the following two ways to gain reservoir information:

Scenario 1: Drill an exploratory well – This will yield core data that can be directly used as “hard” conditioning data for the next generation of models

Scenario 2: Acquire seismic (secondary data which mimics seismic was generated by taking moving window average of a porosity model that was developed for the base case) – This would be reflective of “soft” data that is at a resolution different from the “hard” conditioning data and is imprecisely related to the “hard” data.

Gaining extra information, over and above the existing 5 producing wells, may reduce the uncertainty of our forecasted economic returns and give a more correct estimate for the economic value of the field. Our objective is to evaluate which of two different types of information gives more accurate future economic forecast and more reliable models of uncertainty.

STATIC RESERVOIR MODELING

Base Case: When only initial information is available

The base case is developed using reference hard data for porosity and permeability from 5 producing wells as shown in Table 3-1:

Table 3-1: Hard (core) data of porosity and permeability obtained at the 5 producing well locations

X	Y	Z	Porosity (%)	Permeability (md)
1	10	0	30	40
7	20	0	45	45
15	5	0	32	60
23	40	0	40	80
30	7	0	36	50

The porosity variogram model for the base case is:

Number of Structures = 1

Type = Spherical

Nugget Effect = 0

Maximum, medium, and minimum range = 1000, 100, and 20 units

Azimuth = 45 degrees

Dip = 0

Rake (rotation about X axis, measured counter-clockwise) = 0

The permeability variogram model for the base case is:

Number of Structures = 1

Type = Spherical

Nugget Effect = 0

Max., medium, and min. range = 1500, 200, and 0 units

Azimuth = 30 degrees

Dip = 0

Rake = 0

To obtain multiple realizations of porosity maps, hard data of porosity and variogram model for porosity are used as input in the Sequential Gaussian Simulation SGSIM geostatistical program (Remy et al. 2009). In this algorithm, the local conditional probability distribution at each unknown location on the grid is obtained by kriging using the hard data and previously simulated values in the vicinity of that node. A simulated value is sampled at random from the local conditional probability distribution and that value is added to the conditioning data set at the next simulation node visited along a random path. In this way, the simulation reproduces hard data histogram, and honors spatial variability as indicated by the variogram.

To obtain multiple realizations of permeability maps, hard data of permeability and a model of porosity are specified as primary and secondary data, respectively, along with variogram model for permeability. The Gaussian co-simulation program - COSGSIM (Remy et al. 2009) is used for the simulation. The correlation between primary and secondary variables was assumed as 0.6. In this simulation, the local conditional probability distribution at the simulation node is obtained by cokriging i.e. by extending the estimator to include the conditioning influence of the

secondary porosity data. The interaction between the primary and the secondary variable is approximated using a Markov hypothesis (Remy et al., 2009 [4]) and the specified correlation coefficient. Other than this extended procedure for constructing the local distribution, the remaining steps for sequential simulation are the same..

Figure 3-2 shows the stochastic reservoir model for base case with 5 producing wells whose positions are shown as black dots:

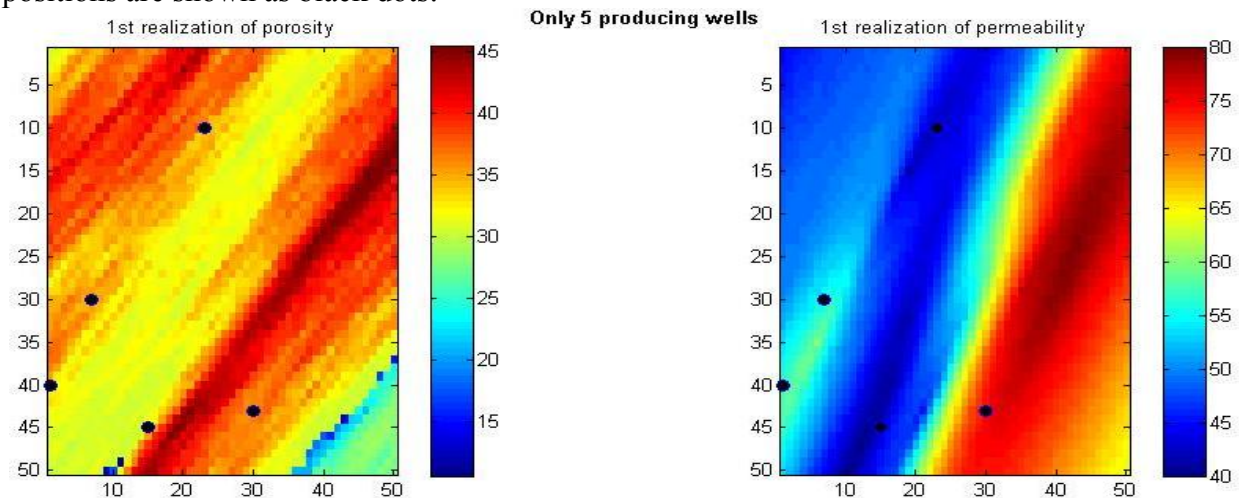


Figure 3-2: Porosity (%) and permeability (md) model on left and right, respectively, for the base case

In order to gain more information about our reservoir, we may decide to go for either of the two scenarios.

Scenario 1: Drill an exploratory well, or,

Scenario 2: Acquire seismic - A secondary data which mimics seismic was generated by taking moving window average of a porosity model by specifying a smoothing window and computing the average of the porosity within the window. The average value was assigned to the central node within the smoothin window.

Scenario 1: Drill an exploratory well to gain reservoir information

The hard data for porosity and permeability obtained from base case and an extra exploratory well are as shown in Table 3-2:

Table 3-2: Hard data of porosity and permeability after drilling an additional well (in yellow)

X	Y	Z	Porosity (%)	Permeability (md)
1	10	0	30	40
7	20	0	45	45
15	5	0	32	60
23	40	0	40	80
30	7	0	36	50
40	40	0	42	65

The porosity variogram model for Scenario 1 is:

Number of Structures = 1

Type = Spherical

Nugget Effect = 0

Max., medium, and min. range = 1000, 100, and 20 units

Azimuth = 45 degrees

Dip = 0

Rake = 0

The permeability variogram model for Scenario 1 is:

Number of Structures = 1

Type = Spherical

Nugget Effect = 0

Max., medium, and min. range = 1500, 200, and 0 units

Azimuth = 30 degrees

Dip = 0

Rake = 0

To obtain multiple realizations of porosity maps after conditioning to the extra information at the exploratory well location, the SGSIM geostatistical program was used. Once the porosity realizations were generated, permeability realization was obtained by conditioning to the hard permeability data as well as the previously simulated porosity model. In order to keep the simulation combinatorial manageable, the simulation was performed by only conditioning to one of the realizations of porosity. The correlation coefficient between porosity and permeability was again assumed to be 0.6.

Figure 3-3 shows the updated reservoir model obtained after conditioning to one extra exploratory well data. Black dots represent position of 5 producing wells from the base case, while green dots represent position of exploratory well.

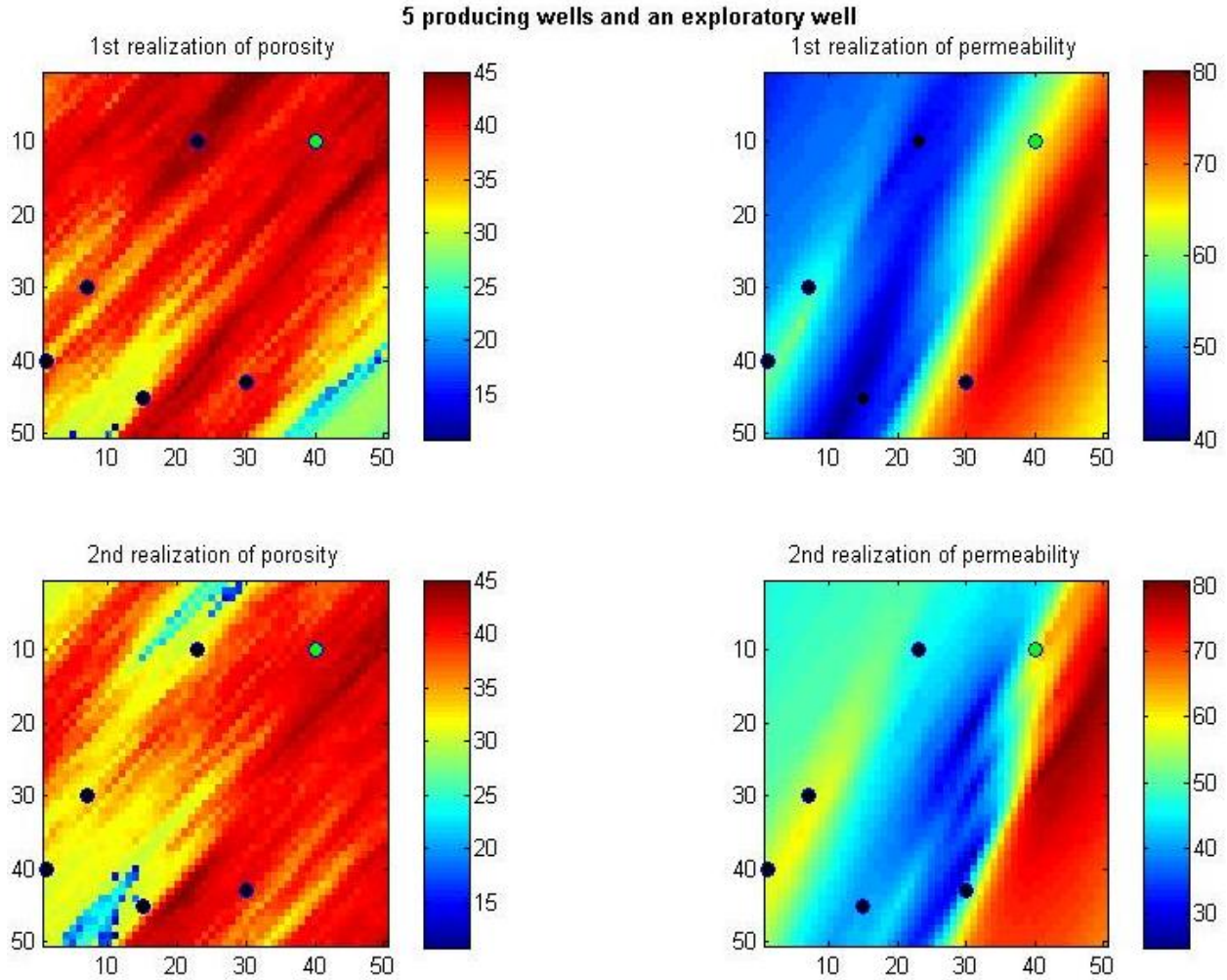


Figure 3-3: Two realizations of each porosity (left side; in %) and permeability (right side; in md), respectively, after drilling an exploratory well (green colored circle)

As a result of adding an extra hard data through exploratory well to the base case, there is a significant change in the model for porosity, and some change in permeability values around the location of the exploratory well. The change in porosity is significant, however the change in the permeability model is more subtle. The additional datum serves to restrict the extent of the low permeability region in the 45° azimuth direction.

Scenario 2: Acquiring Seismic to gain reservoir information

We generate secondary data which mimics seismic by taking moving window average of a porosity model that was developed for the base case. The primary data for porosity and permeability are the 5 hard data from the base case. The variogram models for both porosity and permeability are same for this Scenario.

The porosity and permeability variogram model for Scenario 2 is:

Number of Structures = 1

Type = Spherical

Nugget Effect = 0

Max., medium, and min. range = 1500, 200, and 0 units

Azimuth = 30 degrees

Dip = 0

Rake = 0

To obtain multiple realizations of porosity maps conditioned to primary hard data of porosity and secondary (mimicking seismic) data the COSGSIM geostatistical program was used. The correlation between primary and secondary variables was assumed as 0.6.

Similarly, to obtain multiple realizations of permeability maps, hard data of permeability and any one model of updated porosity (from Scenario 2) were used as primary and secondary data, respectively, along with variogram model for permeability. Cosimulation (COSGSIM) was performed. The correlation between primary and secondary variables was assumed as 0.6.

Figure 3-4a shows the secondary data which mimics the seismic and Figure 3-4b shows the updated reservoir model obtained after conditioning to the secondary data that mimics seismic. Black dots represent position of 5 producing wells from the base case.

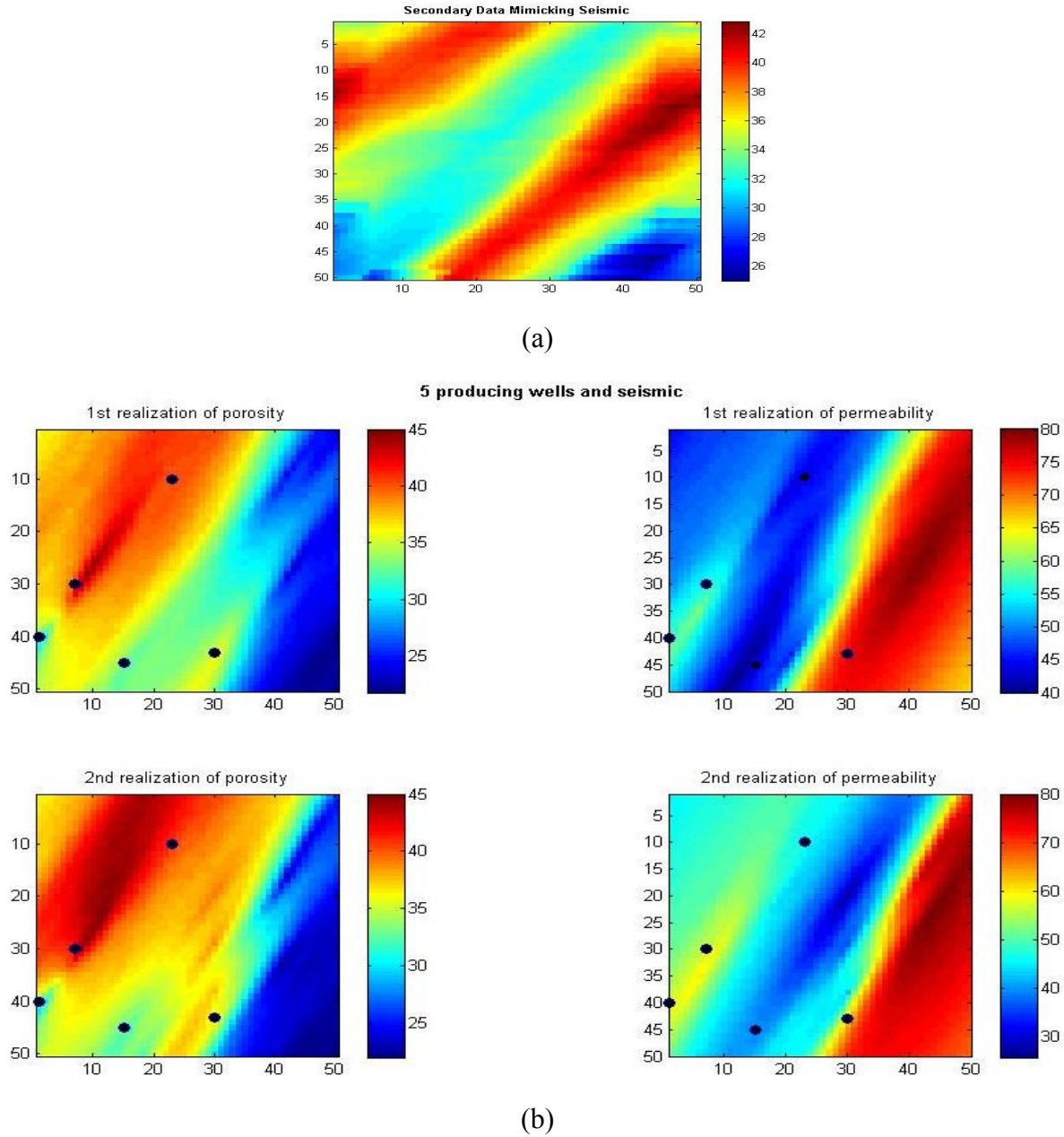


Figure 3-4: a) Secondary data mimicking seismic; b) Two realizations of each porosity (%) and permeability (md) model on left and right, respectively, after acquiring seismic

As a result of adding extra information in the form of seismic data to the base case, there is a significant change in new geological models for both porosity and permeability. Porosity models updated after acquiring seismic are much smoother compared to the porosity model for the base case or porosity models updated after acquiring data from exploratory well. There is also significant change in permeability models updated after acquiring seismic compared to the permeability model for the base case or permeability models updated after acquiring data from exploratory well.

FLOW MODELING

After obtaining static reservoir models for porosity and permeability from geological models, as shown in Figures 3-2 to 3-4, we can input them in a flow model to generate future oil production forecast for the entire life of the reservoir. The following fluid, reservoir and well parameters were assumed for the flow modeling.

Fluid Properties

$$\mu = 0.65 \text{ cp}$$

$$c_i = 2 \times 10^{-6} \text{ psi}^{-1}$$

$$B_o = 1.54 \text{ B/STB}$$

Reservoir and Well Properties

$$\text{Area} = 0.36 \text{ million acres}$$

$$\text{No. of production wells} = 5$$

$$(\text{Shape factor for square reservoir}) C_A = 31.62$$

$$\text{Skin} = 5$$

$$P_i = 3500 \text{ psi}$$

Figure 3-5 shows the oil-water two phase relative permeability curve.

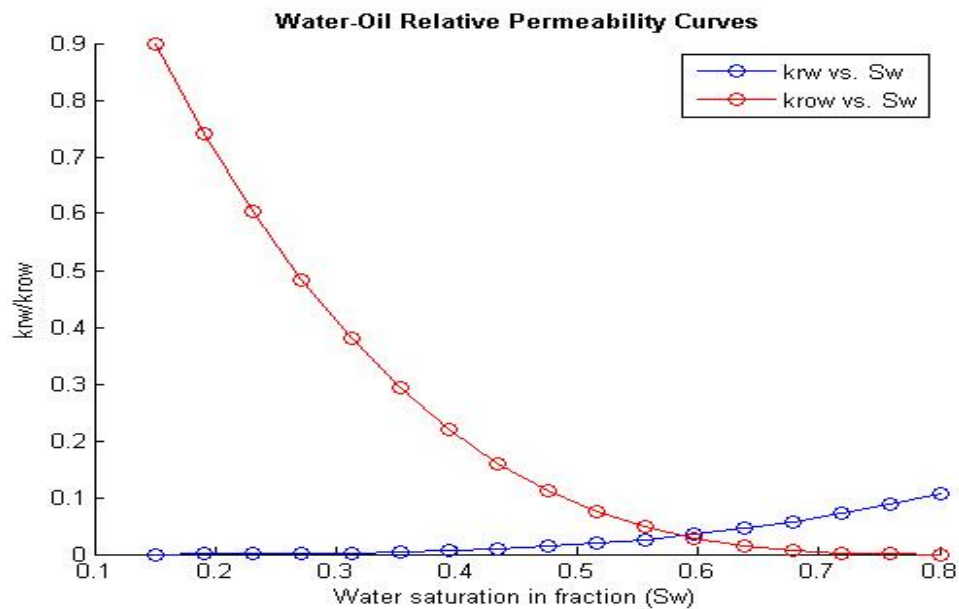


Figure 3-5: Two phase relative permeability curve for oil-water phase

We input these properties and multiple realizations of the static reservoir models in the CMG to get multiple responses from the flow model. Figure 3-6 shows one of the reservoir models setup in CMG gridded for flow with grid dimension of 50 x 50 x 1. There are five production wells which are producing hydrocarbons through natural water drive without the need of any injectors. The wells are located at the locations given in Table 3-1:

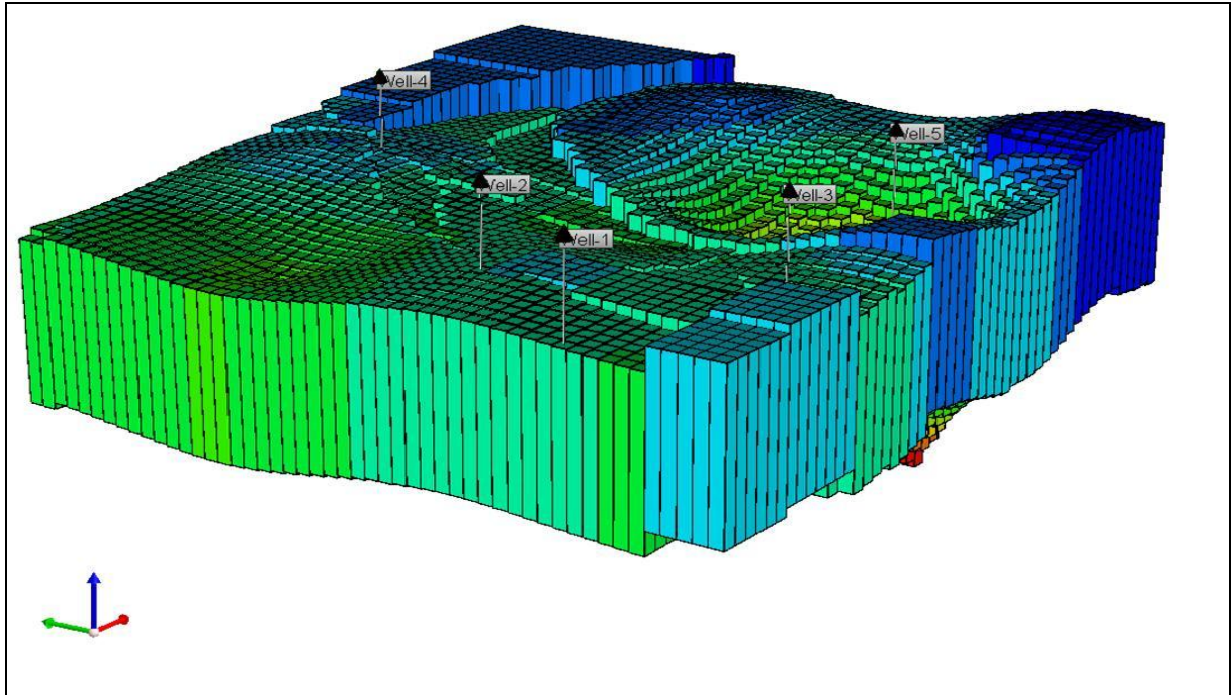


Figure 3-6: Reservoir model setup in CMG for simulations

Once we have the future hydrocarbon production rates from the reservoir for the above two scenarios, we can compare them with future hydrocarbon production rates for base case obtained using the information from only 5 producing wells.

Figure 3-7a, b, c illustrate the uncertainty in oil production rates (spread of production profiles from 100 realizations) from base case, after an exploratory well, and after seismic, respectively.

Figure 3-8 compares the uncertainty in oil production forecast for the base case with that after obtaining information from drilling an exploratory well. Figure 3-9 shows the comparison between the base case and the one obtained after conditioning the reservoir model to the additional secondary attribute in terms of seismic.

Prediction of Production Rate From Different Scenarios and its Uncertainty

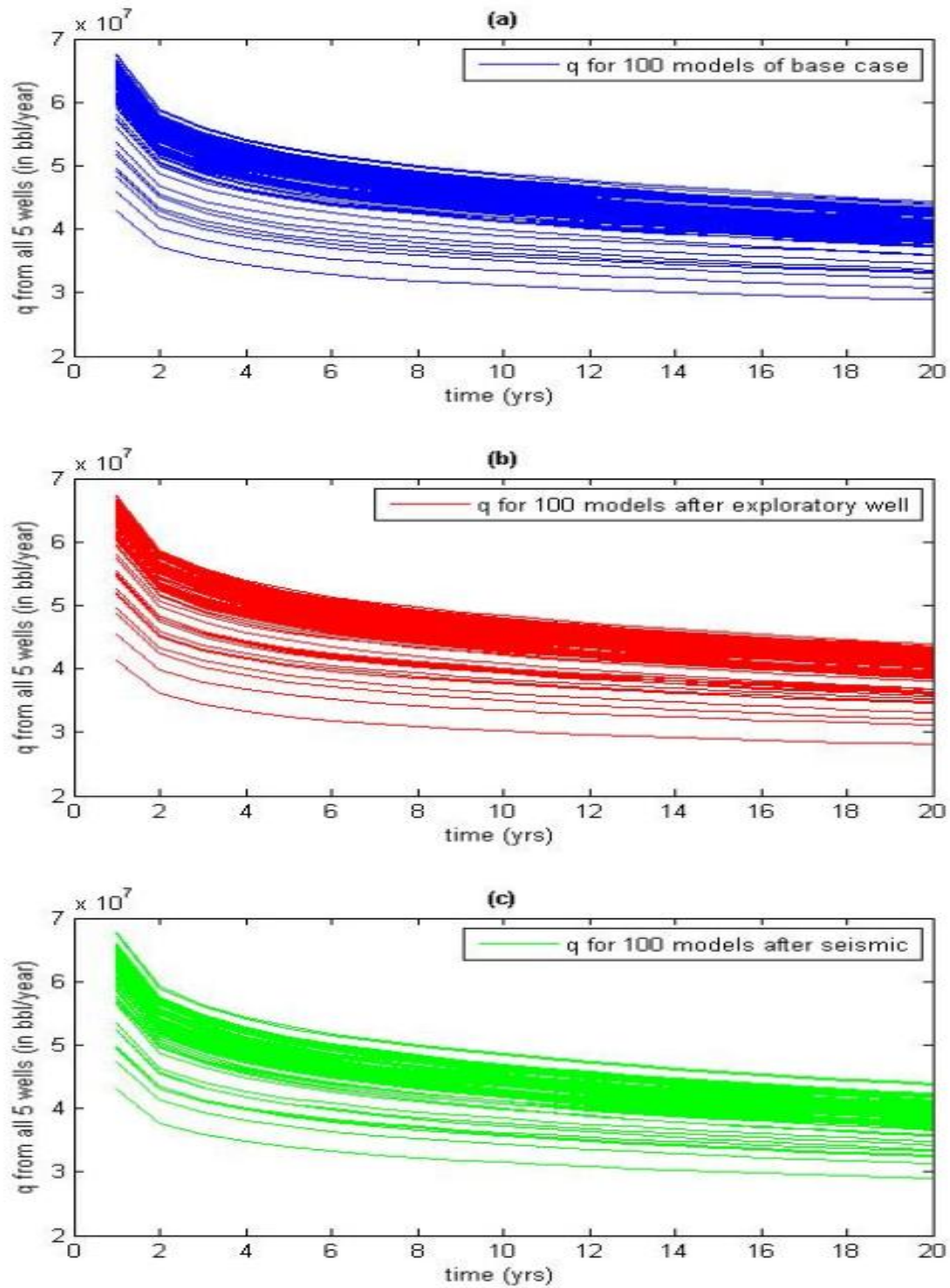


Figure 3-7: Uncertainty in production rate profiles for a) base case, b) after an exploratory well, c) after seismic

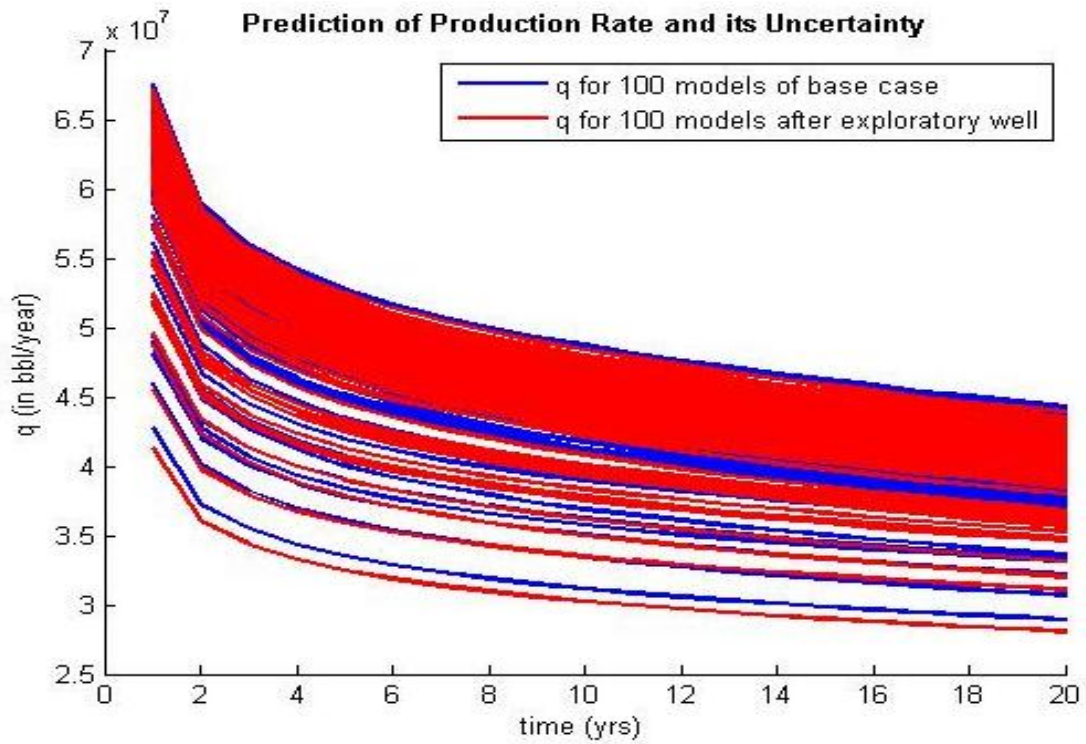


Figure 3-8: Change in uncertainty of oil production forecast after obtaining information from drilling an exploratory well.

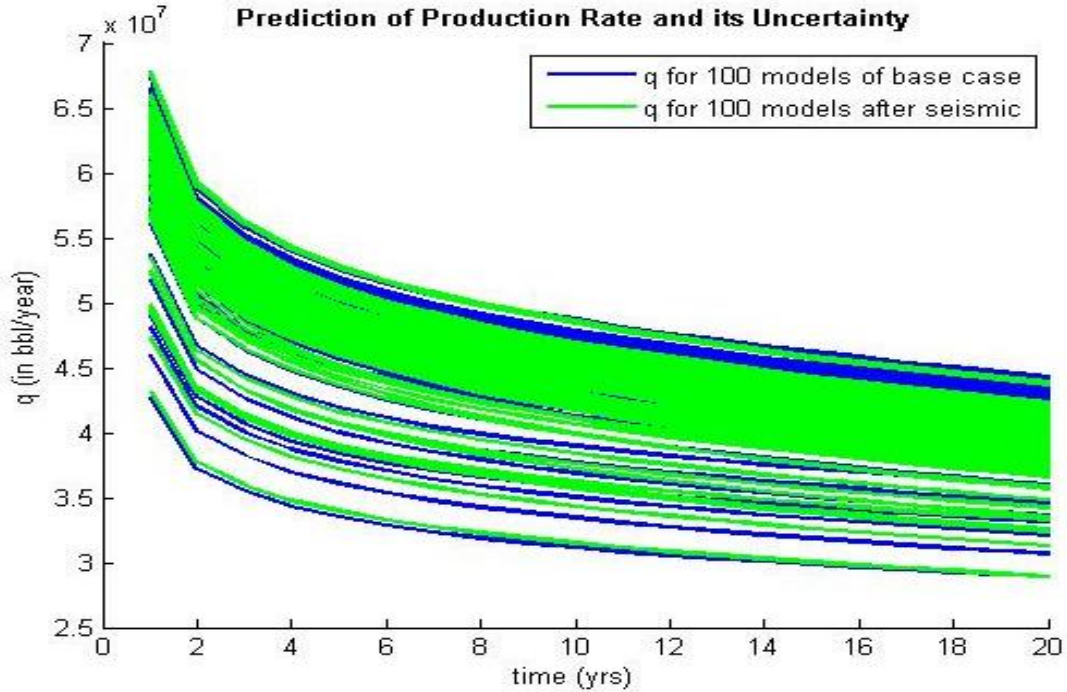


Figure 3-9: Change in uncertainty of oil production forecast after conditioning to secondary data mimicking seismic.

Figure 3-10 compares the uncertainty in oil production forecast for the base case with other two scenarios i.e. after obtaining information from drilling an exploratory well and acquiring a seismic.

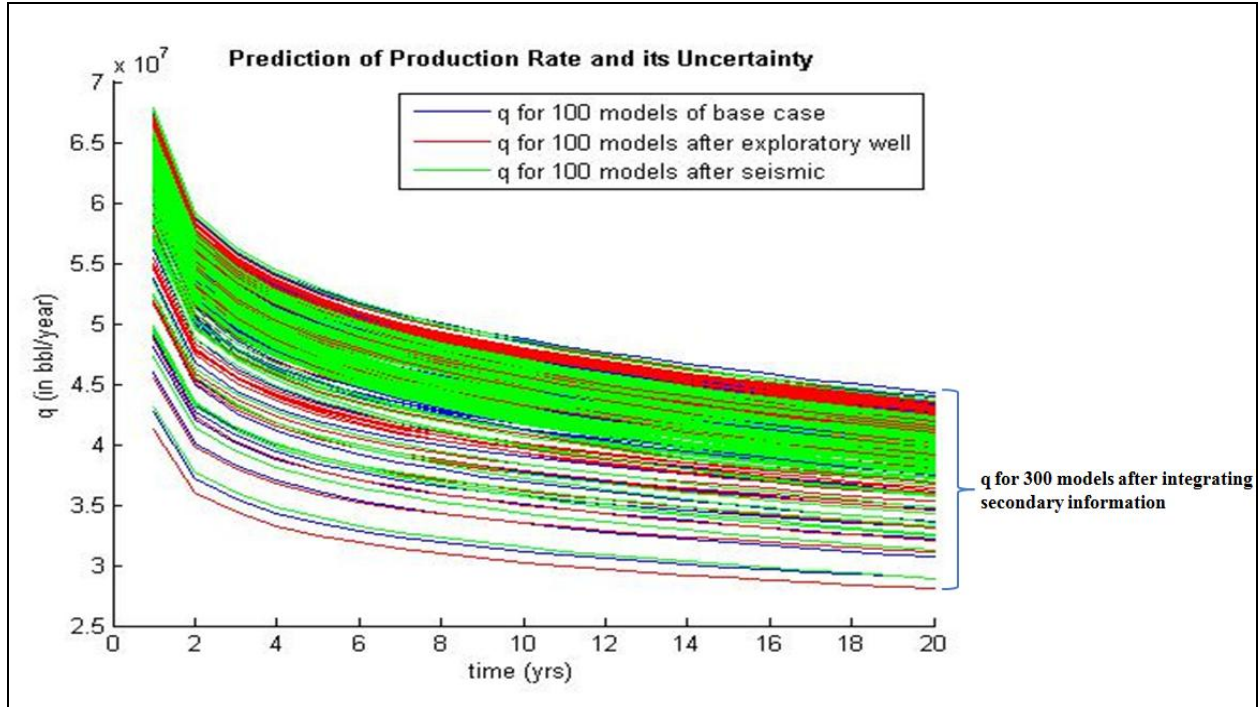


Figure 3-10: Change in uncertainty of oil production forecast

ROV ANALYSIS

ROV is a process of valuing a physical/real asset with real uncertainties. As opposed to NPV, ROV incorporates multi-domain uncertainties. The ROV can be estimated through a closed-form equation known as Black-Scholes equation. Black-Scholes model to compute ROV is given as:

$$C(S, t) = Se^{r(t)} N(d_1) - Xe^{r(t)} N(d_2) \quad \text{--- (3.1)}$$

where,

$$C(S, t) = \text{ROV}$$

$$d_1 = \frac{\ln\left(\frac{S}{X}\right) + \left(r + \frac{\sigma^2}{2}\right)(T - t)}{\sigma\sqrt{T - t}}, \text{ and } d_2 = d_1 - \sigma\sqrt{T - t}$$

$$S = F(t)$$

$$X = \text{capex}$$

$$r = 12\%$$

$$\sigma = \text{Project Volatility}$$

$$T = \text{Time period of maturity}$$

Once we determine the future oil production rates as illustrated in previous section, the following equation is used to obtain forecast of future cash flows for each realization of $q(t)$:

$$F(t) = (q(t) \times p) - \text{opex} \quad \text{--- (3.2)}$$

In equation (3.2) production rate is the only variable that is allowed to vary with time. Oil price can be made to vary by computing time varying oil prices using the Ornstein and Uhlenbeck mean reverting model; however, oil prices are kept constant at \$ 30/barrel to have consistent comparison of the reservoir economic performance by different geological models.

These future cash flows will be used to compute the project volatility through the method explained in Chapter 2. This project volatility is one of the most critical parameter which is used as input in the real options model. We calculated the project volatility as following:

$$PV(t) = F(t) \times DV(t)$$

$$G = \ln \left[\frac{\sum_{i=1}^n PV_i}{\sum_{i=0}^n PV_i} \right]$$

$$\Rightarrow \sigma = std(G)$$

where,

PV_i = Present value at i^{th} year

$std()$ = Standard deviation

σ = Project Volatility

Figure 3-11 shows the time varying project volatility's magnitude decreasing with time. The reason for the decrease in project volatility with time is because there is more prior data of the reservoir's economic performance (in terms of DCF).

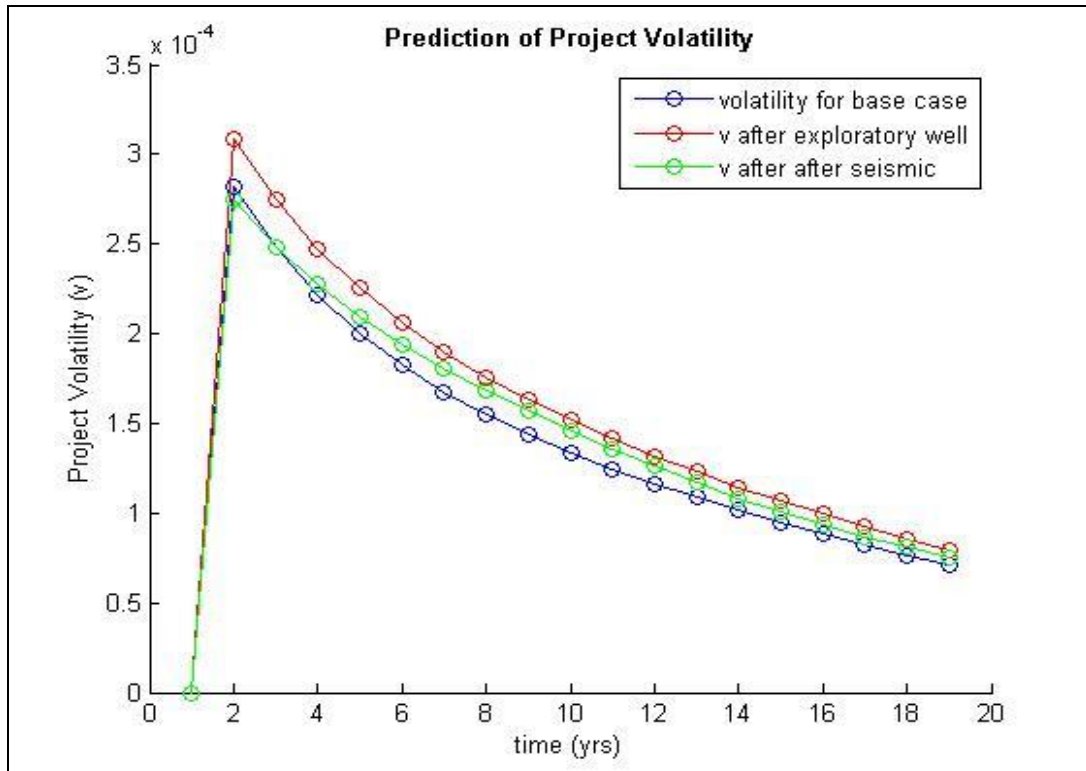


Figure 3-11: Variation of project volatility with time during the life of the reservoir

ROV can be obtained on substituting values for the above variables in equation (3.1). The above calculation is repeated for all the realizations to come up with the uncertainty in the ROV.

RESULTS AND DISCUSSIONS

The cumulative sum of present values gives Net Present Value (or cumulative DCF) which is shown in Figure 3-12. Figure 3-12 compares the uncertainty in cumulative DCF forecast for the base case with that after obtaining information from drilling an exploratory well or acquiring seismic.

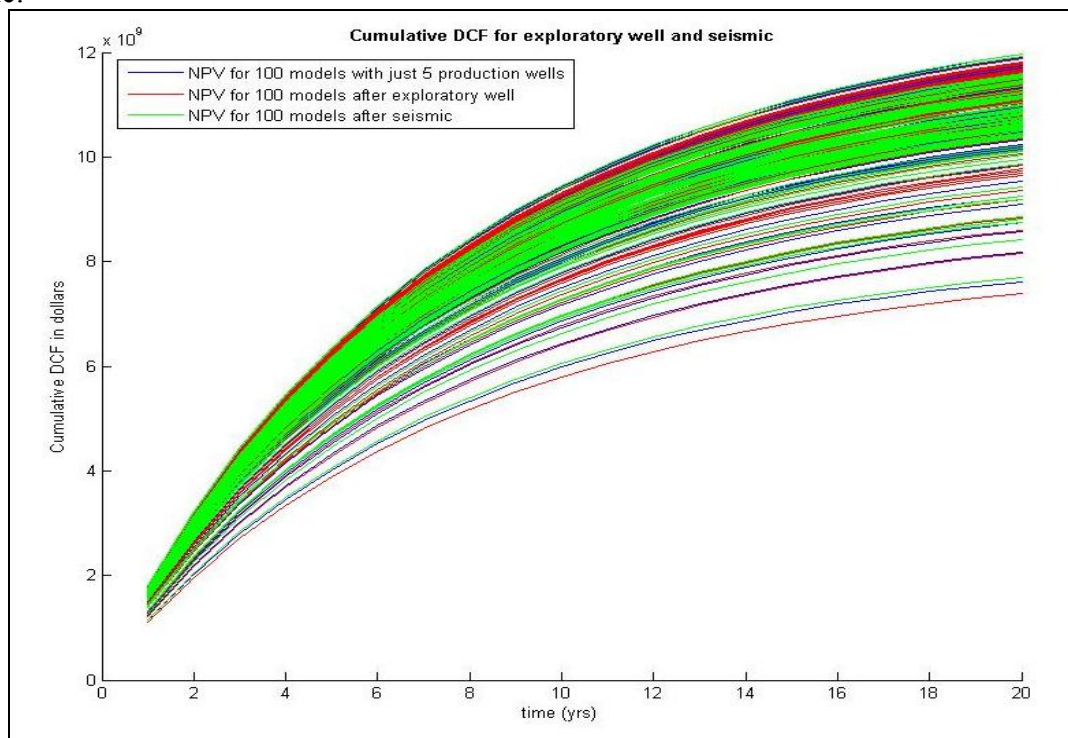


Figure 3-12: Comparison of uncertainty in cumulative DCF for scenarios 1 and 2 with base case

Figure 3-13 compares the uncertainty in ROV for the base case with other two scenarios i.e. after obtaining information from drilling an exploratory well and after conditioning to the secondary

information. Figure 3-14 compares the uncertainty in deterministic valuation (in terms of PV) for the base case with the two data scenarios

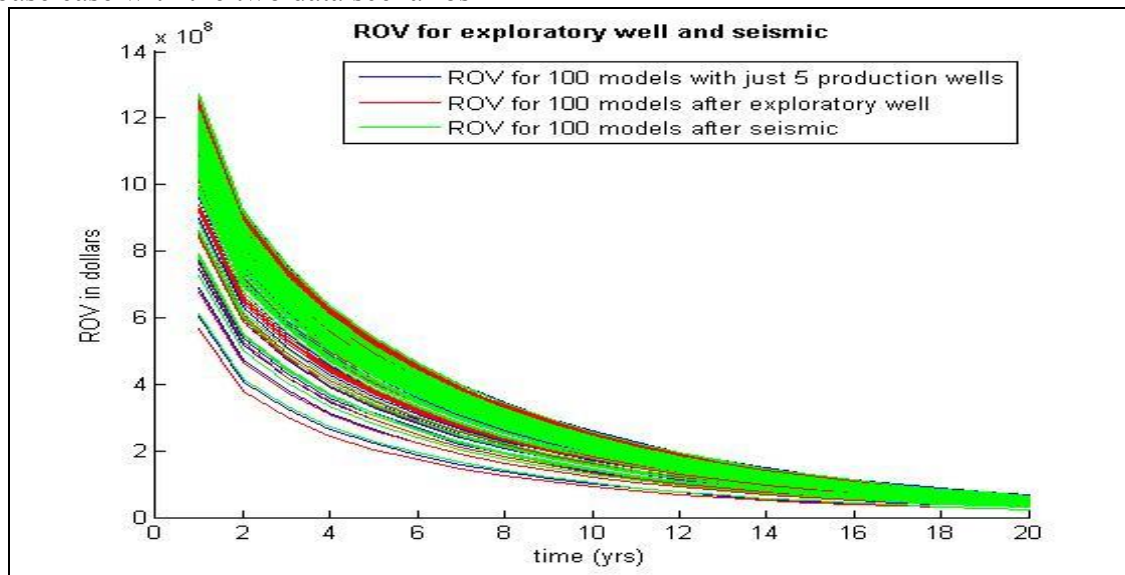


Figure 3-13: Uncertainty in ROV due to uncertainty in production forecasts

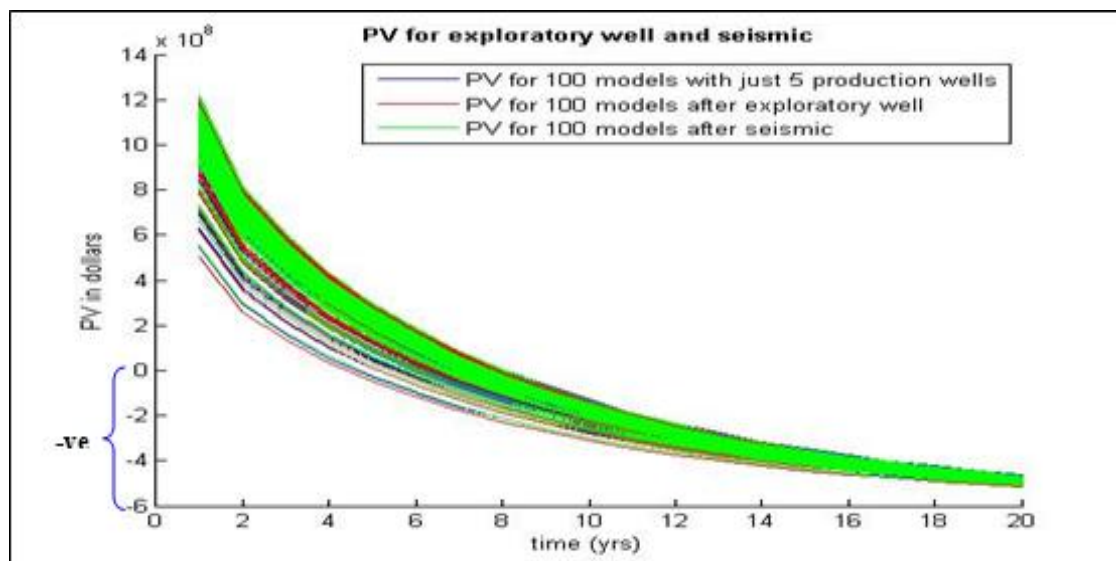


Figure 3-14: Uncertainty in PV due to uncertainty in production forecasts

We can see in Figures 3-13 and 3-14 that the forecast by DCF using PV changes drastically when compared with the forecast by ROV after 2-3 years of production. ROV shows that the option value decrease with time as the uncertainty regarding reservoir performance diminishes.

Comparing the profile of the ROV to that of PV, the ROV analysis preserves the uncertainty in reservoir characteristics till the very end, while the uncertainty in present value decreases practically to zero at the end time

The results further show that both schemes for acquiring additional reservoir related information result in similar reduction in prior uncertainty. The added cost of drilling an additional well or acquiring secondary data causes the DCF value to decrease below zero at later times. However, the ROV by construction, does not dip below zero (option is not exercised if the PV is negative). Even though the ROV is positive for all scenarios (base case, drill an exploratory well, or acquire seismic), there is insignificant monetary gain by acquiring additional reservoir related information over the base case. Therefore, it would not be a judicious decision to invest in either of the scheme for acquiring additional reservoir related information.

Chapter 4: Assessing Economic Implications of Reservoir Modeling Decisions

INTRODUCTION

This chapter presents a method for:

- Using real option valuation to assess the economic forecast of reservoir performance using geological models of varying levels of complexity.
- Using real option valuation to assess the economic forecast of reservoir performance using flow models of varying levels of complexity.

For the first objective, we compared the uncertainty in reservoir's long term performance obtained by geological models with varying levels of complexity. The results suggest that it may be appropriate to use simpler geological models for the forecast of volumetric flow rate uncertainty. We see that the economics in terms of real option value obtained from a simple geological model is not significantly different from that of a complex geological model. Similar results also hold true with DCF analysis.

For the second objective of our research, we compared the uncertainty in reservoir's long term performance obtained by decline curve analysis and a full physics commercial simulator. The results suggest that using decline curve as a flow model predicts the long term production rate fairly accurately and for the case studied, is as good as using a full physics commercial simulator.

These two studies help answer the question – how much detail in reservoir and flow models are necessary if the end objective is to obtain realistic assessment of net economic risk (which would be used to make correct decisions)?

ASSESSING THE IMPACT OF DETAILED GEOLOGICAL MODELING

Research Approach

For geostatistical modeling, we used well established stochastic simulation algorithms like sequential Gaussian Simulation SGSIM (Deutsch & Journel 1997), cosimulation COSGSIM (Xu et al. 1992), indicator simulation SISIM (Zhu & Journel 1993) and multiple point simulation SNESIM (Strabelle 2000). For these techniques semivariogram modeling was performed or in the case of SNESIM, provided a training image. Geostatistical modeling gives us multiple realizations of porosity and permeability models.

For flow modeling we used the CMG simulator (CMG-IMEX 2009) and decline curve analysis (Arps 1945) to obtain production rates. Geostatistical modeling followed by flow modeling is essential for uncertainty assessment of reservoir performance. Finally for economic analysis we use a deterministic discounted cash flow (DCF) technique, as well as real options valuation (ROV) that use the uncertainty models explicitly.

Description of the Problem

The reference truth model for the reservoir has a grid dimension of $200 \times 200 \times 1$. The reference truth model is a truly known model for the reservoir which is used as reference/base case with predicted models. This reservoir has 5 production wells. We use different geological models to

map porosity and permeability of the reservoir. Though all these techniques yield reservoir property variations over a 3D grid; however, we use these models selectively based on the type of reservoir information we want simulated or honored.

Some of the commonly used geological models include SGSIM, SISIM and SNESIM, in the order of increasing complexity. Complexity is in terms of the amount and type of reservoir information needed to generate the porosity and permeability maps as illustrated in next paragraph; the more information a model requires, the more complex it is. Nevertheless, we must give a certain minimum amount of information to all these 3 models, which includes conditioning data to be honored. Other than this information each model requires more information based on the level of complexity. SGSIM and SISIM are semivariogram-based simulations techniques, while SNESIM is a multiple-point simulation technique. Semivariogram-based techniques are less complex than multiple-point technique. Semivariogram is a measure of variability between pairs of locations in the reservoir. It can be typically inferred on the basis of the available “hard” data. Multiple point based techniques such as SNESIM on the other hand require inference of joint variability between several locations (more than two) in the reservoir. Typically, inference of multiple point statistics require exhaustive training data, a spatial template and a sophisticated scheme for scanning and saving statistics and subsequently retrieving the same when performing conditional simulation (Eskandari, 2009). This contributes to the complexity of the algorithm. The amount and type of data that each of these models require, in an increasing order of complexities, are:

SGSIM: Conditioning Data + Semivariogram Model

SISIM: Conditioning Data + User specified indicator threshold values + Marginal Probabilities + Indicator semivariogram Model for each threshold (or median IK)

SNESIM details: Training Image + # of Categories + Target Marginal Distribution + Conditioning Data

Static Reservoir Modeling

Reference Model

As explained above, we must have at least the conditioning data to develop the porosity and permeability distributions. We have this data sampled from a reference model shown in Figure 4-1. The reservoir is modeled on a $200 \times 200 \times 1$ grid scale. There are 5 production wells and the hard data of porosity and permeability from those 5 wells are sampled from the reference as shown in Table 4-1:

Table 4-1: Hard data of porosity and permeability from 5 reference wells

X	Y	Z	Porosity (%)	Permeability (md)
170	150	0	29	521
130	75	0	19	4
70	10	0	17	8
40	100	0	29	529
20	180	0	19	8

Shown in Figure 4-1 is the reference model. Porosity varies from 18% to 33 % and permeability varies from 0.5 md to 1958 md.

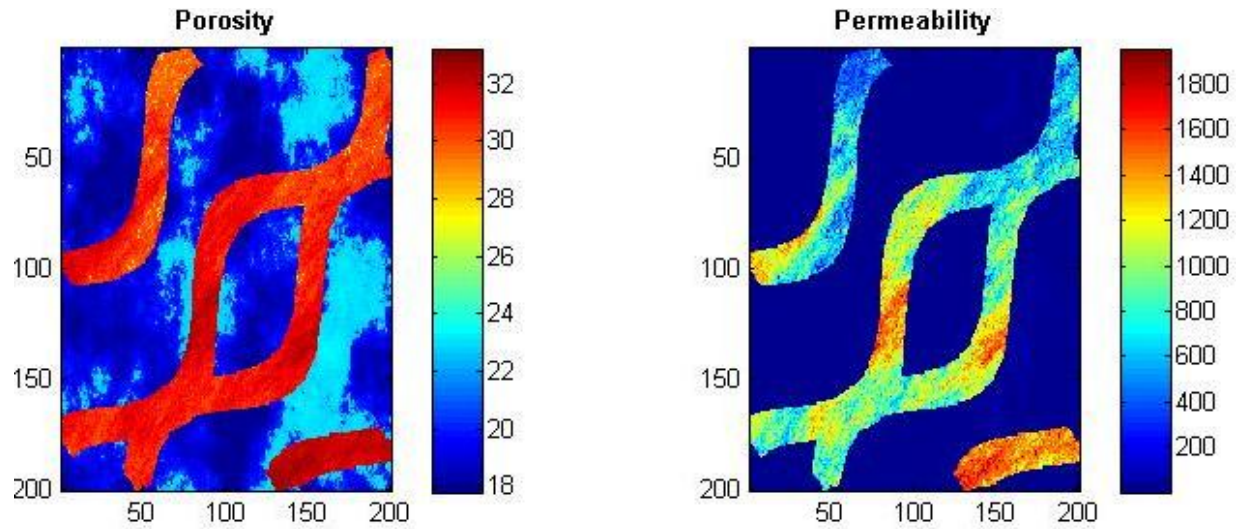


Figure 4-1: Reference Model for porosity (left; in %) and permeability (right; in md)

Sample data of porosity and permeability from reference truth were used to develop semivariogram models for porosity and permeability, respectively. Because information along 5 wells cannot give us a model for the spatial variability of porosity or permeability, the semivariogram model is developed using 105 sampled data from the reference truth model, which includes the data from 5 wells locations as well. Shown in Figures 4-2 is an isotropic model fit (black) for experimental semivariograms (red) of porosity in various directions:

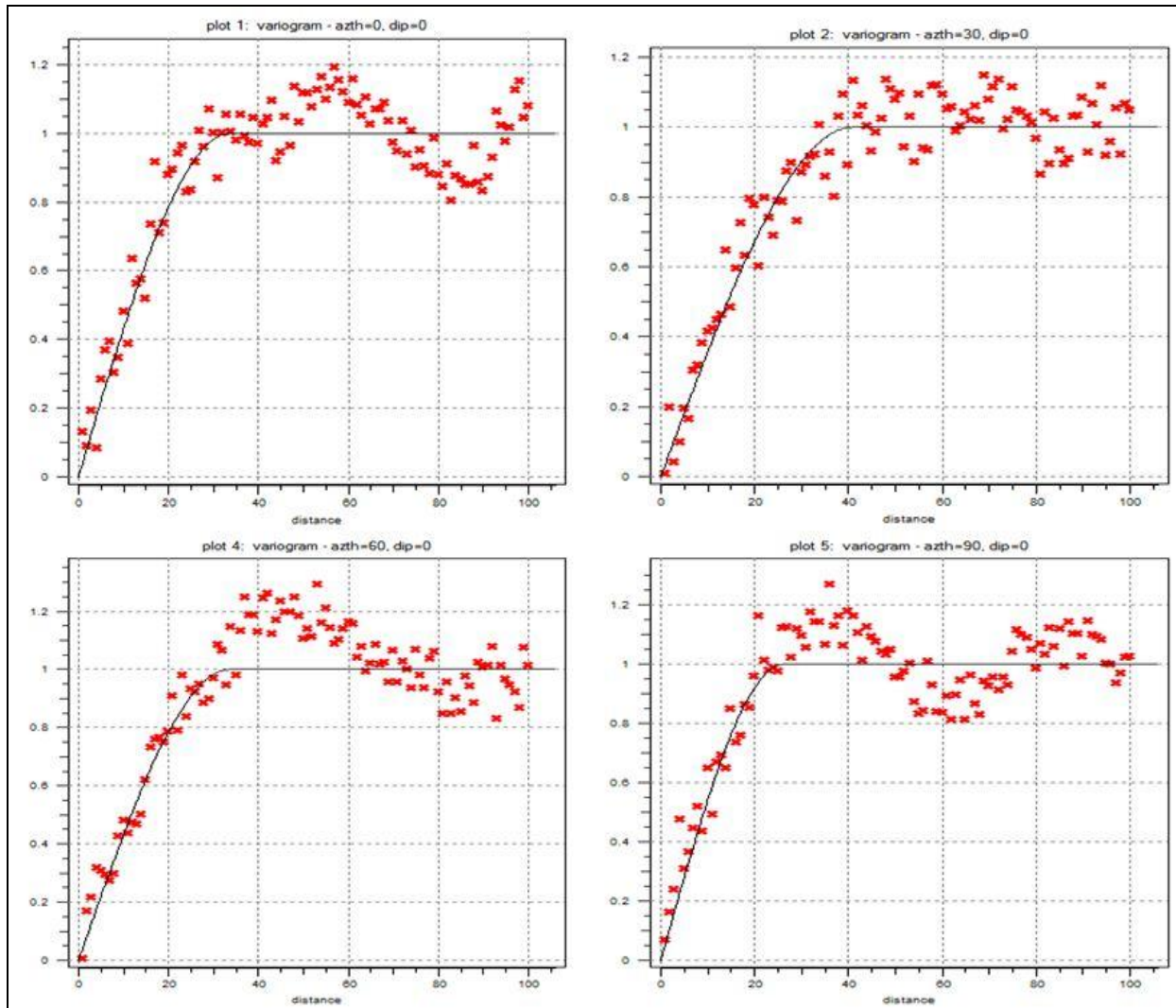


Figure 4-2: Isotropic model fit (black) for experimental semivariograms (red) of porosity in four directions

The isotropic model fitted to experimental semivariograms of porosity is:

Number of Structures = 1

Type = Spherical

Nugget Effect = 0

Max., medium, and min. range = 41, 24, and 24 units

Azimuth = 30

Dip = 0

Rake = 0

Similarly, shown in Figures 4-3 is an isotropic model fit (black) for experimental semivariograms (red) of permeability in various directions:

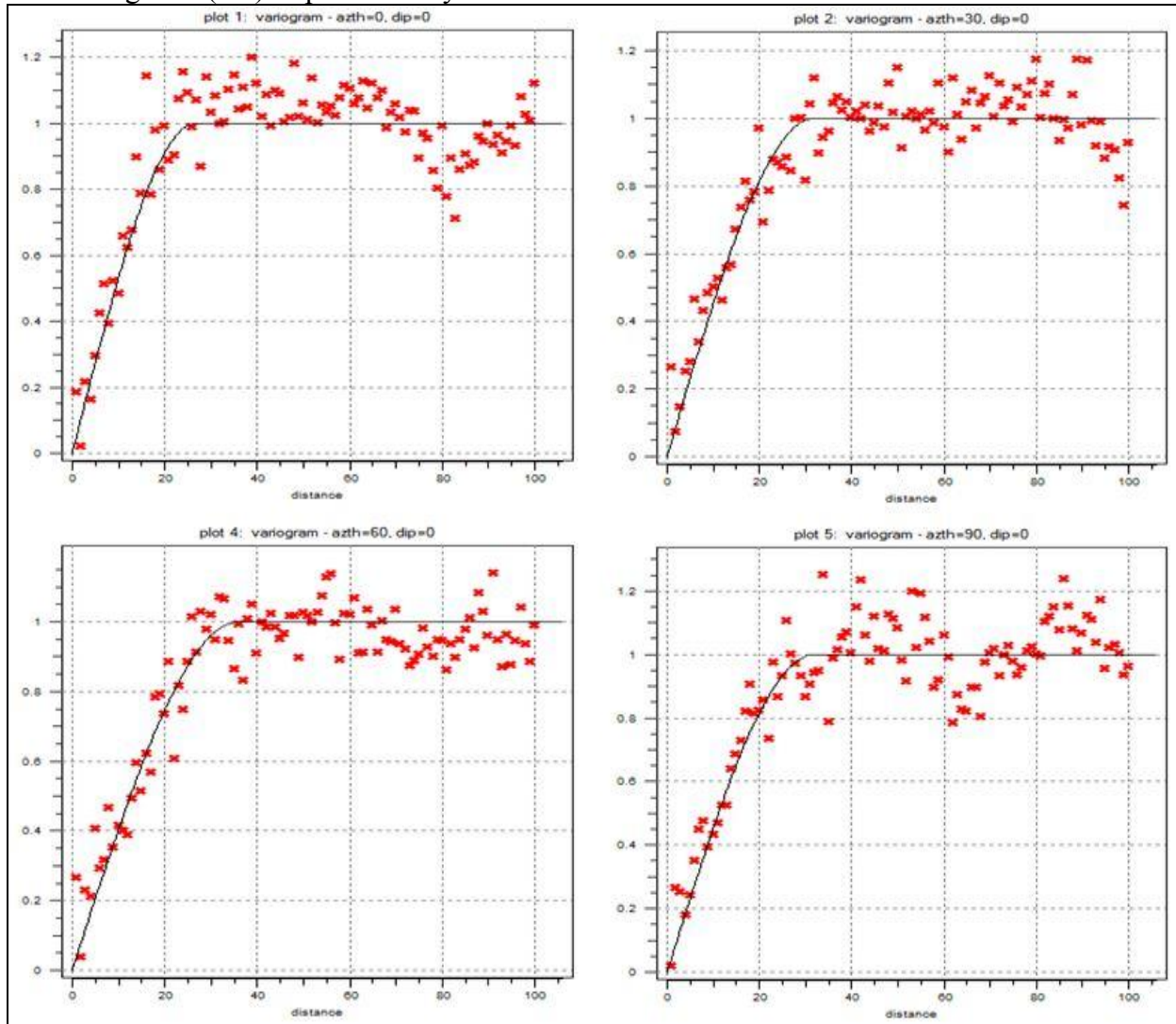


Figure 4-3: Isotropic model fit (black) for experimental semivariograms (red) of permeability in various directions

An isotropic model fitted to experimental normalized semivariograms of permeability is:

Number of Structures = 1

Type = Spherical

Nugget Effect = 0

Max., medium, and min. range = 36, 25, and 20 units

Azimuth = 60

Dip = 0

Rake = 0

The above two semivariogram models for porosity and permeability are used in both SGSIM and SISIM geological models. The median indicator kriging option was selected for the indicator simulation.

SGSIM Model:

We use the hard data of porosity and permeability sampled from the dataset of the reference truth model. Using the conditioning hard data and semivariogram model as input in the SGSIM program, 100 realizations each of porosity and permeability are generated.

Figure 4-4 show one realization each of porosity and permeability obtained using the SGSIM program. Porosity varies from 0.5 % to 30 %, and permeability varies from 0.5 md to 530 md.

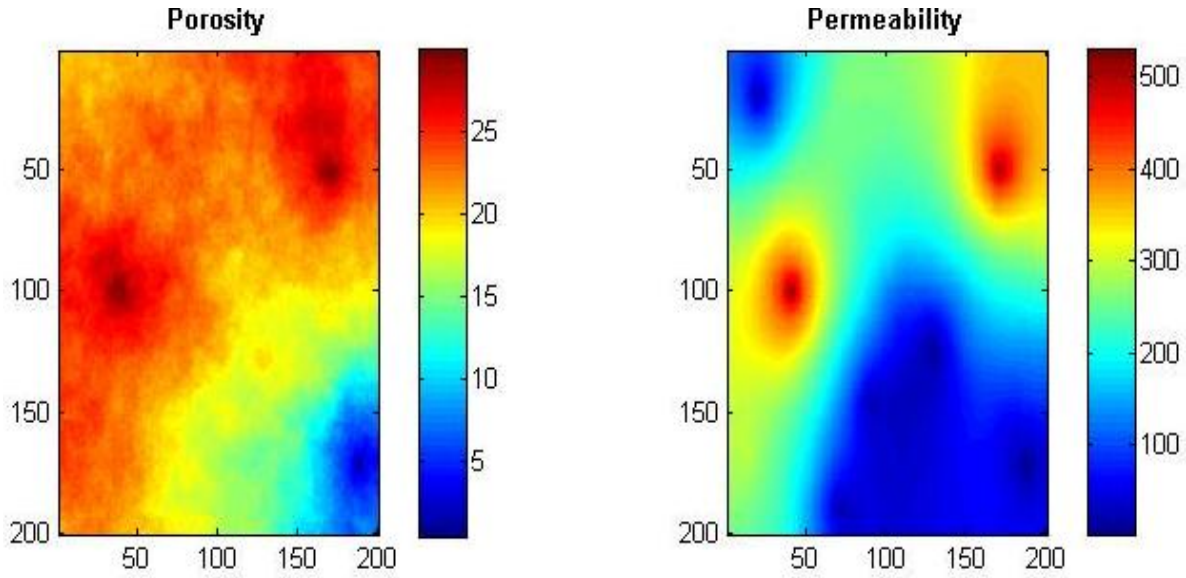


Figure 4-4: Maps from SGSIM

SISIM Model:

We use the hard data of porosity and permeability sampled at 5 wells from the reference. The three threshold values for permeability and porosity are assumed to be [500 1000 1900] and [10 20 40], respectively, with corresponding marginal probabilities of [0.2 0.6 1] and [0.1 0.4 1], respectively, which are based on the reference truth data. These threshold values along with their corresponding marginal probabilities are used to yield a discrete estimate of the conditional cumulative distribution function at the estimation locations. The conditioning hard data, the number of categories along with their marginal probabilities, and semivariogram model are input in the SISIM program, 100 realizations each of porosity and permeability are generated.

Figure 4-5 show one realization each of porosity and permeability obtained using the SISIM. Porosity varies from about 8% to 34 %, and permeability varies from about 4 md to 1900 md.

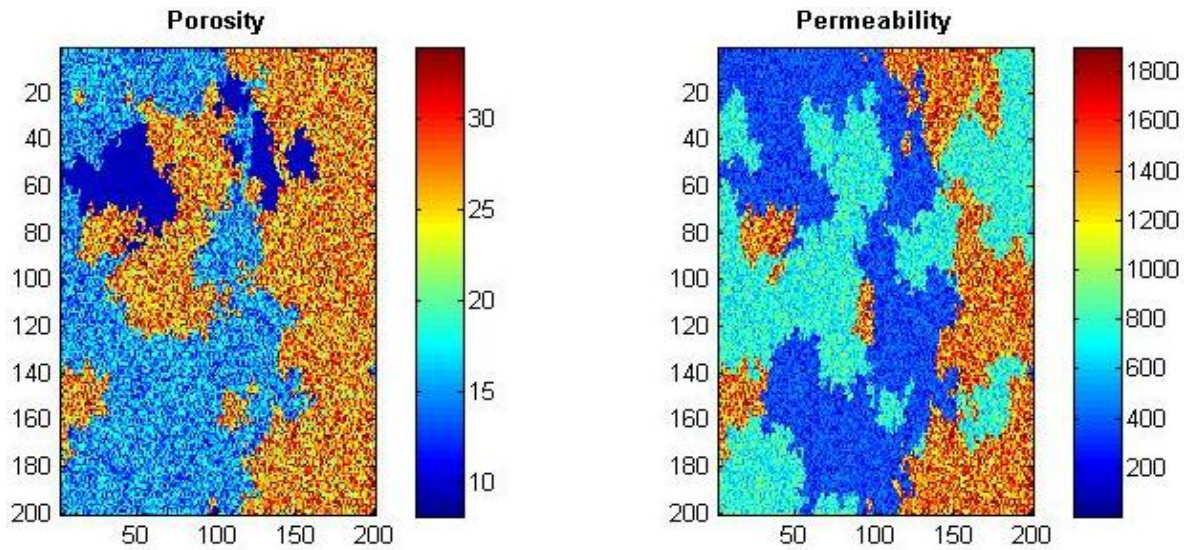


Figure 4-5: Maps from SISIM

SNESIM Model:

A channel model with characteristics similar to the reference model was developed and used as the training image (TI) for inferring multiple point statistics (Figure 4-6). The statistics inferred from the TI was used in conjunction with the same 5 conditioning data shown in Table 4-2. In the first step channel simulation using SNESIM, the number of facies categories modeled were 2 with their corresponding marginal probabilities specified as 0.685 and 0.315, respectively. The data at the conditioning data locations have to be first transformed to the two categories as shown in Table 4-2:

Table 4-2: Conditioning data at well locations in form of two facies

X	Y	Z	TI Hard Data
170	150	0	1
130	75	0	0
70	10	0	0
40	100	0	1
20	180	0	0

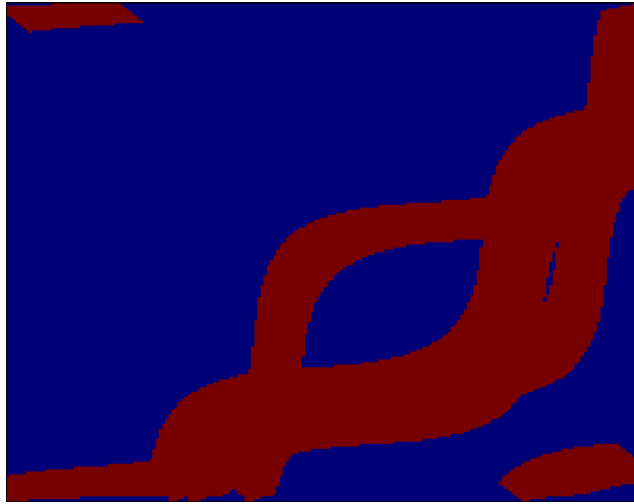


Figure 4-6: TI used as input in the SNESIM program

Using the statistics inferred from the TI, threshold values along with their marginal distributions, and conditioning hard data as input to the SNESIM program, we get 100 realizations of the output in form of 2 facies only i.e. 0 and 1, the same number of facies that our input TI contained. After generating the output in the form of 2 facies, we assign the permeability of the mudstone and channel to each output of 0 and 1 facies, respectively. These permeability values were obtained by performing Gaussian simulations for each facies and finally cutting and pasting values depending on the facies category simulated using SNESIM. Because our conjecture is that the facies geometry has a primary control on the flow characteristics of the models, only one realization of permeability per facies was generated and used with multiple realizations of the facies model generated using SNESIM. This is how the gridded maps of permeability are obtained. Porosity is obtained from the empirical relation between permeability and porosity for the same field.

Figure 4-7 show one realization each of porosity and permeability obtained using the SNESIM program. Porosity varies from 18 % to 33 %, and permeability varies from 0.5 md to 1973 md.

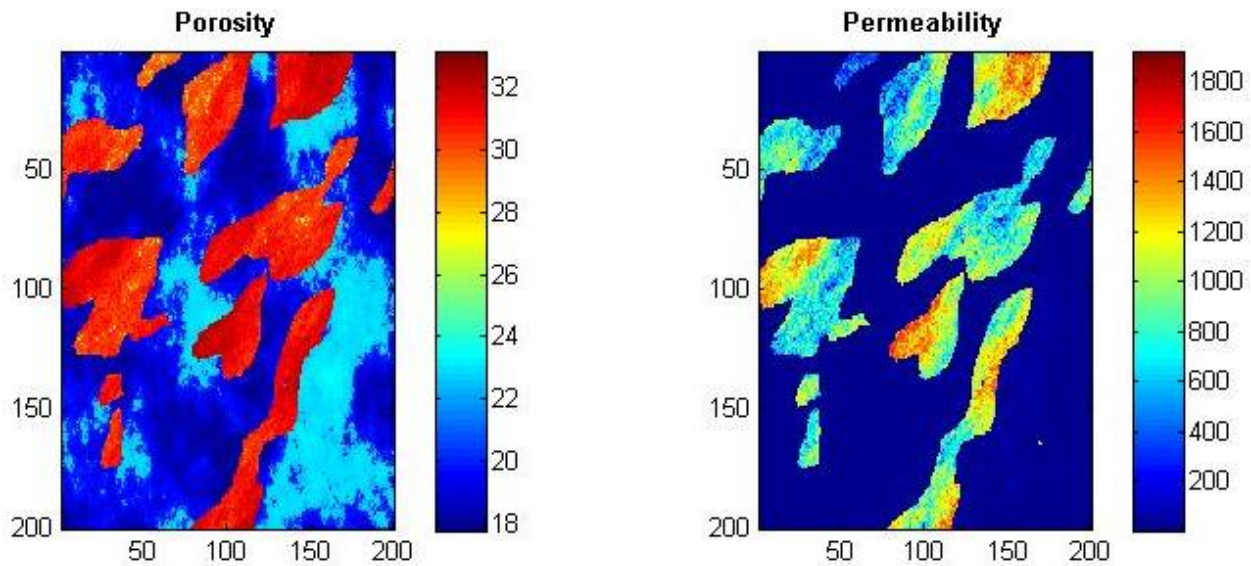


Figure 4-7: Maps from SNESIM

We developed the porosity and permeability maps using different geological models in Figure 4-4 through 4-7. Economic forecast from reference model is used to compare economic forecasts from these different geological models. The level of details and information required increases from SGSIM to SNESIM.

Average Maps for SGSIM, SISIM and SNESIM

Figure 4-8 shows the average variability for SGSIM, SISM and SNESIM maps (porosity in % and permeability in md) over the suite of 100 realizations.

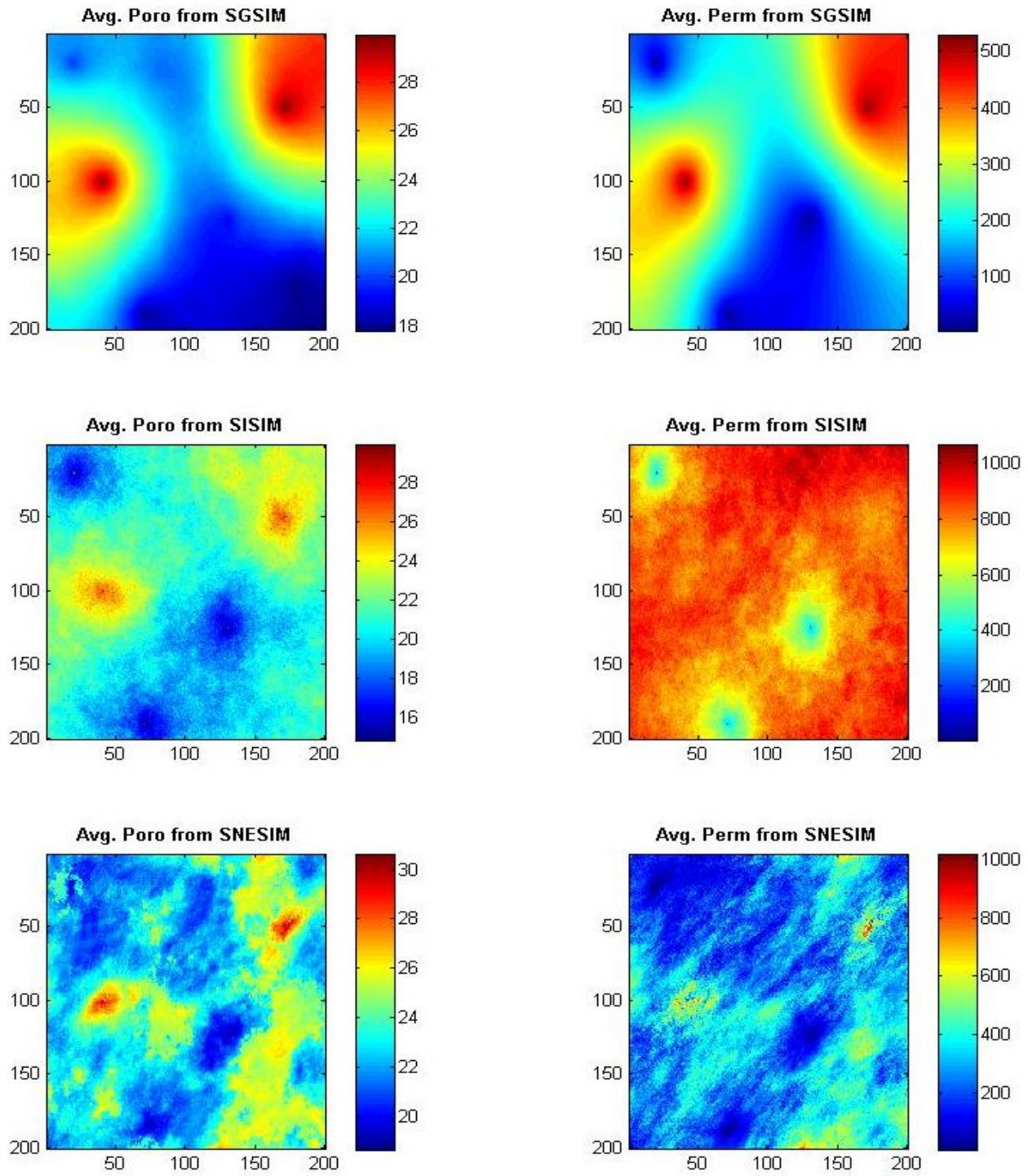


Figure 4-8: Average of SGSIM (top), SISIM (middle) and SNESIM (bottom) maps over the suite of 100 realizations

Flow Modeling

After obtaining static reservoir models for porosity and permeability, we can input them in a flow model to generate future oil production forecast. The following fluid, reservoir and well parameters were assumed for the flow modeling.

Fluid Properties

$$\mu = 0.65 \text{ cp}$$

$$c_i = 2 \times 10^{-6} \text{ psi}^{-1}$$

$$B_o = 1.54 \text{ B / STB}$$

Reservoir and Well Properties

$$\text{Area} = 5.74 \text{ million acres}$$

$$\text{No. of production wells} = 5$$

$$(\text{Shape factor for square reservoir}) C_A = 31.62$$

$$\text{Skin} = 5$$

$$P_i = 3500 \text{ psi}$$

Figure 4-9 shows the oil-water two phase relative permeability curve.

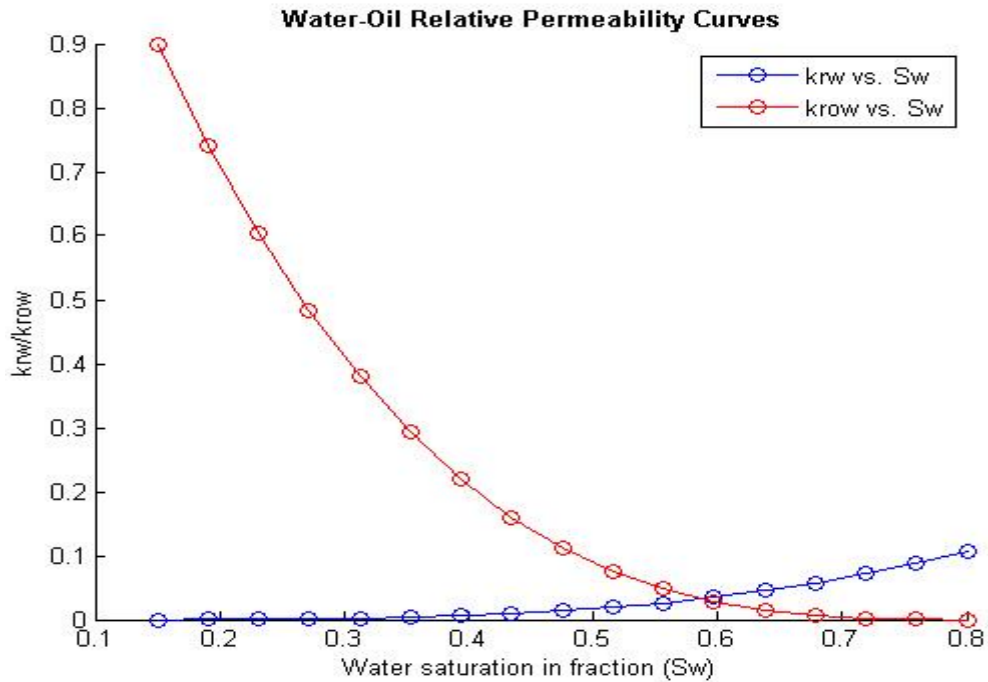


Figure 4-9: Two phase oil-water relative permeability curve assumed for the flow simulations

We input these properties and multiple realizations of the static reservoir models in the CMG to get well flow responses corresponding to each realization. Figure 4-10 shows one of the reservoir models gridded for flow. There are five production wells which are assumed to produce hydrocarbons through natural water drive without any injectors. The wells are located at the locations given in Table 4-1:

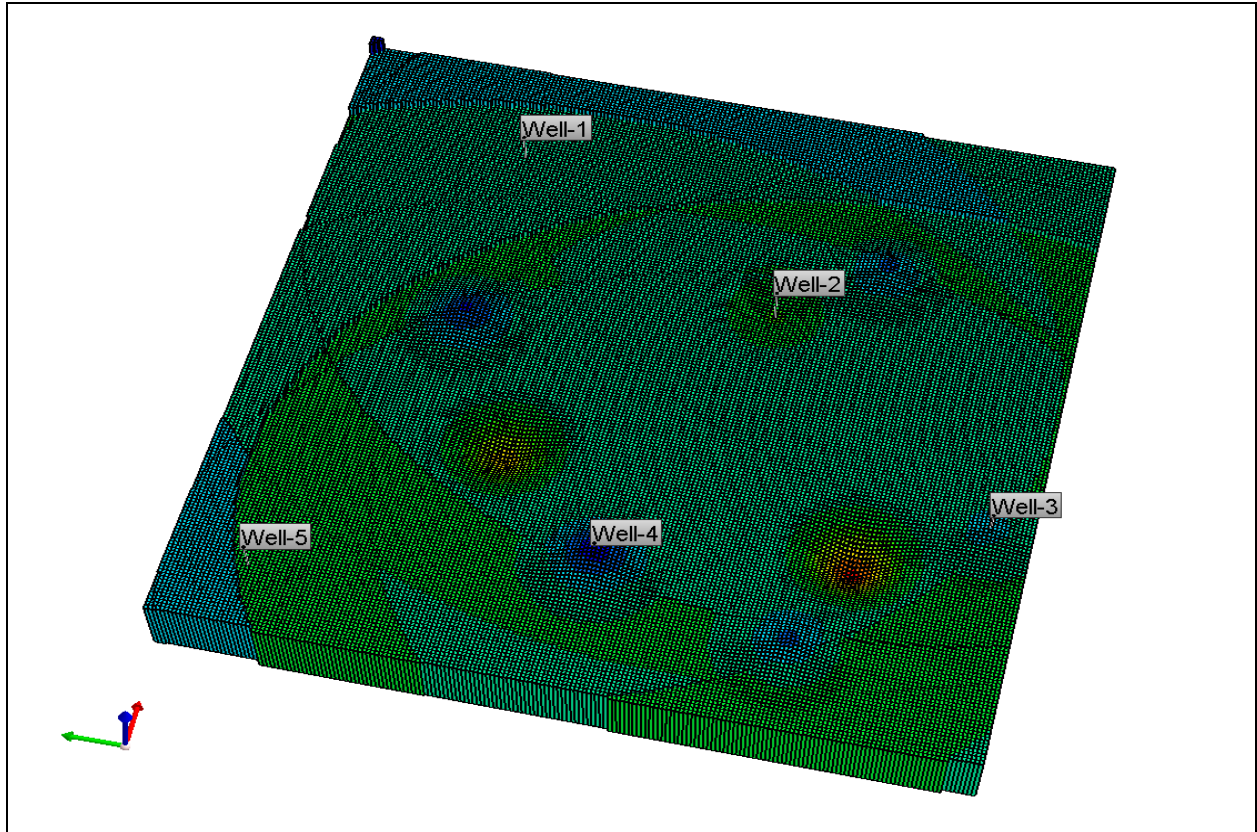


Figure 4-10: Reservoir model setup in CMG for simulations

Once we have the future hydrocarbon production rates from the reservoir for different geological models, we can compare them with future hydrocarbon production rates obtained using the reference model.

Figure 4-11 compares the uncertainty in oil production forecast obtained using SGSIM geological model with the oil production forecast obtained using the reference model. Figures 4-12 and 4-13 show the uncertainty in oil production forecast obtained using SISIM and SNESIM geological models with the reference model, respectively.

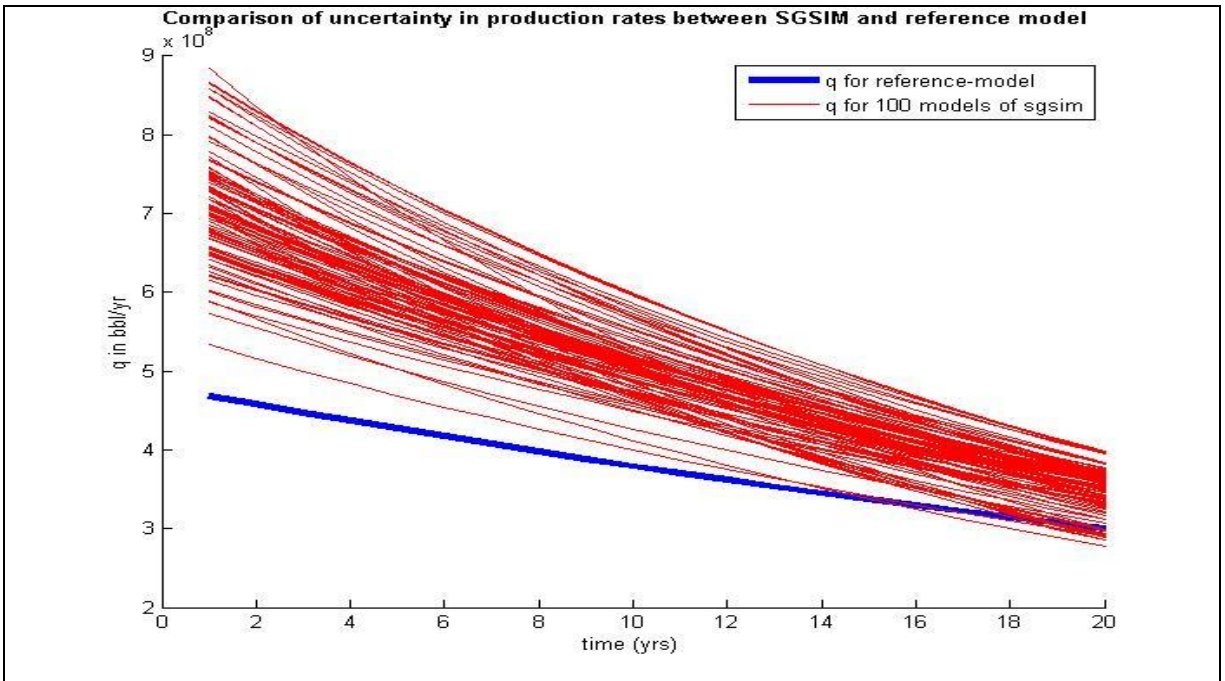


Figure 4-11: Uncertainty in oil production forecast obtained using SGSIM

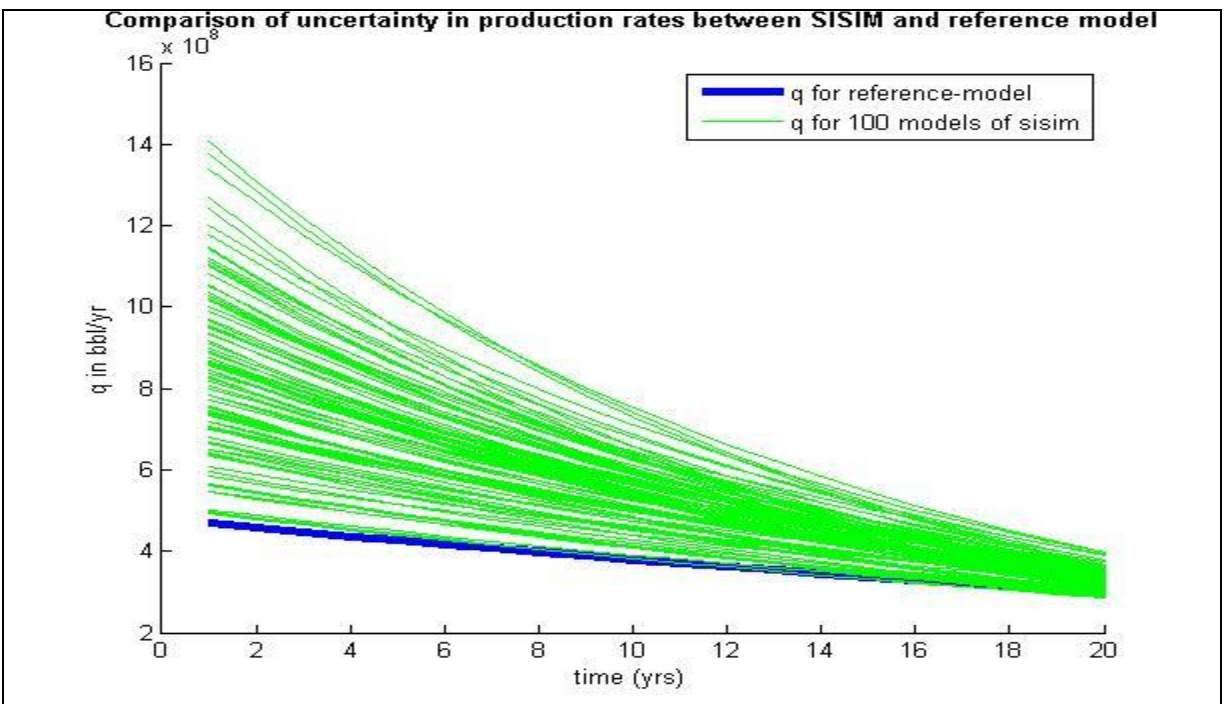


Figure 4-12: Uncertainty in oil production forecast obtained using SISIM

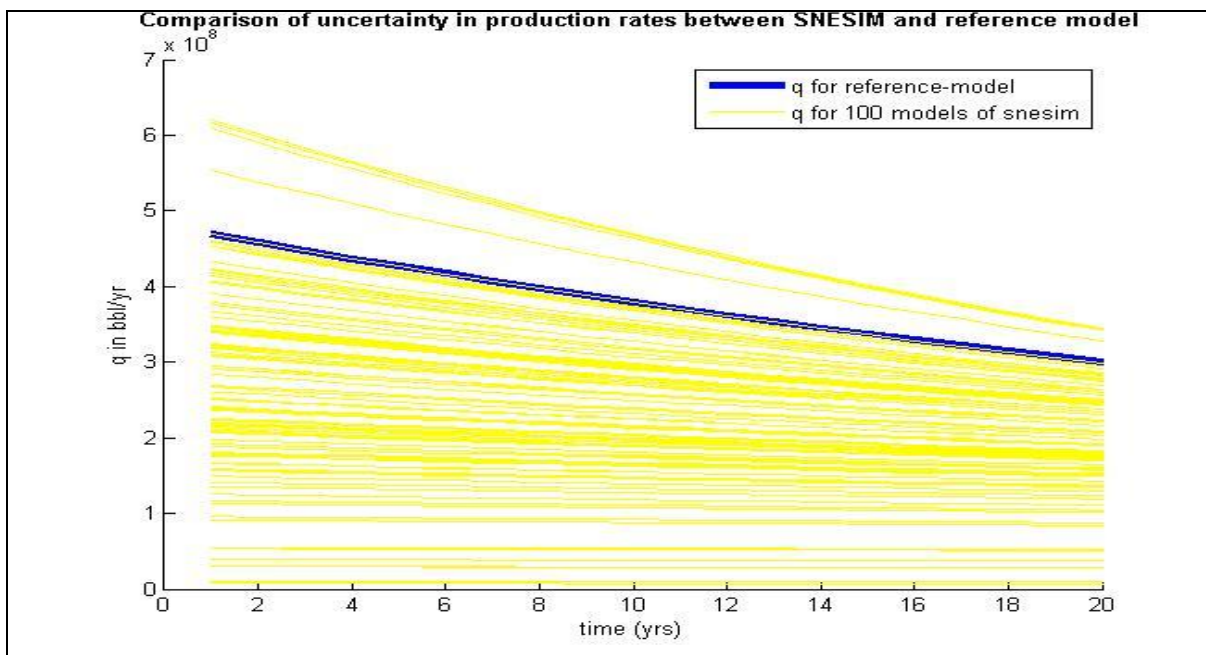


Figure 4-13: Uncertainty in oil production forecast obtained using SNESIM

In both SISIM and SGSIM realizations, the spatial connectivity of high permeability features is underestimated. This results in a more rapid rate of decline of flow rate in the simulated models as compared to the reference model that had good connectivity of high permeability features. The initial rates are higher in the SGSIM and SISIM models because the regions of high permeability are wider than the thin channel shown in the reference model. The connectivity is better represented in the SNESIM models and consequently the reference response is bracketed by the responses simulated for all the realizations obtained using SNESIM.

Figure 4-14 shows the distribution of oil production rates obtained using 3 geological models, which are compared with the production rate from the reference truth model. It can be seen that the production rate distribution obtained from SGSIM is the narrowest and closest to the reference, which is represented by a blue circle.

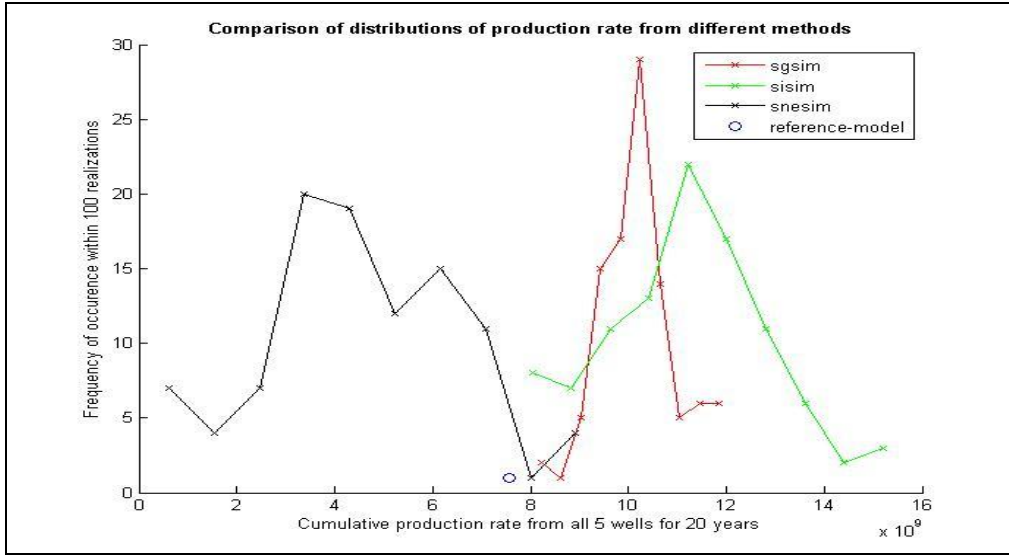


Figure 4-14: Comparison of production rate distributions (histograms) from 3 geological models with the reference truth

ROV Analysis

ROV is a process of valuing a physical/real asset with real uncertainties. As opposed to NPV, ROV incorporates multi-domain uncertainties. The ROV can be estimated through a closed-form equation known as Black-Scholes equation. Black-Scholes model to compute ROV is given as:

$$C(S, t) = Se^{r(t)} N(d_1) - Xe^{r(t)} N(d_2) \quad \text{--- (4.1)}$$

where,

$$C(S, t) = \text{ROV}$$

$$d_1 = \frac{\ln\left(\frac{S}{X}\right) + \left(r + \frac{\sigma^2}{2}\right)(T - t)}{\sigma\sqrt{T - t}}, \text{ and } d_2 = d_1 - \sigma\sqrt{T - t}$$

$$S = F(t)$$

$$X = \text{capex}$$

$$r = 12\%$$

$$\sigma = \text{Project Volatility}$$

$$T = \text{Time period of maturity}$$

Once we determine the future oil production rates as illustrated in previous section, the following equation is used to obtain forecast of future cash flows for each realization of $q(t)$:

$$F(t) = (q(t) \times p) - \text{opex} \quad \text{--- (4.2)}$$

In equation (4.2) production rate is the only variable that is allowed to vary with time. Oil price can be made to vary by computing time varying oil prices using the Ornstein and Uhlenbeck mean reverting model; however, oil prices are kept constant at \$ 30/barrel to have consistent comparison of the reservoir economic performance by different geological models.

These future cash flows will be used to compute the project volatility through the method explained in Chapter 2. This project volatility is one of the most critical parameter which is used as input in the real options model. We calculated the project volatility as following:

$$PV(t) = F(t) \times DV(t)$$

$$G = \ln \left[\frac{\sum_{i=1}^n PV_i}{\sum_{i=0}^n PV_i} \right] \quad \text{--- (4.3)}$$

$$\Rightarrow \sigma = \text{std}(G)$$

where,

PV_i = Present value at i^{th} year

$\text{std}()$ = Standard deviation

σ = Project Volatility

We will obtain G from equation (4.3) for every realization and, therefore, a histogram of G can be plotted. The volatility σ will be the standard deviation of the distribution G .

Figure 4-15 shows the time varying project volatility's magnitude decreasing with time. The reason for the decrease in project volatility with time is because there is more prior data of the reservoir's economic performance (in terms of DCF). In addition to the above factor, the volatility decreases because as fluid is produced for increased duration the effect of geologic uncertainty on reservoir product decreases. This is because larger volume of the reservoir is already contacted by the injected water as time progresses.

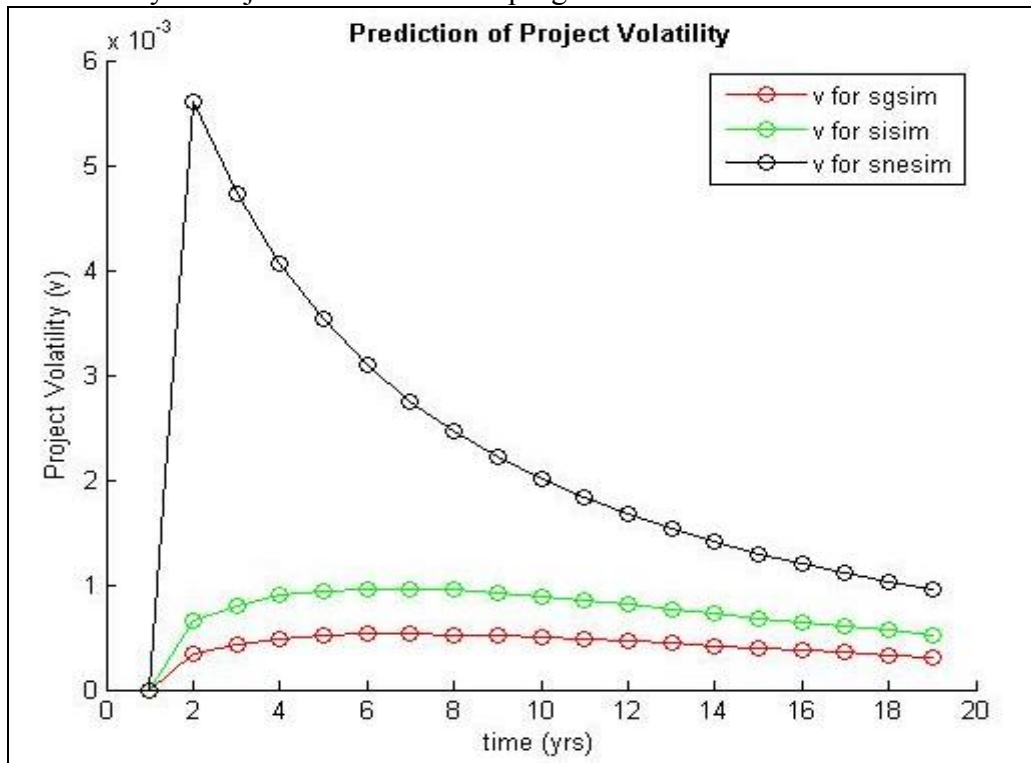


Figure 4-15: Variation of project volatility with time for different models and reference truth

ROV can be obtained on substituting values for the above variables in equation (4.1). The above calculation is repeated for all the realizations to come up with the uncertainty in the ROV.

Results And Discussions On Complexity Of Geological Modeling

The cumulative sum of present values gives Net Present Value (or cumulative DCF) which is shown in Figure 4-16. Figure 4-16 compares the uncertainty in cumulative DCF forecast from SGSIM, SISIM, and SNESIM with the cumulative DCF forecast obtained from reference truth model.

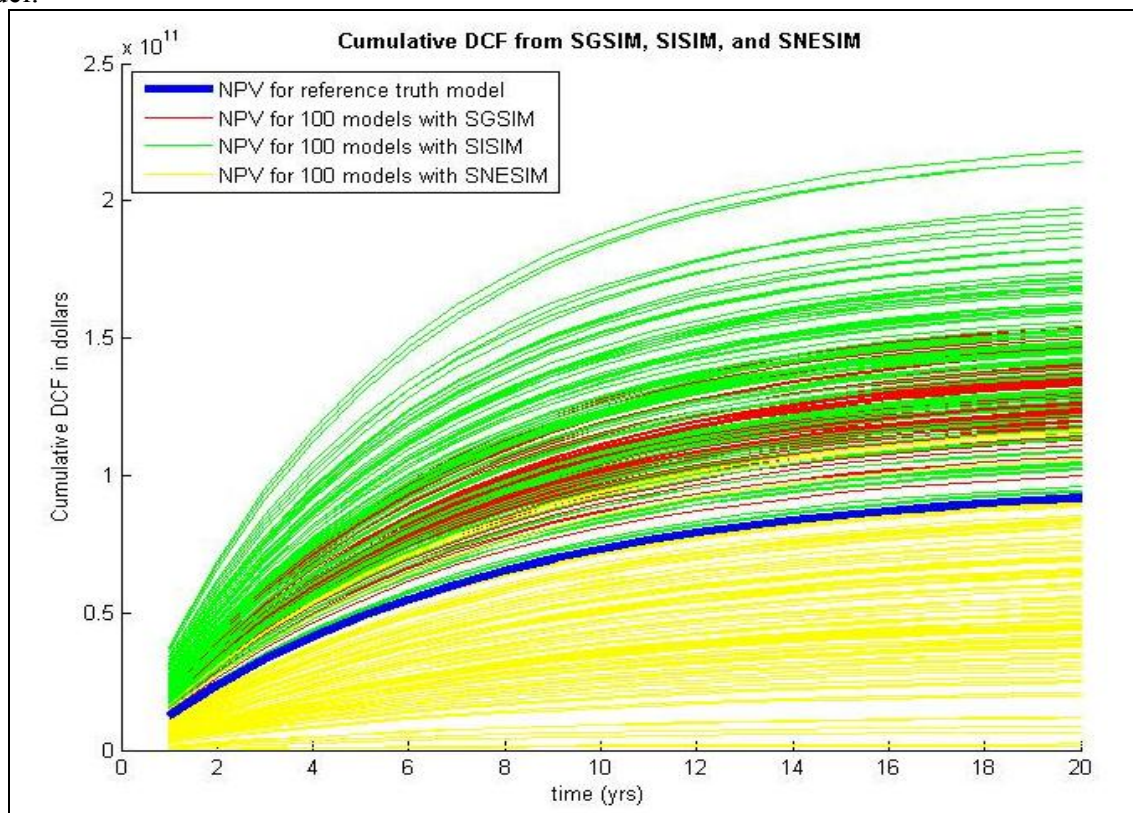


Figure 4-16: Comparison of uncertainty in cumulative DCF from SGISIM, SISIM, and SNESIM with that obtained from reference truth

Once we have the PV or ROV from the reservoir for different geological models, we can compare them with PV or ROV obtained using the reference truth model.

Figure 4-17 compares the uncertainty in PV forecast obtained using SGSIM geological model with the PV forecast obtained using the reference model. Figures 4-18 and 4-19 show the PV forecast obtained using SISIM and SNESIM geological models with the reference model, respectively.

Figure 4-20 compares the uncertainty in ROV forecast obtained using SGSIM geological model with the PV forecast obtained using the reference model. Figures 4-21 and 4-22 compare the ROV forecast obtained using SISIM and SNESIM geological models to that with the reference model, respectively.

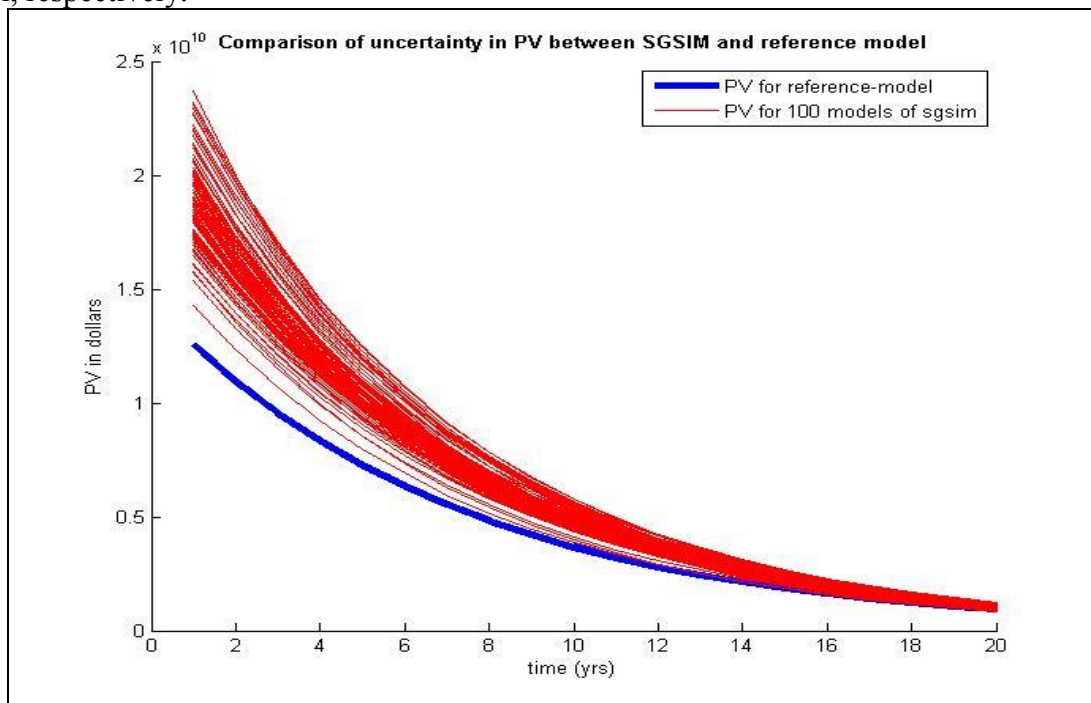


Figure 4-17: Uncertainty in PV forecast obtained using SGSIM

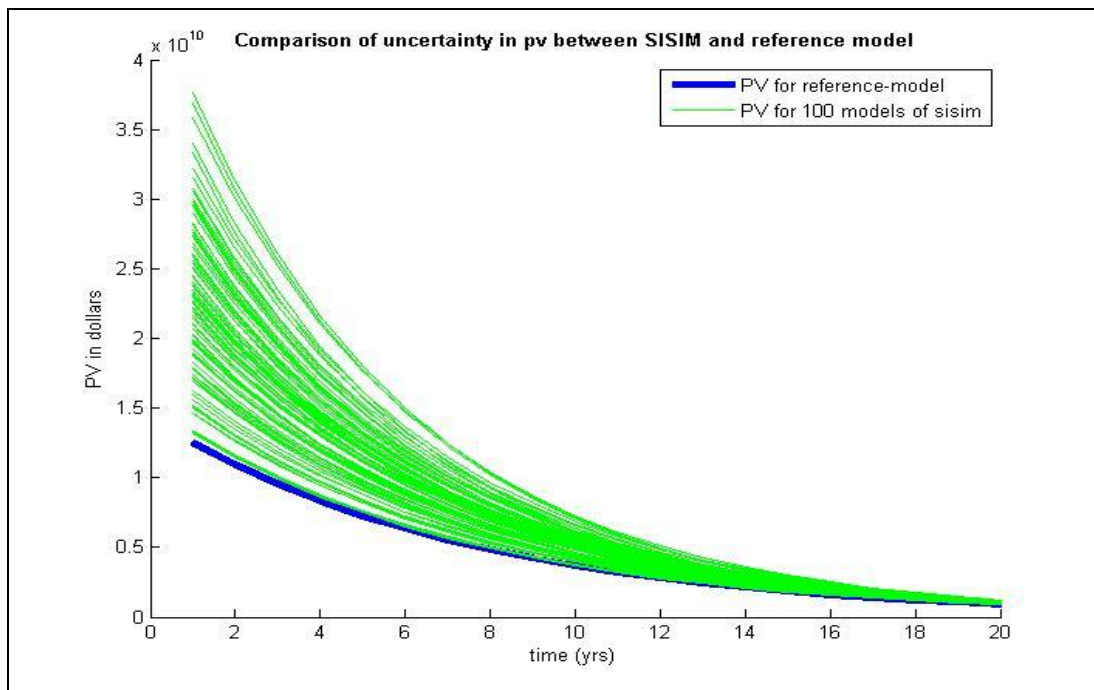


Figure 4-18: Uncertainty in PV forecast obtained using SISIM

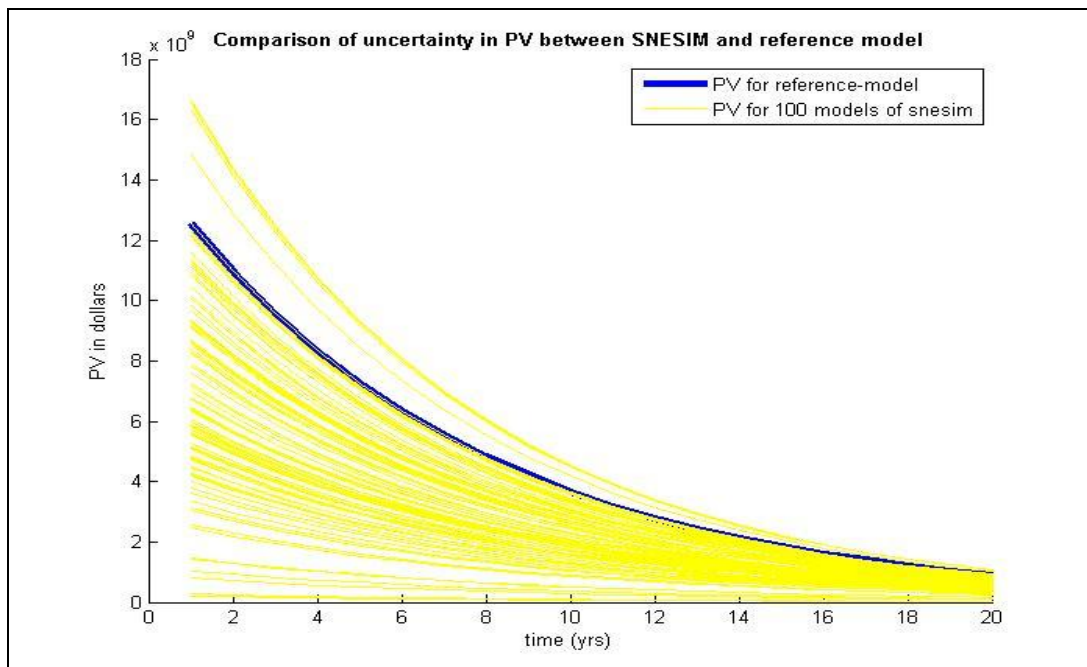


Figure 4-19: Uncertainty in PV forecast obtained using SNESIM

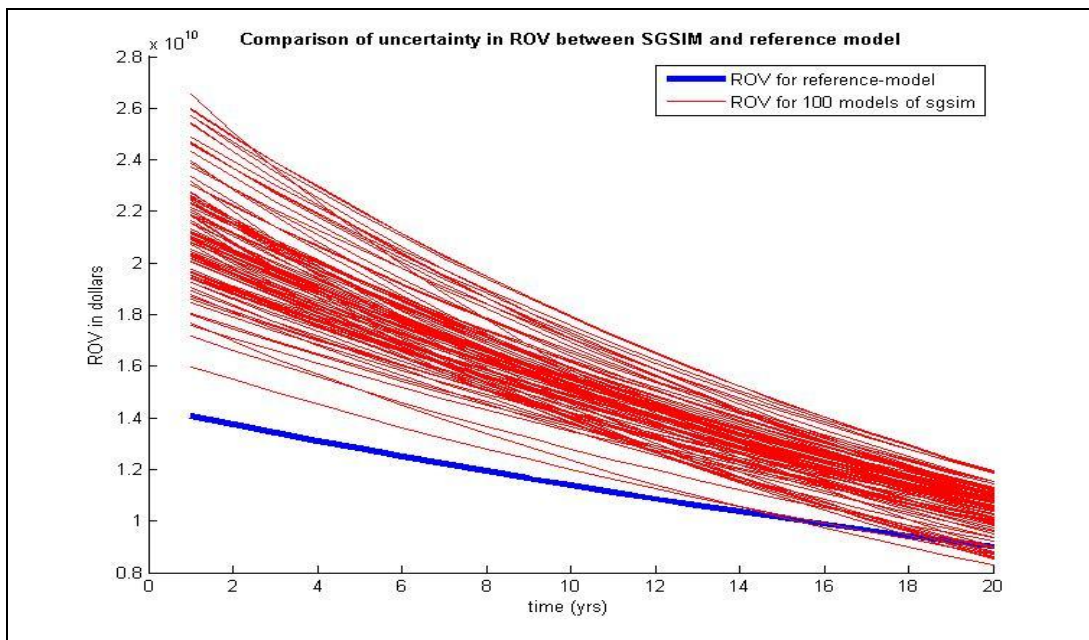


Figure 4-20: Uncertainty in ROV forecast obtained using SGSIM

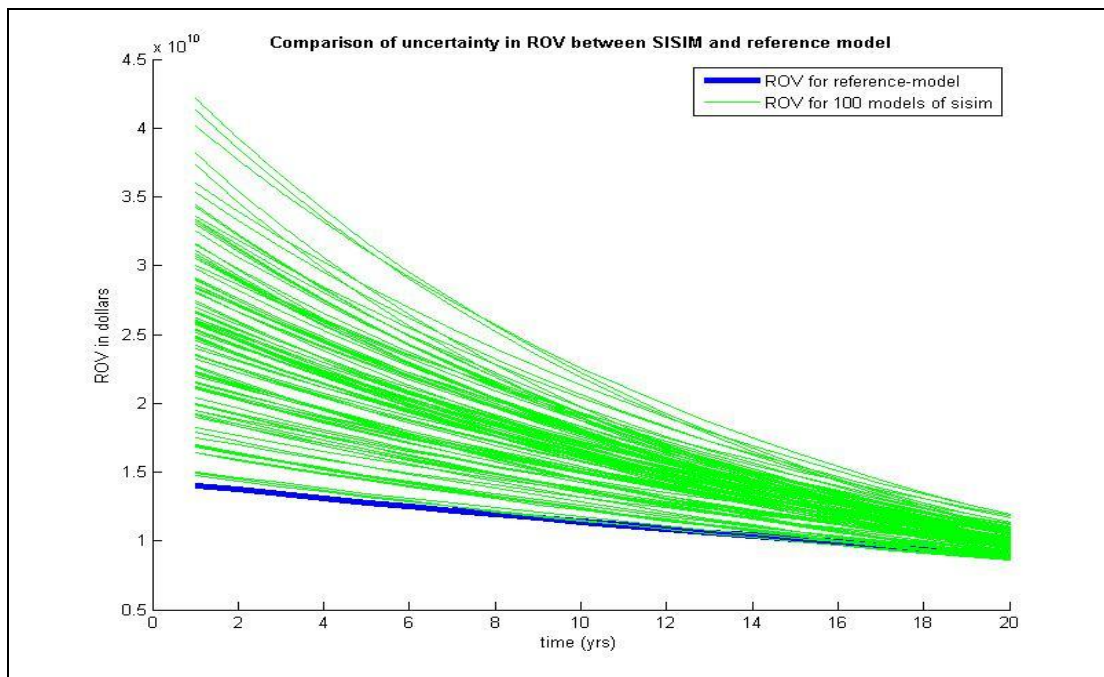


Figure 4-21: Uncertainty in ROV forecast obtained using SISIM

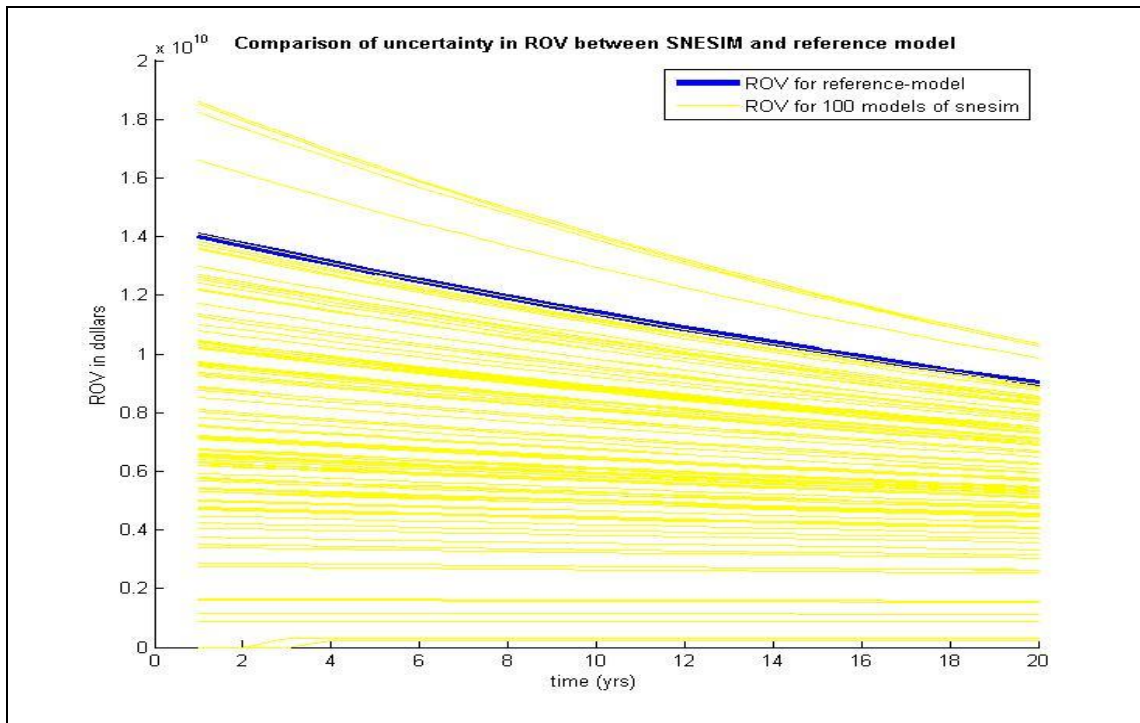


Figure 4-22: Uncertainty in ROV forecast obtained using SNESIM

Therefore, it can be seen that the output of these geological models in terms of economic returns from the reservoir does not show significant variation compared to each other. In fact it is seen that the least complex geological model, SGSIM, matches closely with the reference.

However, if we do the ROV analysis corresponding to the mean production profile from all different models, then the results indicate that ROV corresponding to mean production profile from SNESIM is closest to the reference. Figures 4-23 and 4-24 show mean production histories, and ROV corresponding to the mean production histories from all different models, respectively.

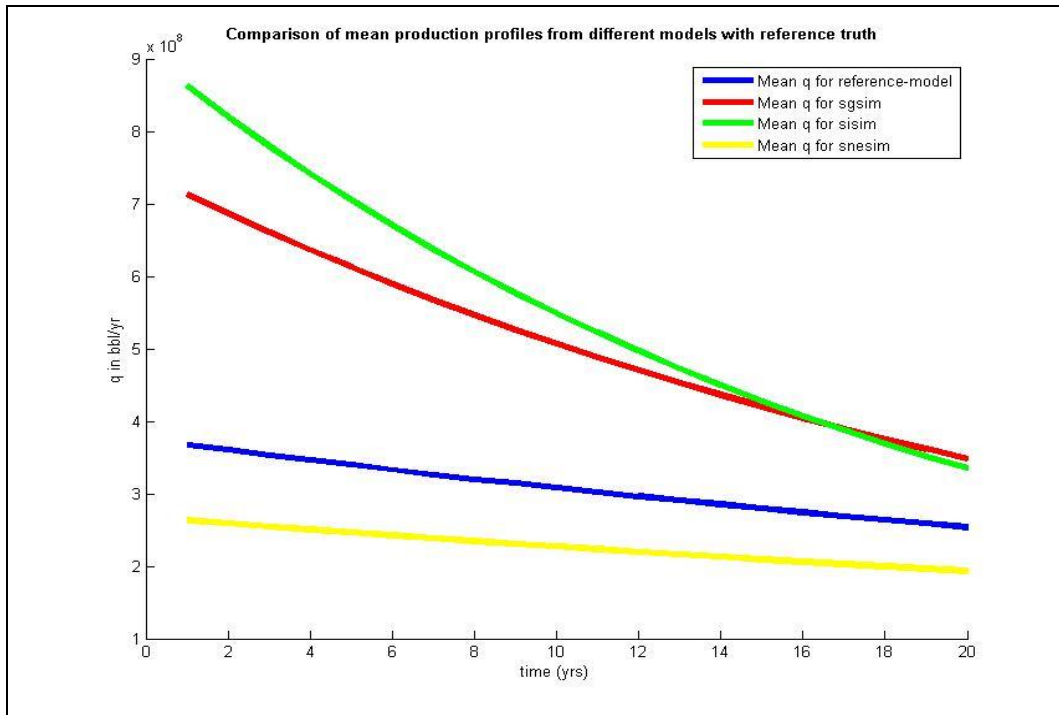


Figure 4-23: Comparison of mean production profiles from different models

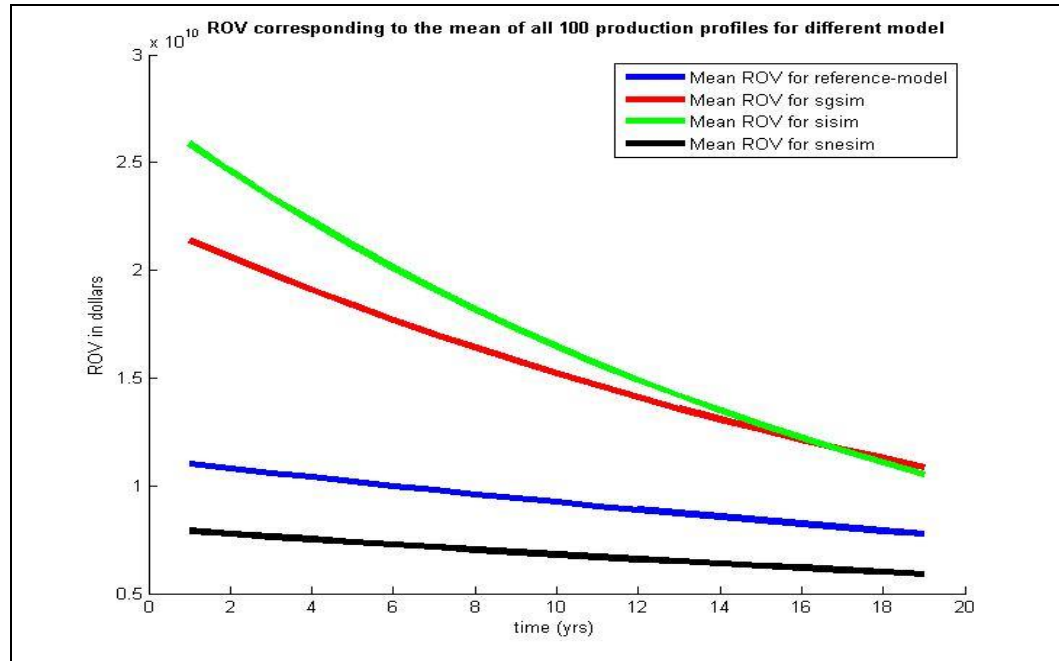


Figure 4-24: Comparison of ROV corresponding to mean production profiles from different models

Overall, the initial economic returns from all the three geological models are about same with respect to the reference, but the PV amount is in general less than the ROV throughout the life of the reservoir. This implies that project valuation using the conventional DCF technique fails to unearth the hidden economic potential of the project that is brought to the fore by the ROV analysis.

ASSESSING THE IMPACT OF DETAILED FLOW MODELING

Research Approach

Similar to the preceding discussion on complexity of the geologic model, it may be useful also to study the impact of complex flow modeling on assessing the uncertainty in flow response characteristics and further on assessing the impact on ROV or NPV. Decline curve analysis can be a good choice if the long term production performance prediction is the ultimate objective.

To forecast the economic performance of the reservoir, we need future hydrocarbon production rates which can be determined using full physics commercial simulator such as CMG or decline curve analysis. For this case study on assessing the economic implication of flow modeling complexity, we use predicted hydrocarbon production rates from the case study in Chapter 3. The description of the case study from Chapter 3 is briefly recounted below.

Description of the Problem

We assume a reservoir with grid dimension of 50 x 50 x 1 that initially has 5 production wells only. The only basic information available about the reservoir characteristics such as porosity

and permeability is from these 5 production wells. Using this base information we can develop multiple realizations of future economic performance of the reservoir. Having multiple scenarios for economic performance of the reservoir helps us to do risk analysis and take appropriate decisions regarding further development of the reservoir.

These multiple realizations of future economic performance of the reservoir represent uncertainty, and to reduce this uncertainty in economic performance we must gain more information about our reservoir. This reduction in uncertainty could be achieved by gaining more information about our reservoir, which can be either by drilling an exploratory well or, acquiring secondary information such as seismic.

Gaining extra information, over and above the existing 5 producing wells, may reduce the uncertainty of our economic returns forecast and give a more correct estimate of the value of the field. Based on the correct economic forecast of the existing field, we can decide whether it will be beneficial to develop the field further or not.

Our purpose of referring to this case study is to use the production rate profiles which were determined using CMG simulator in addition to the production rate profiles which will be computed using decline curve analysis. To get detailed information on how the production rate profiles were determined from CMG simulator, please refer to Chapter 3. The production rate profiles generated from each of these methods will be used to assess the economic implication of flow modeling.

Decline Curve Model

Decline curve model used to predict the field's production rates was taken from Chapter 9 of Walsh and Lake (2003). All the units in following formulas are expressed in oilfield units to maintain consistency.

$$J_k = \frac{0.00708hk_o}{\mu \left(\frac{1}{2} \ln \left(\frac{A_w}{r_w^2 C_A} \right) + 5.75 + s \right)}$$

$$\lambda = \frac{365 N_w J_k}{V_p C_t}$$

$$V_p = 7757.792 Ah\phi$$

$$q_{osci} = \frac{N_w J_k (p_i - p_{wf})}{B_{oi}}$$

$$N_p = 365 \frac{q_{osci}}{\lambda} [1 - \exp(-\lambda t)]$$

$$\bar{p}_t = (p_i - p_{wf}) \exp(-\lambda(t - t_0)) + p_{wf}$$

where,

J_k = Well productivity index [rb/day/psi]

C_A = Shape factor

r_w = Well radius [ft]

h = Reservoir thickness [ft]

k_o = Permeability relative to oil

A = Drainage area [acres]

s = Skin factor

λ = Decay constant [1/year]

N_w = Number of wells

ϕ = Porosity

V_p = Pore volume [rb]

B_{oi} = Formation volume factor [rb/STB]

q_{osci} = Initial producing rate [STB/day]

N_p = Cumulative oil production [STB]

t_0 = Project start time

\bar{p}_t = Average pressure after t years [psi]

p_{wf} = Bottomhole pressure

Flow Modeling

The cases presented here were not run in a history matching mode. In other words, once the decline parameters were established they are not updated. We are simply trying to ascertain if the complexity of the flow model contributes in any way to the assessment of value of information stemming from assimilation of different types of reservoir data. Part of the problem is that we decided to do this on a different case example than that for the rest of the chapter.

Figures 4-25 and 4-26 compare the uncertainty in oil production forecast determined using CMG and decline curve analysis, respectively, for the 2 scenarios from the strategy discussed in Chapter 3.

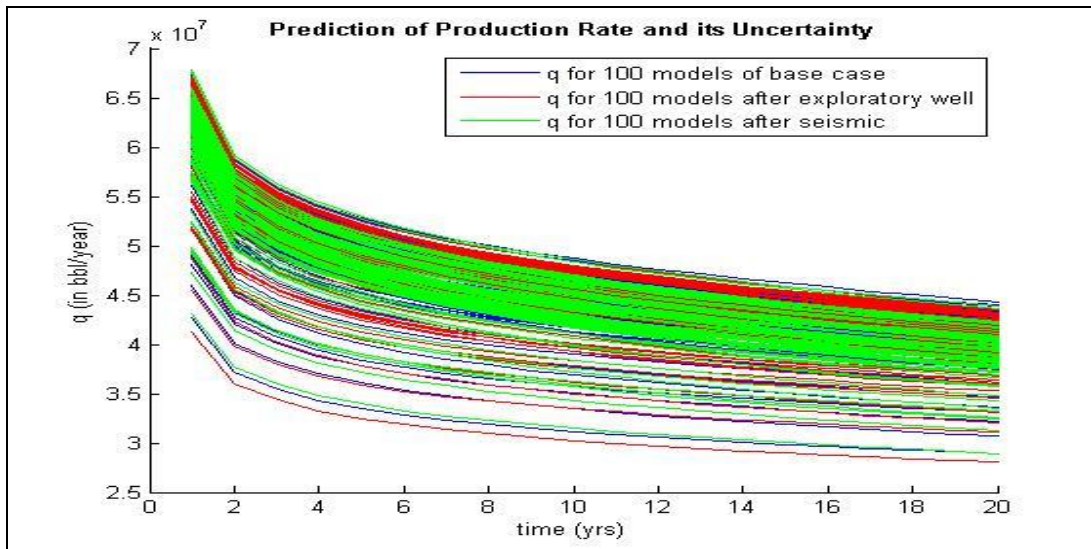


Figure 4-25: Uncertainty in oil production forecast determined using CMG

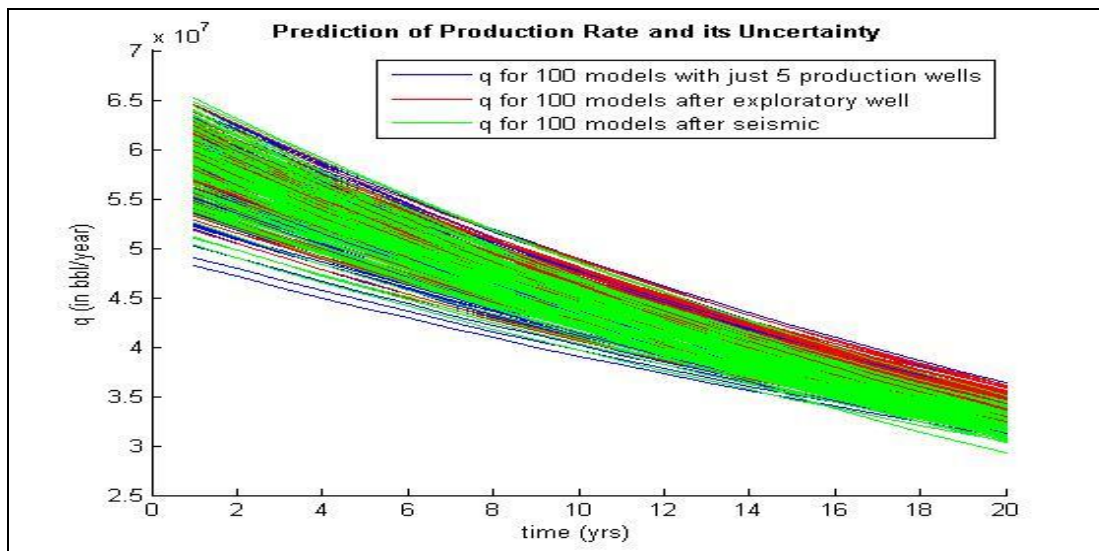


Figure 4-26: Uncertainty in oil production forecast determined using decline curve analysis

Results And Discussions On Complexity Of Flow Modeling

Figures 4-27 and 4-28 show the economic forecast obtained using PV for future hydrocarbon production rates determined through CMG and decline curve analysis, respectively. Figures 4-29 and 4-30 show the economic forecast obtained using ROV for future hydrocarbon production rates determined through CMG and decline curve analysis, respectively.

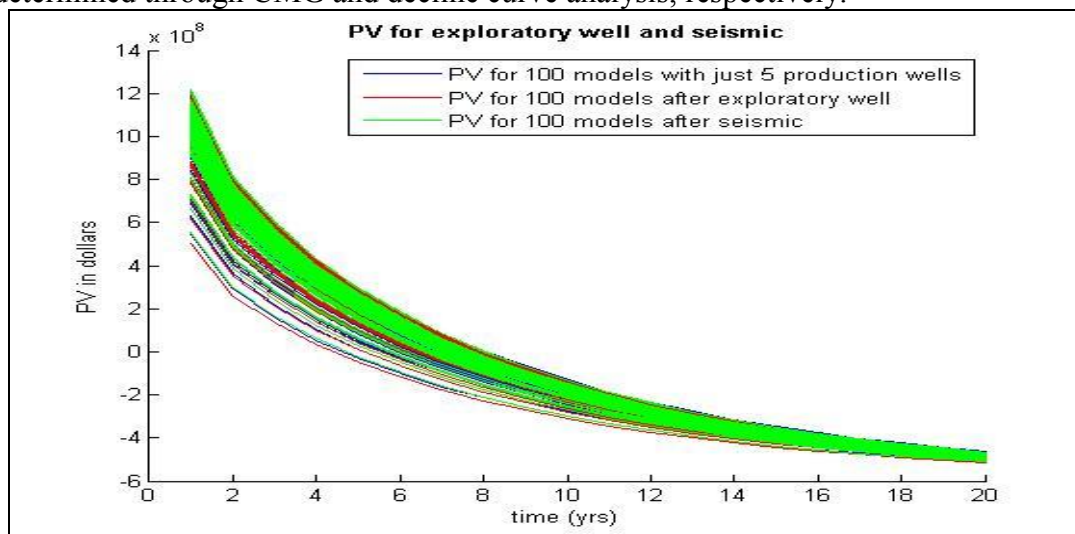


Figure 4-27: Uncertainty in PV obtained using CMG

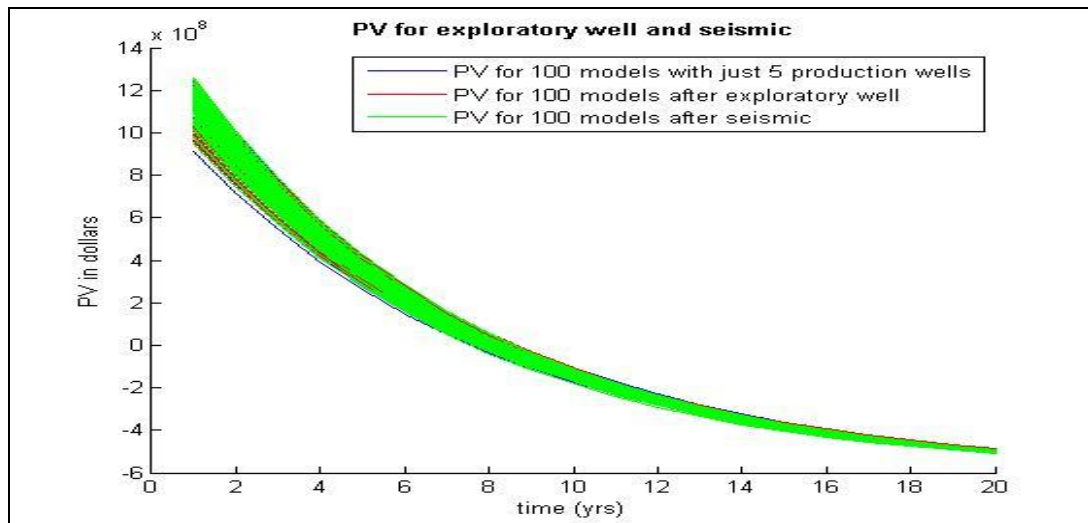


Figure 4-28: Uncertainty in PV obtained using Decline Curve

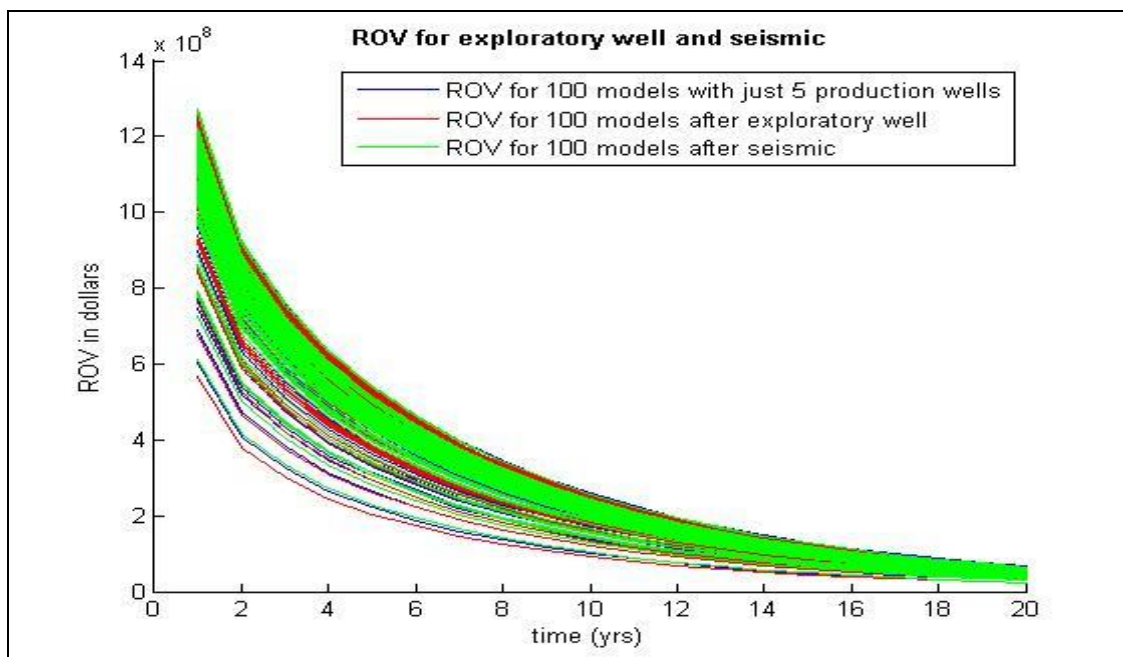


Figure 4-29: ROV obtained using CMG

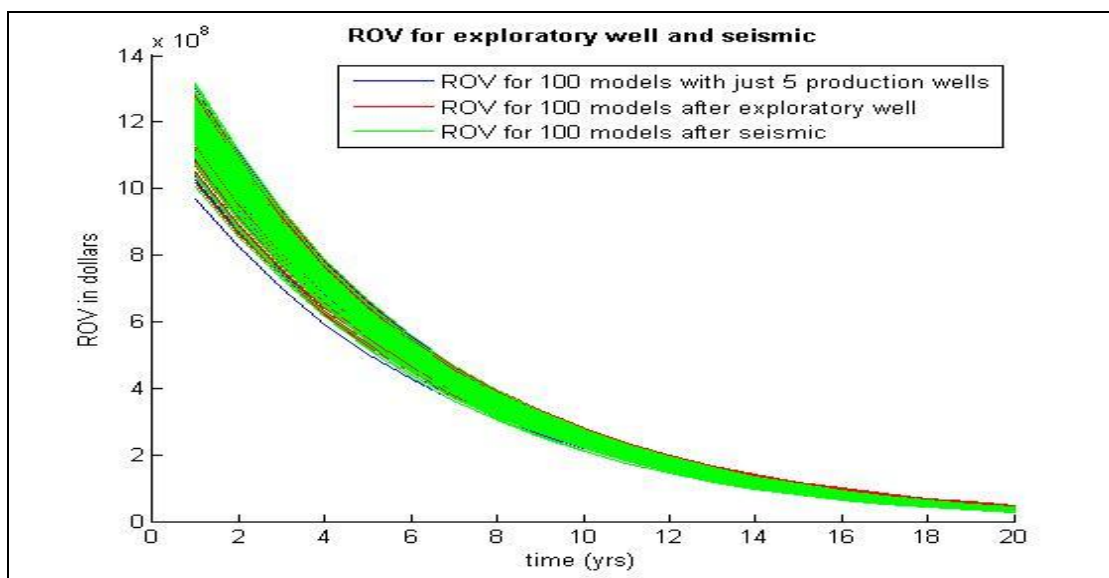


Figure 4-30: ROV obtained using Decline Curve

A key observation, with regards to comparison of figures 4-29 and 4-30 is that the distribution of uncertainty in ROV is reduced when using the decline curve. This is to be expected since the entire spatial variability exhibited by porosity and permeability as depicted over the suite of realizations is reduced to a single effective value that is input into the decline curve model. We can see from the above figures that the results from decline curve analysis, for the economic returns from the reservoir over its life period of 20 years, match quite well with the results from a commercial simulator CMG.

There is a raging debate within the modeling (reservoir, flow and economic) community on the worth of producing sophisticated models that exhibit physical realism. This study explores this issue using economic measures such as PV and ROV. Preliminary results that might be specific to the case study set up in this study seem to indicate that complexity in models might not always translate to improved accuracies in economic forecasts. In fact, project volatility derived using several realizations of the geological model might often dwarf uncertainty in flow performance modeled using sophisticated schemes.

Chapter 5: Binomial-Lattice Option Valuation

INTRODUCTION

Traditional discounted cash flow (DCF) methods of valuation fail to account for the value of managerial flexibility present in many types of projects. For example, NPV analysis does not capture the effects of decision to expand or abandon the project. The real options valuation, a stochastic approach, is a method to value capital investment projects that involve managerial flexibilities (Dixit & Pindyck 1995).

The concept and theory of Real Options is explained in Chapter 2. We also show in Chapter 3 and 4 the utility of real options using Black-Scholes model to discover hidden value in modeling and data acquisition decisions that would not have been evident using conventional DCF analysis.

The main drawback of using the Black-Scholes model is that the Black-Scholes equation is a solution to a stochastic differential equation corresponding to a set of restrictive assumptions. The Binomial lattice on the other hand permits the evaluation of projects that may not follow the strict prescription of initial and boundary conditions specified as part of the Black-Scholes solution.

Binomial Lattice Option Valuation (BLOV) is a generalized numerical method for the valuation of options. In general, the BLOV model does not have closed-form solutions (Cox et al. 1979). Although BLOV is computationally slower than the Black-Scholes model for ROV, it is more

accurate for longer-period (Yound & Wiley 2011) such as options in upstream petroleum industry projects which can last for several years.

Primarily there are two types of options – European and American style options. The difference between these two types of options is the date of exercising the options. A European style option can be exercised only at the date of expiration of option, while American style option can be exercised anytime before the date of expiration of the option. Binomial lattices allow valuation of both the European and American-type options. For judicious decisions, it is wise to wait and analyze the information received until the last moment. And for this reason, the American option is implemented in the oil industry to take advantage of the availability of flexibility in timing. In this chapter we present the procedure to construct a lattice for an American call option.

USE OF THE MODEL

BLOV is a way to show how an asset's value changes over time, provided there is some volatility in the value of that asset. The binomial pricing model traces the evolution of the underlying asset value in discrete-time. This is done by means of a binomial lattice (a tree), for a fixed number of time steps between the option valuation and expiration dates. Each node in the lattice represents a possible value of the asset at a given point in time.

For BLOV at least two lattices must be constructed. The first lattice shows how the underlying **asset value** evolves over time, while the second lattice shows the actual **option values** at different periods of time. Examples of lattices for underlying asset values and option values taken from a case study in Chapter 6 are shown in Figures 5-1 and 5-2, respectively. The y-axis on both lattices in Figures 5-1 and 5-2 represents probability distribution of asset values and option values because at each time step there are multiple asset values and option values,

respectively. Therefore, each time step contains probability distribution as a result of containing multiple values of asset values or option values in their respective lattices. Details of the procedure for constructing the two lattices are explained in the subsequent sections.

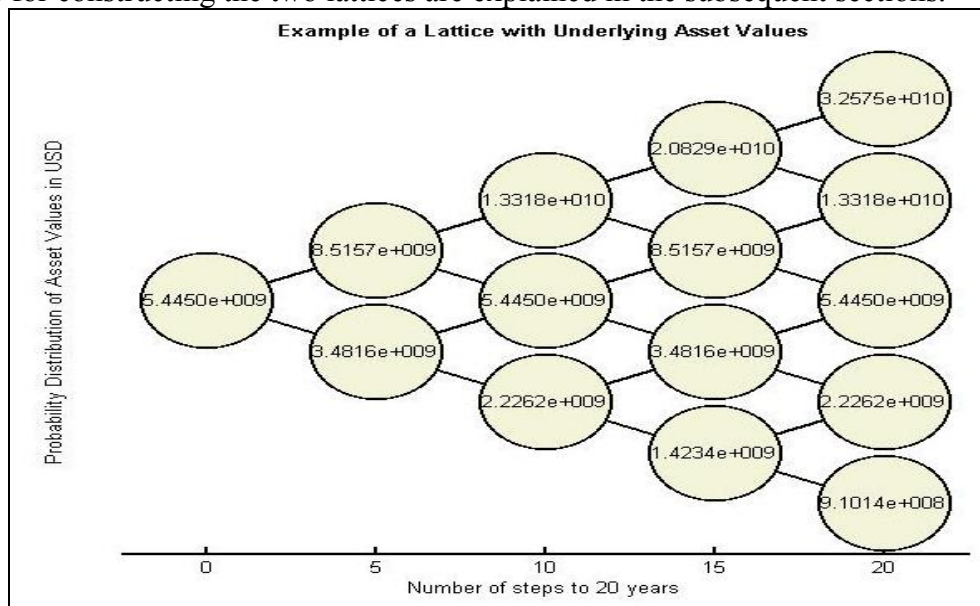


Figure 5-1: Example of a lattice showing underlying asset values

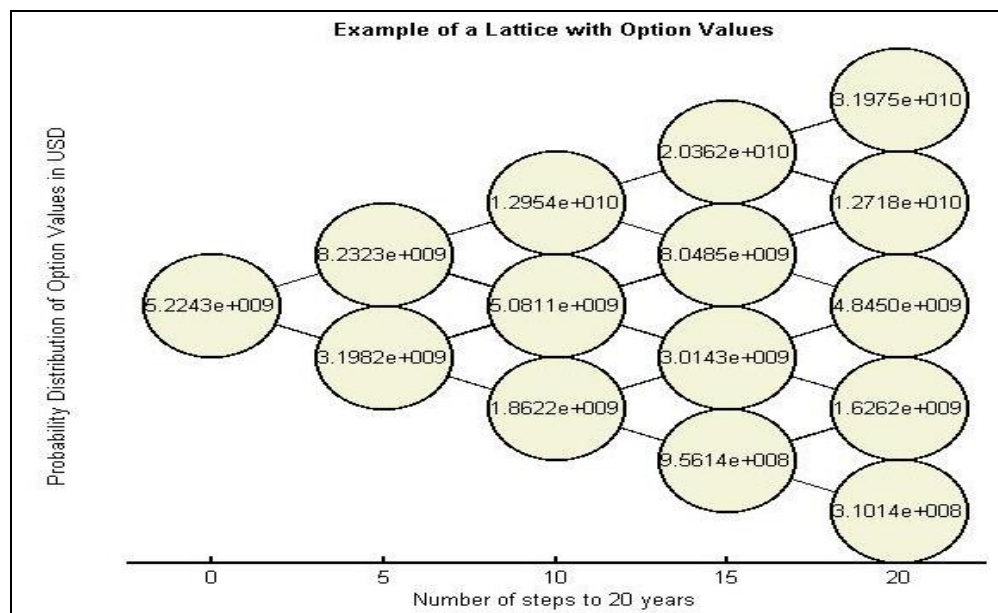


Figure 5-2: Example of a lattice showing option values

METHOD FOR CONSTRUCTING THE LATTICE

A binomial lattice at each node moves along only two possible paths for each time step – up or down i.e. an increase or decrease in the value of a node in the lattice, respectively. The process of option valuation involves first moving forward to form a lattice of the underlying asset, and in the second step working backwards through the lattice from the end nodes (at the expiration date) towards the first starting node to form a final option valuation lattice. In the final valuation lattice, the value computed at each stage is the value of the option at that point in time.

The main aspects of option valuation using Binomial Lattice are thus:

1. Price tree generation,
2. Calculation of option value at the final node,
3. Sequential calculation of the option value at each preceding node.

STEP 1: Creating Lattice of the underlying asset

The lattice of the underlying asset is produced by working forward from left to right towards the terminal nodes at the date of expiration. It shows how the future asset values could possibly evolve. The left most node usually contains the value of the NPV of the underlying asset. At each step the value of the underlying asset will increase or decrease by a factor of u or d respectively ($u \geq 1$ and $0 < d \leq 1$), per time step of the lattice. So, if S_0 is the current price, then in the next time step the price will either go up or go down i.e. $S_{up} = S_0 u$ and $S_{down} = S_0 d$, respectively. The probability of the asset value going up is designated as p , which implies that the probability of the value going down is $1-p$. This is shown in the Figure 5-3:

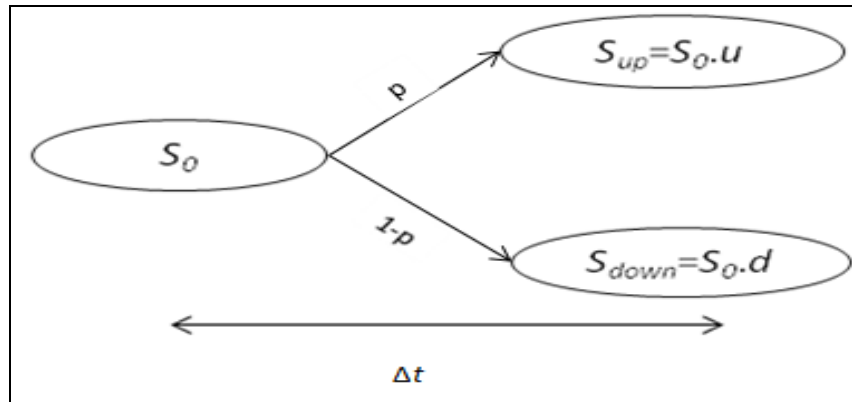


Figure 5-3: Construction of lattice for an underlying asset illustrating the process of construction of lattice for an underlying asset. The value of the asset is first constructed by going from left to right. Subsequently, the option value is computed by traversing the lattice from right to left.

We'll need the probability p in Step 2 below where we'll talk more about it, and also derive its formula. The factors u and d , which determine the upward and downward movements at each node, are functions of the volatility of the underlying asset and the time step between each column of the lattice. They are given as:

$$u = e^{\sigma\sqrt{\Delta t}} \text{ and } d = \frac{1}{u} = e^{-\sigma\sqrt{\Delta t}}$$

σ is the project volatility. The derivation of these expressions for u and d is presented in a subsequent section.

If we repeat this method of filling up the nodes at different time steps, a lattice will evolve as shown in the Figure 5-4. The probability distribution shown in the right side of Figure 5-4 is obtained from asset values in the terminal nodes of the lattice and the spread of that distribution will be controlled by the project volatility (Bailey et al. 2003). This resultant lattice in Figure 5-4 is called as the lattice of the underlying asset.

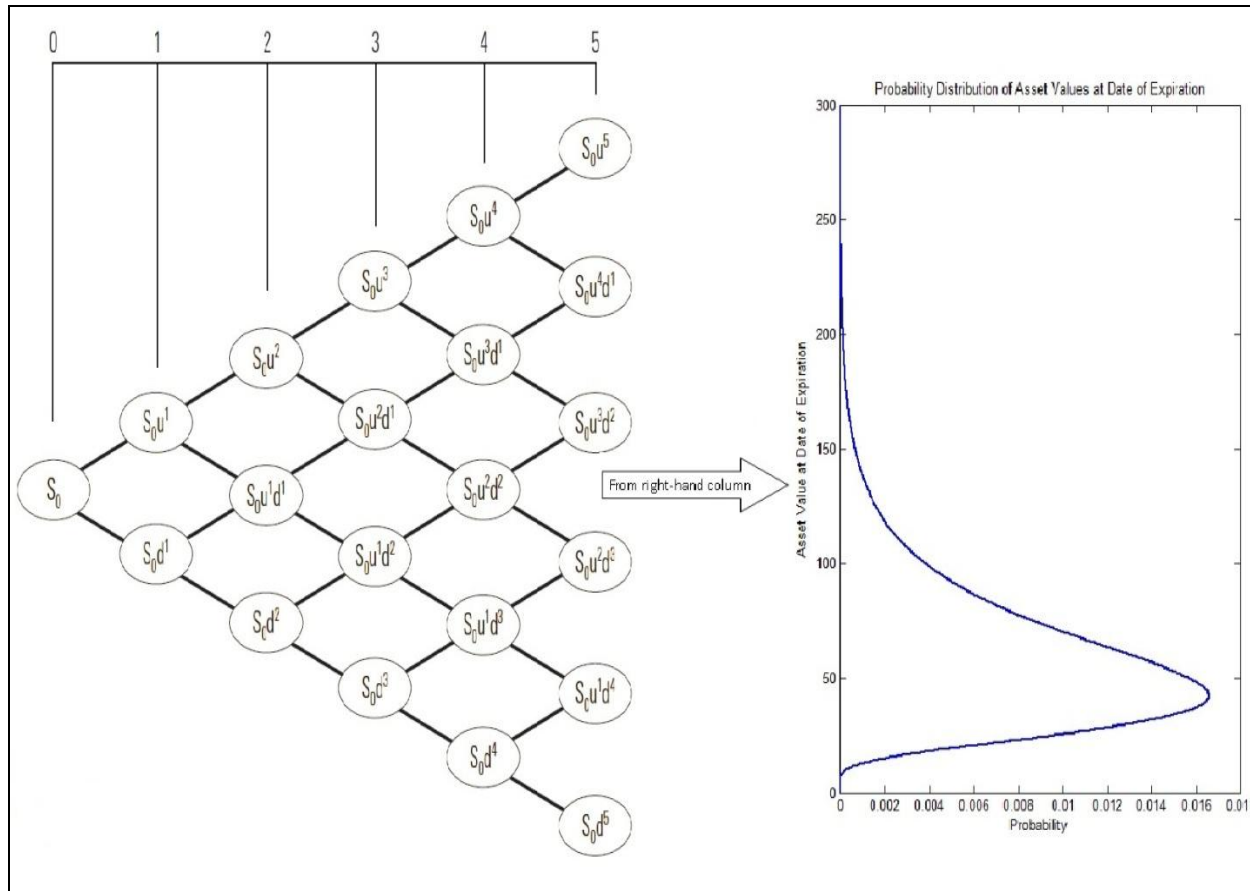


Figure 5-4: Probability distribution of future payoffs obtained from the values in the terminal nodes of the underlying lattice

STEP 2: Creating Option Valuation Lattice

The option valuation lattice consists of equal number of nodes and branches as the lattice of the underlying asset. At each node in the terminal branch of the underlying lattice, i.e. the nodes at the expiration date, the option value is calculated as $Max[(S_n - K), 0]$, where K is the capital expenditure for developing the asset and S_n is the asset value at the date of expiration. Now starting from these values in the terminal nodes, we work backwards towards the first node of the lattice to obtain the value of the option at each node.

Derivation for p, u and d

We start with a condition of the Black-Scholes model whereby we want to match the mean and variance, i.e. moments, of the returns of S in our lattice to the mean and variance in the real world.

In a risk neutral world, the expected gross return after a time Δt is $e^{r\Delta t}$, where r is the risk free rate. As per the risk neutrality assumption, the value of an asset at today's date is equal to the expected value of its future payoff discounted by the risk free rate i.e.

$$S_0 = \frac{E(S_{\Delta t})}{e^{r\Delta t}}, \text{ or } \Rightarrow E\left(\frac{S_{\Delta t}}{S_0}\right) = e^{r\Delta t} \quad \text{--- (5.1)}$$

Where, S_0 is the value of an asset at today's date, and $S_{\Delta t}$ is the future payoff at time Δt .

Because u and d are the gross returns of S_0 and the mean gross return is $e^{r\Delta t}$, therefore we must also have:

$$pu + (1-p)d = e^{r\Delta t} \quad \text{--- (5.2)}$$

Combining Equation (5.2) with (5.1), we have:

$$\begin{aligned} E\left(\frac{S_{\Delta t}}{S_0}\right) &= pu + (1-p)d \\ \Rightarrow E(S_{\Delta t}) &= S_0 [pu + (1-p)d] \end{aligned}$$

Therefore, the variance will be:

$$\begin{aligned} \text{Var}\left(\frac{S_{\Delta t}}{S_0}\right) &= \frac{1}{S_0^2} \text{Var}(S_{\Delta t}) = \frac{1}{S_0^2} \{E(S_{\Delta t}^2) - [E(S_{\Delta t})]^2\} \\ &= \frac{1}{S_0^2} \{S_0^2 [pu^2 + (1-p)d^2] - S_0^2 [pu + (1-p)d]^2\} \end{aligned}$$

$$\text{Var}\left(\frac{S_{\Delta t}}{S_0}\right) = [pu^2 + (1-p)d^2] - [pu + (1-p)d]^2 \quad \text{--- (5.3)}$$

Substituting Eq. (5.2) in Eq. (5.3):

$$\text{Var}\left(\frac{S_{\Delta t}}{S_0}\right) = [pu^2 + (1-p)d^2] - e^{2\sigma\Delta t} \quad \text{--- (5.3A)}$$

In the Black-Scholes model we have a lognormally distributed asset value with variance as:

$$\begin{aligned} \text{Var}(S_{\Delta t}) &= S_0^2 e^{2r\Delta t} (e^{\sigma^2\Delta t} - 1) = S_0^2 (e^{2r\Delta t + \sigma^2\Delta t} - e^{2r\Delta t}) \\ \text{Var}\left(\frac{S_{\Delta t}}{S_0}\right) &= (e^{2r\Delta t + \sigma^2\Delta t} - e^{2r\Delta t}) \quad \text{--- (5.4)} \end{aligned}$$

Equating the right side of Equations 5.3A and 5.4, we obtain:

$$pu^2 + (1-p)d^2 = e^{2r\Delta t + \sigma^2\Delta t} \quad \text{--- (5.5)}$$

To infer the parameters of our lattice p , u and d we need one more equation in addition to Equations (5.2) and (5.5). Different authors have introduced different constraints to obtain a solution. The best known solution is obtained by the constraint introduced by Cox *et al.* (Cox et al. 1979) for asymmetric asset appreciation and decline which we used above in step 1:

$$ud = 1 \quad \text{--- (5.6)}$$

Using Equations (5.2), (5.5) and (5.6), we obtain:

$$\begin{aligned} p &= \frac{e^{r\Delta t} - d}{u - d} \\ u &= e^{\sigma\sqrt{\Delta t}} \text{ and } d = \frac{1}{u} = e^{-\sigma\sqrt{\Delta t}} \end{aligned}$$

We are now ready to value the asset's option at the date of interest using the parameters p , u and d . We use the future payoffs in two adjacent nodes behind the node at the date of interest and calculate the expected value by weighting them with their respective probabilities. This process is shown in Figure 5-5:

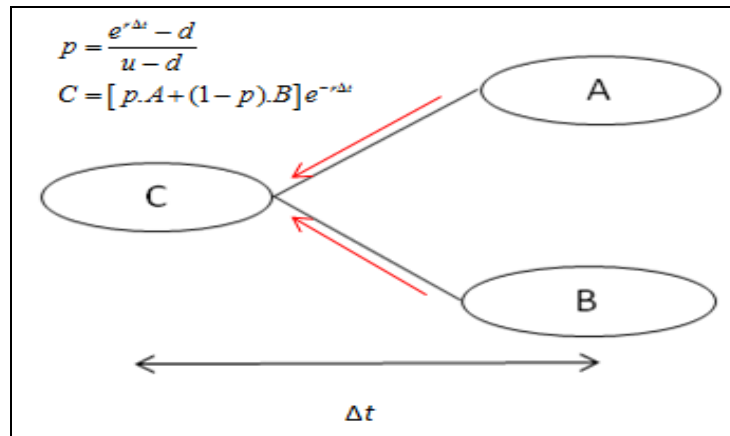


Figure 5-5: Construction of Option Valuation Lattice

If we continue this process for other nodes as well then we get a lattice made up of option values with corresponding up and down movement. On using the above procedure with single volatility for all time steps, a 5-step lattice is developed as shown in Figure 5-6 which was shown as an example in Figure 5-2. For a constant volatility value we will get a lattice which is combining at all nodes. If the volatility is varying with time then we would get a lattice which will not be combining at all the nodes but rather it would be a lattice with nodes growing exponentially. For time varying volatility the construction of lattice is possible, but complicated.

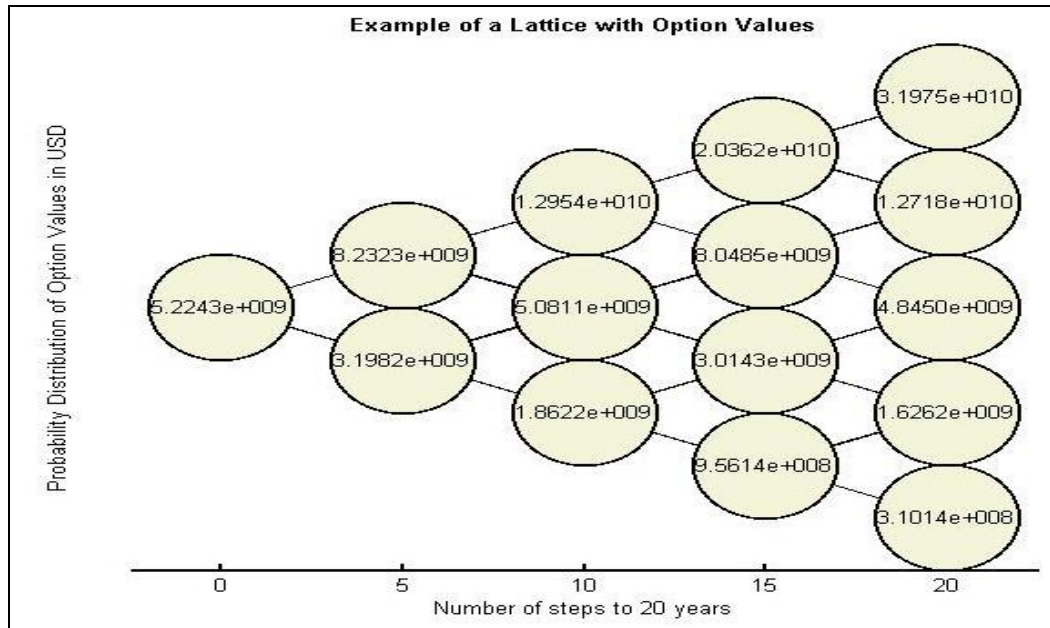


Figure 5-6: Evolution of Option Valuation Lattice

RELATIONSHIP OF BLOV WITH BLACK-SCHOLES MODEL FOR ROV

As evident from the previous discussion, both the binomial model and the Black-Scholes model have common theoretical underpinning. The binomial model can be viewed as a discrete time approximation to the continuous process represented in the Black-Scholes model. For American options without dividends, which are applicable to petroleum industry, the binomial model value converges on the Black-Scholes formula value with an increase in number of time steps. The movement of price in a binomial model is assumed to follow a binomial distribution. For large number of time steps, this binomial distribution in movement of price approaches the normal distribution as assumed in Black-Scholes model. Cox *et al.* (Cox et al. 1979) point out that the BLOV can be viewed as a finite difference solution of the Black-Scholes PDE.

Multiple realizations of stochastic reservoir model that correspond to geologic uncertainty are transferred to the flow model and eventually to the forecast of future hydrocarbon production

rates. Future cash flows are function of future hydrocarbon production rates and, therefore, any variation in future hydrocarbon production rates will result in a variation in the future cash flow stream. Variation in future cash flows is a source of project volatility; hence, the project volatility is also indirectly a function of volumetric flow rate uncertainty (which is related to geologic uncertainty) because future cash flows are a direct function of volumetric flow rate. Chapter 6 applies the framework of BLOV to analyze the economic prospects of an undeveloped, but discovered field.

Chapter 6: Analyzing the Prospects of an Undeveloped Field

INTRODUCTION

This chapter explains in a simple way the application of Binomial Lattice Option Valuation (BLOV) to the valuation of an undeveloped oil reserve. As we discussed earlier that Binomial Lattice Option Valuation (BLOV) (Cox et al. 1979) is a generalized numerical method for the valuation of options. Although its solution is computationally slower than the Black-Scholes formula, it is more accurate, particularly for longer-period options such as those in upstream petroleum industry.

The case example presented in this chapter focuses on the analysis of the reserves of an undeveloped, but discovered, field. The future economic prospects from the field will give an idea of how much a company may want to invest to develop the field. In this case we do the evaluation based on recoverable reserves. Recoverable reserves are the technically and economically recoverable portion of oil volume in the reservoir. To determine recoverable reserves we must first evaluate original oil in place (OOIP), which is defined as the total hydrocarbon content of an oil reservoir. It is often abbreviated as STOOIP, which stands for stock tank original oil in place, or STOIP for Stock Tank Oil Initially In Place, referring to the oil in place before the commencement of production (Energy Information Administration - EIA 2008). Recovery factors for oil fields typically range between 10 and 60 percent. The wide variance is because of the different characteristics of fluid and reservoir properties for different deposits (Energy Information Administration - EIA 2008). By applying the estimate for recovery factor of a field on the OOIP, we can determine the recoverable reserves.

DESCRIPTION OF THE PROBLEM

In the initial phase the only information the company has is sparse data that can be used to develop the model for a reservoir. We use that initial model to do our initial economic valuation using the binomial lattice. Once we have done the economic valuation for the potential reservoir, by using only the initial representation, we will have two options following that economic valuation. The first option is to accept the valuation as is that we computed by using only the initial reservoir model without secondary information. The second option would be to invest money for acquiring new information in the form of 3-D seismic, which can be used together with the initial data to generate new model(s) for the reservoir, and then redo the economic valuation for the reservoir based on the new information. Acquiring additional seismic data will require investment. The objective is to evaluate the option of acquiring additional seismic data in terms of uncertainty reduction over the existing model. We perform this evaluation, by computing the real options valuation (ROV) without and with additional seismic data and use the difference between these numbers to establish the maximum capital expenditure permissible for seismic acquisition, for the project to be still economically viable.

MODELING APPROACH

In the initial stage of reservoir forecasting, only the reference data from 5 wells is available for modeling. The reservoir is represented with a simulation grid dimension of 50 x 50 x 1. Using the reference data we can develop porosity maps of the reservoir by geostatistical techniques. To represent uncertainty we use multiple realizations of the porosity models. For the case example presented in this chapter, we use window average of porosity models to mimic a seismic-like attribute. The value of water saturation is found to be 15% as output from reservoir simulation

and it remains almost constant during the twenty year production period of the field. Using the porosity and water saturation data we can find the OOIP as:

$$N = 6.2898 \frac{V_b \phi (1 - S_w)}{B_{oi}}$$

Where,

N = STOIIP (stb)

V_b = Bulk volume of the rock(m³)

ϕ = Porosity

S_w = Water saturation

B_{oi} = Formation volume factor

Using an approximate estimate of the irreducible water saturation based on the type of reservoir, we find the recovery factor of the reservoir from following relation:

$$R_f = \frac{S_w - S_{wir}}{1 - S_{wir}}$$

Where,

R_f = Recovery factor

S_{wir} = Irreducible water saturation

For this to work we need the average water saturation S_w through the life of the reservoir and so the recovery factor will change with time. Water saturation is computed by running an analog simulation model for the similar field. However, the change in water saturation is quite insignificant over the time period of recovery in which case the recovery factor does not change significantly.

Once we know the recovery factor and STOIIP the recoverable reserves from the reservoir are simply the product of both these two parameters.

$$\text{Recoverable Reserve} = R_f \times N$$

STATIC RESERVOIR MODELING

The important information that we need to know from the reservoir to do the forecast of economic valuation is porosity and permeability. If we do the forecast based on the recoverable reserves method then we only need porosity models of the reservoir. When we have only the reference data we use SGSIM, a geostatistical algorithm, to model the porosity maps of the reservoir. Gridded porosity maps incorporate some reservoir heterogeneity into the OOIP calculation by computing N for each grid block and then finally adding N from the entire grid blocks to get OOIP.

After we obtain seismic as secondary information, we use COSGSIM, a geostatistical program, to model the porosity maps of the reservoir

Scenario 1: Modeling using only data at five wells

The hard data for porosity from 5 producing wells with their locations are shown in Table 6-1:

Table 6-1: Hard data of porosity from 5 wells and their locations

X	Y	Z	Porosity (%)
1	10	0	30
7	20	0	45
15	5	0	32
23	40	0	40
30	7	0	36

The porosity semivariogram model Scenario 1 is:

Number of Structures = 1

Type = Spherical

Nugget Effect = 0

Max., medium, and min. range = 1000, 100, and 20 units

Azimuth = 45 degrees

Dip = 0

Rake = 0

To obtain multiple realizations of porosity maps, hard data of porosity and variogram model for porosity are used as input in the sequential Gaussian simulation (SGSIM) geostatistical program (Deutsch & Journel 1997). This simulation reproduces the histogram of the hard data, and honors spatial variability of the property (variogram).

Figure 6-1 shows one of the porosity models for reference data with 5 wells whose positions are shown as black dots:

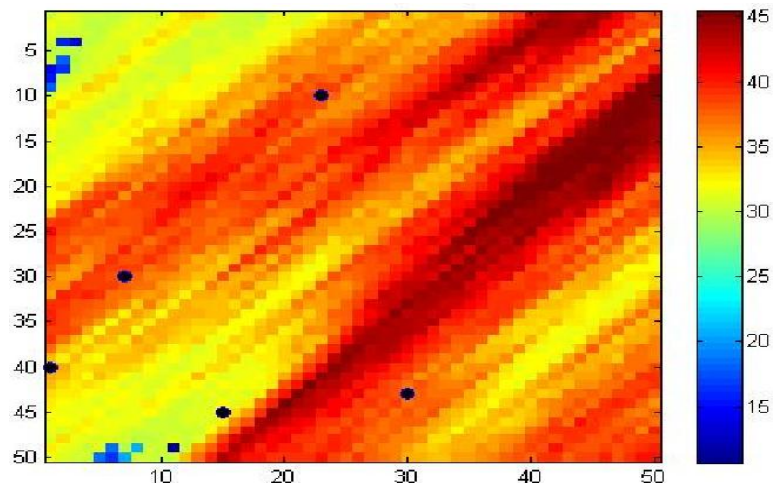


Figure 6-1: Porosity with reference data only

Scenario 2: Well data and Seismic

The primary data for porosity is the data at the five well locations. We generate secondary data which mimics seismic by taking the window average of any single porosity model that was developed under Scenario 1. Figure 6-2 shows a smoothed map which was used as seismic data:

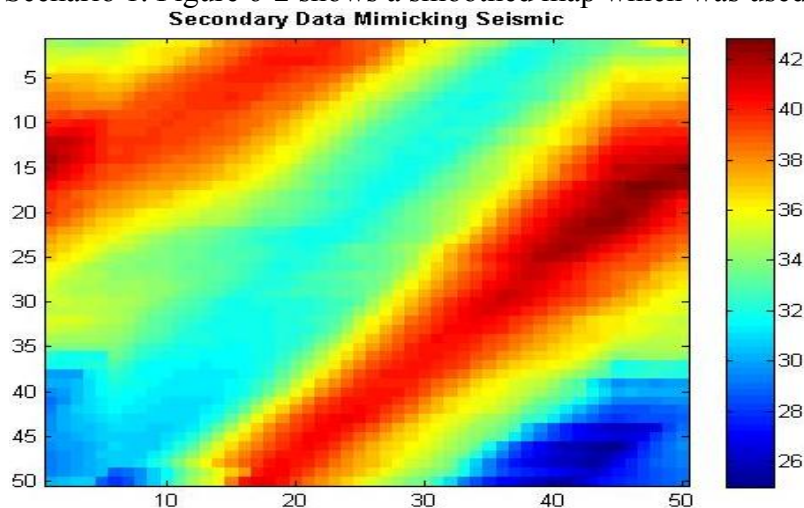


Figure 6-2: Seismic map on a 50 x 50 x 1 grid scale

To obtain multiple realizations of porosity maps after conditioning extra information through secondary information which mimics seismic, primary hard data of porosity and secondary seismic data along with variogram model for porosity are used as input in COSGSIM geostatistical program (Xu et al., 1992) (Xu et al. 1992). The correlation between primary and secondary variables was assumed to be 0.6. A Markov model was assumed for the co-simulation. Under this Markov assumption, only the variogram of the primary variable is required. The cross-variogram between the primary and secondary data is then proportional to the primary variogram with a scaling function that is related to the correlation coefficient between the primary and secondary variable (Xu et al. 1992).

The porosity variogram model for Scenario 2 is similar to the variogram model for Scenario 1.

Figure 6-3 shows one of the porosity models after integrating the seismic information with the reference data. The black dots represent the position of the 5 wells, which act as the primary or “hard” data.

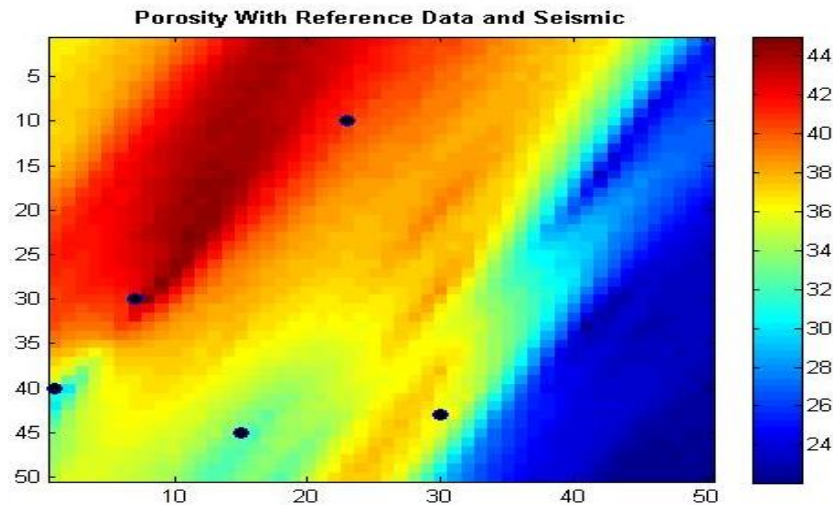


Figure 6-3: Porosity with reference data and seismic

NPV DISTRIBUTION FORECAST

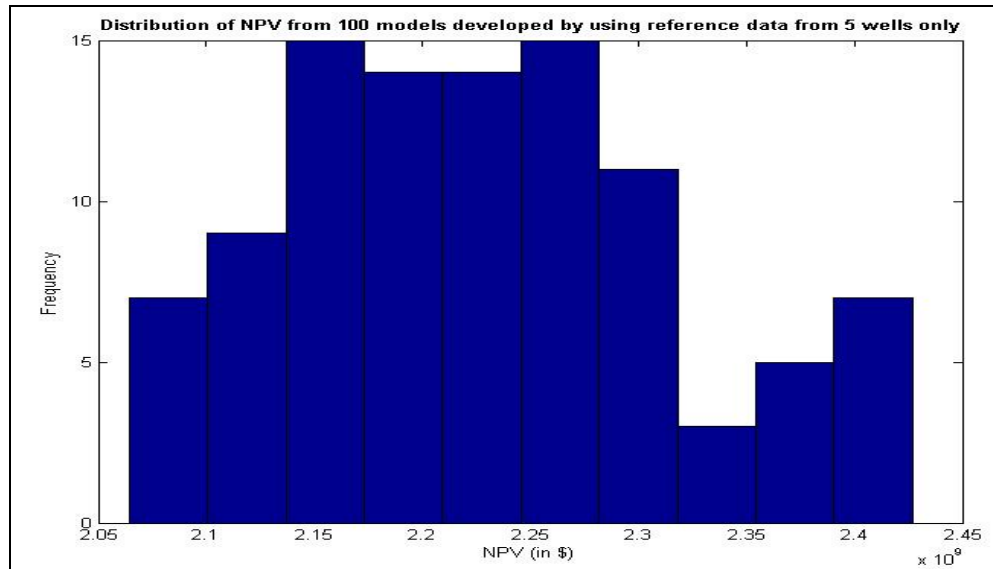
In earlier section we described how to determine recoverable reserves from the reservoir. Using those recoverable reserves and price of oil (constant value of \$70/barrel) we can estimate the Net Present Value (NPV) from the reservoir as follow:

$$\text{NPV(in \$)} = \text{Recoverable Reserve (in bbl)} \times \text{Price of oil (in \$/bbl)}$$

By using multiple realizations of the porosity models we obtain as many NPV values as there are porosity models. Thus, we can find P10, P25, P50, P75, and P90 from the distribution of NPV values. Figure 6-4a and 6-4b show the histogram of the NPV values corresponding to scenario 1 and scenario 2, respectively. The NPV distribution consists of possible economic values before we start producing from the field i.e. economic value of oil reserves that have been discovered but not yet developed.

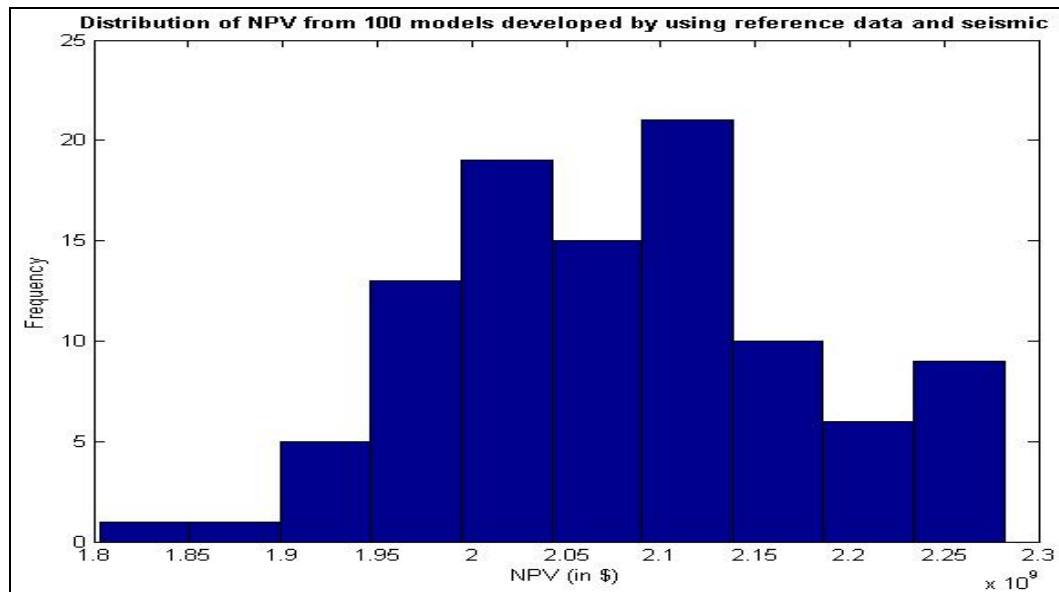
Figure 6-5 compares the P10, P25, P50, P75, and P90 values from the two scenarios.

Scenario 1: Conditioning data at only 5 wells



(a)

Scenario 2: Well data plus Seismic



(b)

Figure 6-4: Distribution of NPV values for a) Scenario 1. The reservoir models have been generated conditioned to only 5 well data; b) Scenario 2. The reservoir models have been generated conditioned to 5 well data and the pseudo-seismic data

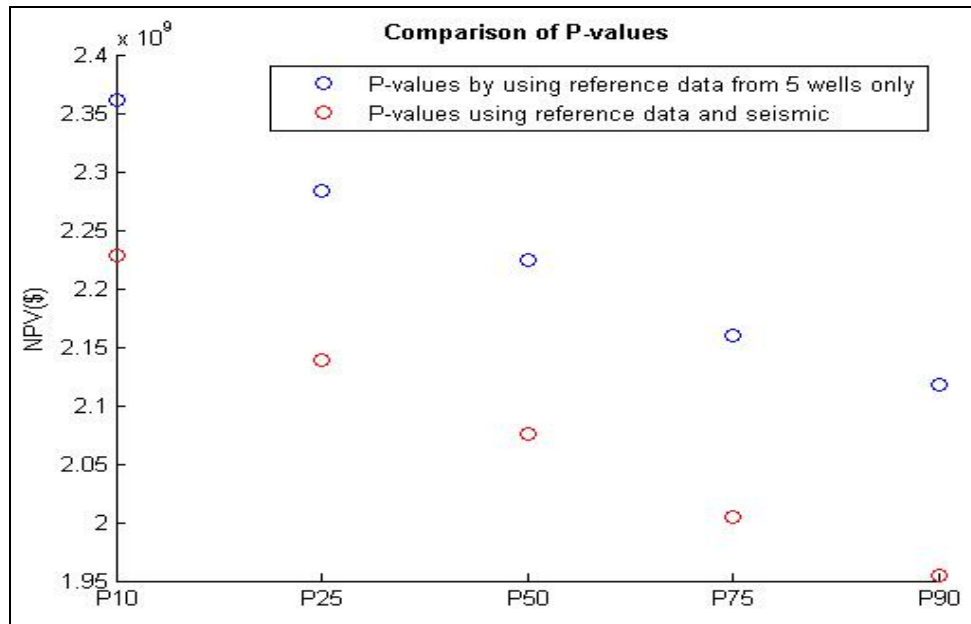


Figure 6-5: P10, P25, P50, P75, and P90 values retrieved from the NPV distribution for Scenario 1 and Scenario 2.

We can see from Figure 6-4a and b that the effective width of the NPV distribution, reflective of the geologic uncertainty decreases after integrating the seismic data. Figure 6-5 shows that the P-values of NPV distribution obtained after acquiring seismic has decreased slightly from base case with reference data only. This indicates that seismic did not bring sufficient reservoir information over the base case with reference data either in terms of adding value or decreasing uncertainty.

We want to incorporate the uncertainty represented by the NPV into the Binomial Lattice Option Valuation (BLOV). BLOV takes a single value of the NPV as input in the starting node of the underlying lattice. To forecast how this total NPV may change over the option time period before we take a decision to invest, we must estimate the project volatility and use it to construct the BLOV model.

OPTION VALUATION BY BLOV

A binomial lattice at each node moves along only two possible paths for each time step – up or down i.e. increase or decrease in value of the lattice, respectively. The process of option valuation involves first moving forward to form a lattice of the underlying asset, and in the second step working backwards through the lattice from the end nodes (at the expiration date) towards the first starting node to form a final option valuation lattice. Shown below is an example of how the underlying lattice and option lattice, respectively, were constructed.

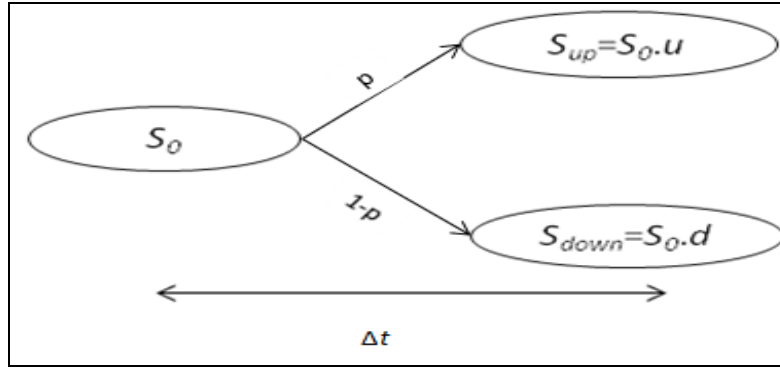
STEP 1: Creating Lattice of the underlying asset

At each step the value of the underlying asset will increase or decrease by a factor of u or d respectively ($u \geq 1$ and $0 < d \leq 1$), per time step of the lattice. Left most node containing S_0 (which is usually taken to be the P50 of NPV distributio) is the current price, then in the next time step the price will either go up or go down i.e. $S_{up} = S_0 \cdot u$ and $S_{down} = S_0 \cdot d$ respectively. The factors u and d are functions of the volatility of the underlying asset and the time step between each column of the lattice. They are calculated from following formulae:

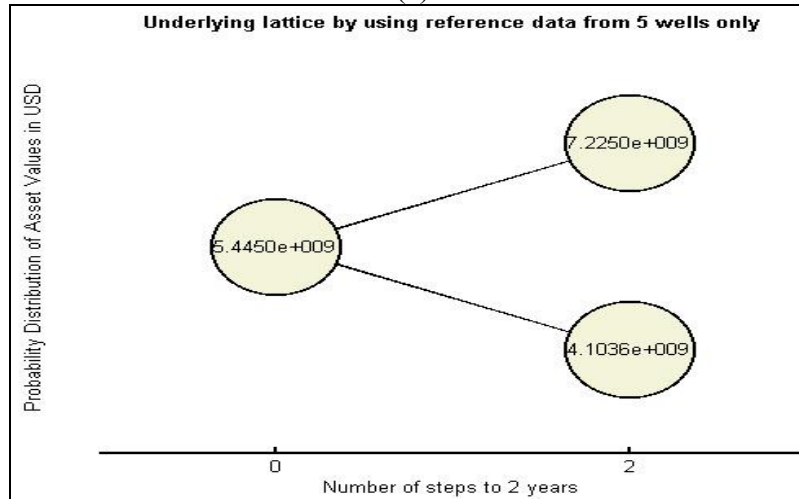
$$u = e^{\sigma\sqrt{\Delta t}} \text{ and } d = \frac{1}{u} = e^{-\sigma\sqrt{\Delta t}}$$

where, σ is the project volatility.

The project volatility is assumed to be constant for lattice construction in this study to keep the construction of lattice process simple. The probability of the asset value going up is designated as p which means that the probability of the value going down is $1-p$. This illustration for single time step is shown in Figure 6-6a and its corresponding lattice for Scenario 1 is shown in Figure 6-6b:



(a)



(b)

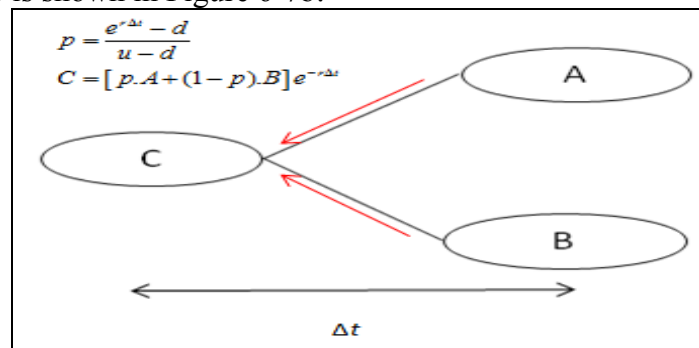
Figure 6-6: a) Illustration for constructing lattice of the underlying asset; b) Calculation of underlying asset value using 5 well data for 1 time step.

In similar fashion we can compute value of the underlying asset at each time step to develop a full lattice for the entire life of the reservoir. This underlying asset lattice shows how the value of the reservoir reserves change with time from the date of lease acquisition.

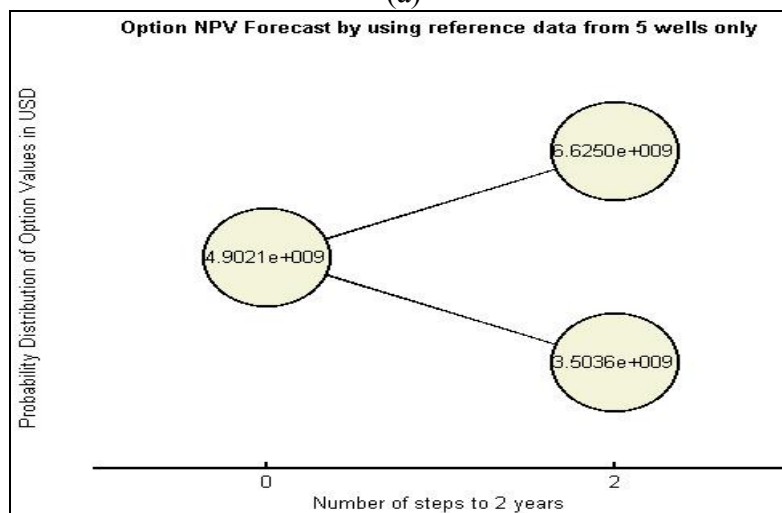
STEP 2: Creating Option Valuation Lattice

At each node in the terminal branch of the underlying lattice, i.e. the nodes at the expiration date, the option value is calculated as $Max[(S_n - K), 0]$, where K is the capital expenditure for

developing the asset and S_n is the asset value at the date of expiration. Now starting from these values in the terminal nodes, we work backwards towards the first node of the lattice to obtain the value of the option at each node. We can now value the asset's option at the date of interest using the parameters p , u and d . We use the future payoffs in two adjacent nodes behind the node at the date of interest and calculate the expected value by weighting them with their respective probabilities. This illustration for single time step is shown in Figure 6-7a and the corresponding lattice for Scenario 1 is shown in Figure 6-7b:



(a)



(b)

Figure 6-7: a) Illustration for constructing option valuation lattice; b) Calculation of option valuation lattice using 5 well data for 1 time step.

In similar fashion we can compute option valuation lattice at each time step to develop a full lattice for entire life of the reservoir. It can be seen the difference in values of underlying lattice and option lattice which occurs because of the capital expenditure (~ \$600 million) subtracted from the underlying asset values at the terminal nodes and then exercising backward induction. In this particular case study the revenue is much greater than the expenditure because the revenue is based on original oil in place for the entire field which in this case is quite large while the expenditure is considered for drilling only 5 wells.

The option lattice shows the distribution of option values, at each time step, to develop the reservoir. The option value corresponding to the undeveloped reservoir is shown in the left most node of the underlying asset's lattice. We can value the option at the end of the lattice starting from year 20 and doing backward induction using risk-neutral binomial option valuation. Under risk neutrality assumption the investor is indifferent to the risk involved and is only interested in expected value which is calculated from later two nodes as shown in Figure 6-7a. The management can either accept an option value at some point to develop the reservoir based on the information they have, or they can decide to opt for further information which will require investment and base their decision on option analysis done with the new information. We have presented two scenarios for data acquisition for improving the reservoir model. For both the scenarios at the termination of the project (year 20), the value of the option equals the maximum of 1) Profit from reservoir after investing in development, or 2) Zero when no investment is made for development of the reservoir. Thus, by construction, the option value cannot be negative.

RESULTS AND DISCUSSIONS

As we have multiple realizations of the NPV for the same reservoir, therefore we can compute P-values of the NPV distribution. The left most node in the lattice of the underlying contains the weighted average of the P-values of the NPV. Following each scenario there are two figures. Figures 6-8 and 6-10 represent lattice of the underlying asset and Figures 6-9 and 6-11 represent option valuation lattice.

Scenario 1: Well data only

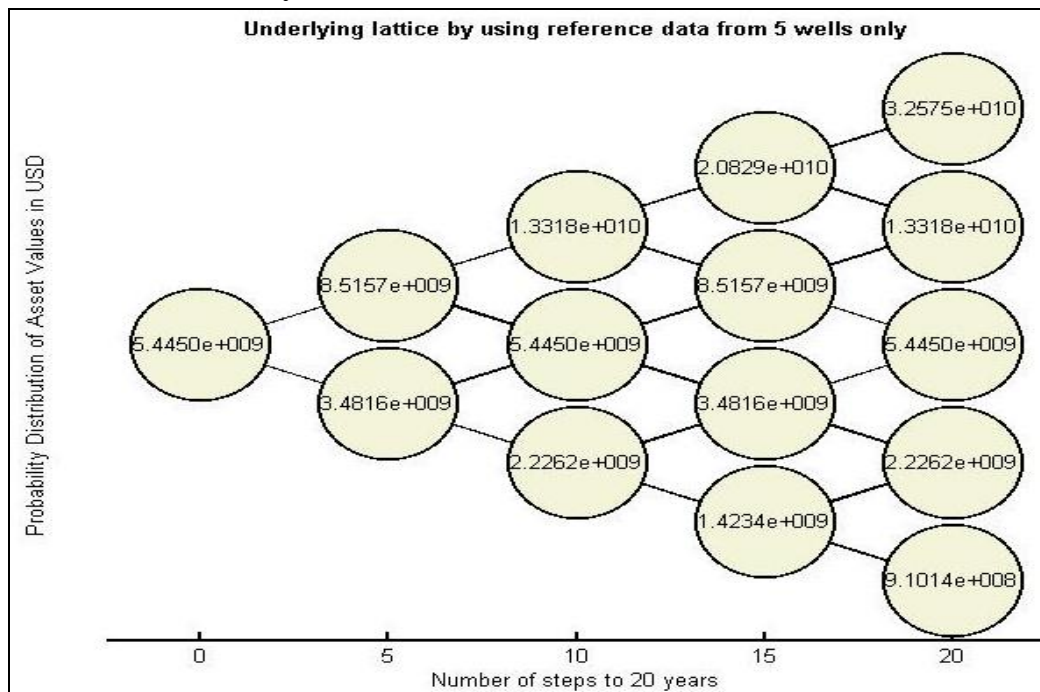


Figure 6-8: Lattice of the underlying asset with reference data only

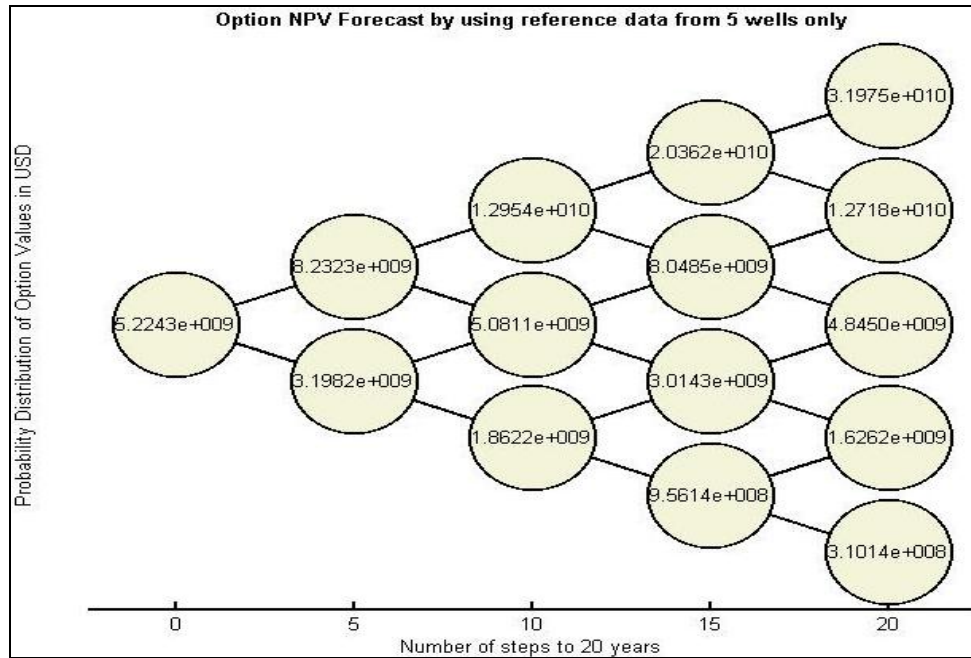


Figure 6-9: Option valuation lattice with reference data only

Scenario 2: Well data and Seismic

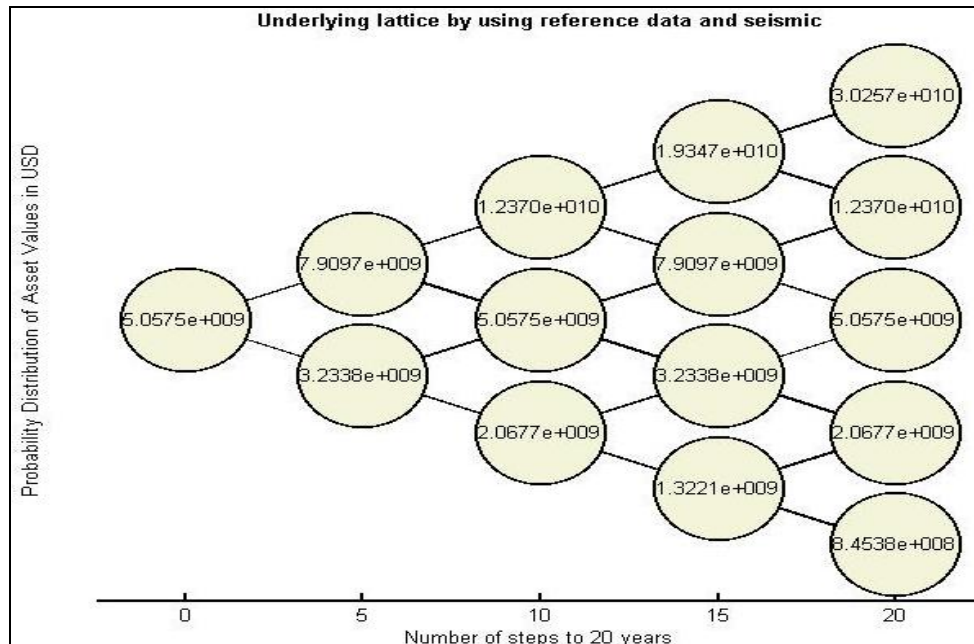


Figure 6-10: Lattice of the underlying asset with reference data and seismic

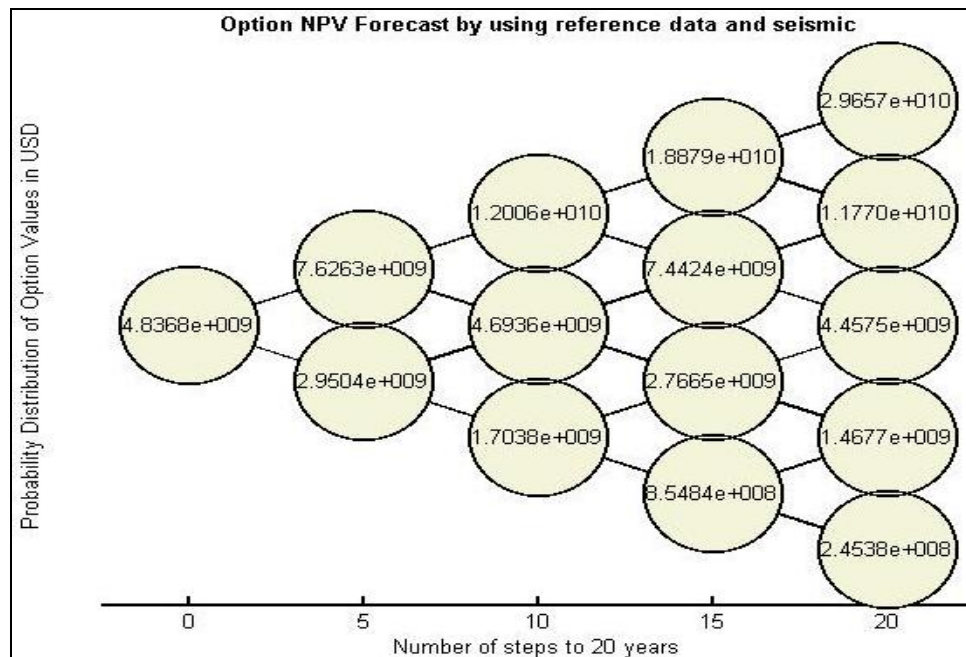


Figure 6-11: Option valuation lattice with reference data and seismic

In Figures 6-9 and 6-11, representing option valuation lattice, the value in the left most node of the lattice is the option value at the start of the project when there is maximum uncertainty or aggregated volatility. It can be seen the difference in values of underlying lattice and option lattice (approximately ~ \$100 million) is significant even without acquiring seismic. There is no significant improvement in option value after acquiring seismic which can be seen by subtracting option values from left most nodes of option lattices in Figures 6-9 and 6-11.

In the previous calculations, we computed the weighted average of the NPV distribution with the probability of each NPV value acting as the weight and used that average as the starting value in the left most node of the underlying asset. However, we can also represent the uncertainty of the NPV distribution more appropriately if we compute the option value corresponding to each NPV

value sampled from the distribution of NPV values. This will result in a distribution of option values at each node and we can then display some critical option values corresponding to a few critical probability values. Figure 6-12 shows option values obtained corresponding to P10, P25, P50, P75 and P90 values.

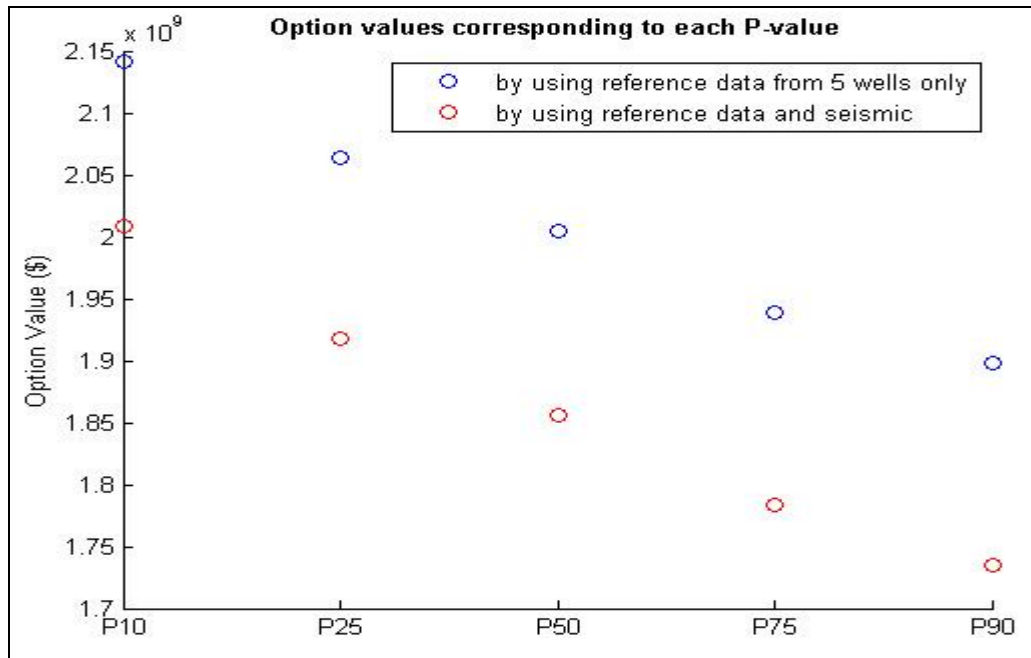


Figure 6-12: Uncertainty in option values generated using P-values of the NPV

We did not add the cost of acquiring the seismic when we did the calculation of NPVs for Scenario 2. In other words we have evaluated solely the economic impact of uncertainty reduction due to integration of seismic. An approximate indication of the maximum cost of acquiring seismic could be determined by subtracting the forecast of option value without seismic from the forecast of option value with seismic. However, the value of the reserve in this particular case study is so large such that it overwhelms any pragmatic value of capital expenditure. The maximum amount that could be invested in acquiring seismic can be obtained

from the Figure 6-12 by subtracting the red colored circle values from their respective blue colored circle values.

The profitability of the field after investing in development costs increases with the increase in option value. In this case study acquiring seismic over and above existing well data did not improve the option value (the profitability) or decrease uncertainty of the field. Based on the results of this specific case study it can be seen that it is hard to improve on value of a large project. In other words, using seismic to firm up porosity estimates does not seem to work in large fields.

Chapter 7: Uncertainty Analysis by Model Selection and Economic Evaluation Using a Binomial Lattice

INTRODUCTION

In general, geological uncertainty analysis implies multiple spatial realizations of geological attributes using stochastic spatial simulation. These multiple realizations represent the spatial variations of the reservoir attributes. Processing these realizations through a transfer function model yields the uncertainty in flow response of the reservoir.

In integrated risk assessment studies, the uncertainty from one aspect of the study is carried to another aspect, and gets aggregated. A model selection framework does the work of refining an initial suite of reservoir models to a final set of reservoir models that depict production characteristics close to the observed field history. In this chapter we present a model selection algorithm which attempts to group reservoir models based on the common connectivity characteristics exhibited by them and then retrieves the group exhibiting characteristics that are closest to the observed response for a reservoir. The model selection technique is thus an efficient way to reduce number of realizations and save computational time for doing uncertainty analysis, and yet be optimally constrained to the available data.

MODEL SELECTION ALGORITHM

We use the distance-metric based approach proposed by Bhowmik et al. (Bhowmik et al. 2010) for reservoir model selection. The method uses a proxy function to discriminate between models on the basis of their connectivity characteristics.

In this approach initially there are multiple realizations of subsurface spatial variables that reflect existing knowledge of possible geology and reservoir architecture. These models are analyzed with a proxy by injecting particles and tracking their movements through the grid. The movement of particles is influenced by a transition probability matrix that takes into account the permeability variations, elevation difference between adjacent nodes and current particle count in grid blocks. The proxy yields information regarding the particle arrival time models are grouped based on the proxy response and projected onto principal component axes for cluster analysis. The representative model for each cluster is run through full-physics simulator and simulation results are compared to field history to derive an updated probability of cluster. The updated probability is used to select a set of models that produce production characteristics close to the observed field history.

The following flowchart explains in brief the methodology for model selection.

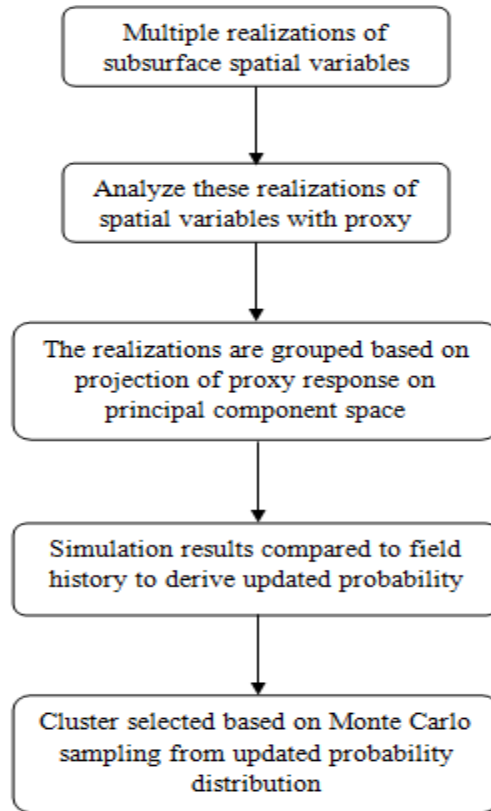


Figure 7-1: Algorithm for model selection by distance-metric approach

This approach to data integration and uncertainty quantification by model selection is especially amenable to real option valuation because parameters such as the volatility and up/down probability can now be calculated more reliably, compared to the initial suite of reservoir models, using the posterior set of models after completing the data integration procedure.

CASE DESCRIPTION

We have a reservoir with grid dimension of 200 x 200 x 1, and having 5 production wells. We start with an initial suite of 100 realizations for permeability and porosity. The objective of this study is to reduce the uncertainty in geological models by a model selection algorithm, and

subsequently apply the binomial lattice option valuation to compare the economics before and after data integration.

We want to reduce the uncertainty in the geological models, but we also want that reduction in uncertainty to be robust. In this case, we assume that well test data is available for two different wells. By assuming that the well test data are non-interfering, we implement the model selection algorithm two times, each time using the well test data for one well to obtain two sets of geologic models. The final set of geologic models is selected by retaining the models that are common between the two sets. This procedure leaves just 4 sets of geologic models as opposed to a suite of 100 models when we started. Additional models that exhibit characteristics similar to the final set of models can be generated by retrieving spatial statistics (variogram or multiple point statistics) that are common to the models and common conditioning data values from the models. These models will share the production characteristics that are reflected in the final set of four models.

Finally, future hydrocarbon production rates are determined from the final set of geologic models and the reservoir's economic performance is assessed using the forecast of hydrocarbon production rates.

STATIC RESERVOIR MODELING

The hard data of porosity and permeability from the 5 production wells are sampled from the reference. Porosity and permeability maps are developed using SISIM program, which is a variogram-based geostatistical simulation technique. As input to the SISIM simulation program, we use 5 hard data sampled from the reference data. The variogram model is developed using

105 sampled data from the reference, which includes the data from 5 wells locations as well, corresponding to the median threshold. The hard data as well as the semivariogram models for porosity and permeability, respectively, are given in Table 7-1:

Table 7-1: Hard data of porosity and permeability from 5 reference wells

X	Y	Z	Porosity (%)	Permeability (md)
170	150	0	29	521
130	75	0	19	4
70	10	0	17	8
40	100	0	29	529
20	180	0	19	8

Shown in Figure 7-2 is an isotropic model fit (black line) fitted on the experimental variograms (red points) of porosity in various directions:

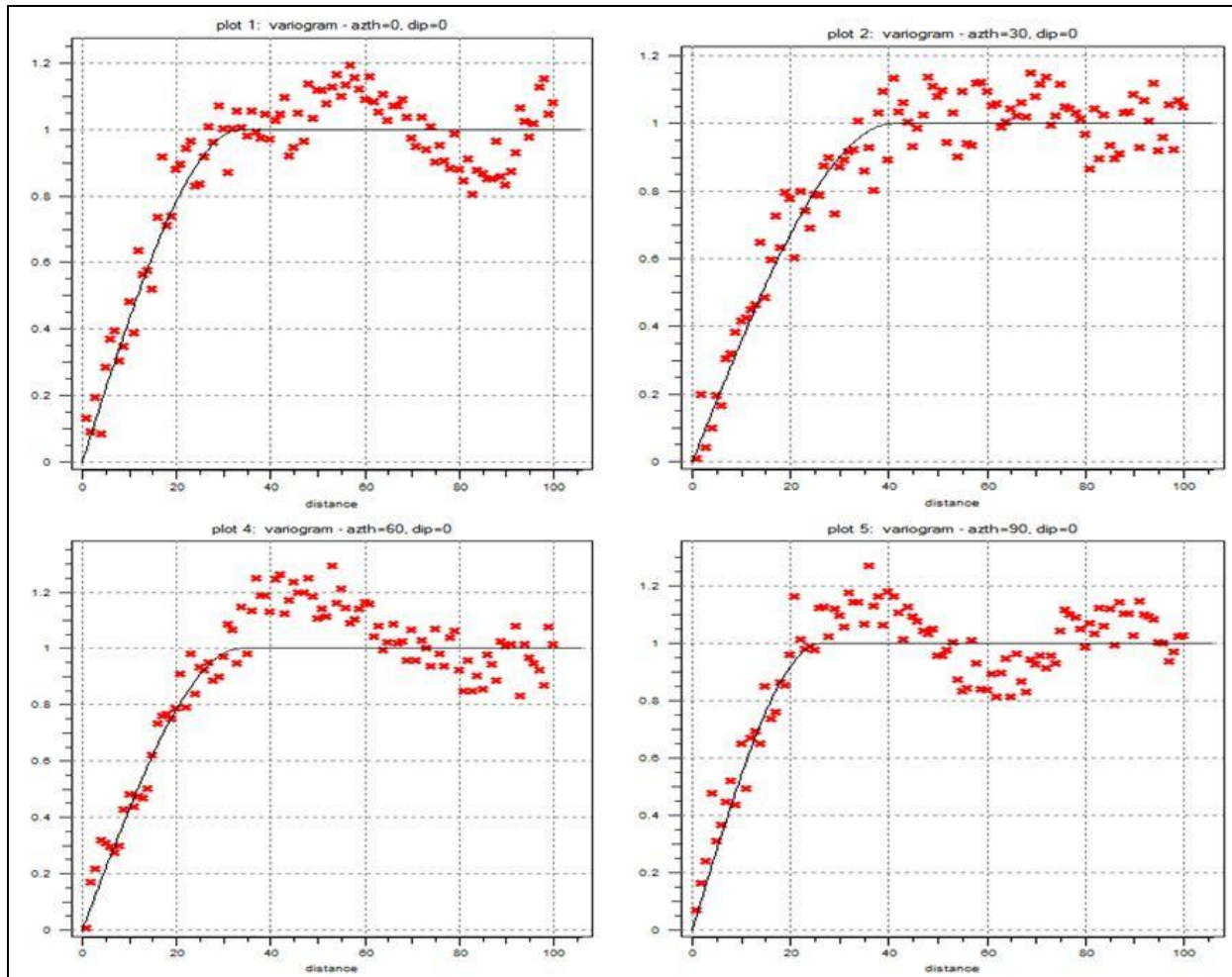


Figure 7-2: Isotropic model fit (black) for experimental variograms (red) of porosity in various directions

An isotropic model fitted to experimental variograms of porosity is:

Number of Structures = 1

Type = Spherical

Nugget Effect = 0

Max., medium, and min. range = 41, 24, and 24 units

Azimuth = 30

Dip = 0

Rake = 0

Similarly, shown in Figure 7-3 is an isotropic model fit (black line) fitted on the experimental variograms (red points) of permeability in various directions:

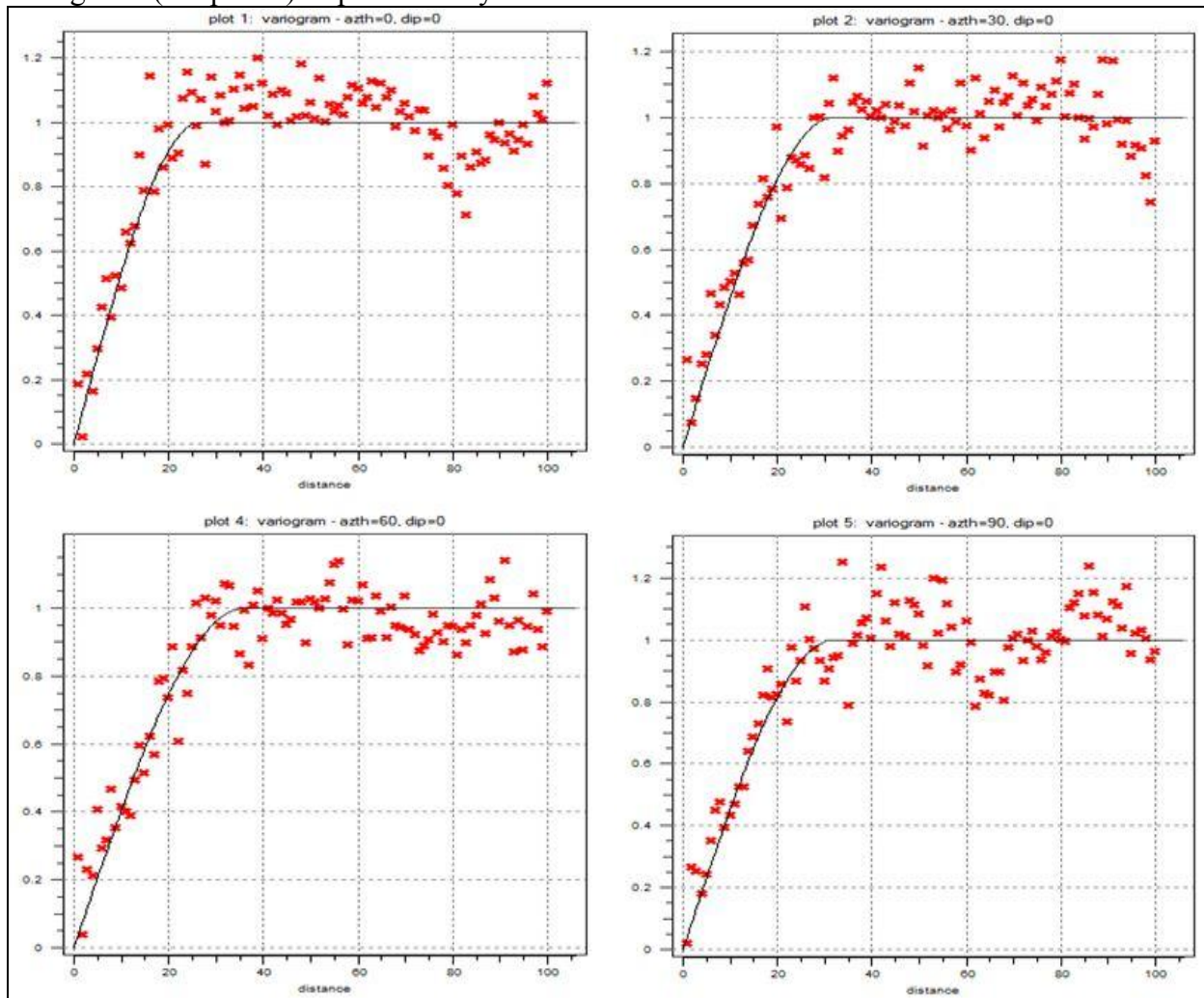


Figure 7-3: Isotropic model fit (black) for experimental variograms (red) of permeability in various directions

An isotropic model fitted to experimental variograms of permeability is:

Number of Structures = 1

Type = Spherical

Nugget Effect = 0

Max., medium, and min. range = 36, 25, and 20 units

Azimuth = 60

Dip = 0

Rake = 0

To perform indicator simulation, three threshold values with corresponding marginal probabilities were specified for permeability and porosity, respectively, as shown in Table 7-2:

Table 7-2: Threshold values of permeability and porosity with their corresponding marginal probabilities

Spatial Variable		Marginal Probabilities	
Permeability (in md)	Porosity (in %)	For Permeability	For Porosity
500	10	0.2	0.1
1000	20	0.6	0.4
1900	40	1	1

These threshold values along with their corresponding marginal probabilities are used to yield a discrete estimate of the conditional cumulative distribution function at these values. Using the conditioning hard data, threshold values along with their marginal probabilities, and variogram model as input in the SISIM program, 100 realizations each of porosity and permeability are generated. The porosity ranges from 8% to 34% and permeability ranges from 4 md to 1900 md. Figure 7-4 shows one realization each of porosity and permeability, and Figure 7-5 shows some of the initial suite of models:

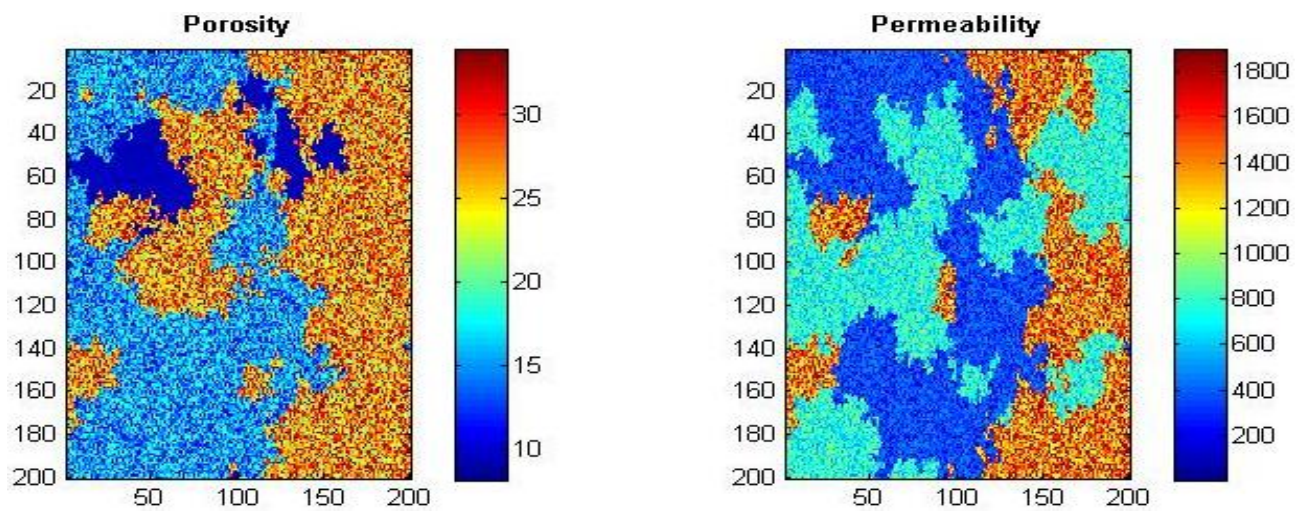


Figure 7-4: Single realization for each porosity (%) and permeability (md)

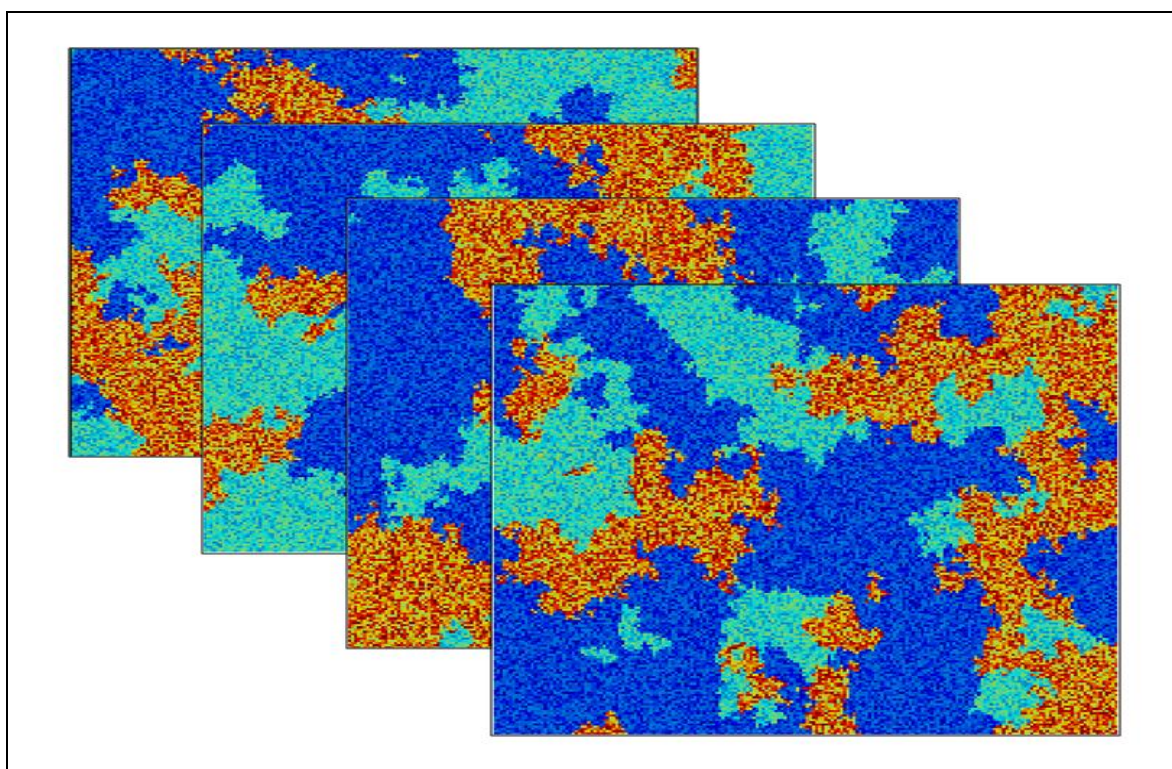


Figure 7-5: Multiple realizations of permeability field

WELL HISTORY

Figure 7-6 shows the reference reservoir model as viewed in CMG with a grid dimension of 200 x 200 x 1. This reservoir model will be used to simulate results for field history. There are five production wells which are assumed to produce hydrocarbons through natural water drive without the need of any injectors. The wells are located at the locations shown in Table 7-3:

Table 7-3: Locations of 5 wells

Well Locations		
X	Y	Z
170	150	1
130	75	1
70	10	1
40	100	1
20	180	1

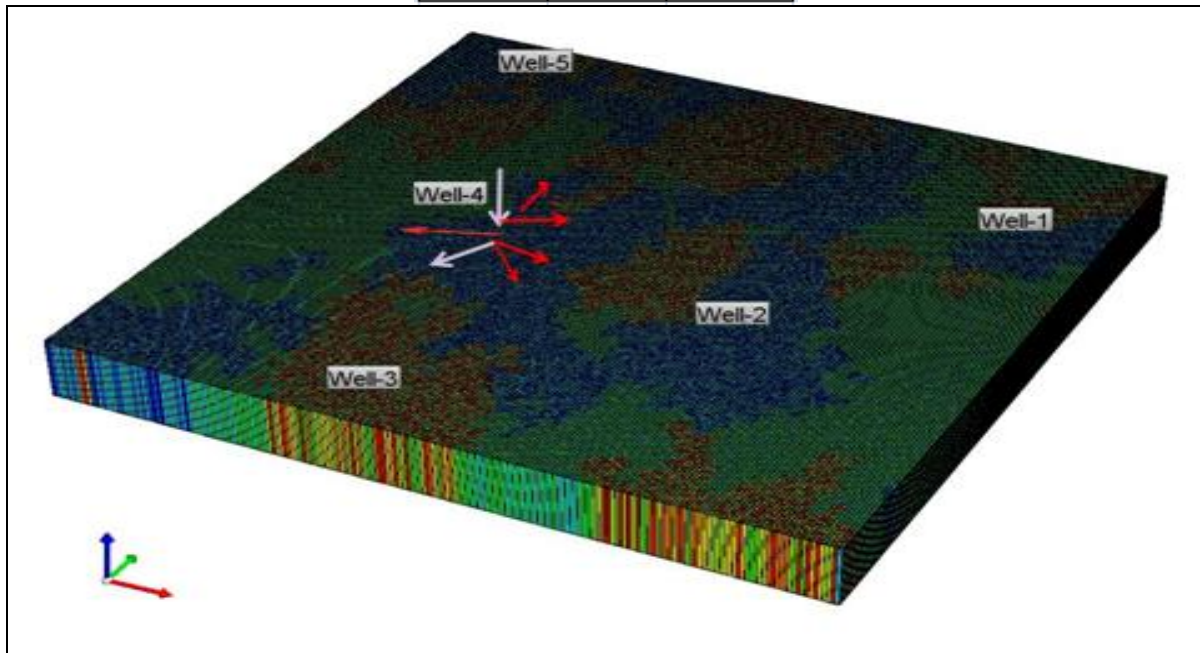


Figure 7-6: Reservoir model setup in CMG for flow simulation.

The well history data is simulated in the form of drawdown and buildup well tests. Out of the five wells in our reservoir, well-1 and well-2 were chosen for well testing. Each well undergoes both drawdown and buildup tests. The well test procedure was implemented exactly as was done for both the wells. For the first 25 days well-1 is set open to mimic drawdown test while well-2, well-3, well-4, and well-5 are shut in. Following the drawdown test, well-1 is shut in for 8 days. The other wells - well-2, well-3, well-4, and well-5 are still assumed to be shut-in. The first set of well history data for well-1 is obtained from this back-to-back drawdown and buildup tests. Similarly, the second set of field history data is obtained for well-2 by producing just from well-2 for 25 days and then shutting it in for 8 days along with other wells.

The bottom-hole pressures corresponding to drawdown and buildup well tests are shown in Figures 7-7 and 7-8 and these are used as two sets of history data for the model selection procedure.

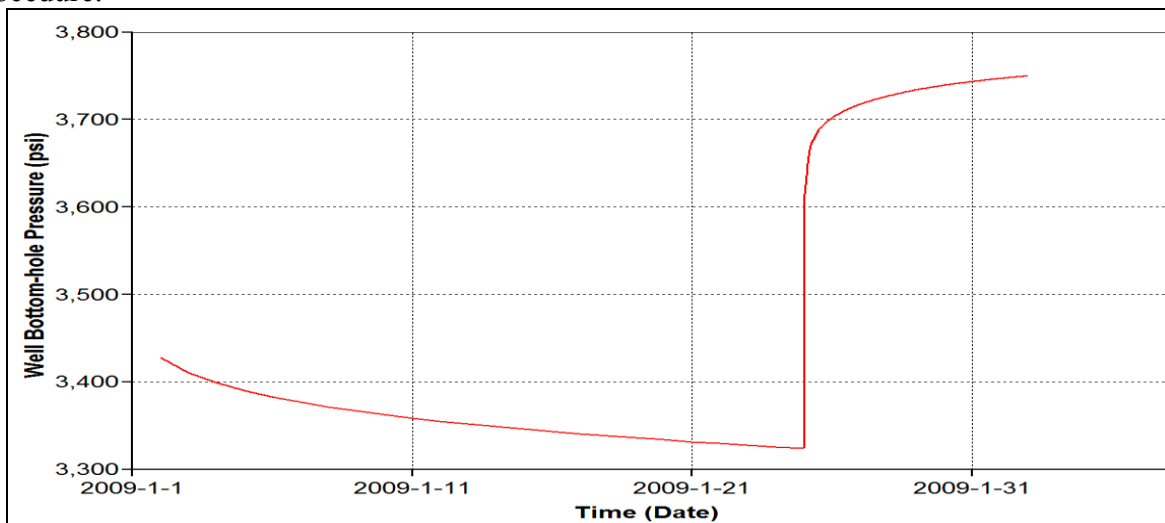


Figure 7-7: Well bottom hole pressure during drawdown and buildup well test for well-1

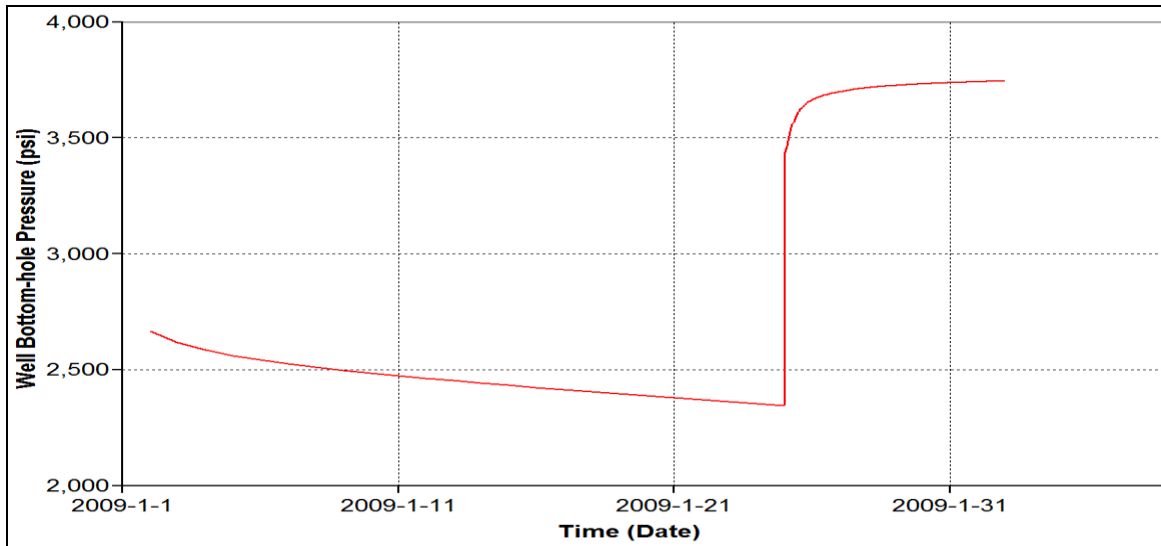


Figure 7-8: Well bottom hole pressure during drawdown and buildup well test for well-2

A particle tracking algorithm that mimics the propagation of the pressure wave during a well test was used as the proxy to assess the flow response of the models in the prior set. Details of this proxy can be found in Bhowmik et al. (Bhowmik et al. 2010).

FINAL SET OF MODELS BY MODEL SELECTION ALGORITHM

After applying the model selection algorithm on the initial suite of models we obtain 5 models for each set of field history data. Out of these 10 total models in the final set, 4 are common. These four models exhibit similar well test characteristics for well – 1 and 2 as observed in the reference.

The reduction of the prior set of 100 models to just 4 models is quite significant. These selected models will not only carry the same statistics from the suite of prior models, but they will also have the same flow characteristic as the prior models. Figure 7-9 shows the uncertainty in future hydrocarbon production rates for 20 years both prior to and after model selection. The

uncertainty in production rates represented by 100 realizations (in blue legend) before model selection reduces to in the spread indicated by the red legend.

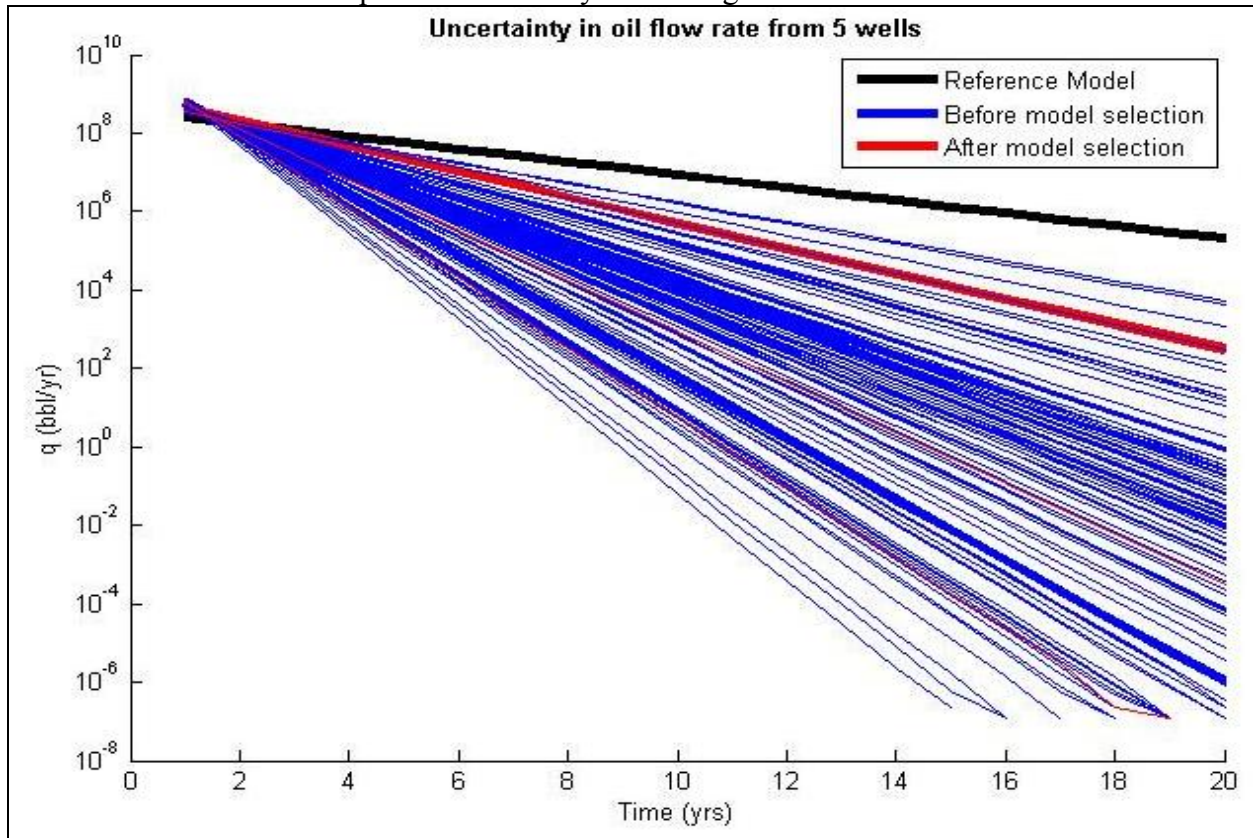


Figure 7-9: Uncertainty in oil flow rates from the reservoir before and after model selection

The oil rate predicted by the final set of models is closer but not exactly the same as the reference. This is because the well test response recorded only at wells 1 and 2 were used for the model selection process and they are insufficient to capture the connectivity characteristics of the entire field. Consequently, the oil rate characteristics are not well represented by the models.

RESULTS

Net Present Value Calculation

We require the oil flow rate from the reservoir to estimate the Net Present Value (NPV). Once we know the flow rates, we can calculate the NPV of total oil production from the reservoir according to the following procedure:

Future Cash Flow in \$/yr : $F(t) = q(\text{in bbl/yr}) \times \text{price of oil}(\text{in \$/bbl})$

Present Value in \$/yr : $PV(t) = \frac{F}{(1+r)^t} - \text{opex}$

$NPV(\text{Net Present Value in \$}) = PV(1) + PV(2) + \dots + PV(20)$

In the above formulas, r is the discount rate (it should be at least inflation rate) assumed constant at 5%, and price of oil is also considered constant with value of \$70/barrel.

NPV Distribution Forecast

By using the multiple realizations of permeability-porosity models we obtain a distribution of NPV values. Thus, we can find P10, P25, P50, P75, and P90 from the distribution of NPV values and compare those before and after model selection. Figure 7-10 presents the histogram of NPV values before model selection and Figure 7-11 are the corresponding percentile values retrieved from that distribution. Figure 7-12 is the histogram of NPV values after model selection and Figure 7-13 presents the P-values of the NPV distribution after model selection.

The uncertainty represented by the NPV distribution, before and after model selection, is because of the uncertainty in geologic models. The forecast of flow rate prediction using models before model selection is quite wide and this is confirmed by the greater spread in NPV values (Figure 7-10). The forecast of flow rate prediction after model selection is narrower than flow rate prediction from initial suite of models and this is also confirmed by the tighter range of NPV distribution (Figure 7-12) after model selection compared to the the greater spread in NPV values before model selection .

Before Model Selection:

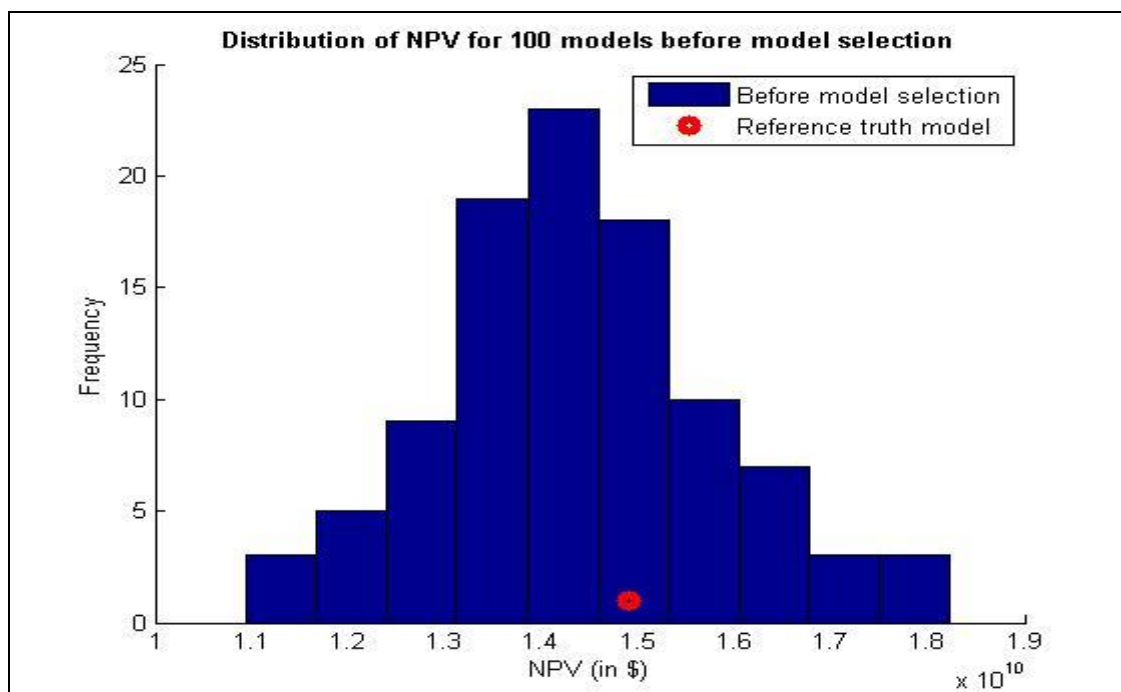


Figure 7-10: NPV distribution before model selection

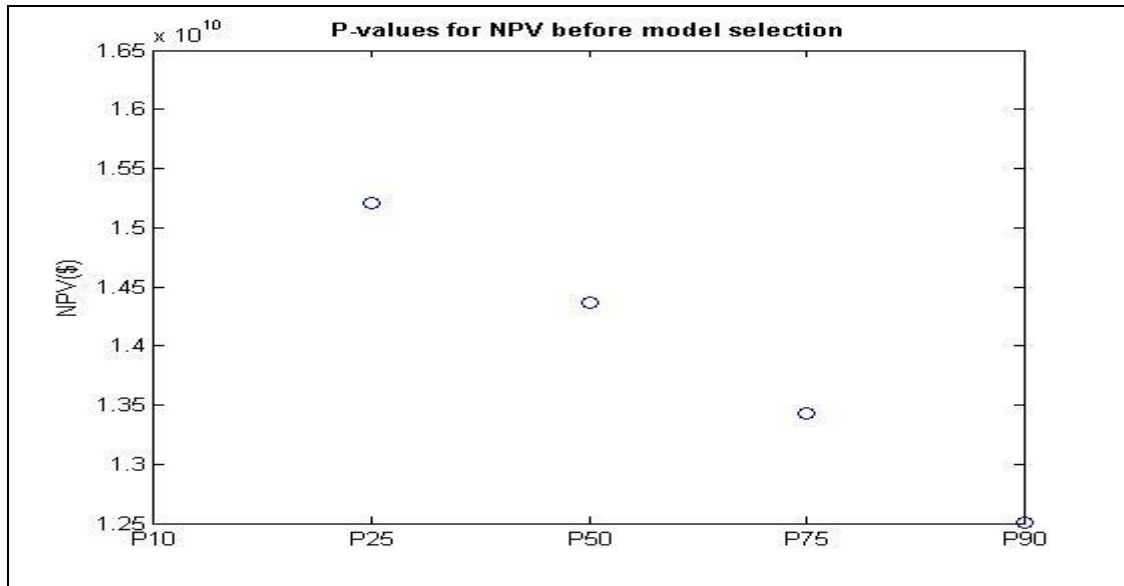


Figure 7-11: Key percentile values of the NPV distribution before model selection

After Model Selection:

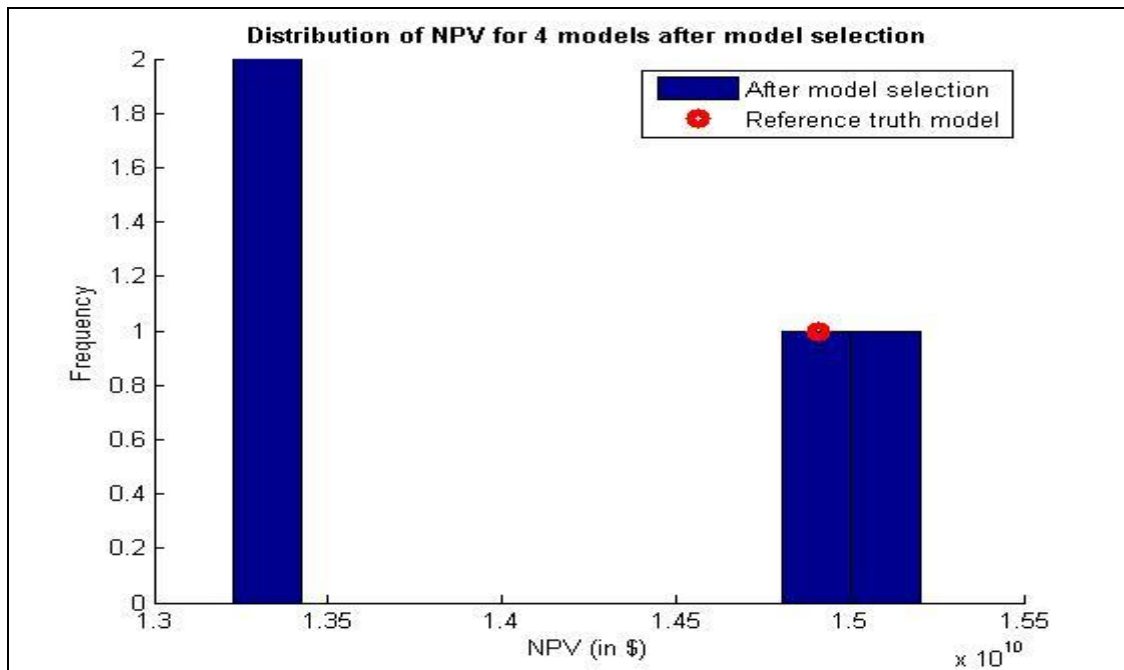


Figure 7-12: NPV distribution after the model selection

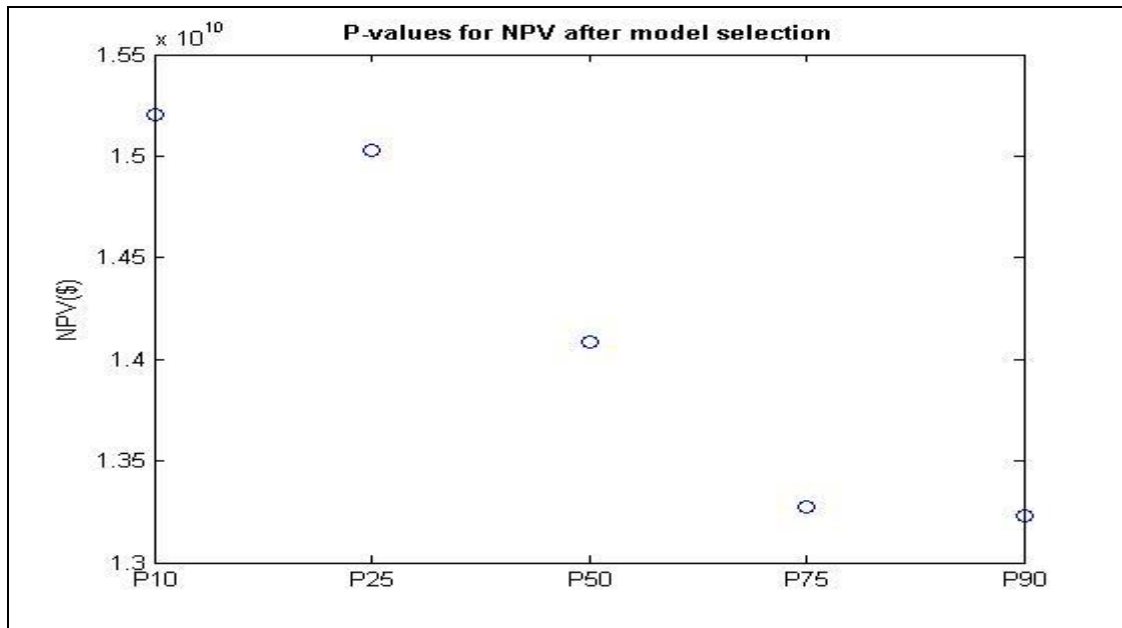


Figure 7-13: Key percentiles of the NPV distribution after the model selection

We want to incorporate the uncertainty represented by the NPV before and after model selection into the Binomial Lattice Option Valuation (BLOV). BLOV takes a single value of the NPV as input in the starting node of the underlying lattice. To incorporate the uncertainty from the NPV distribution, we take the weighted average of the P-values of the NPV distribution to come up with the NPV value at the starting node of the BLOV. This method of computing the single value of NPV, which will be used as input in the underlying lattice, incorporates the uncertainty before and after model selection.

Project Volatility

The future cash flows discussed under the NPV section will be used to compute the project volatility through the method explained in Chapter 2 and implemented in previous chapters.

This project volatility is one of the most critical parameter which is used as input in the real options model. We calculated the project volatility as following:

$$PV(t) = F(t) \times DV(t)$$

$$G = \ln \left[\frac{\sum_{i=1}^n PV_i}{\sum_{i=0}^n PV_i} \right]$$

$$\Rightarrow \sigma = std(G)$$

where,

PV_i = Present value at i^{th} year

$std()$ = Standard deviation

σ = Project Volatility

Figure 7-14 shows that the calculated time-varying project volatility decreases with time. The reason of decrease in project volatility with time is due to the fact that with time there is increase in prior data of the reservoir's economic performance (in terms of DCF). The project volatility for reference truth is developed using the 2nd realization of reference truth available. In total there were only two realizations of reference truth available, and the model comparison is done everywhere with the first realization of reference truth model.

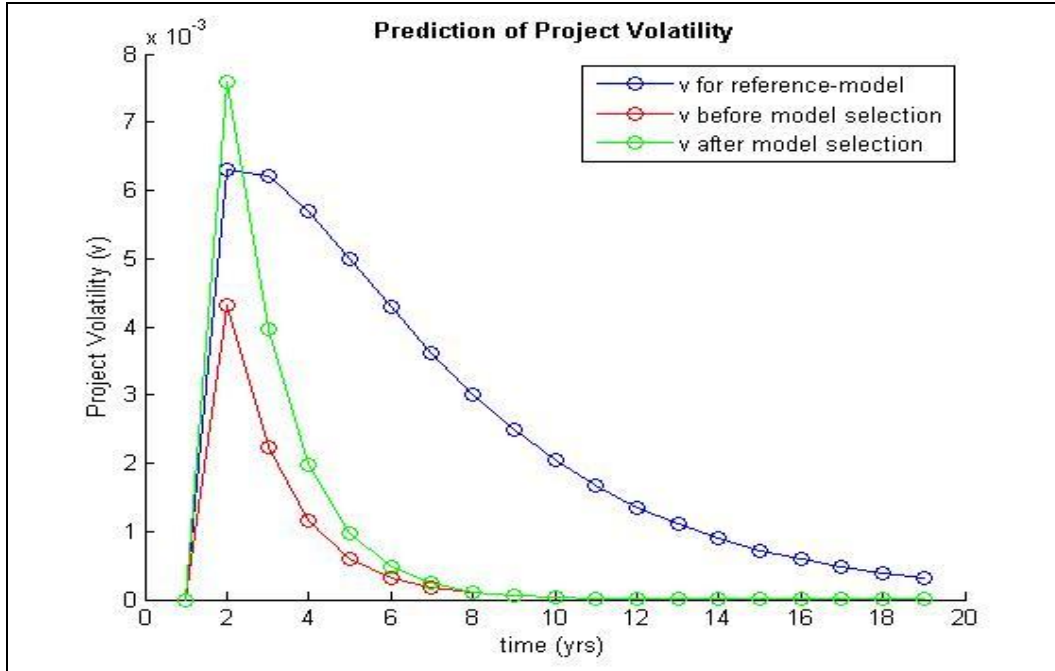


Figure 7-14: Variation of project volatility with time for models before and after selection, and reference truth

For BLOV, the volatility is assumed to be constant throughout the lattice construction. In our case we took the first value of volatility predicted at the second year for all the scenarios. This is a conservative estimate for the project volatility but one that simplifies the lattice generation for ROV calculations.

Option Valuation by BLOV

Figure 7-15 shows the lattice of the underlying asset for reference truth model while Figure 7-16 shows the option valuation lattice. Similarly, Figures 7-17 and 7-19 show the lattice of the underlying asset before and after model selection, respectively, while Figures 7-18 and 7-20 show their corresponding option valuation lattices, respectively.

The underlying asset lattice shows how the value of the reservoir reserves change with time. The left most node in the underlying lattice contains the weighted average of the P-values of the NPV. The lattice evolves into different values, either greater or smaller, with each time step. The multiple values at each time step represent the distribution of NPV values possible at that time. The option lattice shows the distribution of option values, at different time steps, which the company can use to decide about the management of the reservoir. As seen earlier the scenario after model selection presents less uncertainty than the scenario without model selection. The binomial lattice constructed after the model selection is not only less uncertain than the binomial lattice constructed before model selection but the option value for producing oil with 5 wells for 20 years from the reservoir is also higher indicating the incremental worth of using well production data for model selection.

Reference Truth

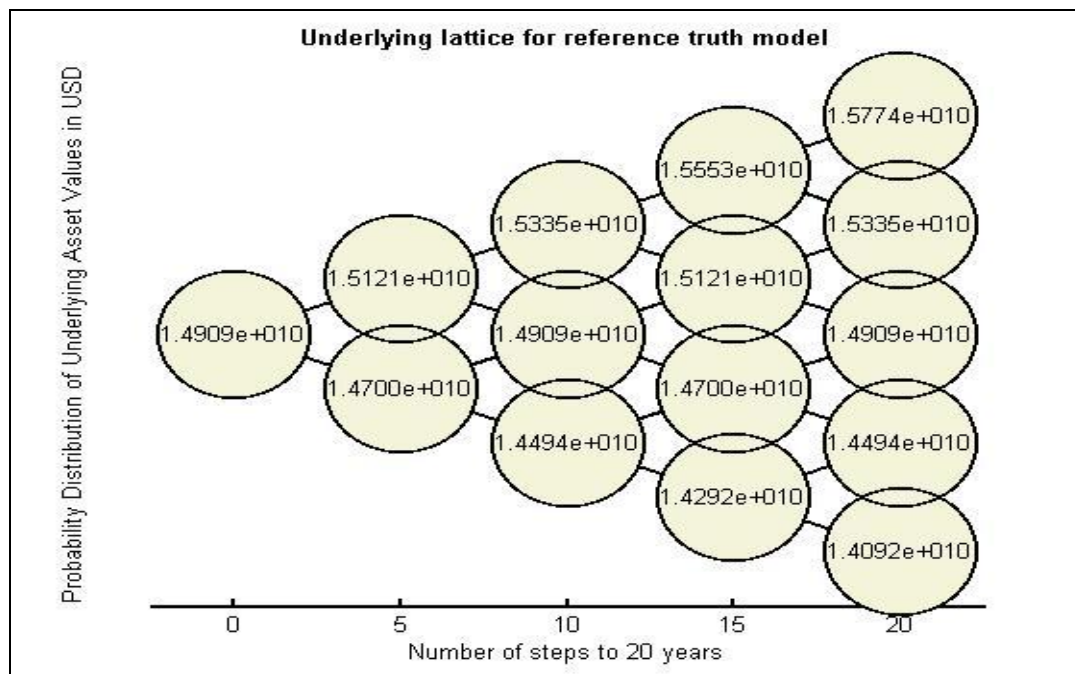


Figure 7-15: Underlying lattice of the reference truth model

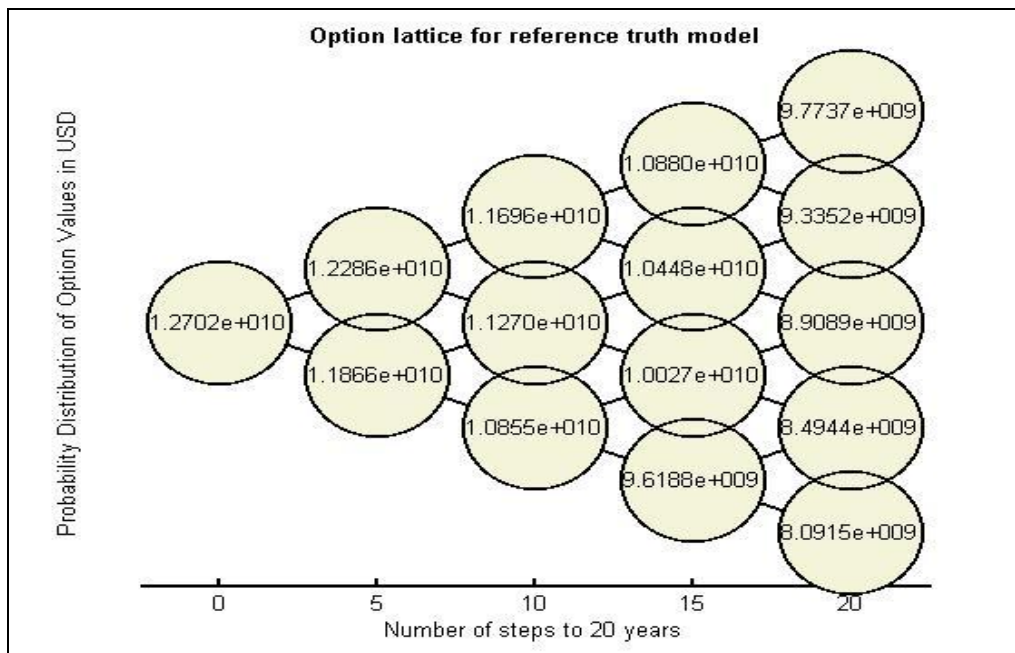


Figure 7-16: Option lattice of the reference truth model

Before Model Selection:

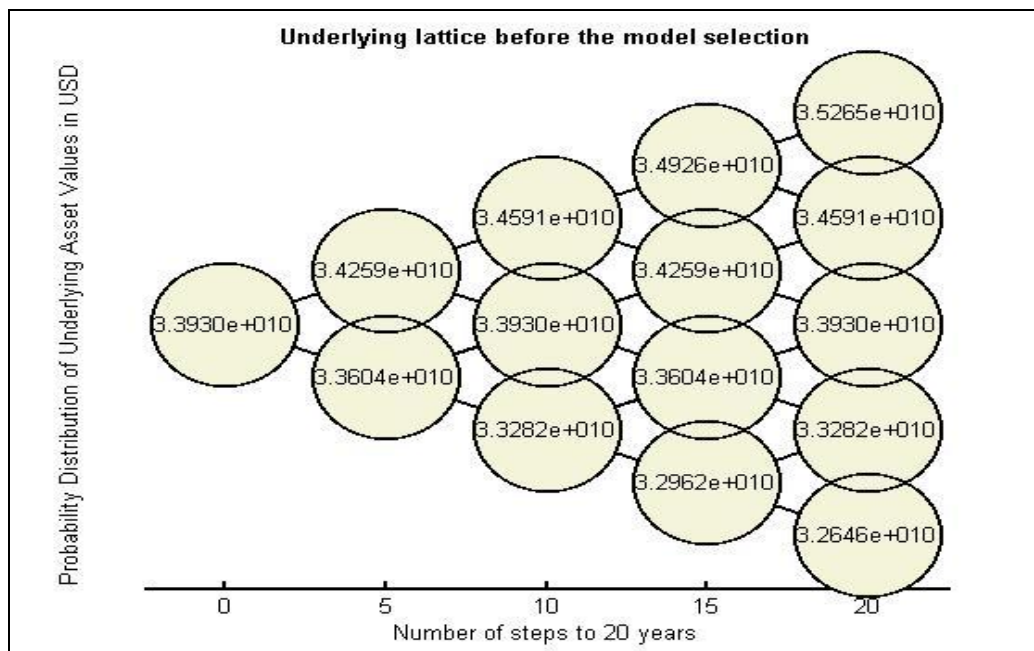


Figure 7-17: Underlying lattice before the model selection

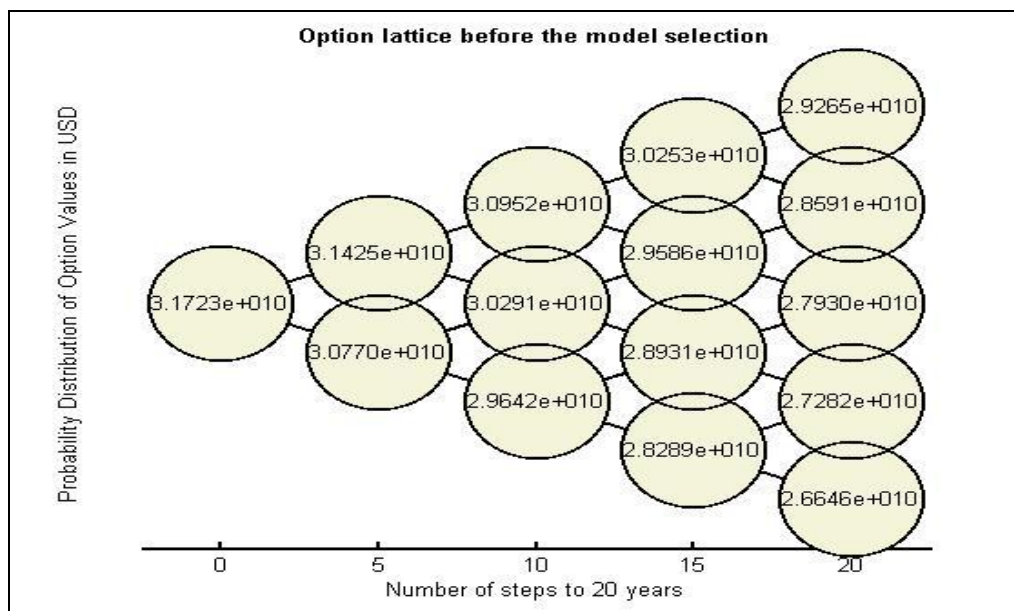


Figure 7-18: Option lattice before the model selection

After Model Selection:

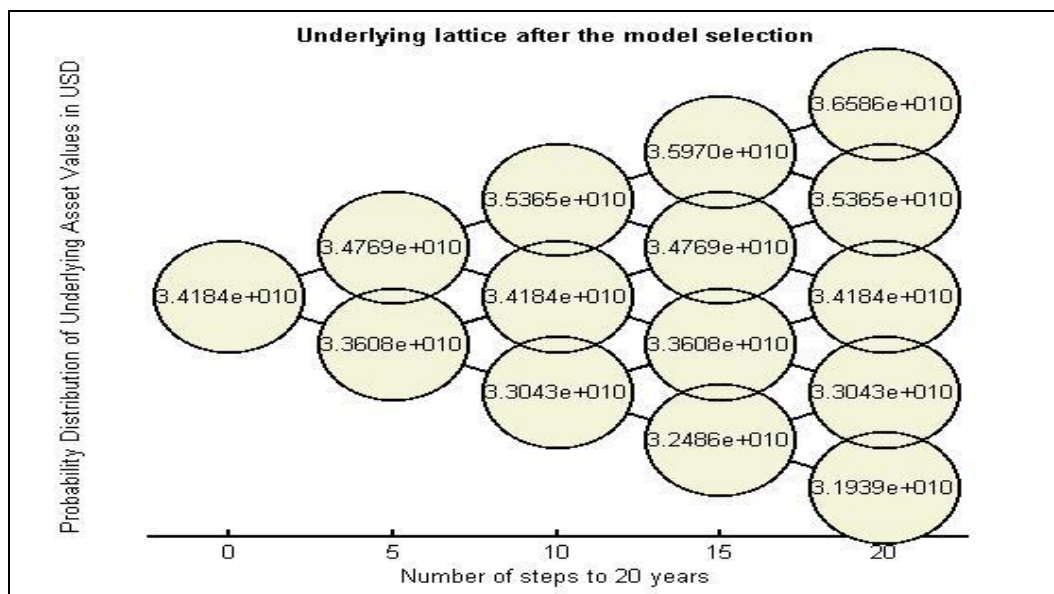


Figure 7-19: Underlying lattice after the model selection

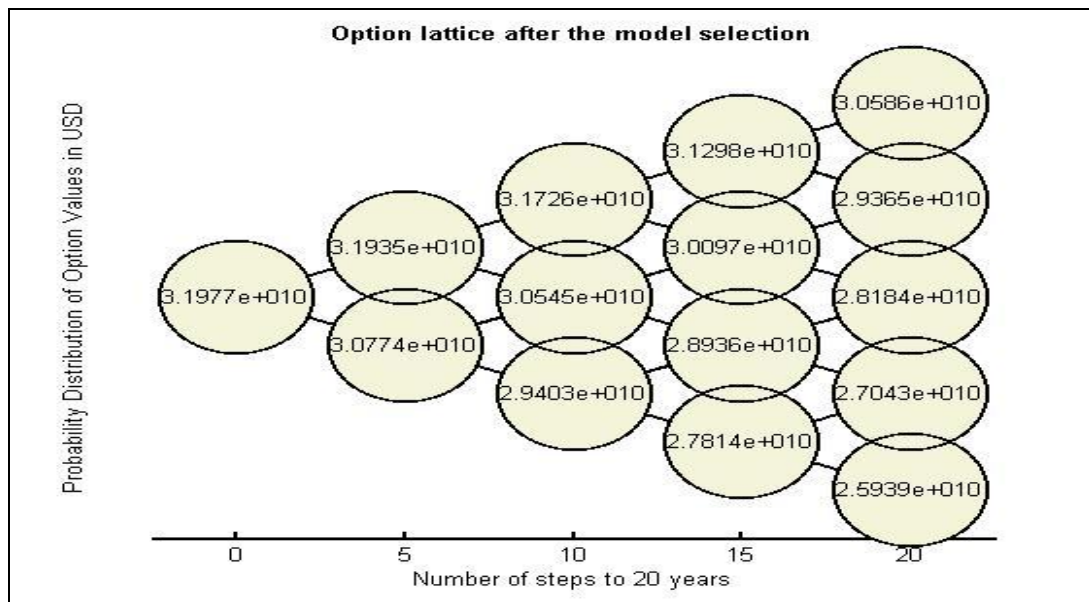


Figure 7-20: Option lattice after the model selection

DISCUSSIONS

In the above figures representing option valuation lattice, the value in the left most node of the lattice is the option value considering the cumulative uncertainty associated with the project. In the above lattices for the underlying asset we have used the weighted average of the key P-values from the NPV distribution as the starting value in the left most node of the underlying asset. However, we can also incorporate the uncertainty of the NPV distribution in the lattice more appropriately if we use each key percentile value from the NPV distribution as the input value of the underlying lattice and obtain as many option values as the key P-values of the NPV distribution, in comparison to obtaining single option value by using the weighted average of the key P-values as the starting value in the left most node of the underlying asset. The spread of those options values would represent the uncertainty in the option values. Figure 7-21 shows

option values obtained corresponding to each percentile value, when used as input in the underlying asset.

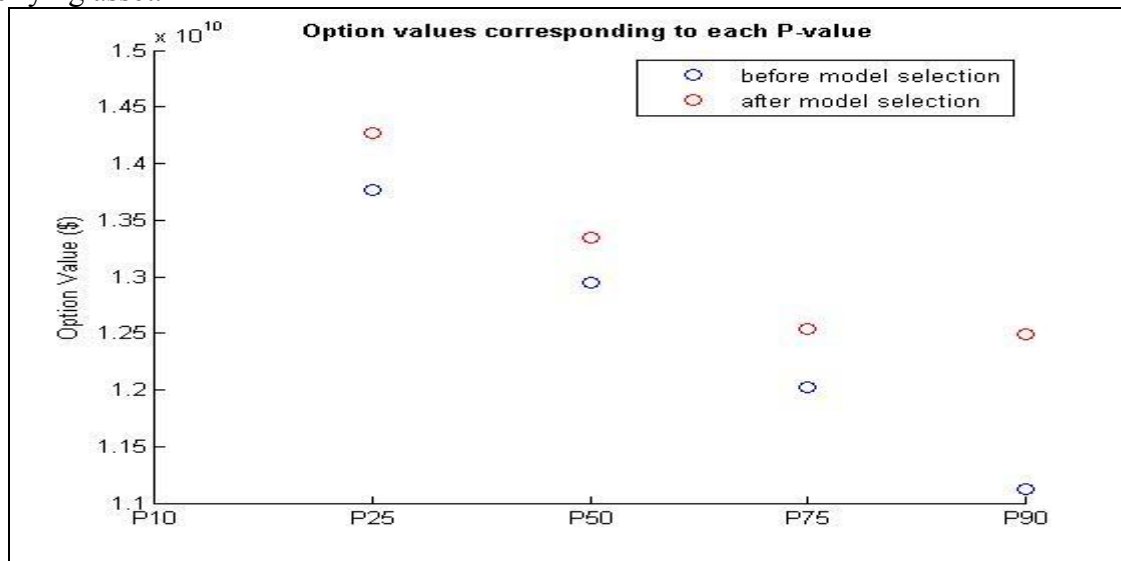


Figure 7-21: Uncertainty in option values generated using P-values of the NPV

Figure 7-21 represents the uncertainty in option values, generated using P-values of the NPV distribution. It is apparent from this figure that there is a decrease in the uncertainty of option values after performing model selection compared to the uncertainty in option values before model selection. Comparing the option values in Figure 7-21 against the option value obtained using the reference model ($=1.2702e+10$ \$), it can be seen that the closest match corresponds to the P75 percentile value.

Chapter 8: Summary, Conclusions, and Future Recommendations

SUMMARY

Project evaluation under uncertainty is a key aspect of reservoir engineering and management that has assumed a critical role in recent times due to the depletion of easy to produce hydrocarbon resources and the increasing hostile operating environments faced by oil and gas operators. In light of the multi-domain uncertainties that confront major projects – flexibility in making development decisions is essential. This necessitates the use of ROV for strategic planning and decision-making in upstream petroleum industry projects.

This thesis addressed the following research questions:

- A strategy to assess the economic worth of incremental data by progressively updating reservoir models. The incremental source of data was either an exploratory well or a seismic. Results suggested that neither of the two information brought significant improvement in resolving the uncertainty within the ROV framework.
- Comparison of reservoir performance based on varying levels of detail in geological model and flow model. ROV analysis is used to address the issue of optimal representation of geology in reservoir models and the role of complex flow models in context of long term uncertainty analysis and risk assessment. Results seem to indicate that complexity in models might not always translate to improved accuracies in economic forecasts. Also, all the economic forecast results suggest that ROV could highlight hidden value of reservoir which NPV fails to uncover.
- Extension of ROV framework using Binomial Lattice, which is easy to use, easy to understand, and more accurate, particularly for longer periods. The BLOV framework is

applied to analyze the economic prospects of an undeveloped, but discovered field. Assessing option values on temporal scale presents the flexibility to make time dependent development decisions.

- A strategy to reduce the cost of investment for performing well test by employing the use of appropriate stochastic reservoir modeling technique and the reference data. The results suggest that SISIM permeability maps translate into less uncertainty in economic valuation than the well test permeability. This is based on the fact that SISIM tries to maintain the continuity in permeability structure of the reservoir as displayed by the SISIM map.
- A strategy to save computational time for doing uncertainty analysis, in context of reservoir performance and risk assessment, by employing the use of model selection algorithm. It results in reduction in prior set of 100 models to just 4 models that exhibit production behavior similar to the observed history. It helps in making the uncertainty quantification feasible and simpler.

CONCLUSIONS

The following conclusions can presented based on the work in this thesis:

- ROV uncovers hidden economic potential of hydrocarbon prospects that conventional DCF analysis might not identify.
- Acquiring extra information might not always be valuable in terms of reducing uncertainty and better economic forecast.
- Complexity in reservoir and flow models might not always translate to improved accuracies in economic forecasts.

- BLOV is easier to use and easy to understand compared to the continuous ROV using Black-Scholes model.
- The model selection algorithm is an efficient and simpler way to do uncertainty quantification by significantly reducing the number of reservoir models from prior suite of reservoir models.

RECOMMENDATIONS FOR FUTURE WORK

On the basis of work done in this thesis, and to explore the full potential of ROV in upstream petroleum industry projects, following can be recommended for future studies:

- Real Data Modeling: The stochastic reservoir models developed in this thesis for uncertainty analysis were not based on real field data or historical data of analogues projects. It would be interesting to see the results of uncertainty modeling and ROV based on reservoir models developed using real field data.
- Explore Model Complexity for Short Term Projects: The forecast of hydrocarbon production rates and economic valuation of the projects done in this thesis are for long term projects in range of several years. Performing ROV for short term projects and the effect of complexity in reservoir models in final economic forecast may be useful in determining the how the ROV is affected by complexity in reservoir models for short term projects.
- Extend Project Volatility Model: Extension of the volatility models which can include negative present worth or market value of a project.
- Explore Facilities Cost Modeling: This thesis assumes an approximate cost for development of facilities. To investigate how the facilities cost influences ROV, it is

important to use the facilities cost models to calculate facilities cost based on the planned production capacity.

- Explore Market Uncertainties: This thesis assumes constant market parameters like interest rate, cost of operational expenses etc. To investigate the effect of market uncertainties, it is important to vary these parameters based on market conditions.

Appendix A: Simulation Data Files for CMG-IMEX

This appendix presents CMG-IMEX simulation data files for various cases presented in this thesis.

A.1 RESERVOIR MODEL: 50 X 50 X 1 GRID DIMENSION, 5 PRODUCTION WELLS (CHAPTER 3)

RESULTS SIMULATOR IMEX 200900

INTERRUPT RESTART-STOP

INUNIT FIELD

WSRF WELL 1

WSRF GRID TIME

WSRF SECTOR TIME

OUTSRF WELL LAYER NONE

OUTSRF RES ALL

OUTSRF GRID BPP OILPOT PRES SO SSPRES SW WINFLUX

WPRN GRID 0

OUTPRN GRID NONE

OUTPRN RES NONE

**\$ Distance units: ft

RESULTS XOFFSET 0.0000

RESULTS YOFFSET 0.0000

RESULTS ROTATION 0.0000 **\$ (DEGREES)

RESULTS AXES-DIRECTIONS 1.0 -1.0 1.0

**\$

**\$ Definition of fundamental cartesian grid

**\$

GRID VARI 50 50 1

KDIR DOWN

DI IVAR

50*2500

DJ JVAR

50*2500

DK ALL

2500*500

DTOP ALL

INCLUDE 'DTOP.INC'

**\$ Property: NULL Blocks Max: 1 Min: 1

**\$ 0 = null block, 1 = active block

NULL CON 1

**\$ Property: Net Pay (ft) Max: 500 Min: 500

NETPAY CON 500

**\$ Property: Porosity Max: 0.3 Min: 0.3

POR ALL

INCLUDE 'poro_model_5wells.inc'

**\$ Property: Permeability I (md) Max: 50 Min: 50

PERMI ALL

INCLUDE 'perm_model_5wells.inc'

PERMJ EQUALSI

PERMK EQUALSI * 0.1

**\$ Property: Pinchout Array Max: 1 Min: 1

**\$ 0 = pinched block, 1 = active block

PINCHOUTARRAY CON 1

CPOR 0.0000001

MODEL BLACKOIL

TRES 200

PVT EG 1

**\$	p	Rs	Bo	Eg	viso	visg	co	
	14.696	3.98796	1.06817	4.44676	3.37768	0.0121185		3e-005
	147.05	23.0822	1.07667	45.3136	2.95187	0.0122544		3e-005
	279.403	45.8345	1.08694	87.6942	2.57656	0.0124489		3e-005
	411.757	70.7697	1.09839	131.636	2.27022	0.0126867		3e-005
	544.11	97.3231	1.11079	177.17	2.0222	0.0129644		3e-005
	676.464	125.182	1.124	224.303	1.81997	0.0132819		3e-005
	808.818	154.143	1.13794	273.011	1.65316	0.0136399		3e-005
	941.171	184.065	1.15256	323.228	1.51388	0.0140399		3e-005
	1073.52	214.84	1.16781	374.838	1.3962	0.0144832		3e-005
	1205.88	246.386	1.18365	427.667	1.29567	0.0149712		3e-005

1338.23	278.635	1.20006	481.48	1.20892	0.0155044	3e-005
1470.59	311.532	1.217	535.986	1.13339	0.0160827	3e-005
1602.94	345.032	1.23447	590.844	1.06708	0.0167049	3e-005
1735.29	379.094	1.25243	645.684	1.00844	0.0173689	3e-005
1867.65	413.685	1.27087	700.13	0.956218	0.0180716	3e-005
2000	448.776	1.28977	753.819	0.909442	0.018809	2.85265e-005
2400	557.61	1.34959	908.451	0.79373	0.0212009	2.25139e-005
2800	670.199	1.41321	1047.64	0.705834	0.023736	1.84332e-005
3200	786.11	1.48035	1169.7	0.636804	0.026304	1.55027e-005
3600	905.01	1.55082	1275.62	0.581138	0.0288299	1.33079e-005
4000	1026.63	1.62442	1367.41	0.535275	0.031271	1.16098e-005

BWI 1

CVO 0

CVW 0

**\$ Property: PVT Type Max: 1 Min: 1

PTYPE CON 1

CW 3.43356e-06

DENSITY OIL 54.6422

DENSITY WATER 60

REFPW 100

VWI 1

DENSITY GAS 0.0686695

ROCKFLUID

RPT 1

SWT

**\$	Sw	krw	krow
	0.15	0	0.9
	0.190625	2.6123e-005	0.741577
	0.23125	0.000208984	0.60293
	0.271875	0.000705322	0.482739
	0.3125	0.00167188	0.379688
	0.353125	0.00326538	0.292456
	0.39375	0.00564258	0.219727
	0.434375	0.00896021	0.160181
	0.475	0.013375	0.1125
	0.515625	0.0190437	0.0753662
	0.55625	0.026123	0.0474609
	0.596875	0.0347698	0.0274658
	0.6375	0.0451406	0.0140625
	0.678125	0.0573923	0.00593262
	0.71875	0.0716816	0.00175781
	0.759375	0.0881653	0.000219727
	0.8	0.107	0

SLT

**\$	Sl	krq	krog
	0.38	0.9	0
	0.41875	0.741577	0.000219727
	0.4575	0.60293	0.00175781
	0.49625	0.482739	0.00593262
	0.535	0.379688	0.0140625

0.57375	0.292456	0.0274658
0.6125	0.219727	0.0474609
0.65125	0.160181	0.0753662
0.69	0.1125	0.1125
0.72875	0.0753662	0.160181
0.7675	0.0474609	0.219727
0.80625	0.0274658	0.292456
0.845	0.0140625	0.379688
0.88375	0.00593262	0.482739
0.9225	0.00175781	0.60293
0.96125	0.000219727	0.741577
1	0	0.9

INITIAL

VERTICAL DEPTH_AVE WATER_OIL EQUIL

REFDEPTH 1000

REFPRES 4000

DWOC 1500

**\$ Property: Bubble Point Pressure (psi) Max: 0 Min: 0

PB CON 0

NUMERICAL

RUN

DATE 2009 1 1

**\$

WELL 'Well-1'

PRODUCER 'Well-1'

OPERATE MIN BHP 2000. CONT

**\$ rad geofac wfrac skin

GEOMETRY K 0.25 0.37 1. 0.

PERF GEOA 'Well-1'

**\$ UBA ff Status Connection

1 40 1 1. OPEN FLOW-TO 'SURFACE'

**\$

WELL 'Well-2'

PRODUCER 'Well-2'

OPERATE MIN BHP 2000. CONT

**\$ rad geofac wfrac skin

GEOMETRY K 0.25 0.37 1. 0.

PERF GEOA 'Well-2'

**\$ UBA ff Status Connection

7 30 1 1. OPEN FLOW-TO 'SURFACE'

**\$

WELL 'Well-3'

PRODUCER 'Well-3'

OPERATE MIN BHP 2000. CONT

**\$ rad geofac wfrac skin

GEOMETRY K 0.25 0.37 1. 0.

PERF GEOA 'Well-3'

**\$ UBA ff Status Connection

15 45 1 1. OPEN FLOW-TO 'SURFACE'

**\$

WELL 'Well-4'

PRODUCER 'Well-4'

OPERATE MIN BHP 2000. CONT

**\$ rad geofac wfrac skin

GEOMETRY K 0.25 0.37 1. 0.

PERF GEOA 'Well-4'

**\$ UBA ff Status Connection

23 10 1 1. OPEN FLOW-TO 'SURFACE'

**\$

WELL 'Well-5'

PRODUCER 'Well-5'

OPERATE MIN BHP 2000. CONT

**\$ rad geofac wfrac skin

GEOMETRY K 0.25 0.37 1. 0.

PERF GEOA 'Well-5'

**\$ UBA ff Status Connection

30 43 1 1. OPEN FLOW-TO 'SURFACE'

DATE 2010 1 1.00000

DATE 2011 1 1.00000

DATE 2012 1 1.00000

DATE 2013 1 1.00000

DATE 2014 1 1.00000

DATE 2015 1 1.00000

DATE 2016 1 1.00000

DATE 2017 1 1.00000
DATE 2018 1 1.00000
DATE 2019 1 1.00000
DATE 2020 1 1.00000
DATE 2021 1 1.00000
DATE 2022 1 1.00000
DATE 2023 1 1.00000
DATE 2024 1 1.00000
DATE 2025 1 1.00000
DATE 2026 1 1.00000
DATE 2027 1 1.00000
DATE 2028 1 1.00000
DATE 2029 1 1.00000
STOP

A.2 RESERVOIR MODEL: 200 X 200 X 1 GRID DIMENSION, 5 PRODUCTION WELLS (CHAPTER 4)

RESULTS SIMULATOR IMEX 200900

INTERRUPT RESTART-STOP

INUNIT FIELD

WSRF WELL 1

WSRF GRID TIME
 WSRF SECTOR TIME
 OUTSRF WELL LAYER NONE
 OUTSRF RES ALL
 OUTSRF GRID BPP OILPOT PRES SO SSPRES SW WINFLUX
 WPRN GRID 0
 OUTPRN GRID NONE
 OUTPRN RES NONE
 **\$ Distance units: ft
 RESULTS XOFFSET 0.0000
 RESULTS YOFFSET 0.0000
 RESULTS ROTATION 0.0000 **\$ (DEGREES)
 RESULTS AXES-DIRECTIONS 1.0 -1.0 1.0
 **\$

 **\$ Definition of fundamental cartesian grid
 **\$

 GRID VARI 200 200 1
 KDIR DOWN
 DI IVAR
 200*2500
 DJ JVAR
 200*2500
 DK ALL

40000*500

DTOP ALL

INCLUDE 'DTOP.INC'

**\$ Property: NULL Blocks Max: 1 Min: 1

**\$ 0 = null block, 1 = active block

NULL CON 1

**\$ Property: Net Pay (ft) Max: 500 Min: 500

NETPAY CON 500

**\$ Property: Porosity Max: 0.3 Min: 0.3

POR ALL

INCLUDE 'poro_model_5wells_sisim.inc'

**\$ Property: Permeability I (md) Max: 50 Min: 50

PERMI ALL

INCLUDE 'perm_model_5wells_sisim.inc'

PERMJ EQUALSI

PERMK EQUALSI * 0.1

**\$ Property: Pinchout Array Max: 1 Min: 1

**\$ 0 = pinched block, 1 = active block

PINCHOUTARRAY CON 1

CPOR 0.0000001

MODEL BLACKOIL

TRES 200

PVT EG 1

**\$	p	Rs	Bo	Eg	viso	visg	co	
14.696	3.98796	1.06817	4.44676	3.37768	0.0121185	3e-005		
147.05	23.0822	1.07667	45.3136	2.95187	0.0122544	3e-005		
279.403	45.8345	1.08694	87.6942	2.57656	0.0124489	3e-005		
411.757	70.7697	1.09839	131.636	2.27022	0.0126867	3e-005		
544.11	97.3231	1.11079	177.17	2.0222	0.0129644	3e-005		
676.464	125.182	1.124	224.303	1.81997	0.0132819	3e-005		
808.818	154.143	1.13794	273.011	1.65316	0.0136399	3e-005		
941.171	184.065	1.15256	323.228	1.51388	0.0140399	3e-005		
1073.52	214.84	1.16781	374.838	1.3962	0.0144832	3e-005		
1205.88	246.386	1.18365	427.667	1.29567	0.0149712	3e-005		
1338.23	278.635	1.20006	481.48	1.20892	0.0155044	3e-005		
1470.59	311.532	1.217	535.986	1.13339	0.0160827	3e-005		
1602.94	345.032	1.23447	590.844	1.06708	0.0167049	3e-005		
1735.29	379.094	1.25243	645.684	1.00844	0.0173689	3e-005		
1867.65	413.685	1.27087	700.13	0.956218	0.0180716	3e-005		
2000	448.776	1.28977	753.819	0.909442	0.018809	2.85265e-005		
2400	557.61	1.34959	908.451	0.79373	0.0212009	2.25139e-005		
2800	670.199	1.41321	1047.64	0.705834	0.023736	1.84332e-005		
3200	786.11	1.48035	1169.7	0.636804	0.026304	1.55027e-005		
3600	905.01	1.55082	1275.62	0.581138	0.0288299	1.33079e-005		
4000	1026.63	1.62442	1367.41	0.535275	0.031271	1.16098e-005		

BWI 1

CVO 0

CVW 0

**\$ Property: PVT Type Max: 1 Min: 1

PTYPE CON 1

CW 3.43356e-06

DENSITY OIL 54.6422

DENSITY WATER 60

REFPW 100

VWI 1

DENSITY GAS 0.0686695

ROCKFLUID

RPT 1

SWT

**\$	Sw	krw	krow
	0.15	0	0.9
0.190625	2.6123e-005	0.741577	
0.23125	0.000208984	0.60293	
0.271875	0.000705322	0.482739	
0.3125	0.00167188	0.379688	
0.353125	0.00326538	0.292456	
0.39375	0.00564258	0.219727	
0.434375	0.00896021	0.160181	
0.475	0.013375	0.1125	
0.515625	0.0190437	0.0753662	
0.55625	0.026123	0.0474609	
0.596875	0.0347698	0.0274658	

0.6375	0.0451406	0.0140625
0.678125	0.0573923	0.00593262
0.71875	0.0716816	0.00175781
0.759375	0.0881653	0.000219727
0.8	0.107	0

SLT

**\$	Sl	krq	krog
	0.38	0.9	0
	0.41875	0.741577	0.000219727
	0.4575	0.60293	0.00175781
	0.49625	0.482739	0.00593262
	0.535	0.379688	0.0140625
	0.57375	0.292456	0.0274658
	0.6125	0.219727	0.0474609
	0.65125	0.160181	0.0753662
	0.69	0.1125	0.1125
	0.72875	0.0753662	0.160181
	0.7675	0.0474609	0.219727
	0.80625	0.0274658	0.292456
	0.845	0.0140625	0.379688
	0.88375	0.00593262	0.482739
	0.9225	0.00175781	0.60293
	0.96125	0.000219727	0.741577
	1	0	0.9

INITIAL

VERTICAL DEPTH_AVE WATER_OIL EQUIL

REFDEPTH 1000

REFPRES 4000

DWOC 1500

**\$ Property: Bubble Point Pressure (psi) Max: 0 Min: 0

PB CON 0

NUMERICAL

RUN

DATE 2009 1 1

**\$

WELL 'Well-1'

PRODUCER 'Well-1'

OPERATE MIN BHP 2000. CONT

**\$ rad geofac wfrac skin

GEOMETRY K 0.25 0.37 1. 0.

PERF GEOA 'Well-1'

**\$ UBA ff Status Connection

170 50 1 1. OPEN FLOW-TO 'SURFACE'

**\$

WELL 'Well-2'

PRODUCER 'Well-2'

OPERATE MIN BHP 2000. CONT

**\$ rad geofac wfrac skin

GEOMETRY K 0.25 0.37 1. 0.

PERF GEOA 'Well-2'
 **\$ UBA ff Status Connection
 130 125 1 1. OPEN FLOW-TO 'SURFACE'
 **\$
 WELL 'Well-3'
 PRODUCER 'Well-3'
 OPERATE MIN BHP 2000. CONT
 **\$ rad geofac wfrac skin
 GEOMETRY K 0.25 0.37 1. 0.
 PERF GEOA 'Well-3'
 **\$ UBA ff Status Connection
 70 190 1 1. OPEN FLOW-TO 'SURFACE'
 **\$
 WELL 'Well-4'
 PRODUCER 'Well-4'
 OPERATE MIN BHP 2000. CONT
 **\$ rad geofac wfrac skin
 GEOMETRY K 0.25 0.37 1. 0.
 PERF GEOA 'Well-4'
 **\$ UBA ff Status Connection
 40 100 1 1. OPEN FLOW-TO 'SURFACE'
 **\$
 WELL 'Well-5'
 PRODUCER 'Well-5'
 OPERATE MIN BHP 2000. CONT

```

**$      rad geofac wfrac skin
GEOMETRY K 0.25 0.37 1. 0.
PERF GEOA 'Well-5'
**$ UBA    ff Status Connection
      20 20 1 1. OPEN  FLOW-TO 'SURFACE'
DATE 2010 1 1.00000
DATE 2011 1 1.00000
DATE 2012 1 1.00000
DATE 2013 1 1.00000
DATE 2014 1 1.00000
DATE 2015 1 1.00000
DATE 2016 1 1.00000
DATE 2017 1 1.00000
DATE 2018 1 1.00000
DATE 2019 1 1.00000
DATE 2020 1 1.00000
DATE 2021 1 1.00000
DATE 2022 1 1.00000
DATE 2023 1 1.00000
DATE 2024 1 1.00000
DATE 2025 1 1.00000
DATE 2026 1 1.00000
DATE 2027 1 1.00000
DATE 2028 1 1.00000
DATE 2029 1 1.00000

```

STOP

A.3 RESERVOIR MODEL: 200 x 200 x 1 GRID DIMENSION, 5 PRODUCTION WELLS, WELL TESTING (CHAPTER 7)

RESULTS SIMULATOR IMEX 200900

INTERRUPT RESTART-STOP

INUNIT FIELD

WSRF WELL 1

WSRF GRID TIME

WSRF SECTOR TIME

OUTSRF WELL LAYER NONE

OUTSRF RES ALL

OUTSRF GRID BPP OILPOT PRES SO SSPRES SW WINFLUX

WPRN GRID 0

OUTPRN GRID NONE

OUTPRN RES NONE

**\$ Distance units: ft

RESULTS XOFFSET 0.0000

RESULTS YOFFSET 0.0000

RESULTS ROTATION 0.0000 **\$ (DEGREES)

RESULTS AXES-DIRECTIONS 1.0 -1.0 1.0

**\$

**\$ Definition of fundamental cartesian grid

**\$

GRID VARI 200 200 1

KDIR DOWN

DI IVAR

200*500

DJ JVAR

200*500

DK ALL

40000*500

DTOP ALL

INCLUDE 'DTOP.INC'

**\$ Property: NULL Blocks Max: 1 Min: 1

**\$ 0 = null block, 1 = active block

NULL CON 1

**\$ Property: Net Pay (ft) Max: 500 Min: 500

NETPAY CON 500

**\$ Property: Porosity Max: 0.3 Min: 0.3

POR ALL

INCLUDE 'poro_model_5wells_sisim_well_testing.inc'

**\$ Property: Permeability I (md) Max: 50 Min: 50

PERMI ALL

INCLUDE 'perm_model_5wells_sisim_well_testing.inc'

PERMJ EQUALSI

PERMK EQUALSI * 0.1

**\$ Property: Pinchout Array Max: 1 Min: 1

**\$ 0 = pinched block, 1 = active block

PINCHOUTARRAY CON 1

CPOR 0.0000001

MODEL BLACKOIL

TRES 200

PVT EG 1

**\$	p	Rs	Bo	Eg	viso	visg
	14.696	3.98796	1.06817	4.44676	3.37768	0.0121185
	147.05	23.0822	1.07667	45.3136	2.95187	0.0122544
	279.403	45.8345	1.08694	87.6942	2.57656	0.0124489
	411.757	70.7697	1.09839	131.636	2.27022	0.0126867
	544.11	97.3231	1.11079	177.17	2.0222	0.0129644
	676.464	125.182	1.124	224.303	1.81997	0.0132819
	808.818	154.143	1.13794	273.011	1.65316	0.0136399
	941.171	184.065	1.15256	323.228	1.51388	0.0140399
	1073.52	214.84	1.16781	374.838	1.3962	0.0144832
	1205.88	246.386	1.18365	427.667	1.29567	0.0149712
	1338.23	278.635	1.20006	481.48	1.20892	0.0155044
	1470.59	311.532	1.217	535.986	1.13339	0.0160827

1602.94	345.032	1.23447	590.844	1.06708	0.0167049
1735.29	379.094	1.25243	645.684	1.00844	0.0173689
1867.65	413.685	1.27087	700.13	0.956218	0.0180716
2000	448.776	1.28977	753.819	0.909442	0.018809
2400	557.61	1.34959	908.451	0.79373	0.0212009
2800	670.199	1.41321	1047.64	0.705834	0.023736
3200	786.11	1.48035	1169.7	0.636804	0.026304
3600	905.01	1.55082	1275.62	0.581138	0.0288299
4000	1026.63	1.62442	1367.41	0.535275	0.031271

BWI 1

CVO 0

CVW 0

**\$ Property: PVT Type Max: 1 Min: 1

PTYPE CON 1

CW 3.43356e-06

DENSITY OIL 54.6422

DENSITY WATER 60

REFPW 100

VWI 1

DENSITY GAS 0.0686695

CO 1.5e-05

**\$ Property: PVT Type Max: 1 Min: 1

PTYPE CON 1

ROCKFLUID

RPT 1

SWT

**\$	Sw	krw	krow
	0.15	0	0.9
	0.190625	2.6123e-005	0.741577
	0.23125	0.000208984	0.60293
	0.271875	0.000705322	0.482739
	0.3125	0.00167188	0.379688
	0.353125	0.00326538	0.292456
	0.39375	0.00564258	0.219727
	0.434375	0.00896021	0.160181
	0.475	0.013375	0.1125
	0.515625	0.0190437	0.0753662
	0.55625	0.026123	0.0474609
	0.596875	0.0347698	0.0274658
	0.6375	0.0451406	0.0140625
	0.678125	0.0573923	0.00593262
	0.71875	0.0716816	0.00175781
	0.759375	0.0881653	0.000219727
	0.8	0.107	0

SLT

**\$	Sl	krq	krog
	0.38	0.9	0
	0.41875	0.741577	0.000219727
	0.4575	0.60293	0.00175781
	0.49625	0.482739	0.00593262

0.535	0.379688	0.0140625
0.57375	0.292456	0.0274658
0.6125	0.219727	0.0474609
0.65125	0.160181	0.0753662
0.69	0.1125	0.1125
0.72875	0.0753662	0.160181
0.7675	0.0474609	0.219727
0.80625	0.0274658	0.292456
0.845	0.0140625	0.379688
0.88375	0.00593262	0.482739
0.9225	0.00175781	0.60293
0.96125	0.000219727	0.741577
1	0	0.9

INITIAL

VERTICAL DEPTH_AVE WATER_OIL EQUIL

REFDEPTH 1000

REFPRES 4000

DWOC 1500

**\$ Property: Bubble Point Pressure (psi) Max: 0 Min: 0

PB CON 0

NUMERICAL

RUN

DATE 2009 1 1

**\$

WELL 'Well-1'
 PRODUCER 'Well-1'
 OPERATE MAX STO 100000. CONT
 **\$ rad geofac wfrac skin
 GEOMETRY K 0.25 0.37 1. 0.
 PERF GEOA 'Well-1'
 **\$ UBA ff Status Connection
 170 50 1 1. OPEN FLOW-TO 'SURFACE'
 **\$
 WELL 'Well-2'
 PRODUCER 'Well-2'
 OPERATE MIN BHP 2000. CONT
 **\$ rad geofac wfrac skin
 GEOMETRY K 0.25 0.37 1. 0.
 PERF GEOA 'Well-2'
 **\$ UBA ff Status Connection
 130 125 1 1. OPEN FLOW-TO 'SURFACE'
 **\$
 WELL 'Well-3'
 PRODUCER 'Well-3'
 OPERATE MIN BHP 2000. CONT
 **\$ rad geofac wfrac skin
 GEOMETRY K 0.25 0.37 1. 0.
 PERF GEOA 'Well-3'
 **\$ UBA ff Status Connection

```

70 190 1 1. OPEN FLOW-TO 'SURFACE'
**$
WELL 'Well-4'
PRODUCER 'Well-4'
OPERATE MIN BHP 2000. CONT
**$      rad geofac wfrac skin
GEOMETRY K 0.25 0.37 1. 0.
PERF GEOA 'Well-4'
**$ UBA      ff Status Connection
40 100 1 1. OPEN FLOW-TO 'SURFACE'
**$
WELL 'Well-5'
PRODUCER 'Well-5'
OPERATE MIN BHP 2000. CONT
**$      rad geofac wfrac skin
GEOMETRY K 0.25 0.37 1. 0.
PERF GEOA 'Well-5'
**$ UBA      ff Status Connection
20 20 1 1. OPEN FLOW-TO 'SURFACE'
WLISTSHUT 'Well-2' 'Well-3' 'Well-4' 'Well-5'
DATE 2009 1 2.00000
DATE 2009 1 3.00000
DATE 2009 1 4.00000
DATE 2009 1 5.00000
DATE 2009 1 6.00000

```

DATE 2009 1 7.00000
DATE 2009 1 8.00000
DATE 2009 1 9.00000
DATE 2009 1 10.00000
DATE 2009 1 11.00000
DATE 2009 1 12.00000
DATE 2009 1 13.00000
DATE 2009 1 14.00000
DATE 2009 1 15.00000
DATE 2009 1 16.00000
DATE 2009 1 17.00000
DATE 2009 1 18.00000
DATE 2009 1 19.00000
DATE 2009 1 20.00000
DATE 2009 1 21.00000
DATE 2009 1 22.00000
DATE 2009 1 23.00000
DATE 2009 1 24.00000
DATE 2009 1 25.00000
WLISTSHUT 'Well-1'
DATE 2009 1 25.04167
DATE 2009 1 25.08333
DATE 2009 1 25.12500
DATE 2009 1 25.16667
DATE 2009 1 25.20833

DATE 2009 1 25.25000
DATE 2009 1 25.29167
DATE 2009 1 25.33333
DATE 2009 1 25.37500
DATE 2009 1 25.41667
DATE 2009 1 25.45833
DATE 2009 1 25.50000
DATE 2009 1 25.54167
DATE 2009 1 25.58333
DATE 2009 1 25.62500
DATE 2009 1 25.66667
DATE 2009 1 25.70833
DATE 2009 1 25.75000
DATE 2009 1 25.79167
DATE 2009 1 25.83333
DATE 2009 1 25.87500
DATE 2009 1 25.91667
DATE 2009 1 25.95833
DATE 2009 1 26.00000
DATE 2009 1 26.04167
DATE 2009 1 26.08333
DATE 2009 1 26.12500
DATE 2009 1 26.16667
DATE 2009 1 26.20833
DATE 2009 1 26.25000

DATE 2009 1 26.29167
DATE 2009 1 26.33333
DATE 2009 1 26.37500
DATE 2009 1 26.41667
DATE 2009 1 26.45833
DATE 2009 1 26.50000
DATE 2009 1 26.54167
DATE 2009 1 26.58333
DATE 2009 1 26.62500
DATE 2009 1 26.66667
DATE 2009 1 26.70833
DATE 2009 1 26.75000
DATE 2009 1 26.79167
DATE 2009 1 26.83333
DATE 2009 1 26.87500
DATE 2009 1 26.91667
DATE 2009 1 26.95833
DATE 2009 1 27.00000
DATE 2009 1 27.04167
DATE 2009 1 27.08333
DATE 2009 1 27.12500
DATE 2009 1 27.16667
DATE 2009 1 27.20833
DATE 2009 1 27.25000
DATE 2009 1 27.29167

DATE 2009 1 27.33333
DATE 2009 1 27.37500
DATE 2009 1 27.41667
DATE 2009 1 27.45833
DATE 2009 1 27.50000
DATE 2009 1 27.54167
DATE 2009 1 27.58333
DATE 2009 1 27.62500
DATE 2009 1 27.66667
DATE 2009 1 27.70833
DATE 2009 1 27.75000
DATE 2009 1 27.79167
DATE 2009 1 27.83333
DATE 2009 1 27.87500
DATE 2009 1 27.91667
DATE 2009 1 27.95833
DATE 2009 1 28.00000
DATE 2009 1 28.04167
DATE 2009 1 28.08333
DATE 2009 1 28.12500
DATE 2009 1 28.16667
DATE 2009 1 28.20833
DATE 2009 1 28.25000
DATE 2009 1 28.29167
DATE 2009 1 28.33333

DATE 2009 1 28.37500
DATE 2009 1 28.41667
DATE 2009 1 28.45833
DATE 2009 1 28.50000
DATE 2009 1 28.54167
DATE 2009 1 28.58333
DATE 2009 1 28.62500
DATE 2009 1 28.66667
DATE 2009 1 28.70833
DATE 2009 1 28.75000
DATE 2009 1 28.79167
DATE 2009 1 28.83333
DATE 2009 1 28.87500
DATE 2009 1 28.91667
DATE 2009 1 28.95833
DATE 2009 1 29.00000
DATE 2009 1 29.04167
DATE 2009 1 29.08333
DATE 2009 1 29.12500
DATE 2009 1 29.16667
DATE 2009 1 29.20833
DATE 2009 1 29.25000
DATE 2009 1 29.29167
DATE 2009 1 29.33333
DATE 2009 1 29.37500

DATE 2009 1 29.41667
DATE 2009 1 29.45833
DATE 2009 1 29.50000
DATE 2009 1 29.54167
DATE 2009 1 29.58333
DATE 2009 1 29.62500
DATE 2009 1 29.66667
DATE 2009 1 29.70833
DATE 2009 1 29.75000
DATE 2009 1 29.79167
DATE 2009 1 29.83333
DATE 2009 1 29.87500
DATE 2009 1 29.91667
DATE 2009 1 29.95833
DATE 2009 1 30.00000
DATE 2009 1 30.04167
DATE 2009 1 30.08333
DATE 2009 1 30.12500
DATE 2009 1 30.16667
DATE 2009 1 30.20833
DATE 2009 1 30.25000
DATE 2009 1 30.29167
DATE 2009 1 30.33333
DATE 2009 1 30.37500
DATE 2009 1 30.41667

DATE 2009 1 30.45833
DATE 2009 1 30.50000
DATE 2009 1 30.54167
DATE 2009 1 30.58333
DATE 2009 1 30.62500
DATE 2009 1 30.66667
DATE 2009 1 30.70833
DATE 2009 1 30.75000
DATE 2009 1 30.79167
DATE 2009 1 30.83333
DATE 2009 1 30.87500
DATE 2009 1 30.91667
DATE 2009 1 30.95833
DATE 2009 1 31.00000
DATE 2009 1 31.04167
DATE 2009 1 31.08333
DATE 2009 1 31.12500
DATE 2009 1 31.16667
DATE 2009 1 31.20833
DATE 2009 1 31.25000
DATE 2009 1 31.29167
DATE 2009 1 31.33333
DATE 2009 1 31.37500
DATE 2009 1 31.41667
DATE 2009 1 31.45833

DATE 2009 1 31.50000
DATE 2009 1 31.54167
DATE 2009 1 31.58333
DATE 2009 1 31.62500
DATE 2009 1 31.66667
DATE 2009 1 31.70833
DATE 2009 1 31.75000
DATE 2009 1 31.79167
DATE 2009 1 31.83333
DATE 2009 1 31.87500
DATE 2009 1 31.91667
DATE 2009 1 31.95833
DATE 2009 2 1.00000
DATE 2009 2 1.04167
DATE 2009 2 1.08333
DATE 2009 2 1.12500
DATE 2009 2 1.16667
DATE 2009 2 1.20833
DATE 2009 2 1.25000
DATE 2009 2 1.29167
DATE 2009 2 1.33333
DATE 2009 2 1.37500
DATE 2009 2 1.41667
DATE 2009 2 1.45833
DATE 2009 2 1.50000

DATE 2009 2 1.54167
DATE 2009 2 1.58333
DATE 2009 2 1.62500
DATE 2009 2 1.66667
DATE 2009 2 1.70833
DATE 2009 2 1.75000
DATE 2009 2 1.79167
DATE 2009 2 1.83333
DATE 2009 2 1.87500
DATE 2009 2 1.91667
DATE 2009 2 1.95833
DATE 2009 2 2.00000
STOP

Appendix B: MatLab Codes to Perform General Operations

The work in this thesis required working with hundreds of realizations of reservoir properties, and syncing those multiple realizations among CMG-IMEX, SGeMS, and MatLab. This appendix presents various MatLab codes written as general functions which were used in this thesis.

B.1 IMPORTING DATA FROM GSLIB FORMAT FILES TO MATLAB

```
function
[property_as_mat_nModels_want,property_as_mat_all_nModels]=gslib_file_to_mat_g
eneral(nModel,nCell,nModel_want,gslib_file_name) % must enter the last
argument, gslib_file_name, in single quotes as its treated as a string

%% making third argument optional, otherwise if entered should be in string
format

if nargin<3, %(code to be executed even when only 2 arguments are provided)
    gslib_file_name=input('Enter the gslib file name: ','s');
end

if ~ischar(gslib_file_name)
    error('gslib_file_name should a be string');
```

```
end
```

```
if length(gslib_file_name)<4 || ~strcmpi(gslib_file_name(end-3:end),'.dat'),  
    gslib_file_name=[gslib_file_name '.dat']; % string concatenation  
end
```

```
%% Reading directly from the .dat files generated from SGEMS and making the  
data of file as a variable
```

```
property_gslib_format=textread(gslib_file_name,'%f\t','headerlines',nModel+2);  
property_as_mat_all_nModels=reshape(property_gslib_format,nModel,nCell)';  
property_as_mat_nModels_want=property_as_mat_all_nModels(:,1:nModel_want); %  
Note: 'nModel_want' instead of 'nModel'
```

B.2 MAKING A DATA FILE WITH GSLIB FORMAT FROM MATLAB WORKSPACE

```
function  
  
[]=write_property_to_gslib_file_general(nModel,name_of_gslib_file_want,header_  
property_name_want,property_as_gslib_want)  
  
if ~ischar(name_of_gslib_file_want)||~ischar(header_property_name_want)  
    error('name_of_gslib_file_want and header_property_name_want should a be  
string');  
end
```



```

%# open the file

name_of_gslib_file_want=[name_of_gslib_file_want '.dat'];

fid = fopen(name_of_gslib_file_want,'w');


%# start writing. First line: title

fprintf(fid,'%s\n',header_property_name_want); %# don't forget \n for newline.
Use \n\r if you want to open this in notepad


%# write number of models

fprintf(fid,'%i\n',nModel)


%# loop to write the rest of the header

for iModel = 1:nModel

    fprintf(fid,'%s_%i\n',header_property_name_want,iModel);

end


%# use your favorite method to write the rest of the data.

%# for example, you could use fprintf again, using \t to add tabs

%# create format-string

%# check the help to fprintf to learn about formatting details

formatString = repmat('%f\t',1,nModel);

formatString = [formatString(1:end-1),'n']; %# replace last tab with newline


%# transpose the array, because fprintf reshapes the array to a vector and

```

```

%# 'fills' the format-strings sequentially until it runs out of data

fprintf(fid,formatString,property_as_gslib_want');

%# close the file

fclose(fid);

```

B.3 CALLING CMG-IMEX FROM MATLAB TO RETRIEVE BOTTOM HOLE PRESSURE (BHP) DATA

```

function

[timesteps_days_BHP,BHP_w1,BHP_w2,BHP_w4,BHP_w5]=BHP_from_CMG_general(nModel,n
Cell,nModel_want,ReservoirModel_CMGBuilder,poro_models_gslib_file,perm_models_
gslib_file,poro_model_inc_file,perm_model_inc_file,ReportBHP)

ReservoirModel_CMGBuilder_dat=[ReservoirModel_CMGBuilder '.dat']; % string
concatenation

%# poro and perm models extracted from gslib files and made into matlab
variable

poro_models=gslib_file_to_mat_general(nModel,nCell,nModel_want,poro_models_gsl
ib_file);

perm_models=gslib_file_to_mat_general(nModel,nCell,nModel_want,perm_models_gsl
ib_file);

```

```

%# poro and perm model '.inc' files

poro_model_inc=[poro_model_inc_file '.inc'];
perm_model_inc=[perm_model_inc_file '.inc'];


%# Report files for BHP, input and output, for CMG
ReportBHP_rwd=[ReportBHP '.rwd'];
ReportBHP_rwo=[ReportBHP '.rwo'];


%% loop to run all nModel

for model_no=1:nModel_want

    %% Writing the porosity and permeability model one at a time in .inc file,
    which will be read and will work as input to porosity and permeability models
    in CMG

    dlmwrite(poro_model_inc,poro_models(:,model_no)/100,'delimiter','\n');
    dlmwrite(perm_model_inc,perm_models(:,model_no),'delimiter','\n');

    %% Calling mx201010.exe and running report.exe from CMG portal

    %# Calls CMG

    [status_mx201010,result_mx201010]=system(['mx201010.exe -f '
ReservoirModel_CMGBuilder_dat ']);

```

```

    %# Calls parameter report file and generates output file

    [status_report,result_report]=system(['report.exe /f "' ReportBHP_rwd '"
/o "' ReportBHP_rwo '"']);

%% Reading and writing the BHP results using .rwd and .rwo files

    %# open the ReportBHP_rwo file
    fid = fopen(ReportBHP_rwo);

    %# read it into one big array, row by row
    fileContents = textscan(fid,'%s','Delimiter','\n');
    fileContents = fileContents{1};
    fclose(fid); %# don't forget to close the file again

    %# find rows containing TABLE NUMBER
    wellStarts = strmatch('TABLE NUMBER',fileContents);
    nWells = length(wellStarts);

    %# loop through the wells and read the numeric data
    wellStarts = [wellStarts];
    nT_BHP=wellStarts(2)-wellStarts(1)-5;

    for w = 1:nWells
        %# read lines containing numbers

```

```

    tmp = fileContents(wellStarts(w)+5:wellStarts(w)+4+nT_BHP);

    %# convert strings to numbers

    tmp = cellfun(@str2num,tmp,'uniformOutput',false);

    %# concatenate array

    tmp = cat(1,tmp{:});

    %# assign output

    BHP_w(:,w)=tmp(:,2);

end

timesteps_days_BHP=tmp(:,1);

BHP_w1(model_no,:)=BHP_w(:,1);

BHP_w2(model_no,:)=BHP_w(:,2);

BHP_w3(model_no,:)=BHP_w(:,3);

BHP_w4(model_no,:)=BHP_w(:,4);

BHP_w5(model_no,:)=BHP_w(:,5);

end % end of the mail loop for running different models

```

B.4 CALLING CMG-IMEX FROM MATLAB TO RETRIEVE PRODUCTION RATE DATA

```

function

[q_yearly]=q_from_CMG_general(nModel,nCell,nModel_want,T,ReservoirModel_CMGBui
lder,poro_models_gslib_file,perm_models_gslib_file,poro_model_inc_file,perm_mo
del_inc_file,Reportq)

```

```

ReservoirModel_CMGBuilder_dat=[ReservoirModel_CMGBuilder '.dat']; % string
concatenation

%# poro and perm models extracted from gslib files and made into matlab
variable

poro_models=gslib_file_to_mat_general(nModel,nCell,nModel_want,poro_models_gsl
ib_file);

perm_models=gslib_file_to_mat_general(nModel,nCell,nModel_want,perm_models_gsl
ib_file);

%# poro and perm model '.inc' files

poro_model_inc=[poro_model_inc_file '.inc'];

perm_model_inc=[perm_model_inc_file '.inc'];

%# Report files for q, input and output, for CMG

Reportq_rwd=[Reportq '.rwd'];

Reportq_rwo=[Reportq '.rwo'];

%% loop to run all nModel

for model_no=1:nModel_want

    %% Writing the porosity and permeability model one at a time in .inc file,
    which will be read and will work as input to porosity and permeability models
    in CMG

```

```

dlmwrite(poro_model_inc,poro_models(:,model_no)/100,'delimiter','\n');
dlmwrite(perm_model_inc,perm_models(:,model_no),'delimiter','\n');

%% Calling mx201010.exe and running report.exe from CMG portal

%# Calls CMG

[status_mx201010,result_mx201010]=system(['mx201010.exe -f '
ReservoirModel_CMGBuilder_dat ']); % Calls CMG

%# Calls parameter report file and generates output file

[status_report,result_report]=system(['report.exe /f "' Reportq_rwd '" /o
"' Reportq_rwo '"]]);

%% Reading and writing the q results using .rwd and .rwo files

%# open the Reportq_rwo file

fid = fopen(Reportq_rwo);

%# read it into one big array, row by row

fileContents = textscan(fid,'%s','Delimiter','\n');
fileContents = fileContents{1};

fclose(fid); %# don't forget to close the file again

%# find rows containing TABLE NUMBER

```

```

wellStarts = strmatch('TABLE NUMBER',fileContents);

nWells = length(wellStarts);

%# loop through the wells and read the numeric data

wellData = cell(nWells,2);

wellStarts = [wellStarts;length(fileContents)];

for w = 1:nWells

    %# read lines containing numbers

    tmp = fileContents(wellStarts(w)+6:wellStarts(w)+6+T-1);

    %# convert strings to numbers

    tmp = cellfun(@str2num,tmp,'uniformOutput',false);

    %# concatenate array

    tmp = cat(1,tmp{:});

    %# assign output

    q_yearly_w(:,w)=tmp(:,2);

end

q_yearly(model_no,:)=(365.*sum(q_yearly_w,2));

end % end of the mail loop for running different models

```

B.5 COMPUTING PRODUCTION RATE THROUGH DECLINE CURVE ANALYSIS

```

%% PRODUCTION DATA COMPUTED USING TANK METHOD EQUATIONS

```



```

function[q_MethodType]=q_from_TankMethod_general(nModel,nCell,nModel_want,A,Nw
,rw,CA,skin,mu,h,ct,Pi,Pwf,Bo,T,xy_wells,poro_models_gslib_file,perm_models_gs
lib_file)

poro_models=gslib_file_to_mat_general(nModel,nCell,nModel_want,poro_models_gsl
ib_file);
perm_models=gslib_file_to_mat_general(nModel,nCell,nModel_want,perm_models_gsl
ib_file);
Aw=A./Nw; % Area of drainage of 1 well. It is not A./6, because the 6th well
is not producing.

%% Mean of Poro and Perm

for model_no=1:nModel_want
    phi_mean(model_no)=mean(poro_models(:,model_no))/100;

    k=reshape(perm_models(:,model_no),sqrt(nCell),sqrt(nCell))';

    % Limit the well perm values taken around the wells to [0,sqrt(nCell)]
    xy_wells_limit1=(xy_wells-5<0);
    xy_wells_limit2=(xy_wells+5>sqrt(nCell));
    xy_wells(xy_wells_limit1)=xy_wells(xy_wells_limit1)+5;
    xy_wells(xy_wells_limit2)=sqrt(nCell)-5;

```

```

    %# mean value of permeability is taken as mean of 10 perm values in X and
    Y direction around each well

    k_mean(model_no)=(mean(mean(k(xy_wells(1,1)-
5:xy_wells(1,1)+5,xy_wells(2,1)-
5:xy_wells(2,1)+5))) +mean(mean(k(xy_wells(1,2)-
5:xy_wells(1,2)+5,xy_wells(2,2)-
5:xy_wells(2,2)+5))) +mean(mean(k(xy_wells(1,3)-
5:xy_wells(1,3)+5,xy_wells(2,3)-
5:xy_wells(2,3)+5))) +mean(mean(k(xy_wells(1,4)-
5:xy_wells(1,4)+5,xy_wells(2,4)-
5:xy_wells(2,4)+5))) +mean(mean(k(xy_wells(1,5)-
5:xy_wells(1,5)+5,xy_wells(2,5)-5:xy_wells(2,5)+5)))) ./5;

end

%% PRODUCTION AT DIFFERENT YEARS FOR 5 WELLS

for j=1:T % Number of year

    t(j)=j;

    for model_no=1:nModel_want % number of models or realizations

        Jk(model_no)=(0.00708*h*k_mean(model_no))/(mu*((0.5*log(Aw/((rw^2)*CA)))+5.75+
skin)); % well productivity index

        Vp(model_no)=7757.792*A.*h.*phi_mean(model_no); % pore volume

        lambda(model_no)=(365*Nw*Jk(model_no))./(Vp(model_no)*ct); % decay
rate of the field

```

```

%      Pi_explorwell(model_no,j)=( (Pi-Pwf)*exp(-
lambda(model_no).*t(j)))+Pwf; % new intial pressure at end of year t(j)

      q_osci(model_no)=(Nw*Jk(model_no)*(Pi-Pwf))/Bo; % intial producing
rate for entire field

      Np(model_no,j)=(365*(q_osci(model_no)./lambda(model_no)).*(1-exp(-
lambda(model_no).*t(j)))); % cumulative oil production by 5 wells for t(j)
years starting year 0 prior to drilling an exploratory well

      if j>1

          q_MethodType(model_no,j)=Np(model_no,j)-Np(model_no,j-1); % oil
production by 5 wells for individual year t(j) prior to drilling an
exploratory well

      else

          q_MethodType(model_no,j)=Np(model_no,j); % oil production by 5
wells for individual year 1 prior to drilling an exploratory well

      end

      end % end of number of models or realizations for any single year
end

```

B.6 PV, NPV AND ROV ANALYSIS

```

function [PV,NPV,ROV,q_MethodType,volatility_LR_sum_PV,volatility_LR_sum_NPV]
=
PV_and_ROV_analysis_general(nModel,nCell,nModel_want,r,p_oil,A,Nw,rw,CA,skin,m
u,h,ct,Pi,Pwf,Bo,T,opex,capex,xy_wells,poro_models_gslib_file,perm_models_gslib

```

```

b_file,ReservoirModel_CMGBuilder,poro_model_inc_file,perm_model_inc_file,Reportq,q_MethodType)

if nargin<27

    q_MethodType=input('Do you want to use q from "CMG", "Tank Method" or from
a saved .mat file? Enter the exact name: ','s');

    if strcmp(q_MethodType,'CMG')

q_MethodType=q_from_CMG_general(nModel,nCell,nModel_want,T,ReservoirModel_CMGB
uilder,poro_models_gslib_file,perm_models_gslib_file,poro_model_inc_file,perm_
model_inc_file,Reportq);

        elseif strcmp(q_MethodType,'Tank Method')

q_MethodType=q_from_TankMethod_general(nModel,nCell,nModel_want,A,Nw,rw,CA,ski
n,mu,h,ct,Pi,Pwf,Bo,T,xy_wells,poro_models_gslib_file,perm_models_gslib_file);

            else

                q_MethodType=load([q_MethodType '.mat']);

            end

        end

    end

if ischar(q_MethodType)

    q_MethodType=load(q_MethodType);

    q_MethodType=struct2cell(q_MethodType);

    q_MethodType=q_MethodType{1};

end

```

```

%% COMPUTATION OF PROJECT VOLATILITY FROM COPELAND AND ANTIKAROV METHOD

logarithmic ratio of NPV

%% COMPUTING FUTURE CASH FLOWS (F) OF THE PROJECT FOR DIFFERENT YEARS

for j=1:T % number of years

    t(j)=j;

    for model_no=1:nModel_want % number of models or realizations

        %% future cash flows

        F(model_no,j)=q_MethodType(model_no,j)*p_oil; % future cash flow
generated for year t(j)

    end

end

%% APPLYING COPELAND AND ANTIKAROV METHOD ON CASH FLOW (PV)

for time_n=1:T

    for model_no=1:nModel_want % number of models or realizations

        MV_n(model_no,time_n)=sum(F(model_no,(time_n+1:T)).*exp(-
r.*((time_n+1:T)-time_n)));

        PW_n(model_no,time_n)=MV_n(model_no,time_n)+F(model_no,time_n);

    end

end

for time_n=2:T

    for model_no=1:nModel_want % number of models or realizations

```

```

k_n_CA(model_no,time_n)=log(PW_n(model_no,time_n)./MV_n(model_no,(time_n-1)));
% k_n_CA is a random number

    end

    v_MethodType(time_n)=std(k_n_CA(:,time_n)); % Volatility of project to be
used in BS equation

end

%% COMPUTING NPV OF THE PROJECT FOR DIFFERENT YEARS

for t=1:T % number of years

    DF(t)=1/((1+r).^t); % Discount Factor for discretely compounded over time

    for model_no=1:nModel_want % number of models or realizations

        % PV and NPV Analysis

        F(model_no,t)=(q_MethodType(model_no,t)*p_oil); % future cash flow
generated in year t with 5 wells only

        PV(model_no,t)=(F(model_no,t).*DF(t))-opex; % profit generated for
year t

        NPV(model_no,t)=sum(PV(model_no,:))-capex; % net profit generated from
year 0 till year t

    end

end

```

```

%% COMPUTING VOLATILITY OF THE PROJECT, BY TWO METHODS INVOLVING PV AND NPV
RESP., FOR DIFFERENT YEARS

for t=2:T

    for model_no=1:nModel_want

        LR_sum_PV(model_no,t)=log(sum(PV(model_no,t:T))/sum(PV(model_no,t-
1:T)));

LR_sum_NPV(model_no,t)=log(sum(NPV(model_no,t+1:T))/sum(NPV(model_no,t:T)));

    end

end

volatility_LR_sum_PV=std(LR_sum_PV);
volatility_LR_sum_NPV=std(LR_sum_NPV);

%% COMPUTING ROV OF THE PROJECT FOR DIFFERENT YEARS

for t=1:T % number of years

    for model_no=1:nModel_want % number of models or realizations

        % ROV Analysis

        if NPV(model_no,t)>0

            S(model_no,t)=NPV(model_no,t)+capex; % future cash flow generated
in year t

            X=capex; % exercise price

            v(t)=volatility_LR_sum_PV(1,t);

```

```

d1(model_no,t)=(log(S(model_no,t)/X)+(r+v(t).^2/2)*t)./(v(t).*sqrt(t));

d2(model_no,t)=d1(model_no,t)-v(t).*sqrt(t);

ROV(model_no,t)=(S(model_no,t).*normcdf(d1(model_no,t)))-(X.*exp(-
r*t)).*normcdf(d2(model_no,t)));

else

    ROV(model_no,t)=0;

end

if ROV(model_no,t)<0

    ROV(model_no,t)=0;

end

end

end

```

B.7 NPV AND RESERVE ESTIMATION BY STOOIP

```

function

[NPV_by_STOOIP,P10,P25,P50,P75,P90,vol_reserve]=NPV_reserve_by_STOOIP(nModel,n
Model_want,nCell,poro_models_gslib_format,Sw) % Sw has to be in percentage

p_oil=70; % $/STB

%% Changing co-ordinate system from SGEMS to CMG

```



```

%# Calling function 'gslib_file_to_mat_general.mat' to convert property values
from gslib format to matlab format

if ischar(poro_models_gslib_format)==1

[poro_as_mat_nModels_want,poro_as_mat_all_nModels]=gslib_file_to_mat_general(n
Model,nCell,nModel_want,poro_models_gslib_format);

else

    poro_as_mat_nModels_want=poro_models_gslib_format;
end

if nargin<5, %(code to be executed even when only 4 arguments are provided)

    Sw_all_nModels=load('Swav_seismic_yearly_CMG');

    Sw_all_nModels=struct2cell(Sw_all_nModels);

    Sw_all_nModels=Sw_all_nModels{1};

    Sw_all_nModels=mean(Sw_all_nModels(2:21,:));

    Sw=mean(Sw_all_nModels);

end

%% Calculating Stock Tank Original Oil in Place (STOOIP)

% Formula for OOIP:  $N \text{ [in stb]} = 6.2898 \cdot (V_b \cdot \phi \cdot (1 - S_w)) / B_{oi}$ ; 6.289808 is
% used to convert 'N' in cubic metres to stb Area of one cell is 500ft x
% 500ft, and paythickness is uniformly 500ft.

for model_no=1:nModel_want

```

```

N(:,model_no)=(((50*500*50*500*1*500)/(3.28^3))*(poro_as_mat_nModels_want(:,model_no)/100)*(1-(Sw/100)))/1.54)*6.2898;

    STOOIP(model_no)=sum(N(:,model_no)); % Adding the 'N' for all the cells
gives STOOIP

end

%% RECOVERY FACTOR (Rf) AND VOLUMETRIC VALUE OF THE RESERVE

% Formula for Recovery Factor: Rf [in fraction]=(Swav-Swirr)/(1-Swirr),
% where Swirr = 0.10

Rf=((Sw/100)-0.10)/(1-0.10);

%# Volumetric Value of the Reserve

vol_reserve=Rf.*STOOIP; % in STB

NPV_by_STOOIP=vol_reserve*p_oil; % in $

percentiles=prctile(NPV_by_STOOIP,[10,25,50,75,90]);

P90=percentiles(1);

P75=percentiles(2);

P50=percentiles(3);

P25=percentiles(4);

P10=percentiles(5);

```

B.8 BLOV ANALYSIS

```
function
[price,BLOV_lattice,underlying_lattice]=BLOV_general(S0,K,sigma,r,T,nColumn,title_of_option_lattice,title_of_underlying_lattice)

% BLOV stands for Binomial Lattice Option Valuation

%% Check if the title_of_lattice is in string format
if nargin==8
    if ~ischar(title_of_option_lattice) &&
~ischar(title_of_underlying_lattice)
        error('title_of_option_lattice and title_of_underlying_lattice should
a be string');
    end
elseif nargin==7
    if ~ischar(title_of_option_lattice)
        error('title_of_option_lattice should a be string');
    end
end

%% Constant parameters
del_T=T./nColumn; % where n is the number of columns in binomial lattice
u=exp(sigma.*sqrt(del_T));
d=1./u;
```

```

p=(exp(r.*del_T)-d)./(u-d);

a=exp(-r.*del_T);

%% Initializing the lattice

Stree=zeros(nColumn+1,nColumn+1);

BLOV_lattice=zeros(nColumn+1,nColumn+1);

%% FORWARD INDUCTION

for i=0:nColumn
    for j=0:i
        Stree(j+1,i+1)=S0.*(u.^(i-j))*(d.^j);
    end
end

underlying_lattice=Stree(:,i+1);

for i=0:nColumn
    BLOV_lattice(i+1,nColumn+1)=max(Stree(i+1,nColumn+1)-K,0);
end

%# Draw the lattice of the underlying asset only if asked in the function
argument

if nargin>7

```

```

%# Drawing the binomial lattice for the underlying asset

N = size(Stree,1);

[xPoints,yPoints] = meshgrid(0:N-1);

yPoints = bsxfun(@plus,-yPoints,0:0.5:(N-0.5)/2);

xLines = [xPoints([1:N+1:N^2-N-1 1:N:N^2-2*N+1]); ...
          xPoints([1:N-1 N:-1:2],N).'];  %'

yLines = [yPoints([1:N+1:N^2-N-1 1:N:N^2-2*N+1]); ...
          yPoints([1:N-1 N:-1:2],N).'];  %'

index = find(triu(reshape(1:N^2,N,N)));

xPoints = xPoints(index);

yPoints = yPoints(index);

values = strtrim(cellstr(num2str(Stree(index),'%1.4e')));

%# Create the figure

hFigure = figure('Color','w');

hAxes = axes('Parent',hFigure,'XLim',[-0.5 N-0.5],...
            'YLim',[min(yPoints)-0.5 max(yPoints)+0.5],...
            'YColor','w','XTick',0:N-1,'LineWidth',2);

set(hAxes,'XTickLabel',linspace(0,T,N).');

hold on;

plot(hAxes,xLines,yLines,'k','LineWidth',2);

plot(hAxes,xPoints,yPoints,'o','MarkerFaceColor',[0.96 0.96 0.86],...
     'MarkerSize',60,'MarkerEdgeColor','k','LineWidth',2);

```

```

text(xPoints,yPoints,values,'Parent',hAxes,...
    'HorizontalAlignment','center');

xlabel(['Number of steps to ', num2str(T), ' years'])
ylabel('Probability Distribution of Underlying Asset in USD','Color','k')
title(title_of_underlying_lattice,'Fontweight','Bold')

hold off;

end

%% BACKWARD INDUCTION

for i=nColumn:-1:1
    for j=0:i-1
        BLOV_lattice(j+1,i)=a.*((1-
p).*BLOV_lattice(j+2,i+1))+(p.*BLOV_lattice(j+1,i+1));
    end
end

price=BLOV_lattice(1,1);

%# Draw the option lattice only if asked in the function argument

if nargin>6

    %# Drawing the binomial lattice for the option

    N = size(BLOV_lattice,1);

```

```

[xPoints,yPoints] = meshgrid(0:N-1);

yPoints = bsxfun(@plus,-yPoints,0:0.5:(N-0.5)/2);

xLines = [xPoints([1:N+1:N^2-N-1 1:N:N^2-2*N+1]); ...

    xPoints([1:N-1 N:-1:2],N).'];   %'

yLines = [yPoints([1:N+1:N^2-N-1 1:N:N^2-2*N+1]); ...

    yPoints([1:N-1 N:-1:2],N).'];   %'

index = find(triu(reshape(1:N^2,N,N)));

xPoints = xPoints(index);

yPoints = yPoints(index);

values = strtrim(cellstr(num2str(BLOV_lattice(index),'%1.4e')));

%# Create the figure

hFigure = figure('Color','w');

hAxes = axes('Parent',hFigure,'XLim',[-0.5 N-0.5],...

    'YLim',[min(yPoints)-0.5 max(yPoints)+0.5],...

    'YColor','w','XTick',0:N-1,'LineWidth',2);

set(hAxes,'XTickLabel',linspace(0,T,N).');

hold on;

plot(hAxes,xLines,yLines,'k','LineWidth',2);

plot(hAxes,xPoints,yPoints,'o','MarkerFaceColor',[0.96 0.96 0.86],...

    'MarkerSize',60,'MarkerEdgeColor','k','LineWidth',2);

text(xPoints,yPoints,values,'Parent',hAxes,...

    'HorizontalAlignment','center');

xlabel(['Number of steps to ', num2str(T), ' years'])

```

```

        ylabel('Probability Distribution of Option Values in USD','Color','k')

        title(title_of_option_lattice,'Fontweight','Bold')

        hold off;

end

%% Converting the lattice of upper traingular matrix to a tree format

N = size(BLOV_lattice,1);  %# The size of the rows and columns in BLOV_lattice
BLOV_lattice = full(spdiags(spdiags(BLOV_lattice),(1-N):2:(N-1),zeros(2*N-
1,N))));

```

B.9 CALLING GSLIB EXECUTABLE ‘TRANS’ FROM MATLAB AND RETRIEVING THE RESULTANT DATA

```

function

[transformed_property_as_gslib,property_as_mat_all_models,result]=generate_data_after_trans_general(nModel,nCell,nModel_want,property_models_gslib_file,property_model_inc_file,transformed_file_out,name_of_gslib_file_want,name_of_header_want)

[property_models_mat,property_as_mat_all_models]=gslib_file_to_mat_general(nModel,nCell,nModel_want,property_models_gslib_file);

%# property model '.inc' file
property_model_inc=[property_model_inc_file '.inc'];

```



```

transformed_file_name_out=[transformed_file_out '.out'];

%% loop to run all nModel

for model_no=1:nModel_want

    prefixData = property_model_inc_file;

    %# write header lines to file

    fid = fopen(property_model_inc, 'wt');

    fprintf(fid,'%s\n',prefixData); %# don't forget \n for newline. Use \n\r
if yow want to open this in notepad

    fprintf(fid,'%i\n',1)

    fprintf(fid,'%s_%i\n',prefixData,1);

    fclose(fid);

    dlmwrite(property_model_inc,property_as_mat_all_models(:,model_no), '-
append', 'delimiter','\t');

    [status,result(:,model_no)]=system('"C:\Documents and
Settings\HSingh2\Desktop\Work\Model - SGEMS, CMG and MATLAB\trans.exe" <
"C:\Documents and Settings\HSingh2\Desktop\Work\Model - SGEMS, CMG and
MATLAB\input_trans_parameter_file.txt"');

```

```

transformed_property_as_gslib(:,model_no)=textread(transformed_file_name_out,'
%f\t','headerlines',2+1);

end % end of the mail loop for running different models

write_property_to_gslib_file_general(nModel_want,name_of_gslib_file_want,name_
of_header_want,transformed_property_as_gslib)

```

B.10 GENERATING SAMPLE DATA AND THEIR CO-ORDINATES FROM A GRIDDED DATA

```

function

[sampled_data_property_without_headers,x_coordinate_sampled_data,y_coordinate_samp
led_data]=generate_sampled_data_with_cells_general(nModel,nCell,nModel_want,nSampl
eData,gslib_file_name,sampled_data_gslib_file_name,sampled_data_gslib_file_header)

% must enter the 2nd last and last argument in single quotes as it's treated
as a string

[property_as_mat_var,property_without_headers]=gslib_file_to_mat_general(nMode
l,nCell,nModel_want,gslib_file_name);

%% Sampling points from property_without_headers

for model_no=1:nModel_want

    for sampled_data=1:nSampleData

        cellno_sampled_data=round(nCell*rand);

```

```

        while cellno_sampledata==0
            cellno_sampledata=round(nCell*rand);
        end

x_coordinate_sampledata(sampledata,model_no)=rem(cellno_sampledata,sqrt(nCell)
);

y_coordinate_sampledata(sampledata,model_no)=fix(cellno_sampledata/sqrt(nCell)
)+ceil(rem(cellno_sampledata,sqrt(nCell))/sqrt(nCell));

        sampledata_property_without_headers(sampledata,
model_no)=property_without_headers(cellno_sampledata,model_no);
        end
end

X=x_coordinate_sampledata;
Y=y_coordinate_sampledata;

%% Writing the sample reference truth data and saving as .dat file in GSLIB
%% format with headers. This sample data could be used in SGEMS as input to
some simulation methods

[r c] = size(X);
prefixX = 'X';

```

```

prefixY = 'Y';

prefixData = sampledata_gslib_file_header;


sampledata_gslib_file_name=[sampledata_gslib_file_name '.dat']; % string
concatenation

%# build a cell array that contains all the header lines
num = strtrim( cellstr(num2str((1:c)', '_%d')) );    %#' SO fix

headers = [ prefixData ;

           num2str(3*c) ;

           strcat(prefixX,num) ;

           strcat(prefixY,num) ;

           strcat(prefixData,num) ];


coordinates_and_property=[X Y sampledata_property_without_headers];


%# write to file

fid = fopen(sampledata_gslib_file_name, 'wt');

fprintf(fid, '%s\n',headers{:});

fclose(fid);


%# append rest of data

dlmwrite(sampledata_gslib_file_name, coordinates_and_property, '-append',
'delimiter','\t');

```

B.11 COMPUTING PERMEABILITY BY DRAWDOWN/BUILDUP WELL TESTING DATA

```
function
[k_well_testing_dd_sisim,k_well_testing_bup_sisim,del_t_dd_hrs,del_P_dd,...

deriv_DP_dd,del_t_bup_hrs,del_P_bup,deriv_DP_bup,t_horner]=k_from_well_testing
_general(...

    nModel_want,P_dd,t_dd_days,P_bup,t_bup_days,tp_days)

%% Reservoir Parameters in oil field units

nCell=40000;

nModel=100;

A=((sqrt(nCell)*2500*sqrt(nCell)*2500))/43560; % Area of reservoir in acres
h=2500; % ft in X and Y direction

%% Fluid Properties in oil field units

qo=450000; % constant flow rate for 1st well in STB/D

mu=0.65; % cp

Bo=1.54;

rw=0.25; % ft

Swir=0.15;

ct=2e-6; % psi^-1

%% Well Properties
```

```

Nw=5; % Number of production wells

Aw=A./Nw; % Area of drainage of 1 well.

T=20; % total time in years of lease and of operating wells

xy_wells=[170,130,70,40,20;50,125,190,100,20];

xy_wells_SGEMS=[xy_wells(1,:);sqrt(nCell)-xy_wells(2,:)];

%% Computing average porosity

poro_models=gslib_file_to_mat_general(nModel,nCell,nModel_want,'poro_models_5w
ells_sisim_gslib_format');

for model_no=1:nModel_want

    phi_mean(model_no)=mean(poro_models(:,model_no))/100;

end

%% Loading Drawdown test data

%# Load time steps data

% t_dd_days=load(t_dd_days);

% t_dd_days=struct2cell(t_dd_days);

% t_dd_hrs=t_dd_days{1}.*24;

%# Load BHP data

% P_dd=load(P_dd);

```

```

% P_dd=struct2cell(P_dd);

% P_dd=P_dd{1}';

t_dd_hrs=t_dd_days.*24;

%% Analyzing the Drawdown data numerically by diagnostic tests

%# Drawdown Pressure Difference

for model_no=1:nModel_want

    for i=1:size(t_dd_hrs,1)

        del_P_dd(i,model_no)=P_dd(1,model_no)-P_dd(i,model_no);

        del_t_dd_hrs(i,:)=t_dd_hrs(i);

    end

end

%# Drawdown Pressure Derivative

for model_no=1:nModel_want

    for i=1:size(t_dd_hrs,1)-2

        deriv_DP_dd(i+1,model_no)=del_t_dd_hrs(i+1)*(((del_P_dd(i+1,model_no)-
        del_P_dd(i,model_no))/(del_t_dd_hrs(i+1)-del_t_dd_hrs(i)))*(del_t_dd_hrs(i+2)-
        del_t_dd_hrs(i+1)))+...
        (((del_P_dd(i+2,model_no)-
        del_P_dd(i+1,model_no))/(del_t_dd_hrs(i+2)-
        del_t_dd_hrs(i+1)))*(del_t_dd_hrs(i+1)-del_t_dd_hrs(i)))/(del_t_dd_hrs(i+2)-
        del_t_dd_hrs(i))));
    end
end

```

```

end

end

deriv_DP_dd(size(t_dd_hrs,1),:)=0;

%% Calculating formation permeability from Drawdown

for model_no=1:nModel_want

    %# Semilog Line Analysis

    m_dd(model_no)=(del_P_dd(2,model_no)-
del_P_dd(1,model_no))/(del_t_dd_hrs(2)-del_t_dd_hrs(1));

    C_dd(model_no)=(qo*Bo)/(24*m_dd(model_no));

    CD_dd(model_no)=(C_dd(model_no)*5.615)/(2*pi*phi_mean(model_no)*ct*h*(rw^2));

    poly_dd=polyfit(log(del_t_dd_hrs(size(t_dd_hrs,1)-
4:size(t_dd_hrs,1))),P_dd(size(t_dd_hrs,1)-4:size(t_dd_hrs,1),model_no),1);

    m_semil_dd(model_no)=poly_dd(1);

    c_1hr_dd(model_no)=poly_dd(2);

    P_1hr_dd(model_no)=(m_semil_dd(model_no)*log(10)*log(1))+c_1hr_dd(model_no);

    %# Computing permeability and skin factor

    k_semil_dd(model_no)=-(162.6*qo*mu*Bo)/(m_semil_dd(model_no)*log(10)*h);

    S_dd(model_no)=1.1513*((P_1hr_dd(model_no)-
P_dd(1,model_no))/(m_semil_dd(model_no)*log(10)))-
log10((k_semil_dd(model_no))/(phi_mean(model_no)*mu*ct*(rw^2)))+3.23);

```



```

end

k_well_testing_dd_sisim=k_semil_dd;

S_well_testing_dd_sisim=S_dd;

save('k_well_testing_dd_sisim','k_well_testing_dd_sisim')

save('S_well_testing_dd_sisim','S_well_testing_dd_sisim')

```

```

%% Drawing Figures for Drawdown Analysis

```

```

hold on

plot(t_dd_hrs,P_dd(:,1:nModel_want),'b-')

xlabel('time (hrs)');

ylabel('BHP(psia)');

legend('Drawown');

title('Linear scale drawdown overview')

hold off

```

```

figure

hold on

semilogx(t_dd_hrs,P_dd(:,1:nModel_want) , 'b-')

xlabel('time (hrs)');

ylabel('BHP(psia)');

legend('Drawown');

title('Drawdown Semilog Plot')

hold off

```

```

figure
hold on
grid on

semilogx(del_t_dd_hrs,del_P_dd(:,1),'b-')
semilogx(del_t_dd_hrs,deriv_DP_dd(:,1),'r-')

xlabel('time (hrs)');
ylabel('DelP and Deriv-DelP');
legend('DelP','Deriv-DelP');
title('Diagnostic Derivative Plot for Drawdown')

%# plotted separately (from model no. 2 to 100) in order to include the 2
legends
if nModel_want>1
    semilogx(del_t_dd_hrs,del_P_dd(:,2:nModel_want),'b-')
    semilogx(del_t_dd_hrs,deriv_DP_dd(:,2:nModel_want),'r-')
    title('Drawdown')
end

hold off

%% Do the buildup Analysis only if the data is provided as input in the
function's argument

if nargin==6

    %% Loading Buildup test data

```

```

    %# Load time steps data

    %     t_bup_days=load(t_bup_days);
    %     t_bup_days=struct2cell(t_bup_days);
    %     t_bup_hrs=t_bup_days{1}.*24;
    tp_hrs=tp_days*24;

    %# Load BHP data

    %     P_bup=load(P_bup);
    %     P_bup=struct2cell(P_bup);
    %     P_bup=P_bup{1}';

    t_bup_hrs=t_bup_days.*24;

    %% Analyzing the Buildup data numerically by diagnostic tests

    %# Buildup Pressure Difference

    for model_no=1:nModel_want

        for i=1:length(t_bup_hrs)

            del_P_bup(i,model_no)=P_bup(i,model_no)-P_bup(1,model_no);

            del_t_bup_hrs(i,:)=(t_bup_hrs(i)-tp_hrs);

            t_horner(i,:)=(tp_hrs+del_t_bup_hrs(i))/del_t_bup_hrs(i);

        end

    end

    %# Buildup Pressure Derivative

```

```

for model_no=1:nModel_want

    for i=1:length(t_bup_hrs)-2

deriv_DP_bup(i+1,model_no)=del_t_bup_hrs(i+1)*((((del_P_bup(i+1,model_no)-
del_P_bup(i,model_no))/(del_t_bup_hrs(i+1)-
del_t_bup_hrs(i)))*(del_t_bup_hrs(i+2)-del_t_bup_hrs(i+1)))+...
((del_P_bup(i+2,model_no)-
del_P_bup(i+1,model_no))/(del_t_bup_hrs(i+2)-
del_t_bup_hrs(i+1)))*(del_t_bup_hrs(i+1)-
del_t_bup_hrs(i)))/(del_t_bup_hrs(i+2)-del_t_bup_hrs(i)));

        deriv_P_bup(i+1,model_no)=((((P_bup(i+1,model_no)-
P_bup(i,model_no))/(del_t_bup_hrs(i+1)-del_t_bup_hrs(i)))*(del_t_bup_hrs(i+2)-
del_t_bup_hrs(i+1)))+...
((P_bup(i+2,model_no)-
P_bup(i+1,model_no))/(del_t_bup_hrs(i+2)-
del_t_bup_hrs(i+1)))*(del_t_bup_hrs(i+1)-
del_t_bup_hrs(i)))/(del_t_bup_hrs(i+2)-del_t_bup_hrs(i)));

        end

    end

    deriv_DP_bup(size(t_bup_hrs,1),:)=0;

%% Calculating formation permeability from Drawdown

for model_no=1:nModel_want

```

```

    %# Horner plot Analysis

    m_bup(model_no)=(del_P_bup(2,model_no)-
del_P_bup(1,model_no))/(del_t_bup_hrs(2)-del_t_bup_hrs(1));

    C_bup(model_no)=(qo*Bo)/(24*m_bup(model_no));

CD_bup(model_no)=(C_bup(model_no)*5.615)/(2*(22/7)*phi_mean(model_no)*ct*h*(rw
^2));

    poly_bup=polyfit(log(t_horner(1:3)),P_bup(1:3,model_no),1);

    m_semil_bup(model_no)=poly_bup(1);

    c_1hr_bup(model_no)=poly_bup(2);

P_1hr_bup(model_no)=(m_semil_bup(model_no)*log(10)*log(tp_hrs+1))+c_1hr_bup(mo
del_no);

    %# Computing permeability and skin factor

    k_semil_bup(model_no)=-
(162.6*qo*mu*Bo)/(m_semil_bup(model_no)*log(10)*h);

    S_bup(model_no)=1.1513*((P_bup(1,model_no)-
P_1hr_bup(model_no))/(m_semil_bup(model_no)*log(10)))-
log10((k_semil_bup(model_no))/(phi_mean(model_no)*mu*ct*(rw^2))+3.23);

    end

    k_well_testing_bup_sisim=k_semil_bup;

    S_well_testing_bup_sisim=S_bup;

    save('k_well_testing_bup_sisim','k_well_testing_bup_sisim')

    save('S_well_testing_bup_sisim','S_well_testing_bup_sisim')

```

```
%% Drawing Figures for Buildup Analysis
```

```
figure  
hold on  
plot(t_bup_hrs,P_bup(:,1:nModel_want),'b-')  
xlabel('time (hrs)');  
ylabel('BHP(psia)');  
legend('Buildup');  
title('Linear scale buildup overview')  
hold off
```

```
figure  
hold on  
semilogx(t_horner,P_bup(:,1:nModel_want),'b-')  
xlabel('Horner Time');  
ylabel('BHP(psia)');  
title('Buildup Horner Semilog Plot')  
hold off
```

```
figure  
hold on  
grid on  
semilogx(del_t_bup_hrs,del_P_bup(:,1),'b-')  
semilogx(del_t_bup_hrs,deriv_DP_bup(:,1),'r-')
```

```

xlabel('time (hrs)');

ylabel('DelP and Deriv-DelP');

legend('DelP','Deriv-DelP');

title('Diagnostic Derivative Plot for Buildup')

%# plotted separately (from model no. 2 to 100) in order to include the 2
legends

if nModel_want>1

    semilogx(del_t_bup_hrs,del_P_bup(:,2:nModel_want),'b-')

    semilogx(del_t_bup_hrs,deriv_DP_bup(:,2:nModel_want),'r-')

    title('Buildup')

end

hold off

end

```

Appendix C: MatLab Codes for Specific Cases and Chapters

This appendix presents various MatLab codes written for specific cases/chapters presented in this thesis.

C.1 MODEL UPDATING AND VALUE OF INFORMATION (CHAPTER 3)

```
%% RESERVOIR PARAMETERS

nModel=100;

nModel_want=2;

nCell=2500;

A=((sqrt(nCell)*2500*sqrt(nCell)*2500))/43560; % Area of reservoir in acres

Nw=5; % Number of production wells

rw=0.25;

CA=31.62; % Shape factor for square reservoir

skin=5;

mu=0.65; % taken from CMG's Components (function of pressure)

h=500; % Paythickness in feets, and constant throughout the reservoir and in
all grids

ct=2*(10^-6);

Pi=3500; % Entered in CMG's Initial Conditions

Pwf=500;

Bo=1.54; % taken from CMG's Components (function of pressure)
```



```

xy_wells=[40,30,45,10,43;1,7,15,23,30];

%% ECONOMIC PARAMETERS FOR ROV and NPV ANALYSIS

%# GENERAL ECONOMIC PARAMETERS

T=20; % total time in years of lease and of operating wells

nT_BHP=24; % number of timesteps in which BHP is generated

p_oil=30; % assuming a constant oil price in dollars per barrel (bbl)

capex_5wells=600*(10^6); % investment to develop a field with 5 wells

opex=2*(10^5); % amount incurred in maintaining a well per year

r=0.12;

v_price=0.17; % volatility or standard deviation of oil prices

%# EXPLORATORY WELL SPECIFIC ECONOMIC PARAMETERS

capex_explorwell=2*(10^6); % amount incurred in drilling one EXPLORATORY well

%# SEISMIC SPECIFIC ECONOMIC PARAMETERS

capex_seismic=2*(10^6); % amount incurred in acquiring a seismic

%% COMPUTING NPV AND ROV OF THE PROJECT FOR DIFFERENT YEARS

%# Before drilling an exploratory or acquiring a seismic

[PV_5wells,NPV_5wells,ROV_5wells,q_5wells_yearly,v_5wells_yearly] =

PV_and_ROV_analysis_general(nModel,nCell,nModel_want,r,p_oil,A,Nw,rw,CA,skin,m

u,h,ct,Pi,Pwf,Bo,T,opex,capex_5wells,xy_wells,'poro_models_5wells_gslib_format

```

```

    'perm_models_5wells_gslib_format', 'ReservoirModel_5wells_CMGBuilder', 'poro_model_5wells', 'perm_model_5wells', 'Reportq_5wells');

%

[price_5wells, lattice_5wells]=BLOV_general(mean(PV_5wells(:,1)), capex_5wells, v_5wells_yearly(2), r, T, nColumn);

%# After drilling an exploratory

[PV_explorwell, NPV_explorwell, ROV_explorwell, q_explorwell_yearly, v_explorwell_yearly] =

PV_and_ROV_analysis_general(nModel, nCell, nModel_want, r, p_oil, A, Nw, rw, CA, skin, mu, h, ct, Pi, Pwf, Bo, T, opex, capex_5wells+capex_explorwell, xy_wells, 'poro_models_explorwell_gslib_format', 'perm_models_explorwell_gslib_format', 'ReservoirModel_ExplorWell_CMGBuilder', 'poro_model_explorwell', 'perm_model_explorwell', 'Reportq_explorwell');

%

[price_explorwell, lattice_explorwell]=BLOV_general(mean(PV_explorwell(:,1)), capex_5wells+capex_explorwell, v_explorwell_yearly(2), r, T, nColumn);

%# After acquiring a seismic

[PV_seismic, NPV_seismic, ROV_seismic, q_seismic_yearly, v_seismic_yearly] =

PV_and_ROV_analysis_general(nModel, nCell, nModel_want, r, p_oil, A, Nw, rw, CA, skin, mu, h, ct, Pi, Pwf, Bo, T, opex, capex_5wells+capex_seismic, xy_wells, 'poro_models_seismic_gslib_format', 'perm_models_seismic_gslib_format', 'ReservoirModel_Seismic_CMGBuilder', 'poro_model_seismic', 'perm_model_seismic', 'Reportq_seismic');

```

```

%

[price_seismic,lattice_seismic]=BLOV_general(mean(PV_seismic(:,1)),capex_5well
s+capex_seismic,v_seismic_yearly(2),r,T,nColumn);

% Taking mean of all 100 models

PV_5wells_mean=mean(PV_5wells,1);

PV_explorwell_mean=mean(PV_explorwell,1);

PV_seismic_mean=mean(PV_seismic,1);


ROV_5wells_mean=mean(ROV_5wells,1);

ROV_explorwell_mean=mean(ROV_explorwell,1);

ROV_seismic_mean=mean(ROV_seismic,1);


%# VOI: ON DRILLING AN EXPLORATORY WELL AND ACQUIRING A SEISMIC RESPECTIVELY


VOI_PV_explorwell=mean(mean(PV_explorwell))-mean(mean(PV_5wells));

VOI_ROV_explorwell=mean(mean(ROV_explorwell))-mean(mean(ROV_5wells));


VOI_PV_seismic=mean(mean(PV_seismic))-mean(mean(PV_5wells));

VOI_ROV_seismic=mean(mean(ROV_seismic))-mean(mean(ROV_5wells));


%% Plotting all 100 models for PV and ROV wrt years


plot(1:T,q_5wells_yearly,'b-');

xlabel('time (yrs)');

```

```

ylabel('q from all 5 wells (in bbl/year)');

legend('q for 100 models with 5 production wells')

title('Prediction of Production Rate and its Uncertainty')

```

```

figure

plot(1:T,q_explorwell_yearly,'r-');

xlabel('time (yrs)');

ylabel('q from all 5 wells (in bbl/year)');

legend('q for 100 models after exploratory well')

title('Prediction of Production Rate and its Uncertainty')

```

```

figure

plot(1:T,q_seismic_yearly,'g-');

xlabel('time (yrs)');

ylabel('q from all 5 wells (in bbl/year)');

legend('q for 100 models after seismic')

title('Prediction of Production Rate and its Uncertainty')

```

```

figure

hold on

plot(1:T,q_5wells_yearly(1,:), 'b-');

plot(1:T,q_seismic_yearly(1,:), 'g-') % FOR SEISMIC VOI

xlabel('time (yrs)');

ylabel('q (in bbl/year)');

```

```

legend('q for 100 models with just 5 production wells','q for 100 models after
seismic');

%# plotted separately (from model no. 2 to 100) in order to include the two
legend colours representing before and after exploratory well

plot(1:T,q_5wells_yearly(2:nModel_want,:), 'b-');

plot(1:T,q_seismic_yearly(2:nModel_want,:), 'g-') % FOR SEISMIC VOI

title('Prediction of Production Rate and its
Uncertainty', 'Fontweight', 'Bold');

figure

hold on

plot(1:T,q_5wells_yearly(1,:), 'b-');

plot(1:T,q_explorwell_yearly(1,:), 'r-'); % FOR EXPLORATORY WELL VOI

plot(1:T,q_seismic_yearly(1,:), 'g-') % FOR SEISMIC VOI

xlabel('time (yrs)');

ylabel('q (in bbl/year)');

legend('q for 100 models with just 5 production wells','q for 100 models after
exploratory well','q for 100 models after seismic');

%# plotted separately (from model no. 2 to 100) in order to include the two
legend colours representing before and after exploratory well

plot(1:T,q_5wells_yearly(2:nModel_want,:), 'b-');

plot(1:T,q_explorwell_yearly(2:nModel_want,:), 'r-'); % FOR EXPLORATORY WELL
VOI

plot(1:T,q_seismic_yearly(2:nModel_want,:), 'g-') % FOR SEISMIC VOI

```

```

title('Prediction of Production Rate and its
Uncertainty','Fontweight','Bold');

figure

hold on

plot(1:T,PV_5wells(1,:), 'b-');

plot(1:T,PV_explorwell(1,:), 'r-'); % FOR EXPLORATORY WELL VOI

plot(1:T,PV_seismic(1,:), 'g-') % FOR SEISMIC VOI

xlabel('time (yrs)');

ylabel('PV in dollars');

legend('PV for 100 models with just 5 production wells','PV for 100 models
after exploratory well','PV for 100 models after seismic');

%# plotted separately (from model no. 2 to 100) in order to include the two
legend colours representing before and after exploratory well

plot(1:T,PV_5wells(2:nModel_want,:), 'b-');

plot(1:T,PV_explorwell(2:nModel_want,:), 'r-'); % FOR EXPLORATORY WELL VOI

plot(1:T,PV_seismic(2:nModel_want,:), 'g-') % FOR SEISMIC VOI

title('PV for exploratory well and seismic','Fontweight','Bold');

figure

hold on

plot(1:T,ROV_5wells(1,:), 'b-')

plot(1:T,ROV_explorwell(1,:), 'r-') % FOR EXPLORATORY WELL VOI

plot(1:T,ROV_seismic(1,:), 'g-') % FOR SEISMIC VOI

xlabel('time (yrs)');

```

```

ylabel('ROV in dollars');

legend('ROV for 100 models with just 5 production wells','ROV for 100 models
after exploratory well','ROV for 100 models after seismic');

%# plotted separately (from model no. 2 to 100) in order to include the two
legend colours representing before and after exploratory well

plot(1:T,ROV_5wells(2:nModel_want,:), 'b-')

plot(1:T,ROV_explorwell(2:nModel_want,:), 'r-') % FOR EXPLORATORY WELL VOI

plot(1:T,ROV_seismic(2:nModel_want,:), 'g-') % FOR SEISMIC VOI

title('ROV for exploratory well and seismic','Fontweight','Bold');


%# Plotting mean of all models for PV and ROV wrt years


figure

hold on

plot(1:T,PV_5wells_mean, 'r-');

plot(1:T,PV_explorwell_mean, 'g-')

plot(1:T,PV_seismic_mean, 'y-')

xlabel('time (yrs)');

ylabel('PV in dollars');

legend('PV for mean of models of 5 production wells','PV for mean of models
after exploratory well','PV for mean of models after seismic');

title(['PV for mean of all ', num2str(nModel), '
models'], 'Fontweight','Bold');


figure

```

```

hold on

plot(1:T,ROV_5wells_mean,'r-');

plot(1:T,ROV_explorwell_mean,'g-')

plot(1:T,ROV_seismic_mean,'y-')

xlabel('time (yrs)');

ylabel('ROV in dollars');

legend('ROV for mean of models of 5 production wells','ROV for mean of models
after exploratory well','ROV for mean of models after seismic');

title(['ROV for mean of all ', num2str(nModel), '
models'],'Fontweight','Bold');

```

C.2 ASSESSING ECONOMIC IMPLICATIONS OF RESERVOIR MODELING DECISIONS (CHAPTER 4)

```

%% RESERVOIR PARAMETERS

%# All units in oil field

nCell=40000;

nModel=100;

nModel_want=100;

nModel_reference=2;

nModel_reference_want=2;

A=((sqrt(nCell)*2500*sqrt(nCell)*2500))/43560; % Area of reservoir in acres

Nw=5; % Number of production wells

```



```

rw=0.25;

CA=31.62; % Shape factor for square reservoir

skin=5;

mu=0.65; % taken from CMG's Components (function of pressure)

h=500; % Paythickness in feets, and constant throughout the reservoir and in
all grids

ct=2*(10^-6);

Pi=3500; % Entered in CMG's Initial Conditions

Pwf=500;

Bo=1.54; % taken from CMG's Components (function of pressure)

T=20; % total time in years of lease and of operating wells

xy_wells=[170,130,70,40,20;50,125,190,100,20];

xy_wells_SGEMS=[xy_wells(1,:);sqrt(nCell)-xy_wells(2,:)];

%% PV and ROV Analysis

%# ECONOMIC PARAMETERS FOR PV and ROV ANALYSIS

T=20; % total time in years of lease and of operating wells

p_oil=30; % assuming a constant oil price in dollars per barrel (bbl)

capex=600*(10^6); % investment to develop a field

opex=2*(10^5); % amount incurred in maintaining a well per year

r=0.12;

[PV_reference_truth,ROV_reference_truth,q_reference_truth_yearly,v_reference_t
ruth_yearly]=PV_and_ROV_analysis_general(nModel_reference,nCell,nModel_referen

```

```

ce_want,r,p_oil,A,Nw,rw,CA,skin,mu,h,ct,Pi,Pwf,Bo,T,opex,capex,xy_wells,'poro_
models_5wells_reference_truth_gslib_format','perm_models_5wells_reference_trut
h_gslib_format','ReservoirModel_5wells_reference_truth_CMGBuilder','poro_model
_5wells_reference_truth','perm_model_5wells_reference_truth','Reportq_5wells_r
eference_truth');

[PV_sgsim,ROV_sgsim,q_sgsim_yearly,v_sgsim_yearly]=PV_and_ROV_analysis_general
(nModel,nCell,nModel_want,r,p_oil,A,Nw,rw,CA,skin,mu,h,ct,Pi,Pwf,Bo,T,opex,cap
ex,xy_wells,'poro_models_5wells_sgsim_gslib_format','perm_models_5wells_trans_
sgsim_gslib_format','ReservoirModel_5wells_sgsim_CMGBuilder','poro_model_5well
s_sgsim','perm_model_5wells_sgsim','Reportq_5wells_sgsim');

[PV_sisim,ROV_sisim,q_sisim_yearly,v_sisim_yearly]=PV_and_ROV_analysis_general
(nModel,nCell,nModel_want,r,p_oil,A,Nw,rw,CA,skin,mu,h,ct,Pi,Pwf,Bo,T,opex,cap
ex,xy_wells,'poro_models_5wells_sisim_gslib_format','perm_models_5wells_sisim_
gslib_format','ReservoirModel_5wells_sisim_CMGBuilder','poro_model_5wells_sisi
m','perm_model_5wells_sisim','Reportq_5wells_sisim');

[PV_snesim,ROV_snesim,q_snesim_yearly,v_snesim_yearly]=PV_and_ROV_analysis_gen
eral(nModel,nCell,nModel_want,r,p_oil,A,Nw,rw,CA,skin,mu,h,ct,Pi,Pwf,Bo,T,opex
, capex,xy_wells,'poro_models_5wells_snesim_gslib_format','perm_models_5wells_s
nesim_gslib_format','ReservoirModel_5wells_snesim_CMGBuilder','poro_model_5wel
ls_snesim','perm_model_5wells_snesim','Reportq_5wells_snesim');

% Taking mean of all 100 models, of both PV and ROV

PV_reference_truth_mean=mean(PV_reference_truth,1);

PV_sgsim_mean=mean(PV_sgsim,1);

PV_sisim_mean=mean(PV_sisim,1);

```

```

PV_snesim_mean=mean(PV_snesim,1);

ROV_reference_truth_mean=mean(ROV_reference_truth,1);

ROV_sgsim_mean=mean(ROV_sgsim,1);

ROV_sisim_mean=mean(ROV_sisim,1);

ROV_snesim_mean=mean(ROV_snesim,1);


% Taking sum of all 20 years' production

q_sum_reference_truth_yearly=sum(q_reference_truth_yearly,2); % sum of all 20
years' production

q_sum_sgsim_yearly=sum(q_sgsim_yearly,2);

q_sum_sisim_yearly=sum(q_sisim_yearly,2);

q_sum_snesim_yearly=sum(q_snesim_yearly,2);


[n_sgsim,x_sgsim] = hist(q_sum_sgsim_yearly);

[n_sisim,x_sisim] = hist(q_sum_sisim_yearly);

[n_snesim,x_snesim] = hist(q_sum_snesim_yearly);


% Plotting distributions of q for comparison

hold on

plot(x_sgsim,n_sgsim,'rx-'); % just an example, plot the pdf with red x's and
a line, instead of bars

plot(x_sisim,n_sisim,'gx-');

plot(x_snesim,n_snesim,'kx-');

```

```

plot(q_sum_reference_truth_yearly(1),1,'ob')

legend('sgsim','sisim','snesim','reference-truth')

title('Comparison of distributions of production rate from different
methods','Fontweight','Bold');

%# Plotting all 100 models for PV and ROV wrt years

figure

hold on

plot(1:T,PV_reference_truth(1,:),'ob-');

plot(1:T,PV_sgsim(1,:),'r-');

plot(1:T,PV_sisim(1,:),'g-')

plot(1:T,PV_snesim(1,:),'k-')

xlabel('time (yrs)');

ylabel('PV in dollars');

legend('PV for 2 models of reference-truth','PV for 100 models of sgsim','PV
for 100 models of sisim','PV for 100 models of snesim');

%# plotted separately (from model no. 2 to 100) in order to include the 4
legends

if nModel_reference_want>=2

    plot(1:T,PV_reference_truth(2:nModel_reference_want,:),'b-')

end

plot(1:T,PV_sgsim(2:nModel_want,:),'r-')

plot(1:T,PV_sisim(2:nModel_want,:),'g-')

plot(1:T,PV_snesim(2:nModel_want,:),'k-')

```

```

title(['PV for all', num2str(nModel), 'models'],'Fontweight','Bold');

figure

hold on

plot(1:T,ROV_reference_truth(1,:), 'ob-');

plot(1:T,ROV_sgsim(1,:), 'r-');

plot(1:T,ROV_sisim(1,:), 'g-')

plot(1:T,ROV_snesim(1,:), 'k-')

xlabel('time (yrs)');

ylabel('ROV in dollars');

legend('ROV for 2 models of reference-truth','ROV for 100 models of
sgsim','ROV for 100 models of sisim','ROV for 100 models of snesim');

%# plotted separately (from model no. 2 to 100) in order to include the 4
legends

if nModel_reference_want>=2

    plot(1:T,ROV_reference_truth(2:nModel_reference_want,:), 'b-')

end

plot(1:T,ROV_sgsim(2:nModel_want,:), 'r-')

plot(1:T,ROV_sisim(2:nModel_want,:), 'g-')

plot(1:T,ROV_snesim(2:nModel_want,:), 'k-')

title(['ROV for all', num2str(nModel), 'models'],'Fontweight','Bold');

%# Plotting mean of all models for PV and ROV wrt years

figure

```

```

hold on

plot(1:T,PV_reference_truth_mean,'ob-');

plot(1:T,PV_sgsim_mean,'r-');

plot(1:T,PV_sisim_mean,'g-')

plot(1:T,PV_snesim_mean,'k-')

xlabel('time (yrs)');

ylabel('PV in dollars');

legend('PV for mean of models of reference-truth','PV for mean of models of
sgsim','PV for mean of models of sisim','PV for mean of models of snesim');

title(['PV for mean of all ', num2str(nModel), '
models'], 'Fontweight', 'Bold');

```

```

figure

hold on

plot(1:T,ROV_reference_truth_mean,'ob-');

plot(1:T,ROV_sgsim_mean,'r-');

plot(1:T,ROV_sisim_mean,'g-')

plot(1:T,ROV_snesim_mean,'k-')

xlabel('time (yrs)');

ylabel('ROV in dollars');

legend('ROV for mean of models of reference-truth','ROV for mean of models of
sgsim','ROV for mean of models of sisim','ROV for mean of models of snesim');

title(['ROV for mean of all ', num2str(nModel), '
models'], 'Fontweight', 'Bold');

```

```

figure

hold on

plot(1:T,v_reference_truth_yearly,'ob-');

plot(1:T,v_sgsim_yearly,'r-');

plot(1:T,v_sisim_yearly,'g-')

plot(1:T,v_snesim_yearly,'k-')

xlabel('time (yrs)');

ylabel('Project Volatility (v)');

legend('v for models of reference-truth','v for models of sgsim','v for models
of sisim','v for models of snesim');

title(['Project Volatility for all ', num2str(nModel), '
models'], 'Fontweight', 'Bold');

```

C.3 ANALYZING THE PROSPECTS OF AN UNDEVELOPED FIELD (CHAPTER 6)

```

%% Required Parameters

%# RESERVOIR PARAMETERS

% All units in oil field

nCell=2500;

nModel=100;

nModel_want=100;

A=((sqrt(nCell)*500*sqrt(nCell)*500))/43560; % Area of reservoir in acres

```

```

%# ECONOMIC PARAMETERS FOR PV and ROV ANALYSIS

T=20; % total time in years of lease and of operating wells

p_oil=30; % assuming a constant oil price in dollars per barrel (bbl)

capex=600*(10^6); % investment to develop a field

opex=2*(10^5); % amount incurred in maintaining a well per year

r=0.05;

nColumn=4;

volatility=0.20;

%% NPV and BLOV Analysis for 5 Scenarios

%# NPV estimation by using 'NPV_reserve_by_STOOIP.m'

[NPV_reference,P10_reference,P25_reference,P50_reference,P75_reference,...

P90_reference,vol_reserve_reference]=NPV_reserve_by_STOOIP_general(nModel,nModel_want,nCell,'poro_models_5wells_gslib_format');

[NPV_seismic,P10_seismic,P25_seismic,P50_seismic,P75_seismic,P90_seismic,...

vol_reserve_seismic]=NPV_reserve_by_STOOIP_general(nModel,nModel_want,nCell,'poro_models_seismic_gslib_format');

percentiles_reference=[P90_reference,P75_reference,P50_reference,P25_reference,P10_reference];

netP_reference=sum([0.90,0.75,0.50,0.25,0.10].*percentiles_reference);

```



```

percentiles_seismic=[P90_seismic,P75_seismic,P50_seismic,P25_seismic,P10_seismic];

netP_seismic=sum([0.90,0.75,0.50,0.25,0.10].*percentiles_seismic);

%# BLOV analysis by using 'BLOV_general.m'

[price_reference,lattice_reference]=BLOV_general(netP_reference, capex, volatility, r, T, nColumn, 'Option NPV Forecast by using reference only', 'Underlying lattice by using reference only');

[price_reference90,lattice_reference90]=BLOV_general(percentiles_reference(1), capex, volatility, r, T, nColumn);

[price_reference75,lattice_reference75]=BLOV_general(percentiles_reference(2), capex, volatility, r, T, nColumn);

[price_reference50,lattice_reference50]=BLOV_general(percentiles_reference(3), capex, volatility, r, T, nColumn);

[price_reference25,lattice_reference25]=BLOV_general(percentiles_reference(4), capex, volatility, r, T, nColumn);

[price_reference10,lattice_reference10]=BLOV_general(percentiles_reference(5), capex, volatility, r, T, nColumn);

[price_seismic,lattice_seismic]=BLOV_general(netP_seismic, capex, volatility, r, T, nColumn, 'Option NPV Forecast by using reference and seismic', 'Underlying lattice by using reference and seismic');

[price_seismic90,lattice_seismic90]=BLOV_general(percentiles_seismic(1), capex, volatility, r, T, nColumn);

```

```

[price_seismic75,lattice_seismic75]=BLOV_general(percentiles_seismic(2),capex,
volatility,r,T,nColumn);

[price_seismic50,lattice_seismic50]=BLOV_general(percentiles_seismic(3),capex,
volatility,r,T,nColumn);

[price_seismic25,lattice_seismic25]=BLOV_general(percentiles_seismic(4),capex,
volatility,r,T,nColumn);

[price_seismic10,lattice_seismic10]=BLOV_general(percentiles_seismic(5),capex,
volatility,r,T,nColumn);


%% Figures


%# Plotting Histograms

figure

hist(NPV_reference)

xlabel('NPV (in $)')

ylabel('Frequency')

title(['Distribution of NPV by using reference only ', num2str(nModel), '
models'], 'Fontweight', 'Bold');


figure

hist(NPV_seismic)

xlabel('NPV (in $)')

ylabel('Frequency')

title(['Distribution of NPV by using reference and seismic ', num2str(nModel),
' models'], 'Fontweight', 'Bold');

```

```

%# Plotting P10, P25, P50, P75, and P90 for NPV

figure

x = 1:5;

y = [P10_reference,P25_reference,P50_reference,P75_reference,P90_reference];

plot(x, y, '-ob')

set(gca, 'XTick',1:5, 'XTickLabel',{'P10' 'P25' 'P50' 'P75' 'P90'})

title('P-values by using reference only','Fontweight','Bold')

ylabel('NPV($)')


figure

x = 1:5;

y = [P10_seismic,P25_seismic,P50_seismic,P75_seismic,P90_seismic];

plot(x, y, '-ob')

set(gca, 'XTick',1:5, 'XTickLabel',{'P10' 'P25' 'P50' 'P75' 'P90'})

title('P-values using reference and seismic','Fontweight','Bold')

ylabel('NPV($)')


%# Plotting option values corresponding to P10, P25, P50, P75, and P90

figure

hold on

x = 1:5;

y_reference =

[price_reference10,price_reference25,price_reference50,price_reference75,price

_reference90];

```

```

y_seismic =

[price_seismic10,price_seismic25,price_seismic50,price_seismic75,price_seismic
90];

plot(x, y_reference, '-ob')
plot(x, y_seismic, '-or')

set(gca, 'XTick',1:5, 'XTickLabel',{'P10' 'P25' 'P50' 'P75' 'P90'})

title('Option values corresponding to each P-value','Fontweight','Bold')

ylabel('Option Value ($)')

legend('by using reference only','by using reference and seismic')

hold off

```

C.4 ANALYZING RESERVOIR PERFORMANCE BY MODEL SELECTION (CHAPTER 7)

```

%% Required Parameters

%# RESERVOIR PARAMETERS

% All units in oil field

nCell=40000;

nModel=100;

nModel_want=100;

A=((sqrt(nCell)*500*sqrt(nCell)*500))/43560; % Area of reservoir in acres

Nw=5; % Number of production wells

rw=0.25;

CA=31.62; % Shape factor for square reservoir

```

```

skin=5;

mu=0.65; % taken from CMG's Components (function of pressure)

h=500; % Paythickness in feets, and constant throughout the reservoir and in
all grids

ct=2*(10^-6);

Pi=3500; % Entered in CMG's Initial Conditions

Pwf=500;

Bo=1.54; % taken from CMG's Components (function of pressure)

xy_wells=[40,30,45,10,43;1,7,15,23,30];

%# ECONOMIC PARAMETERS FOR PV and ROV ANALYSIS

T=20; % total time in years of lease and of operating wells

p_oil=30; % assuming a constant oil price in dollars per barrel (bbl)

capex=6000*(10^6); % investment to develop a field

opex=2*(10^5); % amount incurred in maintaining a well per year

r=0.05;

nColumn=4;

volatility=0.20;

%% Choosing the common models from model selection by two well test history
data

%# reading selected models obtained using two well test history data

model_list1=importdata('model_list_by_well_1_history.txt',' ',1);

model_list1=struct2cell(model_list1);

```

```

model_list1=model_list1{1};

model_list2=importdata('model_list_by_well_2_history.txt',' ',1);

model_list2=struct2cell(model_list2);

model_list2=model_list2{1};

model_list=intersect(model_list1,model_list2);


%# selected perm models

perm_models=importdata('perms.dat',' ',1);

perm_models=struct2cell(perm_models);

perm_models=perm_models{1}; % all models before model selection

selected_perm_models=perm_models(:,[model_list]);


%# selected poro models

poro_models=gslib_file_to_mat_general(nModel,nCell,nModel_want,'poro_models_5w
ells_sisim_gslib_format'); % all models before model selection

selected_poro_models=poro_models(:,[model_list]);


%# writing the selected poro and perm models in gslib file format

write_property_to_gslib_file_general(numel(model_list),'poro_models_after_mode
l_selection_gslib_format','poro_models_after_model_selection',selected_poro_mo
dels)

write_property_to_gslib_file_general(numel(model_list),'perm_models_after_mode
l_selection_gslib_format','perm_models_after_model_selection',selected_perm_mo
dels)

```

```

%% NPV Analysis by Tank Method and BLOV: Before Model Selection

%# NPV estimation by using 'PV_and_ROV_analysis_general.m'

[PV_before_model_selection,NPV_before_model_selection,ROV_before_model_selection,q_before_model_selection,volatility_LR_sum_PV,volatility_LR_sum_NPV] = PV_and_ROV_analysis_general(nModel,nCell,nModel_want,r,p_oil,A,Nw,rw,CA,skin,mu,h,ct,Pi,Pwf,Bo,T,opex,capex,xy_wells,'poro_models_5wells_sisim_gslib_format','perm_models_5wells_sisim_gslib_format');

percentiles_before_model_selection=prctile(NPV_before_model_selection(:,T),[10,25,50,75,90]);

P90_before_model_selection=percentiles_before_model_selection(1);
P75_before_model_selection=percentiles_before_model_selection(2);
P50_before_model_selection=percentiles_before_model_selection(3);
P25_before_model_selection=percentiles_before_model_selection(4);
P10_before_model_selection=percentiles_before_model_selection(5);

netP_before_model_selection=sum([0.90,0.75,0.50,0.25,0.10].*percentiles_before_model_selection);

%# BLOV analysis by using 'BLOV_general.m'

[price_before_model_selection,lattice_before_model_selection]=BLOV_general(netP_before_model_selection,capex,volatility_LR_sum_PV(2),r,T,nColumn,'Option lattice before the model selection','Underlying lattice before the model selection');

```

```

[price_before_model_selection90,lattice_before_model_selection90]=BLOV_general
(percentiles_before_model_selection(1),capex,volatility_LR_sum_PV(2),r,T,nColu
mn);

[price_before_model_selection75,lattice_before_model_selection75]=BLOV_general
(percentiles_before_model_selection(2),capex,volatility_LR_sum_PV(2),r,T,nColu
mn);

[price_before_model_selection50,lattice_before_model_selection50]=BLOV_general
(percentiles_before_model_selection(3),capex,volatility_LR_sum_PV(2),r,T,nColu
mn);

[price_before_model_selection25,lattice_before_model_selection25]=BLOV_general
(percentiles_before_model_selection(4),capex,volatility_LR_sum_PV(2),r,T,nColu
mn);

[price_before_model_selection10,lattice_before_model_selection10]=BLOV_general
(percentiles_before_model_selection(5),capex,volatility_LR_sum_PV(2),r,T,nColu
mn);

%% NPV Analysis by Tank Method and BLOV: After Model Selection

%# NPV estimation by using 'PV_and_ROV_analysis_general.m'

[PV_after_model_selection,NPV_after_model_selection,ROV_after_model_selection,
q_after_model_selection,volatility_LR_sum_PV,volatility_LR_sum_NPV] =
PV_and_ROV_analysis_general(numel(model_list),nCell,numel(model_list),r,p_oil,
A,Nw,rw,CA,skin,mu,h,ct,Pi,Pwf,Bo,T,opex,capex,xy_wells,'poro_models_after_mod
el_selection_gslib_format','perm_models_after_model_selection_gslib_format');

```



```

percentiles_after_model_selection=prctile(NPV_after_model_selection(:,T),[10,2
5,50,75,90]);

P90_after_model_selection=percentiles_after_model_selection(1);
P75_after_model_selection=percentiles_after_model_selection(2);
P50_after_model_selection=percentiles_after_model_selection(3);
P25_after_model_selection=percentiles_after_model_selection(4);
P10_after_model_selection=percentiles_after_model_selection(5);

netP_after_model_selection=sum([0.90,0.75,0.50,0.25,0.10].*percentiles_after_m
odel_selection);

%# BLOV analysis by using 'BLOV_general.m'

[price_after_model_selection,lattice_after_model_selection]=BLOV_general(netP_
after_model_selection, capex, volatility_LR_sum_PV(2), r, T, nColumn, 'Option
lattice after the model selection', 'Underlying lattice after the model
selection');

[price_after_model_selection90,lattice_after_model_selection90]=BLOV_general(p
ercentiles_after_model_selection(1), capex, volatility_LR_sum_PV(2), r, T, nColumn)
;

[price_after_model_selection75,lattice_after_model_selection75]=BLOV_general(p
ercentiles_after_model_selection(2), capex, volatility_LR_sum_PV(2), r, T, nColumn)
;

[price_after_model_selection50,lattice_after_model_selection50]=BLOV_general(p
ercentiles_after_model_selection(3), capex, volatility_LR_sum_PV(2), r, T, nColumn)
;

```

```

[price_after_model_selection25,lattice_after_model_selection25]=BLOV_general(p
ercentiles_after_model_selection(4),capex,volatility_LR_sum_PV(2),r,T,nColumn)
;

[price_after_model_selection10,lattice_after_model_selection10]=BLOV_general(p
ercentiles_after_model_selection(5),capex,volatility_LR_sum_PV(2),r,T,nColumn)
;

%% Figures

%# Plotting Histograms

figure

hist(NPV_before_model_selection(:,T))

xlabel('NPV (in $)')

ylabel('Frequency')

title(['Distribution of NPV for ', num2str(nModel), ' models before model
selection'], 'Fontweight', 'Bold');

figure

hist(NPV_after_model_selection(:,T))

xlabel('NPV (in $)')

ylabel('Frequency')

title(['Distribution of NPV for ', num2str(numel(model_list)), ' models after
model selection'], 'Fontweight', 'Bold');

%# Plotting P10, P25, P50, P75 and P90

```

```

figure

x = 1:5;

y =

[P10_before_model_selection,P25_before_model_selection,P50_before_model_select
ion,P75_before_model_selection,P90_before_model_selection];

plot(x, y, '-ob')

set(gca, 'XTick',1:5, 'XTickLabel',{'P10' 'P25' 'P50' 'P75' 'P90'})

title('P-values for NPV before model selection','Fontweight','Bold')

ylabel('NPV($) ')

```

```

figure

x = 1:5;

y =

[P10_after_model_selection,P25_after_model_selection,P50_after_model_selection
,P75_after_model_selection,P90_after_model_selection];

plot(x, y, '-ob')

set(gca, 'XTick',1:5, 'XTickLabel',{'P10' 'P25' 'P50' 'P75' 'P90'})

title('P-values for NPV after model selection','Fontweight','Bold')

ylabel('NPV($) ')

```

```

%# Plotting option values corresponding to P10, P25, P50, P75, and P90

figure

hold on

x = 1:5;

```

```

y_reference =
[price_before_model_selection10,price_before_model_selection25,price_before_model_selection50,price_before_model_selection75,price_before_model_selection90]
;
y_seismic =
[price_after_model_selection10,price_after_model_selection25,price_after_model_selection50,price_after_model_selection75,price_after_model_selection90];
plot(x, y_reference, '-ob')
plot(x, y_seismic, '-or')
set(gca, 'XTick',1:5, 'XTickLabel',{'P10' 'P25' 'P50' 'P75' 'P90'})
title('Option values corresponding to each P-value','Fontweight','Bold')
ylabel('Option Value ($)')
legend('before model selection','after model selection')
hold off

%# Plotting flow rates
figure
hold on
plot(1:T,q_before_model_selection(1,:), '-b', 'LineWidth', 4)
plot(1:T,q_after_model_selection(1,:), '-r', 'LineWidth', 4)
xlabel('Time (yrs)')
ylabel('q (bbl/yr)')
legend('Before model selection','After model selection')
plot(1:T,q_before_model_selection(2:nModel,:), '-b')

```

```
plot(1:T,q_after_model_selection(2:numel(model_list),:),'-r')  
title('Uncertainty in oil flow rate from 5 wells','Fontweight','Bold')
```

Bibliography

- Arps, J.J., 1945. Analysis of Decline Curves. *Transactions of the American Institute of Mining, Metallurgical and Petroleum Engineers*, 160, pp.228–247.
- Bailey, W., Bhandari, A., Faiz, S., Srinivasan, S., Weeds, H., 2003. Unlocking the Value of Real Options (Oilfield Review), Schlumberger. , 15(4).
- Bhowmik, S., Srinivasan, S. & Bryant, S., 2010. Predicting the Migration of CO₂ Plume Using Injection Data and a Distance-Metric Approach to Reservoir-Model Selection. In *Proceedings of SPE International Conference on CO₂ Capture, Storage, and Utilization*. SPE International Conference on CO₂ Capture, Storage, and Utilization.
- CMG-IMEX, 2009. *IMEX - User's Guide: Advanced IMplicit-EXplicit Black Oil Simulator* 2009th ed., Calgary, Alberta: Computer Modelling Group Ltd.
- Copeland, T.E. & Antikarov, V., 2001. *Real options: a practitioner's guide*, Texere.
- Cox, J.C., Ross, S.A. & Rubinstein, M., 1979. Option pricing: A simplified approach. *Journal of Financial Economics*, 7(3), pp.229–263.
- Coy, P., 1999. Exploiting Uncertainty. *Business Week (US edition)*, (no. 3632), pp.118–124.
- DePamphilis, D.M., 2009. *Mergers, Acquisitions, and Other Restructuring Activities: An Integrated Approach to Process, Tools, Cases, and Solutions*, Academic Press.
- Deutsch, C.V. & Journel, A.G., 1997. *GSLIB: Geostatistical Software Library and User's Guide* 2nd ed., Oxford University Press, USA.

- Dias, M.A., 2004. Monte Carlo Simulation of Stochastic Processes. http://www.puc-rio.br/marco.ind/sim_stoc_proc.html#mc-mrd.
- Dixit, A. & Pindyck, R., 1995. Options Approach to Capital Investment - Harvard Business Review. *Harvard Business Review*, p.13.
- Energy Information Administration - EIA, 2008. Defining the Limits of Oil Production. In *International Energy Outlook 2008*. U.S. Department of Energy.
- Eskandari, K. & Srinivasan, S., 2010. Reservoir Modelling of Complex Geological Systems--A Multiple-Point Perspective. *Journal of Canadian Petroleum Technology*, 49(8).
- Johnson, N.W., 2010. Response to Peter Monkhouse. *Economic Analysis and Policy (EAP)*, 40(1), pp.112–123.
- Lin, J., 2008. *Exploring flexible strategies in engineering systems using screening models : applications to offshore petroleum projects*. PhD Dissertation. Massachusetts: Massachusetts Institute of Technology.
- Mun, J., 2002. *Real options analysis: tools and techniques for valuing strategic investments and decisions*, John Wiley and Sons.
- Ornstein, L.S. & Uhlenbeck, G.E., 1930. On the Theory of the Brownian Motion. *Physical Review*, 36(5), p.823.
- Remy, N., Boucher, A. & Wu, J., 2009. *Applied Geostatistics with SGeMS: A User's Guide 1* Har/Cdr., Cambridge University Press.
- Samuelson, P.A., 1965. Proof that properly anticipated prices fluctuate randomly. *Industrial Management Review*.

- Strabelle, S., 2000. *Sequential simulation drawing structures from training images*. PhD Thesis. Stanford University. Available at: <http://gcmd.nasa.gov/records/SGEMS.html>
- Ugur, O., 2008. *Introduction to Computational Finance*, Imperial College Press.
- Walsh, M.P. & Lake, L.W., 2003. *A generalized approach to primary hydrocarbon recovery*, Elsevier.
- Xu, W., Tran, T., Srivastava, R. M., Journel, A. G., 1992. Integrating Seismic Data in Reservoir Modeling: The Collocated Cokriging Alternative. In Society of Petroleum Engineers.
- Young, E.& & Wiley, J., 2011. *International GAAP 2012: Generally Accepted Accounting Practice Under International Financial Reporting Standards*, John Wiley & Sons.
- Zhu & Journel, 1993. Formatting and integrating soft data: Stochastic imaging via the Markov-Bayes algorithm. Soares, A. (Ed.), *Geostatistics Troia '92*, Kluwer Academic Publishers, Dordrecht, Holland, pp.1–12.